Novel Ferrocenyl Peptide Bioconjugates as Anti-Cancer Agents

by

Lingli Lu

Ph.D. **2018**

Novel Ferrocenyl Peptide Bioconjugates as Anti-Cancer Agents

by

Lingli Lu B.Sc. (Hons.)

A thesis presented for the degree of Doctor of Philosophy

At

Dublin City University

Under the supervision of Dr. Peter T. M. Kenny

Ollscoil Chathair Bhaile Atha Cliath

School of Chemical Sciences

January 2018

Dedicated to my family

Declaration

I hereby certify that this material, which I now submit for assessment on the programme of study leading to the award of Ph.D. is entirely my own work, that I have exercised reasonable care to ensure that the work is original, and does not to the best of my knowledge breach any law of copyright, and has not been taken from the work of others save and to the extent that such work has been cited and acknowledged within the text of my work.

Signed:_____ ID No.:_____

Lingli Lu

Date:_____

Acknowledgements

First and foremost, I would like to thank Dr. Peter T.M. Kenny for giving me the opportunity to conduct research under his supervision, and for his support, and patient throughout the past four years.

I would like to thank Government of Ireland Postgraduate Scholarship for funding this research.

My sincerest thanks to Dr. Patricia González-Barranco and Dr. Mónica A. Ramírez-Cabrera from Universidad Autónoma de Nuevo León México and Karen G. Ontiveros-Castillo from DCU for conducting the biological studies in the SiHa and Chang cells.

Dr. Rosaleen Devery of the school of the School of Biotechnology, Christine Kavanagh and Georgia Pierce for their invaluable assistance with the *in vitro* biological screening in the MCF-7 cell line.

Dr. Dilip K. Rai in Teagasc Food Research Centre Ashtown, for obtaining the MS spectra.

Thanks to all the academic staff and technical staff of the School of Chemical Sciences, especially Dr. Kieran, Dr. Emma Coyle, Dr. Andrew Kellett, Dr. Vickie McKee, Veronica Dobbin, Damien McGuirk, John McLoughlin, Vinny hooper, Ambrose May, and Catherine Keogh.

A special thank you to all members in Peter Kenny Research Group, past and present, especially Dr. Andy G. Harry, Dr. Rachel Elizabeth Tiedt and Karen G. Ontiveros-Castillo.

The fourth year and summer students that have worked with me over the past couple of years, including Simone Wogan, Amy Louise O'Sullivan, Darragh O'Connor, Nessa Cassidy, Shauna Keogh, Georgina Monahan, Lipine Peeno Vanchipurakal, Dannie Loayon, Mark Walsh and Anaïs Loyo Pantel.

I also want to thank my friends in DCU, especially Dong Yang, Karmel Sofia Gkika, Hannah Prydderch, Andrew Jordan and Renhe Chu.

Finally, a huge thank you to my family, my Mum Xiutao Du, Dad JingHu Lu and my husband Yan Zhao, for all their support and encouragement. Couldn't have done it without you.

Abstract

Lingli Lu
Novel Ferrocenyl Peptide Bioconjugates as Anti-Cancer Agents

The aim of this project was to explore the structure-activity relationship (SAR) of novel ferrocenyl based anti-cancer bioconjugates. A series of *N*-(1'-methyl-6-ferrocenyl-2-naphthoyl) and *N*- (1'-ethyl-6-ferrocenyl-2-naphthoyl) amino acid and dipeptide esters and a series of *N*-(ferrocenylmethylamino acid)-fluorinated-benzene carboxamide derivatives have been synthesized, characterized and biologically evaluated for their anti-proliferative activity on various cancer cell lines.

The synthesis of each series of compounds was achieved by coupling the free *N*-terminus of various amino acid and dipeptide esters to the carboxyl group of methyl and ethyl ferrocenyl naphthoic acid or the free *N*-terminus of the ferrocenylmethylamine to the carboxylic acid group of the *N*-(fluorobenzoyl)-amino acid using the conventional *N*-(3-dimethylaminopropyl)-*N*'-ethylcarbodiimide hydrochloride (EDC) and *N*-hydroxysuccinimide (NHS) coupling protocol. All compounds were fully characterized by a combination of spectroscopic techniques, including ^{1}H, ^{13}C and ^{19}F NMR, IR, UV-Vis and MS.

Biological evaluation was performed *in vitro* against the human cervical carcinoma cells (ATCC HTB-35, SiHa) and human liver cells (ATCC CCL-13, Chang liver, HeLa markers) for *N*-(1'-alkyl-6-ferrocenyl-2-naphthoyl) amino acid and dipeptide esters and vincristine. *N*-(1'-ethyl-6-ferrocenyl-2-naphthoyl)-glycine-D-alanine ethyl ester had an IC_{50} of 8.75 μM on cervical cancer cells, which is significantly more cytotoxic than chemotherapeutic medication vincristine. And it has low toxicity against Chang liver cells. The results can suggest that there are differences in susceptibilities to novel ferrocenyl amino acid and dipeptide bioconjugates toxicity between cervical carcinoma and liver cells. Therefore *N*-(1'-ethyl-6-ferrocenyl-2-naphthoyl)-glycine-D-alanine ethyl ester is a potential anti-cancer agent with selectivity.

Another series of *N*-(ferrocenylmethylamino acid) fluorinated benzene carboxamide derivatives were tested on the estrogen positive (ER+) breast cancer cell line, MCF-7. *N*-(ferrocenylmethyl-L-alanine)-3,4,5-trifluorobenzene carboxamide, *N*-(ferrocenylmethyl-L-alanine)-2,3,4,5,6-pentafluorobenzene carboxamide and *N*-(ferrocenylmethylglycine)-2,3,4,5,6-pentafluorobenzene carboxamide all have strong anti-proliferative effects, with the IC_{50} values between 0.57-2.14 μM.

Table of Contents

Abbreviations

A

A	absorbance

B

bs	broad singlet (spectroscopy)

C

C	carbon; concentration
*C*q	quaternary carbon
Cp	cyclopentadienyl ring
COSY	correlated spectroscopy

D

d	doublet (spectroscopy)
D-Ala	D-alanine
dFdDTP	gemcitabine diphosphate
dFdCTP	gemcitabine triphosphate
DCM	dichloromethane
DCU	Dublin City University
dd	doublet of doubles
DEPT-135	distortionless enhancement by polarisation transfer
DMSO-d_6	deuterated dimethylsulfoxide

E

e^-	electron
EAT	ehrlich ascites tumor
EDC	*N*-(3-dimethylaminopropyl)-*N'*-ethylcarbodiimide hydrochloride
ER	estrogen receptor
ER(+)	estrogen receptor positive cells
ER(-)	estrogen receptor negative cells

EtOH	ethanol

F

Fc/Fc^+	ferrocene/ferrocenium ion

G

Gly	glycine
GABA	gamma-amino butyric acid

H

HQMC	heteronuclear multiple quantum coherence
HPLC	high performance liquid chromatography

I

IC_{50}	half maximal inhibitory concentration
IR	infra-red spectroscopy

J

J	coupling constant

L

l	path length (cm)
L-Ala	L-alanine
L-Phe	L-phenyalanine
L-Leu	L-leucine

M

m	*meta*; mass
m	multiplet (spectral)
M	metal; mitosis phase
MLCT	metal-ligand charge transfer
mp	melting point
MS	mass spectrometry

N

NHS	*N*-hydroxysuccinimide
NSCLC	non-small cell lung carcinoma

O

o	*ortho*

P

p	*para*
ppm	parts per million

Q

q	quartet
QM	quinone methide

R

RNA	ribonucleic acid
RSD	relative standard deviation
ROS	reactive oxygen species

S

s	singlet
SAR	structure activity relationship
SERM	selective estrogen receptor modulator

T

TEA	triethylamine
TFA	trifluoroacetic acid
THF	tetrahydrofuran

U

UV	ultraviolet

V

Vis	visible

W

WHO	World Health Organisation

Units

cm	centimetre
cm^{-1}	wavenumber(s) / per centimetre
g	gram
hr	hour
Hz	hertz
M	molar
MHz	megahertz
ml	millilitre
mm	millimetre
mM	millimolar
mmol	millimolar
µL	microlitre
µM	micromolar
^{o}C	degree celcius
ppm	parts per million
s	second
δ	chemical shift
%	percentage

Chapter 1

Cancer, cancer chemotherapy and bioorganometallic anti-cancer agents

1.1. Cancer

1.1.1. Introduction

Cancer is the term used to describe a group of diseases characterized by the uncontrolled cell proliferation and spread of abnormal cells. It is one of the leading causes of death and disease. According to the World Health Organization, it causes one in seven deaths worldwide during the year 2012. Worldwide 14.1 million new cancer cases raised in 2012 and it is expected to grow to 21.7 million with 13 million deaths by 2030. [1]

When normal cells are under uncontrolled growth, multiplication and loss of differentiation, cancer cells are formed. If the cancer is localized it is said to be benign. If the cancer cells invade other parts of the body, it is said to be malignant. Cancer is a complex dynamic human disease. There are more than 200 different cancers resulting from different cellular defects, therefore an effective treatment against one type may ineffective against another.

The cause of cancer is not clearly defined whereas both external and internal factors can be involved. Environmental chemicals (chemical carcinogenesis), radiation (irradiation carcinogenesis, *e.g.* X-rays and ultraviolet radiation), lifestyle (smoking, unhealthy diet) and aging (free radicals) can be referred as external factors, while immune system defects, genetic mutations, hormones and infections (*e.g.* human papillomavirus HPV) are treated as internal factors. Those factors may act together to cause cancer.

5-year survival rate is a useful term used in monitoring progress in the early detection and treatment of cancer. The survival statistics vary greatly by the type of cancer and the stage of diagnosis. However, higher survival rates can be related with early detection or effective treatment of the cancer site. Especially if the cancers can be detected *via* screening. Female breast cancer and colorectal cancer are typical examples.

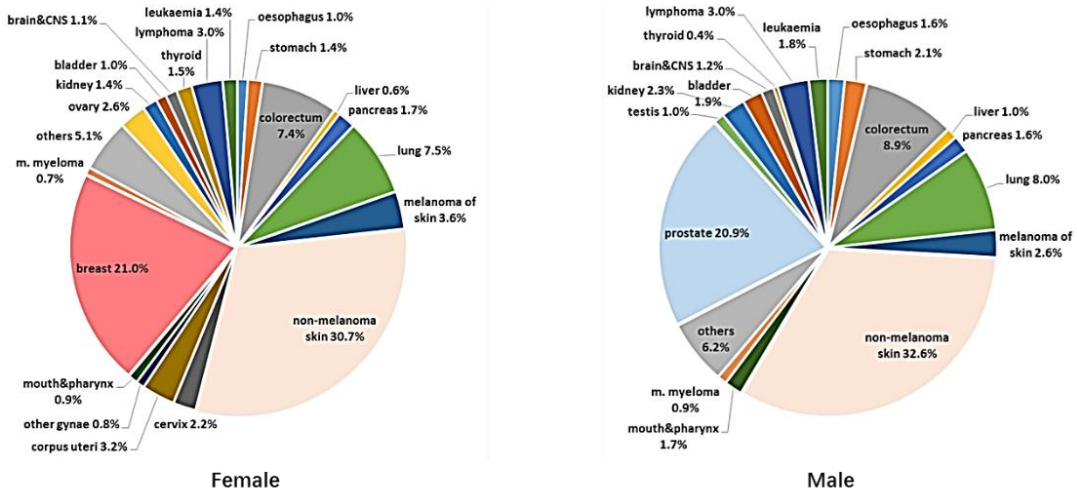

Figure 1. 1: Relative frequency of the most common invasive cancers (including non-melanoma skin cancer) diagnosed during 2011-2013 in Ireland. Reported from the National Cancer Registry. [2]

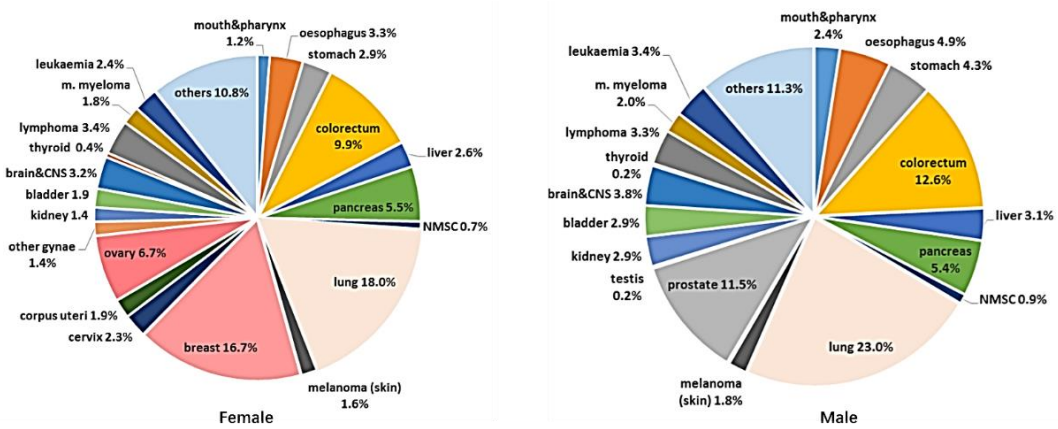

Figure 1. 2: Relative frequency for the cancer deaths between 2011 and 2012 in Ireland. Reported from the National Cancer Registry. [2]

According to the annual report form the national cancer registry, cancer was continuously as the second most common cause of death in Ireland after circulatory disease between 2011-2012. Lung, colorectal and breast cancers are the top three causes of cancer death whereas prostate, breast and colorectal are the most commonly diagnosed invasive cancers (Figure 1.1 and 1.2). [2]

The research within this project is focused on the synthesis of *N*-(1'-alkyl-6-ferrocenyl-2-naphthoyl) amino acid and dipeptide esters, and *N*-(ferrocenylmethylamino acid)-fluorinated benzene carboxamides, and their biological evaluation as potential chemotherapeutic agents for the treatment of cervical and breast cancer.

1.1.2. Cervical cancer

Cervical cancer was reported as the third most common type of cancer in women worldwide and the fourth most common cause of female mortality. [3] Cervical cancer begins when healthy cells on the cervix surface change and grow out of control, and a mass of tumor is formed. This tumor can be benign or cancerous. A benign tumor will not spread into other tissue while cancerous tumor will. There are mainly two types of cervical cancer: squamous cell carcinoma and adenocarcinoma. Around 80% to 90% of cervical cancers are squamous cell carcinoma, these cancers arise from the outer surface cells that cover the cervix. The cancer cells arise in the glandular cells that line the lower birth canal, and are named as adenocarcinoma, which contributed to 10%-20% of all cervical cancers. [4]

A few factors have influence with the development of cervical cancer. Human papillomavirus (HPV) infection is the most important risk. [5] There are over 180 types with HPV, HPV16 and HPV18 that are most frequently associated with cervical cancer. [6] Women with lowered immune systems have a higher risk of cervical cancer development, since the patient is less able to fight cancer. Woman who have genital herpes will have a higher risk of developing cervical cancer. Smoking is another factor linked to cervical cancer. Women who smoke are more likely to develop cervical cancer. Surgery, radiation therapy and chemotherapy are the most common treatments against cervical cancer. [4, 7]

1.1.3. Breast cancer

Breast cancer is a malignant tumor arising from the cells of the breast, it is the most frequently diagnosed cancer in women. Every one woman in eight suffers with breast cancer in the western world, and reported as the third most common causes of cancer death with 7.9% death rate between 2011-2012 in Ireland. [2] Genetic factors, diet and life style are the main causes of breast cancer.

There are many types of breast cancer, the most common types are ductal carcinoma *in situ*, invasive ductal carcinoma and invasive lobular carcinoma. Ductal carcinoma *in situ* can be diagnosed within the breast ducts, it is the type not spread therefore has a higher cure rate. About 80% of invasive breast cancers are caused by invasive ductal carcinoma. This cancer starts in a duct of the breast and grows into the surrounding tissue. Approximately 10% of invasive breast cancers belongs to invasive lobular carcinoma, the cancer starts to spread from the glands of the breast that produce milk. [8]

Breast cancer is often referred to as a hormonal cancer, knowing the hormone receptor status is important for treatment. Breast cancer cells that have estrogen receptors are called ER-positive cancers, the cancer cells have progesterone receptors are referred as PR-positive cancers, and the breast cancer cells that have none of the receptors as above are called triple-negative cancer cells. [9] The hormone receptor-positive patients can use hormone therapy drugs that lower estrogen levels or block estrogen receptors, while patients diagnosed as triple-negative can be treated with chemotherapy and surgery. [8]

1.2. Cancer chemotherapy

Cancer can be treated by different approaches. Surgery, radiotherapy and chemotherapy are the traditional methods, which can be used alone or in combination. The treatment depends on the different stages of cancer and its locations. Surgery and radiotherapy are used to remove, kill or damage cancer cells in a specific area whereas chemotherapy can work throughout the whole body. In some cases, one or more anti-cancer drugs are used to achieve higher effect. The advantages include decreased toxicity, increased efficiency of action and evasion of drug resistance. [10]

The drugs used in chemotherapy are cytotoxic, powerful chemicals that are designed to interrupt cell replication process and stop cells from growing. There are a few subtypes of anti-cancer agents, based on its unique mode of actions. Alkylating agents, anti-metabolites, anti-microtubule agents and metallating agents are the typical examples.

1.2.1. Alkylating agents

Alkylating agents are highly electrophilic compounds that can react with nucleophilic sites of one or both strands in DNA. The main nucleophilic regions of DNA are the *N*-1 and *N*-3 of adenine **1**, *N*-3 of cytosine **2** and in particular *N*-7 of guanine **3**. The alkylation prevents DNA replication and transcription, which results in cell death of affected cells.

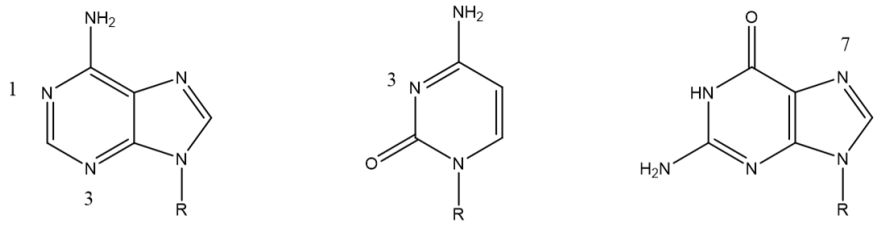

Adenine **1** Cytosine **2** Guanine **3**

Figure 1. 3: Nucleophilic groups on adenine, guanine and cytosine.

The nitrogen mustards were the first alkylating agent used medicinally in 1942. In chlormethine **4**, the nitrogen atom is able to displace a chloride ion intramolecularly to form the highly electrophilic aziridinium ion, the alkylation can take place. [10]

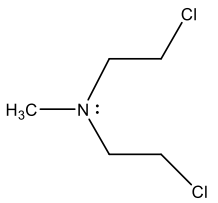

4

Dacarbazine **5** is a prodrug which generate a methyldiazonium ion **7** to act as the alkylating agent for metastatic melanoma cancer treatment. [11] Dacarbazine undergoes an activation by cytochrome P450 enzymes in liver. Methyltriazenoimidazole carboxamide forms and spontaneously degrades to AIC (5-aminoimidazole-4-carboxamide) **6** and the methyldiazonium ion **7**. This active ion reacts with RNA or DNA mainly at 7-position of guanine.

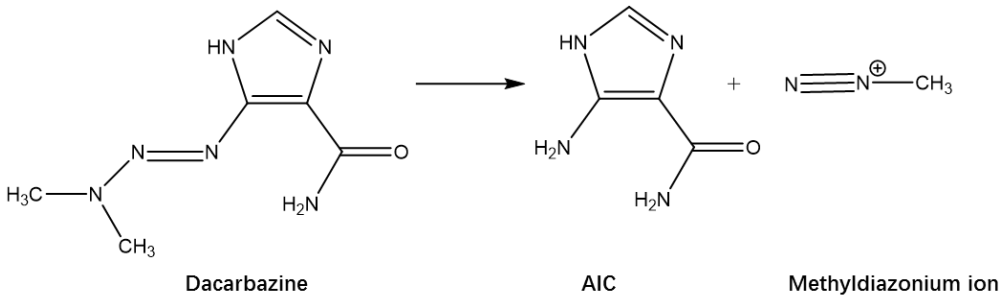

5 **6** **7**

Figure 1. 4: Formation of AIC and methyldiazonium ion from dacarbazine.

1.2.2. Anti-metabolites

Anti-metabolites are a type of anti-cancer agent that can disrupt DNA function *via* inhibition of the enzymes involved in the synthesis of DNA or its nucleotide building blocks. [10]

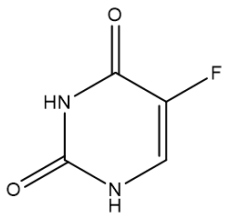

8

5-Fluorouracil **8** inhibits thymidylate synthase. It forms a suicide substrate by irreversibly binding to the active site of the enzyme and disrupting the thymidine synthesis. Therefore, replication and cell division are blocked.

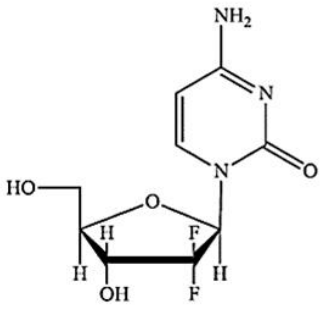

9

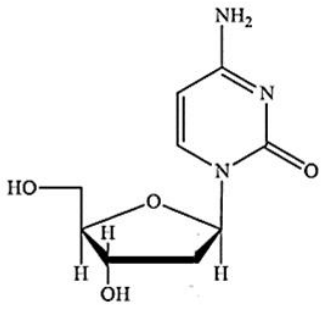

10

Gemcitabine **9** is a widely used chemotherapy medication for several types of cancer treatment, including breast cancer, pancreatic cancer, ovarian cancer and non-small cell lung cancer. [12] It was patented in 1983 and released to market in 1995. This synthetic pyrimidine nucleoside prodrug is a fluorinated analogue of 2-deoxycytidine **10**. After transported into the cell, this prodrug will be phosphorylated by deoxycytidine kinase to form two active metabolites: gemcitabine diphosphate (dFdCDP) and gemcitabine triphosphate (dFdCTP). Gemcitabine diphosphate inhibits the enzyme responsible for catalyzing the synthesis of deoxynucleotide triphosphates that is required for DNA synthesis, and gemcitabine triphosphate competes with endogenous deoxynucleotide triphosphates required in the DNA synthesis. [12]

1.2.3. Anti-microtubule agents

An anti-microtubule agent is a type of drug that blocks cell growth by stopping mitosis, by interfering with the formation of the mitotic spindle required for cell division. Agents acting on microtubules may either bind to tubulin and stop polymerisation or bind to the microtubules themselves and prevent depolymerisation. Hence inhibits cell dividing and induces cell death. [10]

Vincristine **11** and vinblastine **12** are naturally occurring vinca alkaloids. They act as anti-microtubule agents to treat a number of types of cancers, *e.g.* small cell lung cancer, acute lymphocytic leukaemia and neuroblastoma. [13]

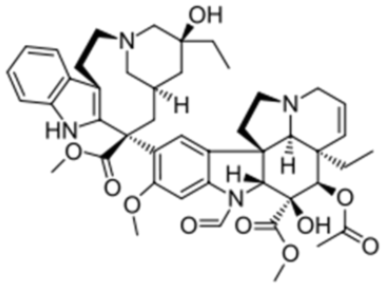

11

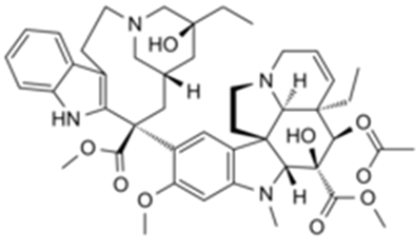

12

Vindesine **13** is a synthetic vinca alkaloid. It binds to the microtubular proteins of the mitotic spindle, leading to crystallization of the microtubule, and mitotic arrest or cell death. [13]

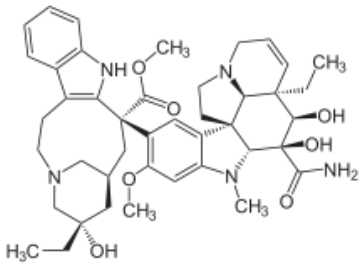

13

1.2.4. Metallating agents (platinum anti-cancer agents)

Since Rosenberg and colleagues found the products of hydrolysis of the platinum electrode can inhibit bacterial growth in the 1960s, cisplatin (*cis*-diamminedichloroplatinum(II)) **14** has been extensively studied. [14] Cisplatin and other related platinum-based anti-cancer drugs belong to a class of agents called metallating agents. Cisplatin and other platinate derivatives are now commonly used as anti-cancer drugs for ovary, testes, head and neck and other cancers' treatments. [15]

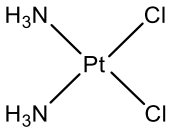

14

Cisplatin is a square planar complex composed of two ammonia ligands and two chloro substituents coordinated to the platinum in *cis* configuration. The mode of action has been studied. Following administration, cisplatin enters the cell, where the environment has a low chloride ion concentration, aquated cisplatin acts as a positively charged complex. The highly active electrophilic complexes function as metalating agents to target nitrogen atoms of DNA. Indeed, the covalent Pt-DNA links within the same strand to form intra-strand bridges. The formation of these DNA-cisplatin adducts causes a change in the structure of the double helix therefore disrupts the replication and transcription of DNA, halting cancer cell proliferation.

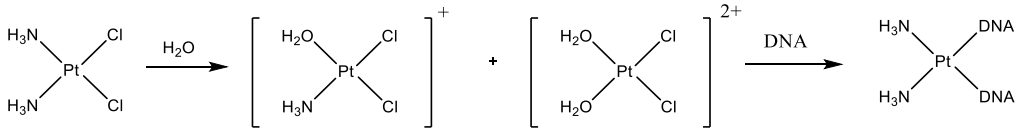

Figure 1. 5: Loss of chloro substituents in water and binding with DNA. [10]

Despite its huge success, the dose limiting toxicities associated with cisplatin has presented a serious concern in clinic. Therefore, different generations of derivatives of cisplatin have been developed.

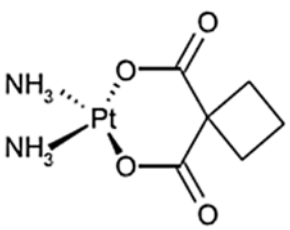

15

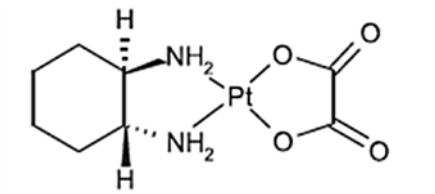

16

Carboplatin (cis-diammine(1,1-cyclobutanedicarboxylate) platinum(II)) **15**, was created by substituting the readily exchangeable chloride ligands with a bidentate dicarboxylate ligand. This well-known second-generation platinum drug reduces the dose limiting toxicity of cisplatin by slowing down the rate of aquation reactions. This anti-cancer drug was released to the market in 1989, and used to treat ovarian cancer and non-small cell lung cancer in combination with paclitaxel.

The third-generation platinum complexes were designed to overcome cellular resistance to cisplatin and carboplatin. Oxaliplatin (1, 2-diaminocyclohexane platinum(II) oxalate) **16** is a successful one approved in 1999. It also has great potential as a treatment option after failure of cisplatin or carboplatin therapy with less toxicity. Oxaliplatin is used for colorectal cancer treatment, typically along with folinic acid and 5-fluorouracil **8**.

A group of octahedral Pt(IV) complexes were called as fourth-generation platinum complexes. These complexes are prodrugs are eventually transformed into Pt (II) complexes, due to the reduction of Pt (IV) and loss of axial ligands. Satraplatin **17** is an orally bioavailable platinum chemotherapeutic agent belonging to this group.

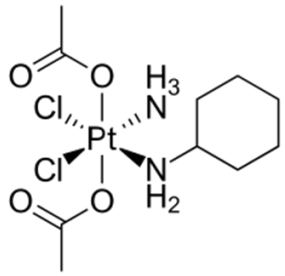

17

1.3. Bioorganometallic chemistry and organometallic anti-cancer agents

Compounds contain metals (e.g. Fe, Rh, Ru and Ti) have appeared as chemotherapeutic agents with anti-proliferative and anti-neoplastic properties in recent years. [16] Those metal-containing substances can be divided into two types: organometallic and metal-organic compounds. Metal atom covalently bound to carbon atoms of organic ligands, such as, ferrocene **18** and its derivatives, are defined as organometallic compounds; metal-organic compounds refer to heteroatoms donates coordinate bond to the metal accepters, like cisplatin **14** and its derivatives in clinical use.

1.3.1. Ferrocene

The orange compound ferrocene which is also called di (η^5-cyclopentadienyl) iron (II) was first isolated in 1951 by two independent research groups, Kealy and Pauson and Miller *et al*. [17] Both groups noted that it was an air-stable, water insoluble and nontoxic compound with good redox properties. The *d* orbitals of the central iron atom overlap with π-electrons of *p* orbitals of the two parallel cyclopentadienyl rings, by forming π-complexation, resulting in the famous "sandwich" structure. This "sandwich" structure was confirmed by Ernst Fischer and Geoffrey Wilkinson through chemical, physical, spectroscopic and X-ray crystallography methods [17]. Based on this, Wilkinson and Fischer shared the Nobel Prize for Chemistry in 1973 for their work in organometallic chemistry.

Ferrocene can be viewed as consisting of an Fe^{2+} ion (six valence *d*-electrons) bonded with two electron rich, aromatic cyclopentadienyl anions (six π-electron species each), all valence shell electrons are paired and obey the 18-electron rule, and leaves the anti-bonding orbitals unpopulated, resulting in a stable diamagnetic compound. The bonding within ferrocene is illustrated as Figure 1.6 (the semi-quantitative molecular orbital diagram), 12 paired electrons (a_{1g}, a_{2u}, e_{1g} and e_{1u}) are in strong bonding orbitals, which leaves 6 electrons (e_{2g} and a_{1g^*}) in the non-bonding orbitals. The HOMO of ferrocene is a_{1g^*} while LUMO is e_{1g^*}. These electrons in the high energy level, non-bonding orbitals are crucial for redox behaviour of ferrocene.

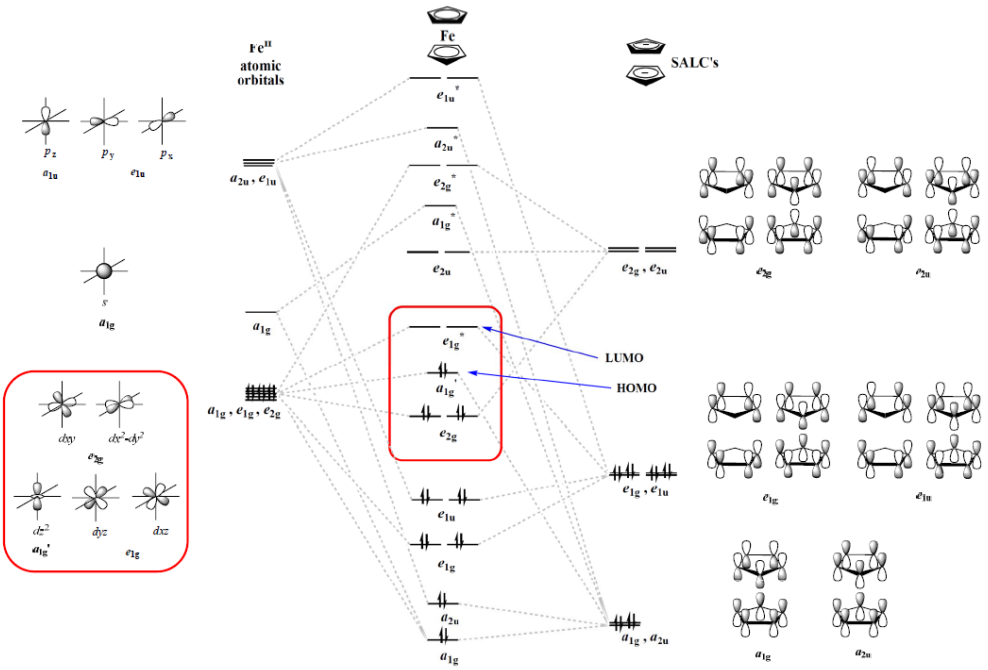

Figure 1. 6: The semi-quantitative molecular orbital diagram of ferrocene (D_{5d} symmetry assignments).

The aromatic character of the ferrocene rings facilitates electrophilic substitution due to six π-electrons delocalized over five carbon atoms. The two main mechanistic routes for electronic substitution of ferrocene are shown in scheme 1.1. In the first mechanism, the electrophile interacts with the iron atom and transferred to the aromatic ring, and undergoes deprotonation. While in the second mechanism, the electrophile directly adds the ring and deprotonated by losing H^+ without direct metal participation.

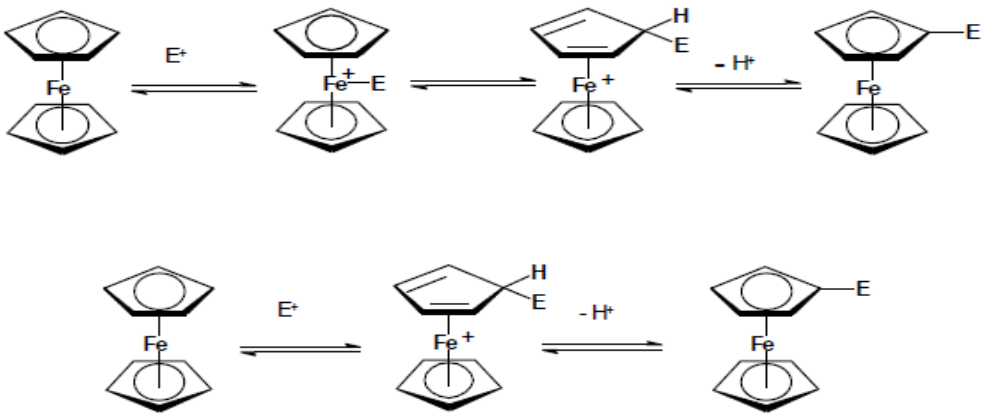

Scheme 1. 1: Two main electrophilic substitution mechanisms for ferrocene.

There are six electrons in the high energy non-bonding orbitals, one electron can be easily removed to yield the ferricenium cation, which is a typical free-radical possessing an unpaired electron.

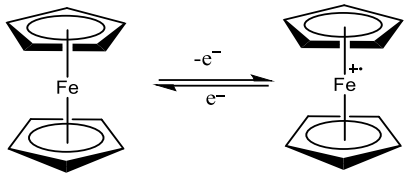

Ferrocene Ferricenium cation

18

Scheme 1. 2: One-electron transfer in the ferrocene/ferricenium system.

1.3.2. Ferricenium salts

Nowadays, ferrocene and its derivatives attract special attention for cancer treatment [18-20]. Reports have shown that ferrocene derivatives are highly active *in vitro* against several types of cancer cell lines [21]. Because of its unique properties, like aromaticity, low toxicity, kinetic stability, relatively lipophilic and redox activity. It has been wildly incorporated in drug design.

Preparation of water-soluble ferrocenyl derivatives that have anti-cancer activity has attracted much attention. [22] Koepf-Maier is one of the pioneers in this field. [23]. His group compared ferrocene and some ferricenium salts with different counter anions against mice bearing Ehrlich ascites tumor (EAT). It was observed that the neutral ferrocene complex lacked anti-tumor efficacy against EAT, whereas the ferricenium tetrachloroferrate, $[Cp_2Fe]^+[FeCl_4]^-$ **19** with survival rate up to 83% against CH 1 human ovarian carcinoma cells. [23]

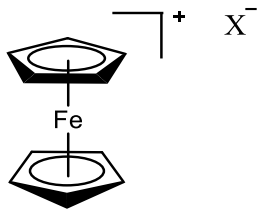

$X^- = [FeCl_4]^-$

19

Soon after, a series of ferrocenylalkylazoles were synthesized by Popova *et al.* and analyzed *in vivo*. For compound **20**, it presented up to 100% of tumor growth inhibition and 45% regression. The success of this compound was attributed to several reasons: the hydrophilic benzotriazolyl group facilitates transportation in aqueous media and the lipophilic ferrocenyl moiety provides permeability into the cell membrane; the swinging alkyl bridge allows the ligand-receptor complex formation; and the planar heterocyclic ring can intercalate between the planes of DNA nucleic bases. [24]

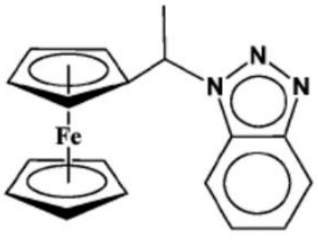

20

1.3.3. Ferrocifen type anti-cancer agents

Tamoxifen (Tam) **21** is an estrogen receptor antagonist present in breast tissue. It can metabolize to form its metabolite hydroxytamoxifen (OH-Tam) **22**. This hydroxylated form produced *in vivo* binds competitively to the estrogen receptor binding site to produce an anti-estrogenic effect, therefore tamoxifen has anti-proliferative effect. [25] The selective estrogen receptor modulators (SERMs) is commonly used in the endocrine therapy to treat with hormone-dependent breast cancers. The breast cancer cells have estrogen receptor (ER) are classified as ER positive cells [ER (+)], and the cancer cells do not express ER are referred as ER negative cells [ER(-)]. [25]

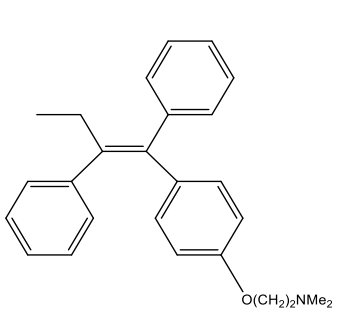

21

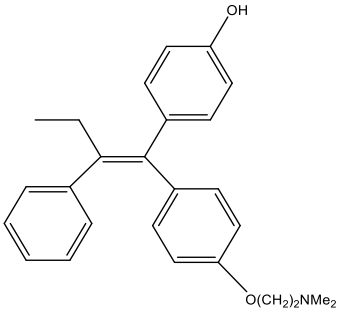

22

Ferrocifen is a ferrocenyl derivative of tamoxifen. Over the past decade, ferrocifen anti-cancer agents have been extensively studied by Jaouen's group. [26] The ferrocifens **23** (Fc-OH-Tam) and **24** (Fc-diOH) derived from hydroxytamoxifen (OH-Tam) **22** are among the earliest organometallic SERMs (selective estrogen receptor modulators). [26, 27] Compound **23** exhibits a strong anti-proliferation effect on both hormone-dependent and hormone-independent breast cancer cells. With IC_{50} as 0.8 μM and 0.5 μM on MCF-7 and MDA-MB-231 cells respectively. Since the corresponding purely organic form shows antiestrogenic activity only on hormone-dependent cancer cells (MCF-7), a dual mode of ferrocifens action was suggested by Jaouen and co-workers: the anti-cancer pathway in the body depends both on the unique properties of ferrocene moiety, and mimic structure like tamoxifen. [28]

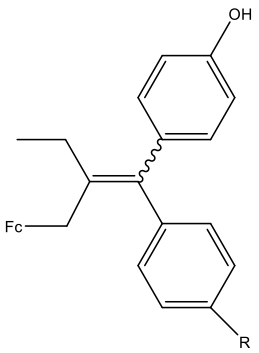

23, R = $O(CH_2)_2N(CH_3)_2$ **24**, R = OH

With the aim to seek related molecules that may have higher anti-cancer efficacy than **23**, and to understand their mechanism of action, several series of ferrocifens have been designed and studied. [27] [28] [29] [30] [31]

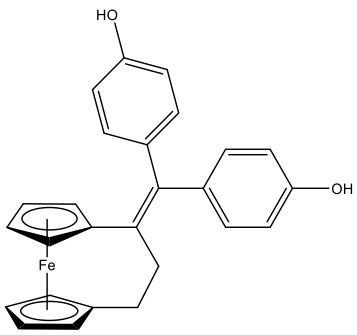

25

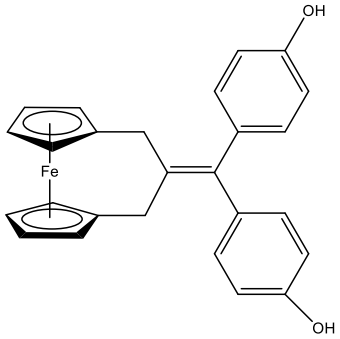

26

Compounds possess the [3]-ferrocenophane motif stand out with their excellent anti-cancer activity. Molecules **25** possesses a direct linkage between the cyclopentadienyl ring and the double bond, while in **26**, the ferrocenyl is symmetrically linked to the double bond by a methylene bridge. Compound **25** showed an exceptional anti-proliferative effect on the hormone-independent MDA-MB-231 and PC-3 cells, both with an IC_{50} value of 0.09 μM. This compound is eight times more active than compound **23**. [32] Compound **26** had a weaker toxicity than **25**, with an IC_{50} as 0.96 and 1.08 μM on MDA-MB-231 and PC-3 cell lines. Cyclic voltammetry experiments were performed by Plazuk *et al.* for both compounds **25** and **26** to understand the possible mechanism. The cytotoxic effect of those ferrocenyl phenols is based on the *in situ* transformation to a quinone methide (QM). The intramolecular proton coupled electron transfer from the phenol to the ferricenium in **25** was due to the π-delocalized mechanism. For unconjugated **26**, the electron transfer proceeds *via* the formation of an intermediate α-methylene radical, which can delocalize over the π system and undergo oxidation step to yield the QM. [32]

Jaouen's group proposed that the ferrous cation undergoes a Fenton-type reaction to generate free hydroxyl radicals, the active metabolite hydroxyferrocifen is readily oxidized to yield a quinone methide (QM) intermediate. [29] These reactive intermediates undergo nucleophilic attack by nucleophiles and react with glutathione or nucleobases to generate toxicity. Scheme 1.3 is the mechanism of the redox activation of ferrocifens proposed by Jaouen and co-workers. The arrows indicate the position readily attacked by nucleophiles. [21] [33]

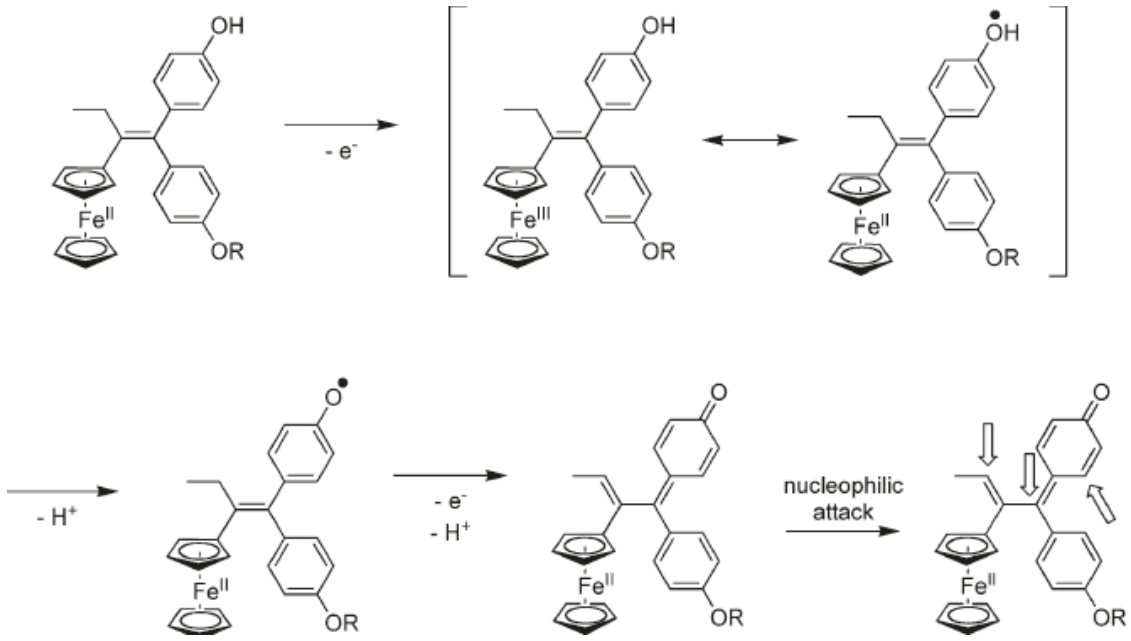

Scheme 1. 3: Redox activation of ferrocifens proposed by Jaouen and co-workers.

1.3.4. ROS-mediated mechanisms of ferrocenyl derivatives as anti-cancer agents

Reactive oxygen species (ROS) are defined as reactive chemical species containing oxygen which is mainly divided into a type of free radicals and another type has unpaired electrons in outer molecular orbitals. Due to its highly reactive property, free radicals can react with biological molecules. A slight rise of ROS level in cells may lead to short-lived cellular alteration, while a severe increase could result in irreversible oxidative damage leading to cell death. Consequently, it is crucial for normal cells to maintain ROS homeostasis. [34]

Recent studies suggest that cancer tissue is known to be in an oxidative stress state. Most cancer cells exhibit high aerobic glycolysis, and are more vulnerable to damage by exogenous agents through increased ROS level. [34] Therefore, increasing the concentration of ROS may vanquish cancer cells by leaving the normal cells unaffected. Combining with the character of cancer cells, modulation of ROS production in cell is a way to selectively destroy cancer cells with no significant toxicity to normal cells.

The redox properties of ferrocene in biological systems have been considered as one of the main reasons for ferrocenyl derivatives as an anti-cancer candidate. Many studies showed that the Fe (II) ferrocenyl compounds have higher activity than Fe (III) ones. [21] The ferrocifens bind with ERβ protein to form ferrocifen-ERβ complexes will attach to a specific region of DNA, and the generation of highly reactive hydroxyl radicals from H_2O_2 through oxidizing Fe^{2+} into Fe^{3+}. This could damage the binding site of DNA strand, resulting in anti-proliferative effect. [33, 35] Overall, the high activity of ferrocene compounds relies on its good redox properties and the formation of ·OH radicals to damage the cancer cell, represent anti-proliferative effects.

1.3.5. Ferrocenyl amino acid and peptide bioconjugates as anti-cancer agents

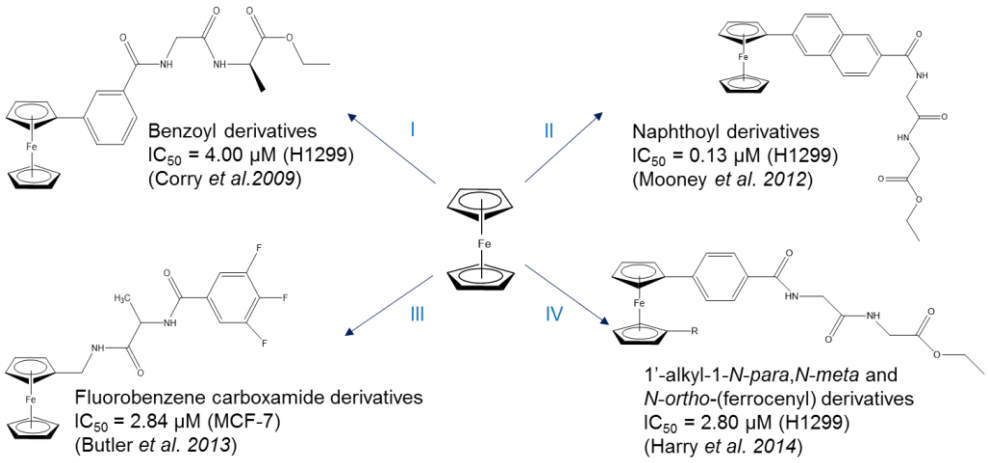

A series of *N*-(ferrocenylmethyl)fluorobenzene-carboxamide derivatives were prepared by Kelly *et al.* using standard peptide coupling procedures. [36] By replacing hydrogen with fluorine, the 4-fluoro derivative **27** shows strongest anti-proliferative effect on MDA-MB-435-S-F breast cancer cell with an IC_{50} value between 11-14 µM. A dose-dependent relationship observed when tested **27** against a wider range of concentrations (1-40 µM). [36]

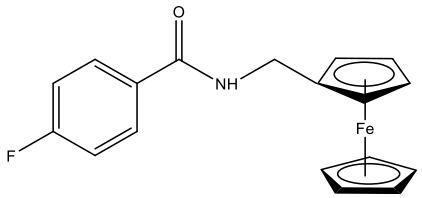

27

Butler *et al.* prepared a series of *N*-(ferrocenylmethyl amino acid) fluorinated benzene carboxamide derivatives using glycine and alanine as linkers, found compound *N*-(ferrocenylmethyl-L-alanine)-3, 4, 5-trifluorobenzene carboxamide **28** is the most active one against MCF-7 cancer cells, with an IC_{50} value of 2.84 µM. [37] The position and the number of fluorine atoms on the aromatic ring were also investigated. 3,4,5-Trifluoro and 2,3,4,5,6-pentafluoro analogues were identified as having a higher inhibitory effect on the MCF-7 cell line. [37]

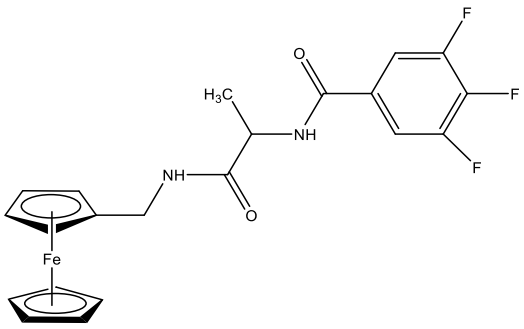

28

A series of *N*-(ferrocenyl) benzoyl dipeptide esters have been extensively studied and have shown to be highly active *in vitro*. *N*-{*ortho*-(ferrocenyl)-benzoyl}-glycine ethyl ester and its starting material *ortho*-ferrocenyl ethyl benzoate were both tested against H1299 non-small cell lung cancer (NSCLC) cell line. Results showed that the derivative has anti-cancer activity (IC_{50} = 48 µM) whereas its starting material was completely inactive. Therefore, more derivatives were designed to have higher anti-cancer activity. Savage *et al.* prepared a series of *N*-{*meta*-(ferrocenyl)-benzoyl} dipeptides, containing L-alanine as the first amino acid in the peptide chain. The derivative with L-alanine-glycine ether ester had an IC_{50} value as 21 µM. [38]

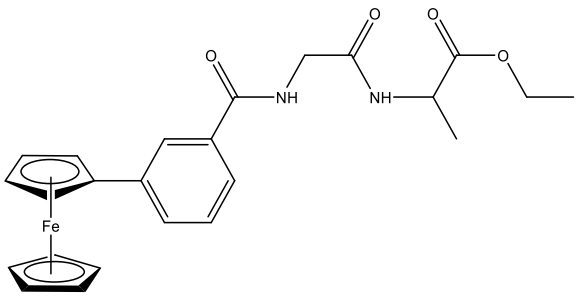

29

Corry *et al*. prepared *N-ortho*, *meta* and *para* ferrocenyl benzoyl amino acid and dipeptide derivatives, *N*-{*meta*-(ferrocenyl)-benzoyl}-glycine-L-alanine ethyl ester **29** found to be the most active one with IC_{50} of 4.0 µM in H1299 cells, whilst the *ortho* and *para* derivatives had a higher IC_{50} values of 5.3 µM and 6.6 µM. These results indicate that the orientation around the benzoyl linker is not a crucial factor for bioactivity. Cell cycle analysis was performed on the cells treated with control sample and test compound *N*-{*ortho*-(ferrocenyl)-benzoyl}-glycine-L-alanine ethyl ester at different concentrations (5, 10, 20, 40 µM). As the concentration of test compound increase, the percentage of cells in G1 phase decreases, suggesting a block in the G2/M phase. [39]

The peptide region of the compounds has been extensively studied by Corry *et al.*, [40] *N*-(ferrocenyl) benzoyl tripeptide and tetrapeptide ethyl ester derivatives were designed to have higher cytotoxicity,

however they showed a negative effect on cytotoxicity by extending the peptide chain. The *N*-{*ortho*-(ferrocenyl) benzoyl}-glycine-glycine-glycine ethyl ester had an IC_{50} value of 63 μM against H1299 cancer cells whereas the tetra-glycine analogue did not show IC_{50} value within 1-100 μM concentration range. Thus, a dipeptide chain is required for optimum activity. [40]

Higher activities were reported by Mooney *et al. via* replacing the benzoyl conjugate with a naphthoyl linker. A series of *N*-(ferrocenyl) naphthoyl amino acid and dipeptide ethyl esters were prepared. [41] *N*-(6-ferrocenyl-2-naphthoyl) derivatives were found to be significantly more active: *N*-(6-ferrocenyl-2-naphthoyl)-glycine-L-alanine ethyl ester having an IC_{50} of 1.3 μM against H1299 lung cancer lines, which was three times more active than the *N*-{*ortho*-(ferrocenyl) benzoyl}-glycine-L-alanine ethyl ester. The *N*-(6-ferrocenyl-2-naphthoyl) derivatives were tested in H1299 cells, with amino acid and peptide and IC_{50} as: γ-aminobutyric acid ethyl ester (IC_{50} = 0.62 μM), glycine-glycine methyl ester (IC_{50} = 0.3 μM), glycine-D-alanine ethyl ester (IC_{50} = 0.33 μM) and glycine-glycine ethyl ester **30** (IC_{50} = 0.13 μM). [42]

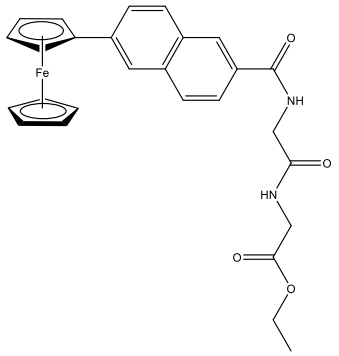

30

It is worth investigating the mechanisms of action for those highly active *N*-(6-ferrocenyl-2-naphthoyl) derivatives. Cell cycle analysis was performed on control samples and H1299 cells treated with the most active compound **30**, at concentrations of 0.5 μM and 1.0 μM. A significant increase in the sub-G_0/G_1 population and decrease in the cells number in the S phase were detected after 48 hours at 0.5 μM, the similar observations were made following incubation for 72 hours. At higher concentration of 1.0 μM, similar trends recorded, and due to the higher concentration, the increase in the sub-G_0/G_1 and S phase cell population were reported. Thus, the exposure of H1299 cells with **30** leads to an accumulation of hypodiploid. This finding suggests that compound **30** most likely induces apoptosis in H1299 cells since apoptotic cells are characterized by DNA fragmentation and consequently a decrease in nuclear DNA content. [43] Oxidation studies were carried out to investigate if compound **30** is capable of causing oxidative damage to guanine. 8-Oxo-Gua concentrations were consistently higher than control levels confirming that oxidation is Fenton-mediated. [43]

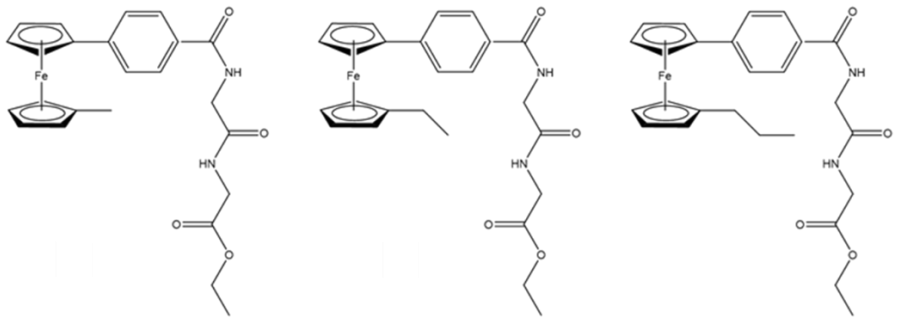

31 **32** **33**

As an extension of structure-activity relationship study, disubstituted derivatives of *N*-(ferrocenyl)benzoyl amino acid and dipeptide esters were prepared. The alkyl group is thought to be important in further decreasing the redox potential of these compounds. Results show they have a greater cytotoxicity than the monosubstituted ones. The most active analogues are 1-methyl-1'-*N*-{*para*-(ferrocenyl)-benzoyl}-glycine-glycine ethyl ester **31**, 1-ethyl-1'-*N*-{*para*-(ferrocenyl)-benzoyl}-glycine-glycine ethyl ester **32** and 1-propyl-1'-*N*-{*para*-(ferrocenyl)-benzoyl}-glycine-glycine ethyl ester **33** with IC_{50} values as 2.8 ± 1.23, 3.5 ± 0.82 and 5.4 ± 1.21 μM in H1299 cell line, respectively. Therefore, the bioactivity decreases with the longer alkyl chains. [44]

1.3.6. Other ferrocenyl derivatives in cancer research

Topoisomerase II is an important enzyme that unwinds DNA to facilitate in nuclear replication, transcription and repair process, this behaviour was highly regulated in normal cells. In cancer cells, high levels of topoisomerase II exist, therefore inhibiting topoisomerase II actions will lead to chromosomal aberrations, followed by cell death. Thus, developing isoform-specific topoisomerase II inhibitors has become interest for researchers. Kondopi and co-workers reported a series of ferrocenyl derivatives act as topoisomerase II inhibitors, 1, 1'-dicarboxaldoxime of ferrocene was a powerful topoisomerase II inhibitor [45]. This complex has a strong anti-proliferative activity against Colon 205 adenocarcinoma [45]. It was proposed that the interaction between nitrogen and oxygen with the topoisomerase II enzyme is the key for anti-cancer activities. Meanwhile, azalactone ferrocene **34** and thiomorpholide amido methyl ferrocene **35** are potential inhibitors. These two compounds interacted with topoisomerase II and inhibited its activity causing genetic implications. [46]

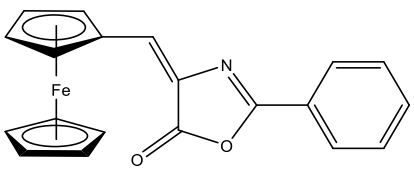

34

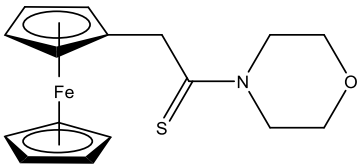

35

Retinoids are a class of chemicals that are vitamers of vitamin A. Retinoids have many important functions throughout the body including roles in vertebrate bone growth, supporting cell differentiation and immune response [47]. Retinoids can incorporate ferrocenyl derivatives to form anti-tumor agents. The actions are mediated through binding and activation of the retinoic acid receptors or retinoid X receptors. Compound **36** was tested against three types of human cancer cell line: lung cancer cell (A549), liver cancer cell line (BEL7404) and tongue cancer cell line (Tca) and it was found that the ferrocenyl analogues have modest IC_{50} values in the range of 19 to 40 μM against all those cell lines. [48]

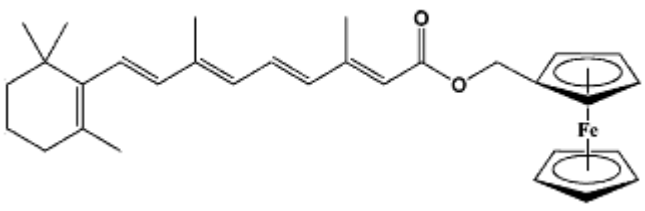

36

Illudin M **37** is a fungal cytotoxin that belongs to a family of sesquiterpenes, produced by some mushrooms. Although the illudins are highly active against various tumors, their extreme toxicity has prevented clinical applications. Schobert and co-workers have prepared a series of compounds attached to illudins. Bis(illudinyl M) 1,1'-ferrocenedioate **38** was much less toxic and displayed better anti-cancer selectivity than its parent Illudin M.[49] These improvements may be due to the shielding function of ferrocene and avoiding attack at the enone group by glutathione.

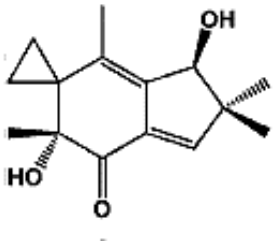

37

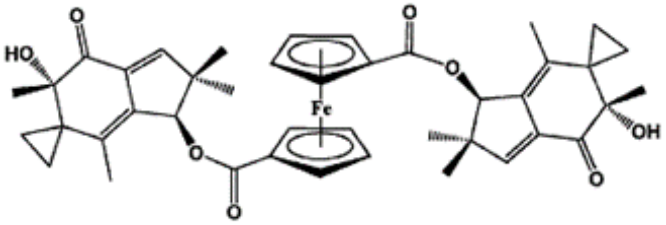

38

Metallocenes with Fe and Ru metal centers have also shown anti-cancer activity. There are two reasons for the promising anti-tumor activity: firstly, ruthenium has accessible range of oxidation states (II, III and IV) under physiological conditions; secondly, ruthenium complexes spontaneously accumulate in rapidly dividing cells.

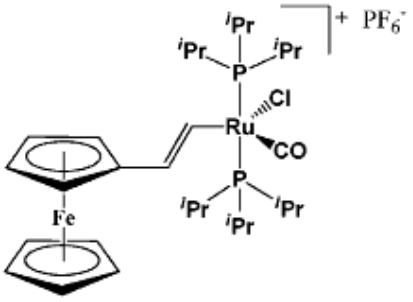

39

Ott *et al.* prepared compound **39**, which has an ethylene linker between ferrocene and ruthenium complexes. When evaluated against colon and breast cancer cells, similar anti-tumor activity to cisplatin was reported. The high bioactivity may relate to the enhanced electron delocalization than corresponding monometallic ruthenium compounds. [50]

1.4. Conclusions

Cancer is a major cause of death worldwide; breast and cervical cancer are two main cancers causing of female mortality. The use of chemotherapeutic agents was restricted by severe toxicity and spontaneous or acquired resistance. Therefore, new therapeutic agents for cancer chemotherapy are constantly required.

Organometallic agents have recently been found to be promising anti-cancer drug candidates, due to organometallics having a great structural variety and far more diverse stereochemistry than organic compounds. Furthermore, they are kinetically stable, relatively lipophilic and their metal atom is in a low oxidations state. The medicinal application of ferrocene derivatives has become a thriving area of anti-cancer research [51]. Ferrocenyl compounds contain a [3]-ferrocenophane motif express anti-proliferative effect in breast and prostate cancer cell lines, [32] and the ferrocenyl tamoxifen derivatives have promising anti-cancer activity, against both ER(+) and ER(-) breast cancer cell lines. [29 52] Kenny *et al.* synthesizing a series of novel ferrocene derivatives with anti-cancer activity. Therefore, a continued investigation is required.

References

1. *Global Cancer Facts and Figures*, American Cancer Society.
2. *Cancer in Ireland 1994-2013: Annual Report of the National Cancer Registry*, Cork, Ireland, 2015.
3. K. U. Jansen and A. R. Shaw, *Annual Review of Medicine*, 2004, **55**, 319-331.
4. D. Pectasides, K. Kamposioras, G. Papaxoinis and E. Pectasides, *Cancer Treatment Reviews*, 2008, **34**, 603-613.
5. P. L. Stern, S. H. v. d. Burg, I. N. Hampson, T. R. Broker, A. Fiander, C. J. Lacey, H. C. Kitchener and M. H. Einstein, *Vaccine*, 2011, **30**, 71-82.
6. R. Koivusalo and S. Hietanen, *Cancer Biology & Therapy*, 2004, **3**, 1177-1183.
7. T. Kamura and K. Ushijima, *Taiwanese Journal of Obstetrics & Gynecology*, 2013, **52**, 161-164.
8. S. Nilsson and K. F. Koehler, *Basic & Clinical Pharmacology & Toxicology*, 2004, **96**, 15-25.
9. A.-L. Laine, E. Adriaenssens, A. Vessières, G. Jaouen, C. Corbet, E. Desruelles, P. Pigeon, R.-A. Toillon and C. Passirani, *Biomaterials*, 2013, **34**, 6949-6956.
10. G. L. Patrick, *An introduction to medicinal chemistry*, Oxford University Express, 5th edn., 2013.
11. H. J. Gogas, J. M. Kirkwood and V. K. Sondak, *Cancer*, 2007, **109**, 455-464.
12. W. Plunkett, P. Huang, Y. Z. Xu, V. Heinemann, R. Grunewald and V. Gandhi, *Seminars in Oncology*, 1995, **22**, 3-10.
13. N. H and H. S, *Gan To Kagaku Ryoho*, 1993, **20**, 34-41.
14. B. Rosenberg, L. VanCam, J. E. Trosko and V. H. Mansour, *Nature*, 1969, **222**, 385-386.
15. L. Kelland, *Nature Reviews Cancer*, 2007, **7**, 573-584.
16. E. W. Neuse, *Journal of Inorganic and Organometallic Polymers and Materials*, 2005, **15**, 3-31.
17. N. J. Long, *Metallocenes: An Introduction to Sandwich Complexes*, Wiley-Blackwell, 1st Edition edn., 1998.
18. M. F. R. Fouda, M. M. Abd-Elzaher, R. A. Abdelsamaia and A. A. Labib, *Applied Organometallic Chemistry*, 2007, **21**, 613-625.
19. G. Sava, G. Jaouen, E. A. Hillard and A. Bergamo, *Dalton Transactions*, 2012, **41**, 8226-8234.
20. G. Jaouen, S. Top, A. Vessières and R. Alberto, *Journal of Organometallic Chemistry*, 2000, **600**, 23-36.
21. E. A. Hillard and G. Jaouen, *Organometallics*, 2011, **30**, 20-27.
22. L. Weissfloch, M. Wagner, T. Probst, R. Senekowitsch-Schmidtke, K. Tempel and M. Molls, *BioMetals*, 2001, **14**, 43-49.
23. P. Kopf-Maier, H. Kopf and E. W. Neuse, *Journal of Cancer Research and Clinical Oncology*, 1984, **108**, 336-340.
24. L V Popova, V N Babin, Yu A Belousov, Yu S Nekrasov, A E Snegireva, N P Borodina, G M Shaposhnikova, O B Bychenko, P M Raevskii, N B Morozova, A I Iiyina and K. G. Shitkov, *Applied Organometallic Chemistry*, 1993, **7**, 85-94.
25. G. Jaouen and M. Salmain, *Bioorganometallic Chemistry: Applications in Drug Discovery, Biocatalysis, and Imaging*, Wiley-VCH, 2015.
26. S. Top, A. Vessières, C. Cabestaing, I. Laios, G. Leclercq, C. Provot and G. Jaouen, *Journal of Organometallic Chemistry*, 2001, **637-639**, 500–506.

27. S. Top, J. Tang, A. Vessières, D. Carrez, C. Provot and G. Jaouen, *Chemical Communications*, 1996, **8**, 955-956.
28. P. Pigeon, S. Top, A. Vessières, M. Huche, M. Gormen, M. E. Arbi, M.-A. Plamont, M. J. McGlinchey and G. Jaouen, *New Joural of Chemistry*, 2011, **35**, 2212-2218.
29. D. Hamels, P. M. Dansette, E. A. Hillard, S. Top, A. Vessières, P. Herson, G. Jaouen and D. Mans, *Angewandte Chemie International Edition*, 2009, **48**, 9124-9126.
30. J. d. J. Cázares-Marinero, S. Top and G. Jaouen, *Journal of Organometallic Chemistry*, 2014, **751**, 610-619.
31. G. Jaouen, A. Vessières and S. Top, *Chemical Society Reviews*, 2015, **44**, 8802-8817.
32. D. Plazuk, A. Vessières, E. A. Hillard, O. Buriez, E. Labbe, P. Pigeon, M. A. Plamont, C. Amatore, J. Zakrzewski and G. Jaouen, *Journal of Medicinal Chemistry Brief Article*, 2009, **52**, 4964-4967.
33. E. Hillard, A. Vessières, L. Thouin, G. Jaouen and C. Amatore, *Angewandte Chemie International Edition*, 2005, **45**, 285-290.
34. D. Trachootham, J. Alexandre and P. Huang, *Nature Reviews*, 2009, **8**, 579-591.
35. J. d. J. Cázares-Marinero, O. Buriez, E. Labbé, S. Top, C. Amatore and G. Jaouen, *Organometallics*, 2013, **32**, 5926-5934.
36. P. N. Kelly, A. Prêtre, S. Devoy, I. O'Rielly, R. Devery, A. Goel, J. F. Gallagher, A. J. Lough and P. T. M. Kenny, *Journal of Organometallic Chemistry*, 2007, **692**, 1327-1331.
37. W. E. Butler, P. N. Kelly, A. G. Harry, R. Tiedt, B. White, R. Devery and P. T. M. Kenny, *Applied Organometallic Chemistry*, 2013, **27**, 361-365.
38. A. Goel, D. Savage, S. R. Alley, P. N. Kelly, D. O'Sullivan, H. Mueller-Bunz and P. T. M. Kenny, *Journal of Organometallic Chemistry*, 2007, **692**, 1292-1299.
39. A. J. Corry, N. O'Donovan, Á. Mooney, D. O'Sullivan, D. K. Rai and P. T. M. Kenny, *Journal of Organometallic Chemistry*, 2009, **694**, 880-885.
40. A. J. Corry, Á. Mooney, D. O'Sullivan and P. T. M. Kenny, *Inorganica Chimica Acta*, 2009, **362**, 2957-2961.
41. Á. Mooney, A. J. Corry, D. O'Sullivan, D. K. Rai and P. T. M. Kenny, *Journal of Organometallic Chemistry*, 2009, **694**, 886-894.
42. Á. Mooney, A. J. Corry, C. Ni Ruairc, T. Mahgoub, D. O'Sullivan, N. O'Donovan, J. Crown, S. Varughese, S. M. Draper, D. K. Rai and P. T. M. Kenny, *Dalton Transactions*, 2010, **39**, 8228-8239.
43. Á. Mooney, R. Tiedt, T. Maghoub, N. O'Donovan, J. Crown, B. White and P. T. M. Kenny, *Journal of Medicinal Chemistry*, 2012, **55**, 5455-5466.
44. A. G. Harry, W. E. Butler, J. C. Manton, M. T. Pryce, N. O'Donovan, J. Crown, D. K. Rai and P. T. M. Kenny, *Journal of Organometallic Chemistry*, 2014, **757**, 28-35.
45. L. V. Popova, V. N. Babin, Y. A. Belousov, Y. S. Nekrasov, A. E. Snegireva, N. P. Borodina, G. M. Shaposhnikova, O. B. Bychenko, P. M. Raevskii, N. B. Morozova, A. I. Ilyina and K. G. Shitkov, *Applied Organometallic Chemistry*, 1993, **7**, 85-94.
46. O. B. Sutcliffe and M. R. Bryce, *Tetrahedron: Asymmetry*, 2003, **14**, 2297-2325.
47. P. Meunier, I. Ouattara, B. Gautheron, J. Tirouflet, D. Camboli and J. Besancon, *European Journal of Medicinal Chemistry*, 1991, **26**, 351-362.
48. A. Nudelman and A. Rephaeli, *Journal of Medicinal Chemistry*, 2000, **43**, 2962-2966.
49. B. H. Long, S. Z. Liang, D. C. Xin, Y. B. Yang and J. N. Xiang, *European Journal of Medicinal Chemistry*, 2009, **44**, 2572-2576.
50. C. Bincoletto, I. L. S. Tersariol, C. R. Oliveira, S. Dreher, D. M. Fausto, M. A. Soufen, F. D. Nascimento and A. C. F. Caires, *Bioorganic & Medicinal Chemistry*, 2005, **13**, 3047-3055.

51. M. Gormen, D. Plażuk, P. Pigeon, E. A. Hillard, M.-A. Plamont, S. Top, A. Vessières and G. Jaouen, *Tetrahedron Letters*, 2010, **51**, 118-120.
52. M. Görmen, P. Pigeon, S. Top, A. Vessières, M.-A. Plamont, E. A. Hillard and G. Jaouen, *Medicinal Chemistry Communications*, 2010, **1**, 149-151.

Chapter 2

Synthesis and structural characterisation of *N*-(1'-methyl-6-ferrocenyl-2-naphthoyl) and *N*-(1'-ethyl-6-ferrocenyl-2-naphthoyl) amino acid and dipeptide esters

2.1. Introduction

Organometallic complexes have been successfully incorporated in a wide variety of materials that with diverse applications. Platinum coordination compounds, such as cisplatin, carboplatin and oxaliplatin are widely used in the cancer treatment. However, they exhibit many disadvantages such as poor selectivity, cross-resistance, acquired resistance and severe side effects. [1] Therefore, new metal-based therapeutic agents for cancer chemotherapy are constantly required.

Recently, ferrocene is a particularly attractive candidate for incorporation into biomolecules and biologically active compounds for biological applications due to its aromatic nature, redox properties, stability and low toxicity.[2] Ferrocene derivatives has been shown to have antiparasitic [3], antibacterial [3, 4], antifungal [5] and indeed anti-cancer [6] activity. Ferrocene itself is not cytotoxic, however its derivatives, for example ferricenium salts, are known to inhibit tumor growth. The ability to form reactive oxygen species under physiological conditions that lead to the oxidative damage of DNA and other biomolecules is thought to be important to their mode of action. *Jaouen et al.* have prepared the earliest organometallic SERMs (selective estrogen receptor modulators), named ferrocifens. They have antiproliferative on both hormone-dependent (MCF-7) and hormone-independent (MDA-MB-231) breast cancer cell lines. [7]

Kenny's research group have shown the conjugation of amino acids and peptides with ferrocene complexes offers a desirable and alternative method to target cancer cells. [6] Mooney and Tiedt *et al.* have presented *N*-(ferrocenyl)naphthoyl amino acid and dipeptide derivatives that have excellent anti-proliferative activity in the lung cancer cell lines H1299 and A549 and the melanoma cell lines Sk-Mel-28, HT-144, MalMe-3M and Lox-IMVI.[8] Compounds **30**, **40-43** all showed activity greater than that of cisplatin against H1299 cell line (Table 2.1).

Table 2.1: IC_{50} values for the most active compounds in the *N*-(6-ferrocenyl-2-naphthoyl) series against H1299 cell line.

Compound	No.	IC_{50} (μM)
Cisplatin	**14**	1.50 ± 0.10
N-(6-ferrocenyl-2-naphthoyl)-γ-aminobutyric acid ethyl ester	**40**	0.62 ± 0.07
N-(6-ferrocenyl-2-naphthoyl)-glycine-glycine methyl ester	**41**	0.30 ± 0.04
N-(6-ferrocenyl-2-naphthoyl)-glycine-glycine ethyl ester	**30**	0.13 ± 0.02
N-(6-ferrocenyl-2-naphthoyl)-glycine-L-alanine ethyl ester	**42**	1.30 ± 0.10
N-(6-ferrocenyl-2-naphthoyl)-glycine-D-alanine ethyl ester	**43**	0.33 ± 0.02

The aim of this research is synthesis, characterization and biological evaluation the disubstituent derivatives of *N*-(ferrocenyl) naphthoyl amino acid and dipeptide (Figure 2.1) for further structure-activity relationship study. Four key moieties have been identified for the modification:

(i) A redox active centre

(ii) A conjugate linker (lowers the oxidation potential of the ferrocene moiety)

(iii) An alkyl group (further lowers the oxidation potential of the ferrocene moiety)

(iv) An amino acid or dipeptide ester chain (can interact with other biomolecules *via* hydrogen bonds).

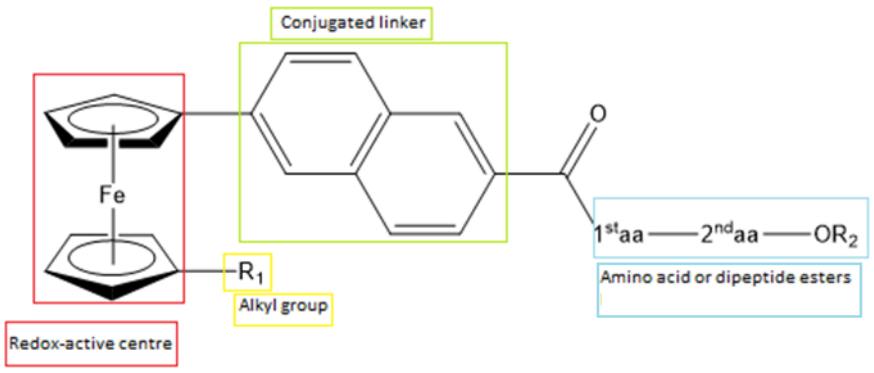

R_1 = -CH_3, -CH_2CH_3

R_2 = -CH_3, -CH_2CH_3

Figure 2.1: General structures of the *N*-(1'-methyl-6-ferrocenyl-2-naphthoyl) and *N*-(1'-ethyl-6-ferrocenyl-2-naphthoyl) amino acid and dipeptide esters **62-77**.

The first region for modification is the ferrocene core of the molecule. The electroactive core has been shown to be required for activity. Mooney *et al.* prepared a *N*-(2-naphthoyl)-glycine-glycine ethyl ester **44** analogue of the *N*-(6-ferrocenyl-2-naphthoyl)-glycine-glycine ethyl ester **30**. When tested at 1 μM against either H1299 lung cancer or Sk-Mel-28 melanoma cell lines, the non-organometallic analogue did not show any inhibitory effect compared with other dipeptide esters. The percentage cell growth was 87.6 ± 18.4 and 95.6 ± 10.9 for H1299 cells and Sk-Mel-28 cells respectively.

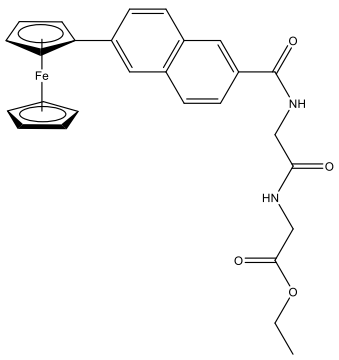

30

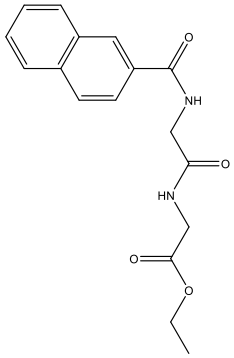

44

Harry *et al.* synthesized disubstituted derivatives of *N*-(ferrocenyl)benzoyl amino acid and dipeptide esters, by having a methyl, ethyl and propyl group on the previously unsubstituted cyclopentadiene ring. The alkyl group is thought to be important in further decreasing the redox potential of these compounds. Those novel compounds have shown a greater cytotoxicity than the monosubstituted ones. The most active analogues are 1-methyl-1'-*N*-{*para*-(ferrocenyl)-benzoyl}-glycine-glycine ethyl ester **31**, 1-ethyl-1'-*N*-{*para*-(ferrocenyl)-benzoyl}-glycine-glycine ethyl ester **32** and 1-propyl-1'-*N*-{*para*-(ferrocenyl)-benzoyl}-glycine-glycine ethyl ester **33** with IC_{50} values as 2.8 ± 1.23, 3.5 ± 0.82 and 5.4 ± 1.21 μM in H1299 cell line, respectively. Since the cytotoxicity of the derivatives decreased with the increased size of the alkyl chain, the methyl group and ethyl group were maintained for this study.

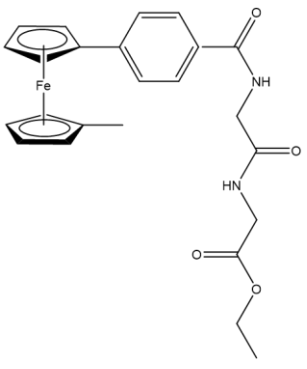

31

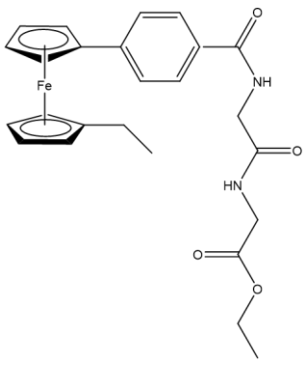

32

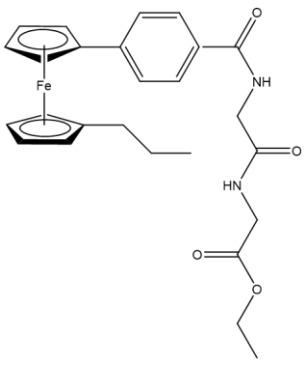

33

The second region for consideration is the conjugated linker. Corry *et al*. prepared *N-ortho*, *meta* and *para* ferrocenyl benzoyl amino acid and dipeptide derivatives, *N*-{*ortho*-(ferrocenyl)benzoyl} glycine-L-alanine ethyl ester **29** found to be the most active one with IC_{50} of 4.0 μM in H1299 cells1. [9] Mooney *et al*. replaced benzoyl linker with a naphthoyl. The naphthoyl spacer is thought to be important in decreasing the redox potential of these compounds. Based on commercial availability, both *N*-(3-ferrocenyl-2-naphthoyl) and *N*-(6-ferrocenyl-2-naphthoyl) derivatives were synthesized. It was found that the *N*-(6-ferrocenyl-2-naphthoyl) derivatives were significantly more active: *N*-(6-ferrocenyl-2-naphthoyl)-glycine-L-alanine ethyl ester **42** having an IC_{50} of 1.3 μM which is three times more active than the *N*-{*ortho*-(ferrocenyl) benzoyl}-glycine-L-alanine ethyl ester **45** (IC_{50} = 5.3 μM). Since the introduction of a naphthoyl linker between the redox active ferrocene unit and the peptide chain has been shown to dramatically enhance the anti-proliferative effect of the ferrocenyl-peptide bioconjugates, this unit was retained for further studies.

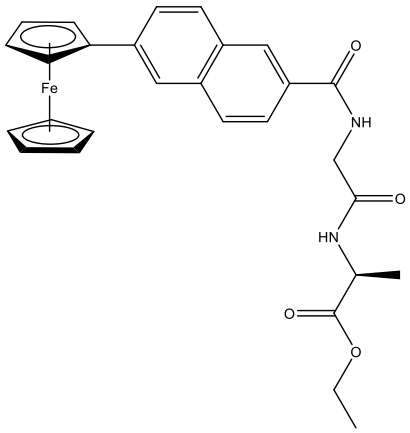

42

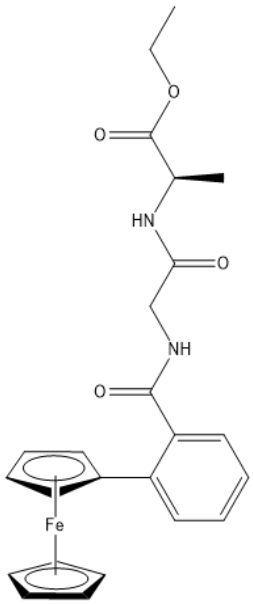

45

The peptide region of the compounds has been extensively studied [10]. An amino acid or dipeptide chain have shown to be essential for the cytotoxic activity of the molecule. Methyl-6-ferrocenylnaphthalene-2-carboxylate **46** was tested against H1299 and Sk-Mel-28 cell lines and displayed no activity. [8] Corry *et al*. have synthesized *N*-(ferrocenyl)benzoyl tripeptide and tetrapeptide derivatives, however increase chain leads to a decrease bioactivity. [10] As shown in table 2.1, the most active derivatives of the *N*-(6-ferrocenyl-2-naphthoyl) amino acid and dipeptide esters are with single α-amino acid or dipeptide. Therefore, the amino acid and dipeptide groups employed in this investigation were maintained as follows: glycine glycine (Gly-Gly), glycine-L-alanine (Gly-L-Ala), glycine-D-alanine (Gly-D-Ala) and γ-aminobutyric acid (GABA).

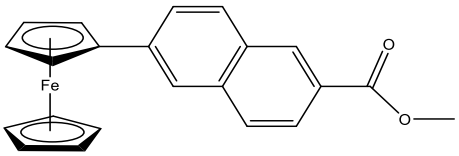

46

The final moiety of the compounds which can be modified is the ester protecting group. In this study, a series of methyl and ethyl esters were prepared to investigate if ester chain length exerts an influence on the cytotoxicity of the molecule.

2.2. The synthesis of *N*-(1'-methyl-6-ferrocenyl-2-naphthoyl) and *N*-(1'-ethyl-6-ferrocenyl 2-naphthoyl) amino acid and dipeptide ester derivatives

The *N*-(1'-methyl-6-ferrocenyl-2-naphthoyl) and *N*-(1'-ethyl-6-ferrocenyl-2-naphthoyl) amino acid and dipeptide esters were prepared *via* standard peptide coupling methods using the conventional *N*-(3-dimethylaminopropyl)-*N*'-ethylcarbodiimide hydrochloride (EDC) and *N*-hydroxysuccinimide (NHS) coupling protocol. A solution of 1'-methyl-6-ferrocenyl-2-naphthoic acid or 1'-ethyl-6-ferrocenyl-2-naphthoic acid in dichloromethane at 0 °C, was treated with EDC, NHS and triethylamine (Et_3N) and allowed to stir for 45 minutes. An equimolar amount of the corresponding amino acid or dipeptide ester hydrochloride was added to the solution with stirring. The procedure is similar to that used for the synthesis of 1-alkyl-1'-*N*-(ferrocenyl) benzoyl dipeptide esters.[11] Scheme 2.1 outlines the synthetic route employed in the synthesis of *N*-(1'-methyl-6-ferrocenyl-2-naphthoyl) and *N*-(1'-ethyl-6-ferrocenyl-2-naphthoyl) amino acid and dipeptide esters.

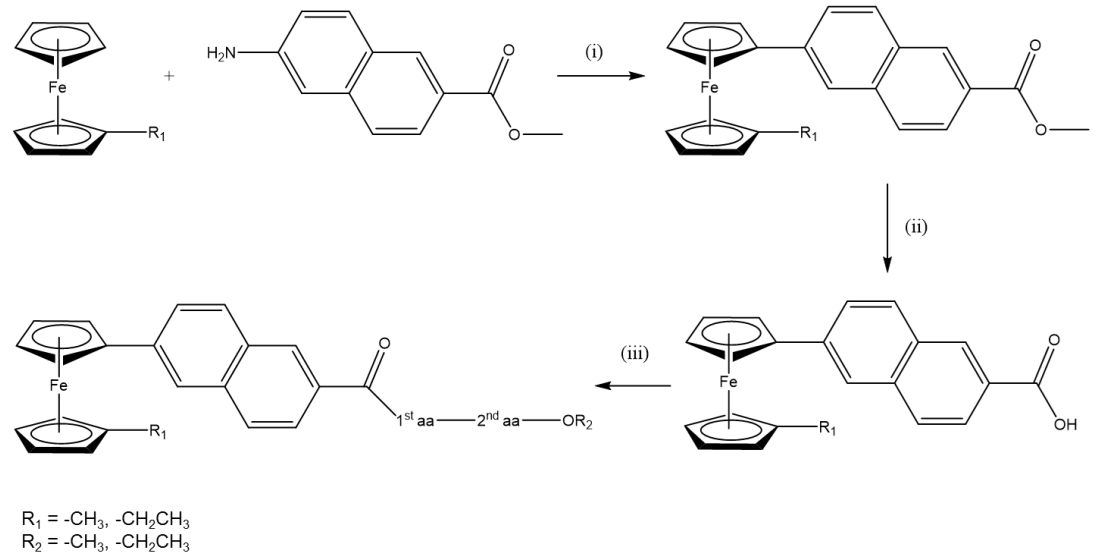

R_1 = -CH_3, -CH_2CH_3
R_2 = -CH_3, -CH_2CH_3

(i) $NaNO_2$, HCl, 5 °C; (ii) NaOH, MeOH; (iii) EDC, NHS, Et_3N, amino acid or dipeptide methyl/ethyl esters.

Scheme 2.1: The general reaction scheme for the synthesis of *N*-(1'-methyl-6-ferrocenyl-2-naphthoyl) and *N*-(1'-ethyl-6-ferrocenyl-2-naphthoyl) amino acid and dipeptide derivatives.

2.2.1. Synthesis of the methyl and ethyl ferrocene

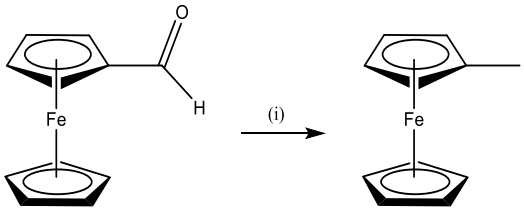

55

(i) $LiAlH_4$, $AlCl_3$.

Scheme 2.2: Synthesis of methyl ferrocene **55** through reductive deoxygenation of ferrocenecarboxaldehyde.

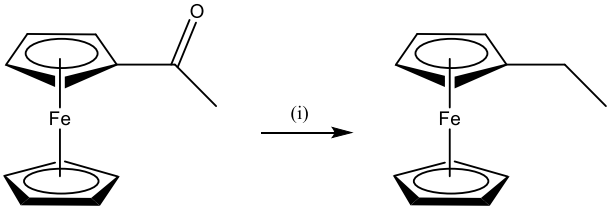

56

(i) $LiAlH_4$, $AlCl_3$.

Scheme 2.3: Synthesis of ethyl ferrocene **56** through reductive deoxygenation of acetyl ferrocene.

The reductive deoxygenation of acylferrocenes to the corresponding hydrocarbons *via* the combined action of lithium aluminium hydride and the use of the strong Lewis acid aluminium trichloride in diethyl ether, is shown in Scheme 2.2 and Scheme 2.3 yielded the desired alkylated ferrocene derivatives with percentage yields varying between 86-90 %.

2.2.2. Preparation of 1’-methyl and 1’-ethyl-6-ferrocenyl-methyl-2-naphthoates

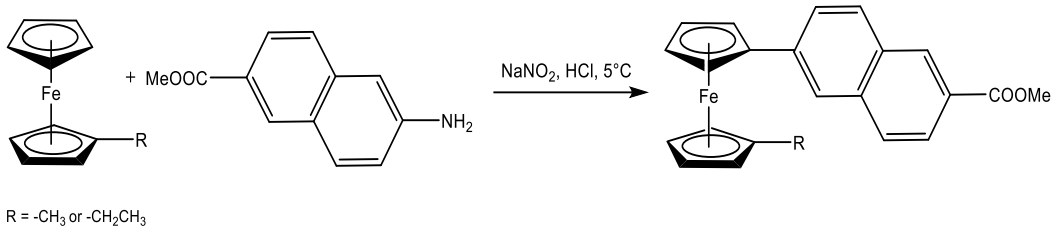

Scheme 2.4: Synthesis of 1’-methyl-6-ferrocenyl-methyl-2-naphthoate and 1’-ethyl-6-ferrocenyl-methyl-2-naphthoate *via* diazonium coupling reaction.

Methyl 6-aminonaphthalene-2-carboxylate hydrochloride or ethyl 6-aminonaphthalene-2-carboxylate hydrochloride was treated with sodium nitrite in the presence of hydrochloric acid at a temperature below 5 °C to yield the diazonium salt (Scheme 2.4).

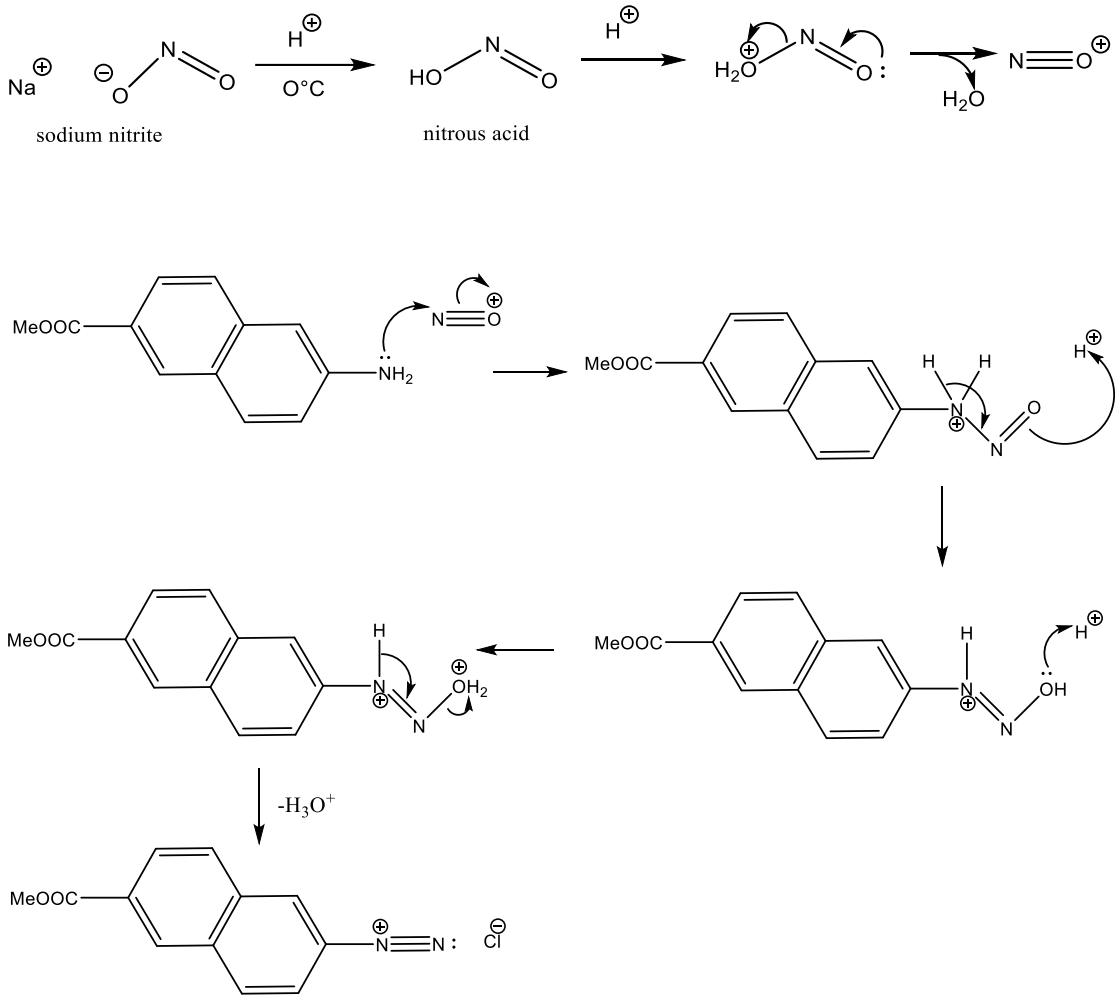

Scheme 2.5: Diazonium salt formation.

The mechanism for the diazonium coupling using 6-amino-2-naphthonic acid is shown in Scheme 2.6. 6-Amino-2-naphthonic acid was treated with sodium nitrite and converted into the diazonium cation. Electrophile chlorine activates the reaction and alkylferrocene present *in situ* reacts with the aryl carbocation *via* electrophilic aromatic substitution to give the product as an orange solid or a red oil.

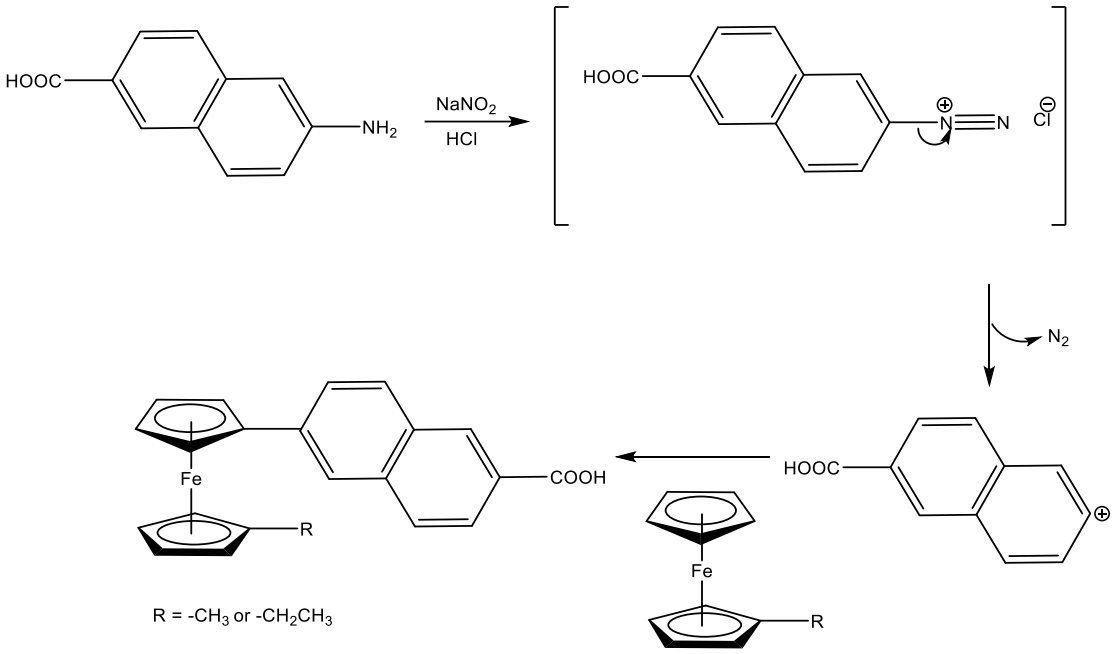

Scheme 2.6: The mechanism of diazonium coupling reaction.

At room temperature, by-product 6-hydroxy-2-naphthoic acid formed by reacting aryl carbocation with water (Scheme 2.7). Therefore, the reaction should be kept at around 0°C to stabilize the diazonium salts.

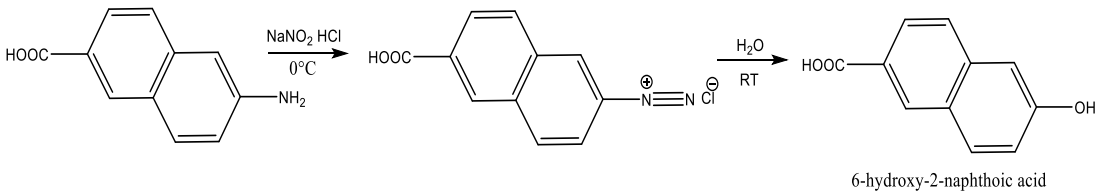

Scheme 2.7: Stability of diazonium salts.

2.2.3. Base hydrolysis

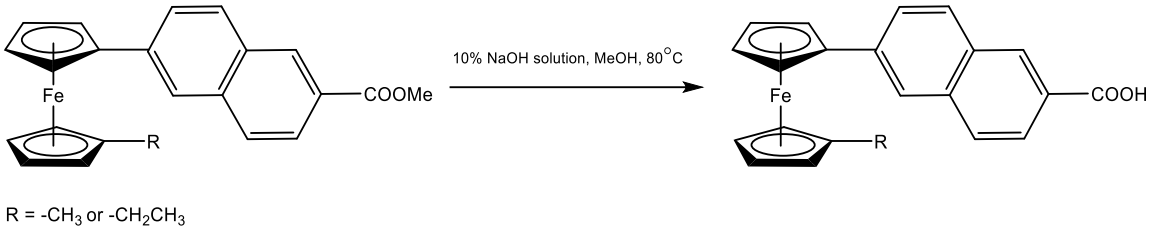

R = -CH_3 or -CH_2CH_3

Scheme 2.8: Synthesis of 1'-methyl-6-ferrocenyl-2-naphthoic acid **60** and 1'-ethyl-6-ferrocenyl-2-naphthoic acid **61**.

Base hydrolysis of ferrocenyl carboxylate ester in 10% sodium hydroxide solution effectively removes the ester group to produce ferrocenyl carboxylate. In the ^{1}H NMR spectra a broad singlet between δ 12.7 to δ 13 indicates the presence of the carboxylic acid proton. Hydrolysis can also be monitored by the disappearance of the methyl ester peak from the ^{1}H and ^{13}C NMR spectra.

2.2.4. The synthesis of *N*-(1'-methyl-6-ferrocenyl-2-naphthoyl) and *N*-(1'-ethyl-6 ferrocenyl-2-naphthoyl) amino acid and dipeptide esters

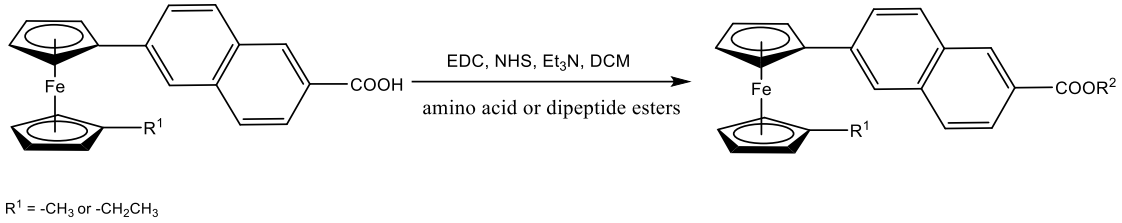

R^1 = -CH_3 or -CH_2CH_3

Scheme 2.9: Synthesis of *N*-(1'-methyl-6-ferrocenyl-2-naphthoyl) and *N*-(1'-ethyl-6-ferrocenyl-2-naphthoyl) amino acid and dipeptide esters **62-77**.

Table 2.2: Compounds **62-77** synthesized in this study.

R^1	R^2	Compound No.
-CH_3	Gly-Gly-OMe	**62**
	Gly-Gly-OEt	**63**
	Gly-L-Ala-OMe	**64**
	Gly-L-Ala-OEt	**65**
	Gly-D-Ala-OMe	**66**
	Gly-D-Ala-OEt	**67**
	GABA-OMe	**68**
	GABA-OEt	**69**
-CH_2CH_3	Gly-Gly-OMe	**70**
	Gly-Gly-OEt	**71**
	Gly-L-Ala-OMe	**72**
	Gly-L-Ala-OEt	**73**
	Gly-D-Ala-OMe	**74**
	Gly-D-Ala-OEt	**75**
	GABA-OMe	**76**
	GABA-OEt	**77**

EDC/NHS coupling reactions allow introduction of the methyl-ferrocenyl naphthoyl and ethyl-ferrocenyl naphthoyl group onto an amino acid or dipeptide esters under solution phase peptide

coupling conditions. A solution of 1'-methyl-6-ferrocenyl-2-naphthoic acid or 1'-ethyl-6-ferrocenyl-2-naphthoic acid in dichloromethane at 0 ^{o}C, was treated with *N*-(3-dimethylaminopropyl)-*N*'-ethylcarbodiimide hydrochloride (EDC), *N*-hydroxysuccinimide (NHS) and triethylamine (Et_3N) and allowed to stir for 45 min. An equimolar amount of the required amino acid or the dipeptide ester hydrochloride was added to this solution with stirring at room temperature for 48 hours. The crude product was purified by column chromatography {eluent 1:1 hexane: ethyl acetate} yielding the title compound as an orange solid or an orange oil.

As showed in Scheme 2.9, the EDC/NHS mediated coupling of the 1'-methyl-6-ferrocenyl-2-naphthoic acid and 1'-ethyl-6-ferrocenyl-2-naphthoic acid with the dipeptide methyl or ethyl ester hydrochloride salts of Gly-Gly, Gly-L-Ala, Gly-D-Ala and GABA, progresses through a formation of an unstable intermediate, an *O*-acylisourea ester. This compound is formed by the reaction of the EDC with the 1'-methyl-6-ferrocenyl-2-naphthoic acid or 1'-ethyl-6-ferrocenyl-2-naphthoic acid. Attack of the nearby nucleophile on the activated carbon can result in an O to N shift intramolecular acyl transfer giving an *N*-acylurea as a by-product, which can limit product yield and interfere with product purification (Scheme 2.10).

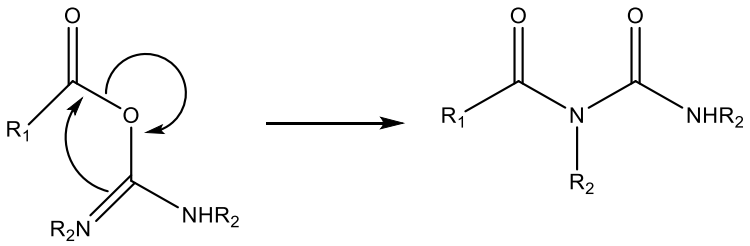

Scheme 2.10: Intramolecular acyl transfer from *O*-acylisourea to *N*-acylurea.

The addition of NHS that act as a secondary nucleophile can stabilizes the *O*-acylisourea intermediate by converting it to an amine-reactive NHS ester, which is a much more stable compound and remains reactive with the amine moiety of the amino acid or dipeptide ester hydrochloride salts. Upon addition of the amino acid or dipeptide ester hydrochloride salts of Gly Gly, Gly L-Ala, Gly D-Ala and GABA, the NHS is displaced resulting in the formation of *N*-(1'-methyl-6-ferrocenyl-2-naphthoyl) and *N*-(1'-ethyl-6-ferrocenyl-2-naphthoyl) amino acid and dipeptide esters **62-77**.

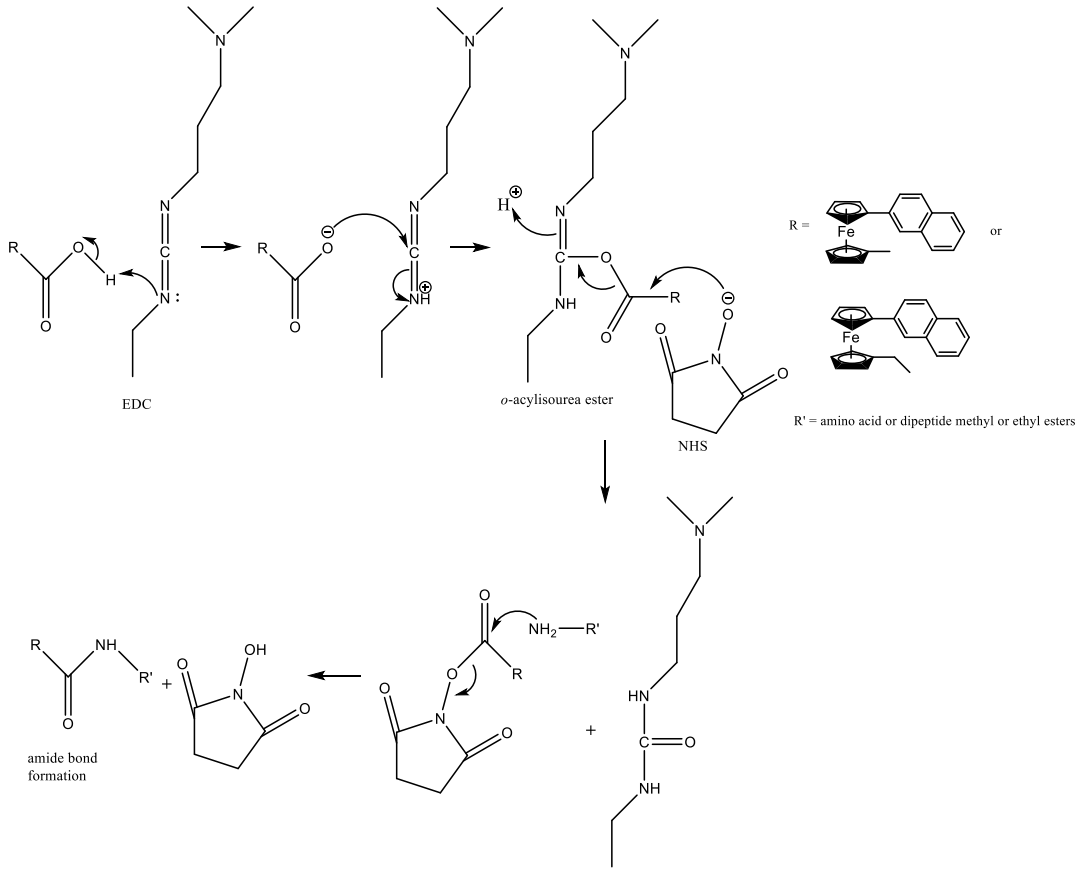

Scheme 2.11: Amide bond formation *via* EDC and NHS coupling.

2.3. Purification and yields of *N*-(1'-methyl-6-ferrocenyl-2-naphthoyl) and *N*-(1'-ethyl-6-ferrocenyl-2-naphthoyl) amino acid and dipeptide ester derivatives

The *N*-(1'-methyl-6-ferrocenyl-2-naphthoyl) and *N*-(1'-ethyl-6-ferrocenyl-2-naphthoyl) amino acid and dipeptide esters were synthesized by the condensation of 1'-methyl-6-ferrocenyl-2-naphthoic acid and 1'-ethyl-6-ferrocenyl-2-naphthoic acid with the amino acid or dipeptide esters of glycine-glycine, glycine-L-alanine, glycine-D-alanine and γ-aminobutyric acid, under the standard EDC/NHS coupling conditions outlined in Section 2.2. Crude *N*-(1'-methyl-6-ferrocenyl-2-naphthoyl) and *N*-(1'-ethyl-6-ferrocenyl-2-naphthoyl) amino acid and dipeptide esters were purified by column chromatography, using a mixture of hexane and ethyl acetate as the eluent. The purified compounds were furnished as orange solids or an orange oil, with yields in the range of 13 % to 60 %, shown in Table 2.3. All compounds gave spectroscopic and analytical data in accordance with their proposed structures.

General trend showed the larger the amino acid and dipeptide esters the lower the yield. And yield decreases with increasing the size of the alkyl chain in general. The side chains of the reacting amino acids or dipeptide and the alkyl chain incorporated can have an influence on the overall yield. γ-aminobutyric acid ester derivatives gave highest yields due to its simple amino acid structure. Yields are lowest in Gly-L-Ala and Gly-D-Ala ester analogues where the side chain of these dipeptides are larger than Gly-Gly esters to exert greater steric hindrance.

Table 2.3: Percentage yields for *N*-(1'-methyl-6-ferrocenyl-2-naphthoyl) and *N*-(1'-ethyl-6-ferrocenyl-2-naphthoyl) amino acid and dipeptide esters.

Compound Name	Compound No.	% Yields
N-(1'-methyl-6-ferrocenyl-2-naphthoyl)-Gly-Gly-OMe	**62**	18
N-(1'-methyl-6-ferrocenyl-2-naphthoyl)-Gly-Gly-OEt	**63**	37
N-(1'-methyl-6-ferrocenyl-2-naphthoyl)-Gly-L-Ala-OMe	**64**	17
N-(1'-methyl-6-ferrocenyl-2-naphthoyl)-Gly-L-Ala-OEt	**65**	23
N-(1'-methyl-6-ferrocenyl-2-naphthoyl)-Gly-D-Ala-OMe	**66**	20
N-(1'-methyl-6-ferrocenyl-2-naphthoyl)-Gly-D-Ala-OEt	**67**	15
N-(1'-methyl-6-ferrocenyl-2-naphthoyl)-GABA-OMe	**68**	57
N-(1'-methyl-6-ferrocenyl-2-naphthoyl)-GABA-OEt	**69**	32
N-(1'-ethyl-6-ferrocenyl-2-naphthoyl)-Gly-Gly-OMe	**70**	13
N-(1'-ethyl-6-ferrocenyl-2-naphthoyl)-Gly-Gly-OEt	**71**	16
N-(1'-ethyl-6-ferrocenyl-2-naphthoyl)-Gly-L-Ala-OMe	**72**	18
N-(1'-ethyl-6-ferrocenyl-2-naphthoyl)-Gly-L-Ala-OEt	**73**	23
N-(1'-ethyl-6-ferrocenyl-2-naphthoyl)-Gly-D-Ala-OMe	**74**	17
N-(1'-ethyl-6-ferrocenyl-2-naphthoyl)-Gly-D-Ala-OEt	**75**	15
N-(1'-ethyl-6-ferrocenyl-2-naphthoyl)-GABA-OMe	**76**	36
N-(1'-ethyl-6-ferrocenyl-2-naphthoyl)-GABA-OEt	**77**	60

2.4. Infra-red studies of *N*-(1'-methyl-6-ferrocenyl-2-naphthoyl) and *N*-(1'-ethyl-6-ferrocenyl-2-naphthoyl) amino acid and dipeptide derivatives

Almost any compounds which has covalent bonds absorbs various frequencies of electromagnetic radiation in the infrared region of the electromagnetic spectrum. This wavelength region lies approximately 400 to 800 nm. Compounds can excite to a higher energy state when they absorb infrared radiation, and hence various molecular vibrations are induced, e.g. stretching, bending, rocking etc. However, only the molecules with bonds have a dipole moment that changes as a function of time are capable to absorb this radiation. Symmetric bonds do not absorb infrared radiation. Since different types of bond have a different natural frequency of vibrations, these localized vibrations can be used for the identification of key functional groups. [12]

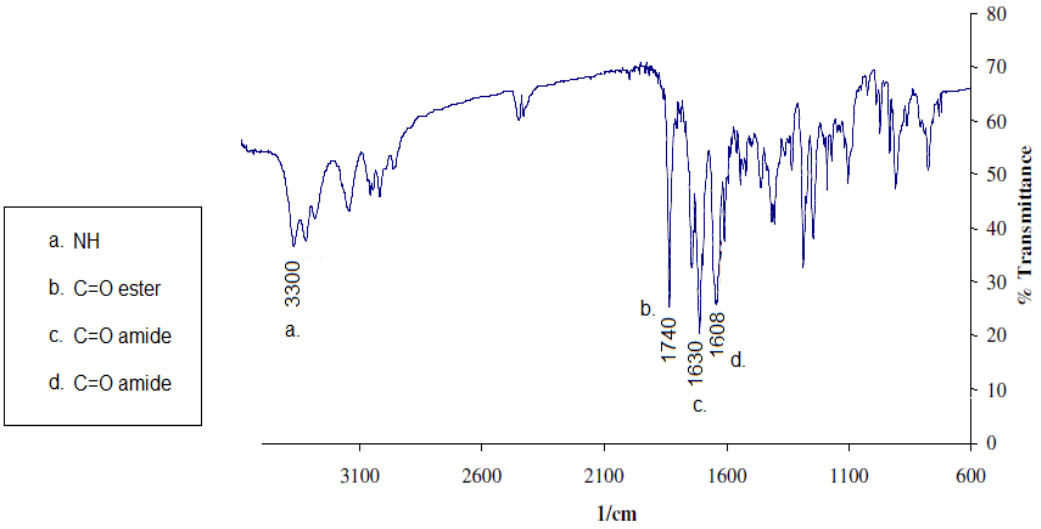

Figure 2.2: IR spectrum of *N*-(1'-methyl-6-ferrocenyl-2-naphthoyl)-glycine-glycine ethyl ester **63**.

Table 2.4: IR data for *N*-(1'-methyl-6-ferrocenyl-2-naphthoyl) and *N*-(1'-ethyl-6-ferrocenyl-2-naphthoyl) amino acid and dipeptide esters. Values are given in cm^{-1}.

Compound No.	N-H	$C=O_{ester}$	$C=O_{amide\ I}(cm^{-1})$	$C=O_{amide\ II}$
62	3307, 3064	1748	1629, 1603	1600
63	3300	1740	1630	1608
64	3290, 3090	1747	1640, 1620	1521
65	3289, 3079	1733	1640, 1623	1521
66	3285, 3078	1739	1642, 1625	1521
67	3286, 3093	1735	1626, 1608	1517
68	3280	1721	1600	*
69	3283	1726	1605	*
70	3303, 3081	1744	1643, 1625	1521
71	3371, 3350	1723	1644, 1626	1532
72	3387, 3090	1737	1642, 1627	1529
73	3315, 3061	1750	1642, 1628	1534
74	3379, 3090	1734	1642, 1627	1531
75	3305, 3061	1734	1641, 1627	1532
76	3274	1730	1622	*
77	3318	1729	1636	*

* GABA derivatives have only one $C=O_{amide}$ present

The IR spectra of the *N*-(1'-methyl-6-ferrocenyl-2-naphthoyl) and *N*-(1'-ethyl-6-ferrocenyl-2-naphthoyl) amino acid and dipeptide esters were obtained as pure solids (Table 2.4). The spectra of these compounds generally showed two bands above 3000 cm^{-1} that correspond to the presence of the secondary amide groups. In the carbonyl region it is usual to observe at least two bands for primary and secondary amides. Amide I band that near 1650 cm^{-1} arises mainly from the C=O stretching vibration with minor contribution form the out-of-phase C-N stretching vibration, the C-C-N deformation or the NH in-phase bend. The one at lower frequency is the out-of-phase combination of the NH in phase bend and CN stretching vibration; which is called the amide II band that typically lying between 1600 and 1500 cm^{-1}. In the carbonyl region, the carbonyl attached to the ester moiety ($C=O_{ester}$) usually appears between 1720-1750 cm^{-1} whilst carbonyl attached to the NH ($C=O_{amide}$) appears between 1600-1640 cm^{-1}.

2.5. UV-Vis studies of *N*-(1'-methyl-6-ferrocenyl-2-naphthoyl) and *N*-(1'-ethyl-6-ferrocenyl-2-naphthoyl) amino acid and dipeptide derivatives

Most organic molecules and functional groups absorb wavelengths in the range from 190 to 800 nm. The transitions result in the absorption of electromagnetic radiation in this region corresponding to transitions between electronic energy levels. An electron is promoted from an occupied orbital to an unoccupied orbital of greater potential since the molecule absorbs quantized energy. Generally, the most probable translation is form the highest occupied molecular orbital (HOMO) to the lowest unoccupied molecular orbital (LUMO). For most molecules, the lowest-energy occupied molecular orbitals are the σ orbitals, π orbitals lie at higher energy levels and orbitals hold unshared pairs n lie at even higher energies. The antibonding orbitals π* and σ* are the orbitals with highest energy.

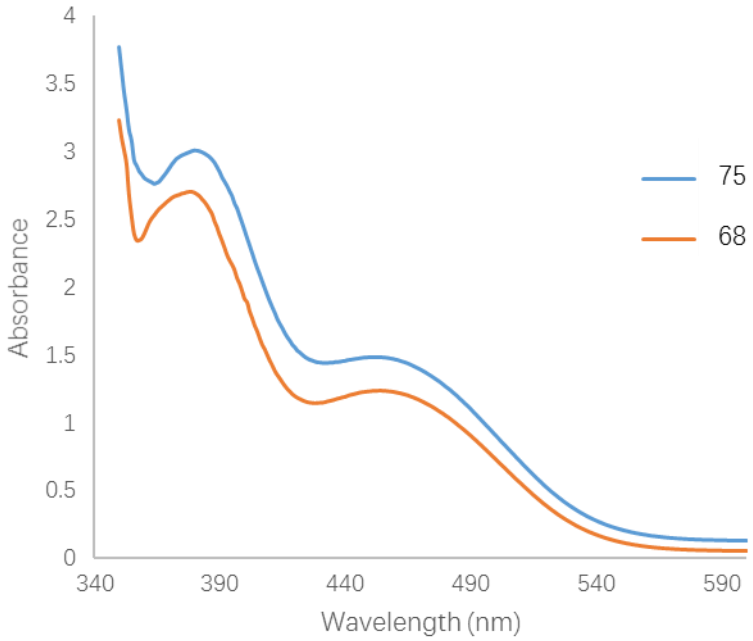

Figure 2.3: UV-Vis data for selected *N*-(1'-methyl-6-ferrocenyl-2-naphthoyl)-γ-aminobutyric acid methyl ester **68** and *N*-(1'-ethyl-6-ferrocenyl-2-naphthoyl)-glycine-D-alanine ethyl ester **75**.

Table 2.5: UV-Vis data for selected *N*-(1'-methyl-6-ferrocenyl-2-naphthoyl) and *N*-(1'-ethyl-6-ferrocenyl-2-naphthoyl) amino acid and dipeptide esters.

Compound No.	$\lambda_{max1\ (nm)}$	ε_1	$\lambda_{max2\ (nm)}$	ε_2
62	379	3132	454	1216
63	371	3216	435	1308
64	369	3081	450	1334
65	367	3482	450	1497
66	376	3211	452	1312
67	373	3453	453	1483
68	367	3283	452	1406
69	378	3048	455	1388
70	372	3040	449	1257
71	367	3264	45	1326
72	368	3086	454	1357
73	367	3491	454	1499
74	373	3217	452	1316
75	372	3465	452	1497
76	376	3306	450	1422
77	380	3542	452	1483

From the UV-Vis data of compound **62-77** in Table 2.5, the strongest absorptions in the UV spectrum are with local maxima at 375 nm and 450 nm, respectively. The absorptions are similar with those of the *N*-(6-ferrocenyl-2-naphthoyl) derivatives. [13] Low energy bands observed approximately at 450 nm with a distinct $\lambda_{max\ 2}$ values can be assigned as metal to ligand charge transfer (MLCT) band transition arising from the ferrocene moiety. The high energy band around 375 nm, with distinct $\lambda_{max\ 1}$ values are due to the π - π^* transitions of the aromatic spacer group. It is well known from literature that the addition of a conjugate system to ferrocene causes the λ_{max} value of ferrocene (400 nm) to shift toward the red region because of extended conjugation. In this UV-Vis study, the spectra of all compounds were obtained at a concentration of 1 x 10^{-4} M in acetonitrile. The molar extinction coefficient ε is calculated from the Beer-Lambert Law $A=\varepsilon cl$, where A is the absorbance, c is the concentration and l is the path length of the sample cell.

2.6. ^{1}H NMR and HPLC studies of *N*-(1'-methyl-6-ferrocenyl-2-naphthoyl) and *N*-(1'-ethyl-6-ferrocenyl-2-naphthoyl) amino acid and dipeptide derivatives

Nuclear magnetic resonance spectra (NMR) were obtained using a Bruker Avance 400 or 600 NMR spectrometer for ^{1}H NMR. Chemical shifts are reported as ppm and all coupling constants (*J*) are in Hertz. All the ^{1}H NMR experiments were performed in $CDCl_3$.

Table 2.6: ^{1}H NMR spectral data for *N*-(1'-methyl-6-ferrocenyl-2-naphthoyl) and *N*-(1'-ethyl-6-ferrocenyl-2-naphthoyl) amino acid and dipeptide esters.

Compound No.	NH's	αH	*ortho* on η^5-$C_5\underline{H}_4$-naphthoyl	*meta* on η^5-$C_5\underline{H}_4$-naphthoyl	*meta* on η^5-$C_5\underline{H}_4$-alkyl	*ortho* on η^5-$C_5\underline{H}_4$-alkyl
62	7.13, 6.73	-	4.59	4.26	3.91	3.87
63	7.53, 7.18	-	4.64	4.29	3.91-3.87	3.91-3.87
64	7.21, 6.84	4.54	4.62	4.29	4.00	3.87
65	7.22, 6.83	4.54	4.63	4.29	4.00	3.85
66	7.35, 7.09	4.59	4.67	4.32	3.94	3.90
67	6.98, 6.51	4.58	4.74	4.39	4.07	3.97
68	6.65	-	4.66	4.29	4.00	3.87
69	6.68	-	4.65	4.29	4.00	3.86
70	7.14, 6.79	-	4.67	4.31	3.94-3.71	3.94-3.71
71	6.99, 6.51	-	4.68	4.33	3.95-3.91	3.95-3.91
72	7.25, 6.91	4.44	4.56	4.29	3.92-3.86	3.92-3.86
73	7.29, 6.96	4.53	4.71	4.35	4.05	3.93
74	7.00, 6.56	4.58	4.68	4.26	3.93-3.88	3.93-3.88
75	7.33, 6.99	4.56	4.66	4.29	4.11-3.93	4.11-3.93
76	6.62	-	4.62	4.27	4.00-3.85	4.00-3.85
77	6.67	-	4.76	4.38	4.02-3.96	4.02-3.96

The typical chemical shifts observed for the *N*-(1'-methyl-6-ferrocenyl-2-naphthoyl) and *N*-(1'-ethyl-6-ferrocenyl-2-naphthoyl) amino acid and dipeptide esters in $CDCl_3$ include the appearance of amide protons (Table 2.6). These signals can be found between δ 7.53 and δ 6.51. The naphthoyl spacer region confirms the presence of six protons, which appear as multiplets from δ 8.27-7.55. This complexity is due to six protons being magnetically inequivalent, following the second order splitting pattern.

For the disubstituted ferrocene moiety, four splitting patterns are observed. For the cyclopentadiene ring attached to the naphthoyl spacer (η^5-$C_5\underline{H}_4$-naphthoyl), the *ortho* protons appear as an apparent triplet in the region of δ 4.76 to δ 4.56 with coupling constant *J* equal to 2 Hz; and the *meta* protons appear as a triplet signal in the region between δ 4.38 and δ 4.26 with the same coupling constants *J* equal to 2 Hz. Refer to the protons on the alkylated cyclopentadiene ring (η^5-$C_5\underline{H}_4$-alkyl), the *meta* and *ortho* protons of *N*-(1'-methyl-6-ferrocenyl-2-naphthoyl) amino acid and dipeptide esters both appear as a triplet in the region of δ 4.07 to δ 3.91 and δ 3.97 to δ 3.85, respectively, with coupling constants *J* equal to 2 Hz. For the protons on the alkylated cyclopentadiene ring (η^5-$C_5\underline{H}_4$-alkyl) of *N*-(1'-ethyl-6-ferrocenyl-2-naphthoyl) amino acid and dipeptide derivatives, *ortho* and *meta* protons generated a multiplet between δ 4.11 to δ 3.92.

The methylene protons (-O$C\underline{H}_2CH_3$) of the ethyl ester derivatives appear between δ 4.10 and δ 4.21 as a quartet while the methyl protons (-$OCH_2C\underline{H}_3$) appear as a triplet between δ 1.17 and δ 1.24. The methyl protons (-O$C\underline{H}_3$) of the methyl derivatives appear as a singlet between δ 4.12 and δ 3.58.

The methyl protons of the alkyl group (-$C\underline{H}_3$) attached to the cyclopentadiene ring appear as three singlets between δ 2.22-1.61 for *N*-(1'-methyl-6-ferrocenyl-2-naphthoyl) amino acid and dipeptide esters. In the *N*-(1'-ethyl-6-ferrocenyl-2-naphthoyl) derivatives, the methylene protons of the alkyl group (-$C\underline{H}_2CH_3$) appear as two to three quartets, from δ 2.64-2.05, and the methyl protons of the alkyl group (-$CH_2C\underline{H}_3$) typically appear as one to two triplet signals from δ 1.21 to δ 0.89. Those signals multiplicities are discussed in section 2.6.1.

2.6.1. ^{1}H NMR spectroscopic studies of alkyl group of 1'-methyl-6-ferrocenyl-methyl-2-naphthoate (58) and 1'-ethyl-6-ferrocenyl-methyl-2-naphthoate (59)

Previous ^{1}H NMR study shows the protons of the alkyl group attached to the cyclopentadiene ring of 1-alkyl-1'-*N-para*, *N-meta* and *N-ortho*-(ferrocenyl) benzoyl dipeptide esters generally follow (n+1) splitting pattern, and each proton generates one signal with corresponding integrations.[11] However this pattern was not observed in this NMR study. The presence of methyl and ethyl groups attached to the cyclopentadiene ring were found to have a strong influence on the appearance of these spectra. Signal multiplicities were observed in the ^{1}H spectra for all resonating nuclei in starting material **51**, **52** and all *N*-(1'-methyl-6-ferrocenyl-2-naphthoyl) and *N*-(1'-ethyl-6-ferrocenyl-2-naphthoyl) amino acid and dipeptide esters (**62-77**). The methyl ferrocene and ethyl ferrocene were directly reacted with methyl-6-aminonaphthalene-2-carboxylate hydrochloride without protection, therefore there are two possibilities for methyl-6-aminonaphthalene-2-carboxylate hydrochloride to attack alkyl ferrocenyl groups. Methyl-6-aminonaphthalene-2-carboxylate hydrochloride can bound to the same or different cyclopentadienyl rings as the alkyl group. Figure 2.5 illustrates the proposed structure of those isomers. The proposed structures of atropisomers (I, II and III) is shown in Figure 2.5. Atropisomers formed because of two planar are unsymmetrically substituted. Atropisomerism restricts the rotation about the two planar. The naphthoyl moiety can also bound to the same planar as the alkyl group (Figure 2.5). Atropisomers I, II and III thought to be the main products due to steric effects of the alkyl group. Since it is impossible to separate those isomers, structures like in Figure 2.5 are still possible. Variable temperature ^{1}H NMR and HPLC-UV studies have been discussed in section 2.6.2 and 2.6.3.

The ^{1}H NMR spectrums of 1'-methyl-6-ferrocenyl-methyl-2-naphthoate **58** and 1'-ethyl-6-ferrocenyl-methyl-2-naphthoate **59** in DMSO-d_6 are shown in Figure 2.6 and Figure 2.7.

In the spectrum of 1'-methyl-6-ferrocenyl-methyl-2-naphthoate **58**, the methyl protons of the alkyl group (-CH_3) attached to the cyclopentadiene ring appears as three separate singlets at δ 2.22, δ 2.02 and δ 1.64, with total integration of three (Figure 2.6). This pattern maintains the same for all *N*-(1'-methyl-6-ferrocenyl-2-naphthoyl) amino acid and dipeptide derivatives.

For 1'-ethyl-6-ferrocenyl-methyl-2-naphthoate **59**, the methylene protons of the alkyl group (-CH_2CH_3) appear as three separate quartets, from δ 2.72-2.16, and the methyl protons of the alkyl group (-CH_2CH_3) appear as two separate triplet signals from δ 1.29 to δ 1.07 (Figure 2.7). This pattern maintains the same for all *N*-(1'-ethyl-6-ferrocenyl-2-naphthoyl) amino acid and dipeptide.

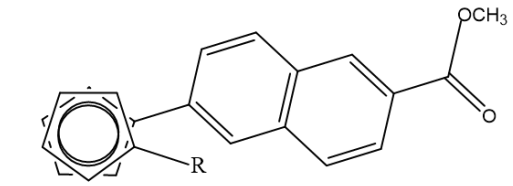

Atropisomer I

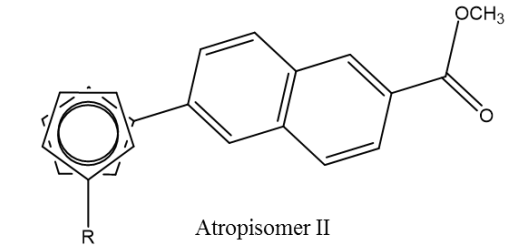

Atropisomer II

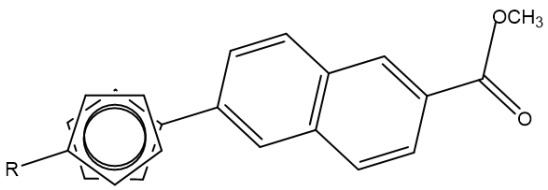

Atropisomer III

R= -CH_3 or -CH_2CH_3

Figure 2.4: The proposed structure of atropisomers I, II and III of compound **58** and **59**.

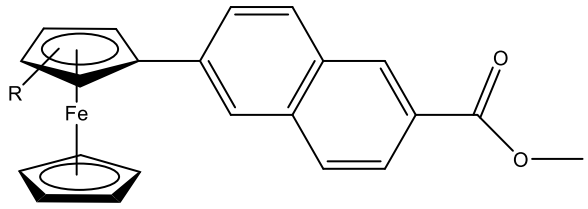

R= -CH_3 or -CH_2CH_3

Figure 2.5: The proposed structure of isomers of compound **58** and **59**.

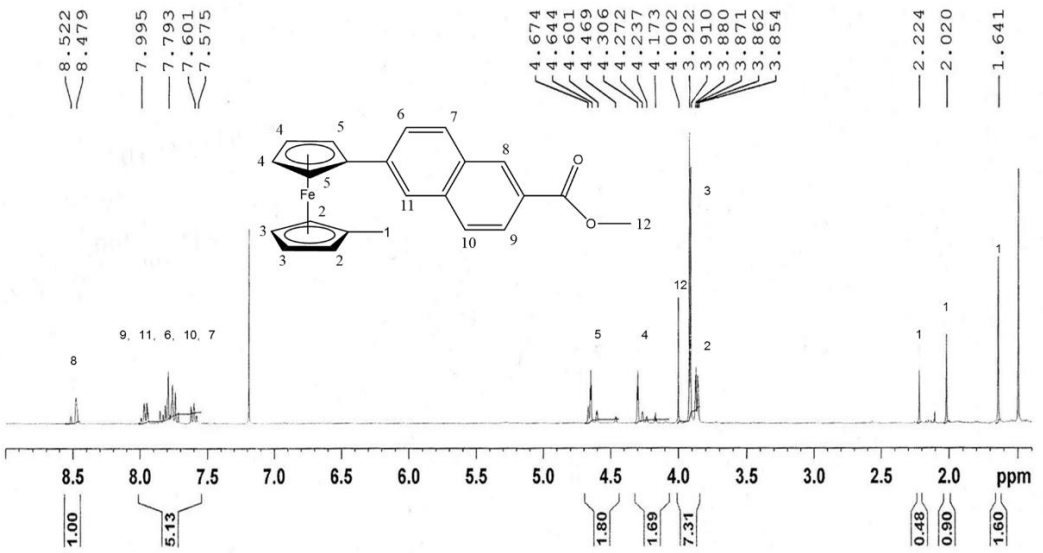

Figure 2.6: ^{1}H NMR spectrum of 1'-methyl-6-ferrocenyl-methyl-2-naphthoate **58** in $CDCl_3$.

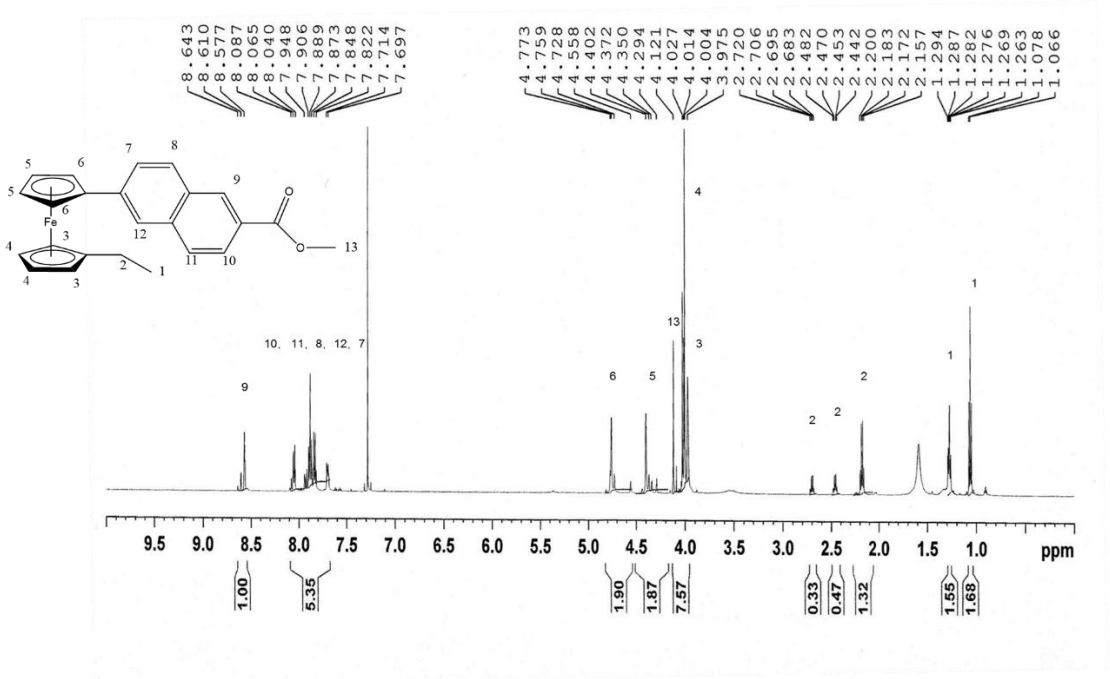

Figure 2.7: ^{1}H NMR spectrum of 1'-ethyl-6-ferrocenyl-methyl-2-naphthoate **59** in $CDCl_3$.

2.6.2. Variable temperature ^{1}H NMR studies of *N*-(1'-methyl-6-ferrocenyl-2-naphthoyl)-γ-aminobutyric acid ethyl ester (69)

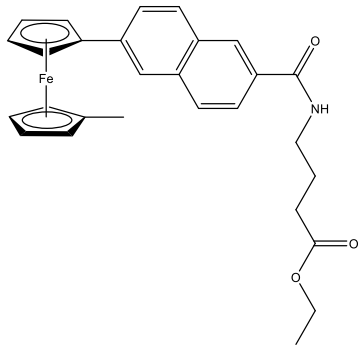

Figure 2.8: *N*-(1'-methyl-6-ferrocenyl-2-naphthoyl)-γ-aminobutyric acid ethyl ester **69**.

The ^{1}H NMR spectrum of *N*-(1'-methyl-6-ferrocenyl-2-naphthoyl) and *N*-(1'-ethyl-6-ferrocenyl-2-naphthoyl) amino acid and dipeptide **62-77** obtained at room temperature is highly complex due to the presence of atropisomers in solution for which the rate of interconversion is slow on the NMR time scale. A strong point of NMR spectroscopy is that information at various temperatures can be obtained without difficultly. When the temperature is lowered enough, different signals appear due to the exchange rate is slow enough for NMR to detect. Whereas a sole signal that corresponds to an average of those sites detected can be seen at higher temperature. This merging of the different signals is called coalescence. The line shapes of NMR spectra change dramatically at temperature slightly above or below coalescence temperature (Tc). Thus, a variable temperature study of the ^{1}H NMR spectrum of *N*-(1'-methyl-6-ferrocenyl-2-naphthoyl)-γ-aminobutyric acid ethyl ester **69** was performed at 20, 40, 60, 80, 100, and 120 °C in DMSO-*d6* (Figure 2.9).

The aromatic region of the ^{1}H NMR spectrum of *N*-(1'-methyl-6-ferrocenyl-2-naphthoyl)-γ-aminobutyric acid ethyl ester **69**, the amide proton of the γ-aminobutyric acid residue gives rise to two triplets at δ 8.39 and 8.61 at 20 °C (Figure 2.10). As the temperature is raised these signals shifting slightly upfield at 80 °C. Above 80 °C the signal sharpens. The ferrocenyl region (Figure 2.11) does not alter significantly upon heating. In contrast, the methylene protons from the γ-aminobutyric acid residue is more informative (Figure 2.12). At 20 °C, the signal belongs to the methylene protons attached to amide bond (-NHC$\underline{H_2}$CH_2CH_2-) is masked by the large signal due to H_2O contained in the DMSO-*d6* solvent. The methylene signal is shifted gradually downfield upon heating due to weakening of hydrogen bonds present in solution. No informative spectrum was recorded for the alkyl region (Figure 2.12). Therefore, the coalescence temperature of compound **69** is not within the range between 20 and 120 °C. Compared with other deuterated solvent *e.g.* acetone-*d6*, benzene-*d6*, chloroform-*d6* and dimethylformamide-*d6*, DMSO-*d6* is the deuterated solvent that have highest boiling point, hence no further investigation carried out for temperature ^{1}H NMR study.

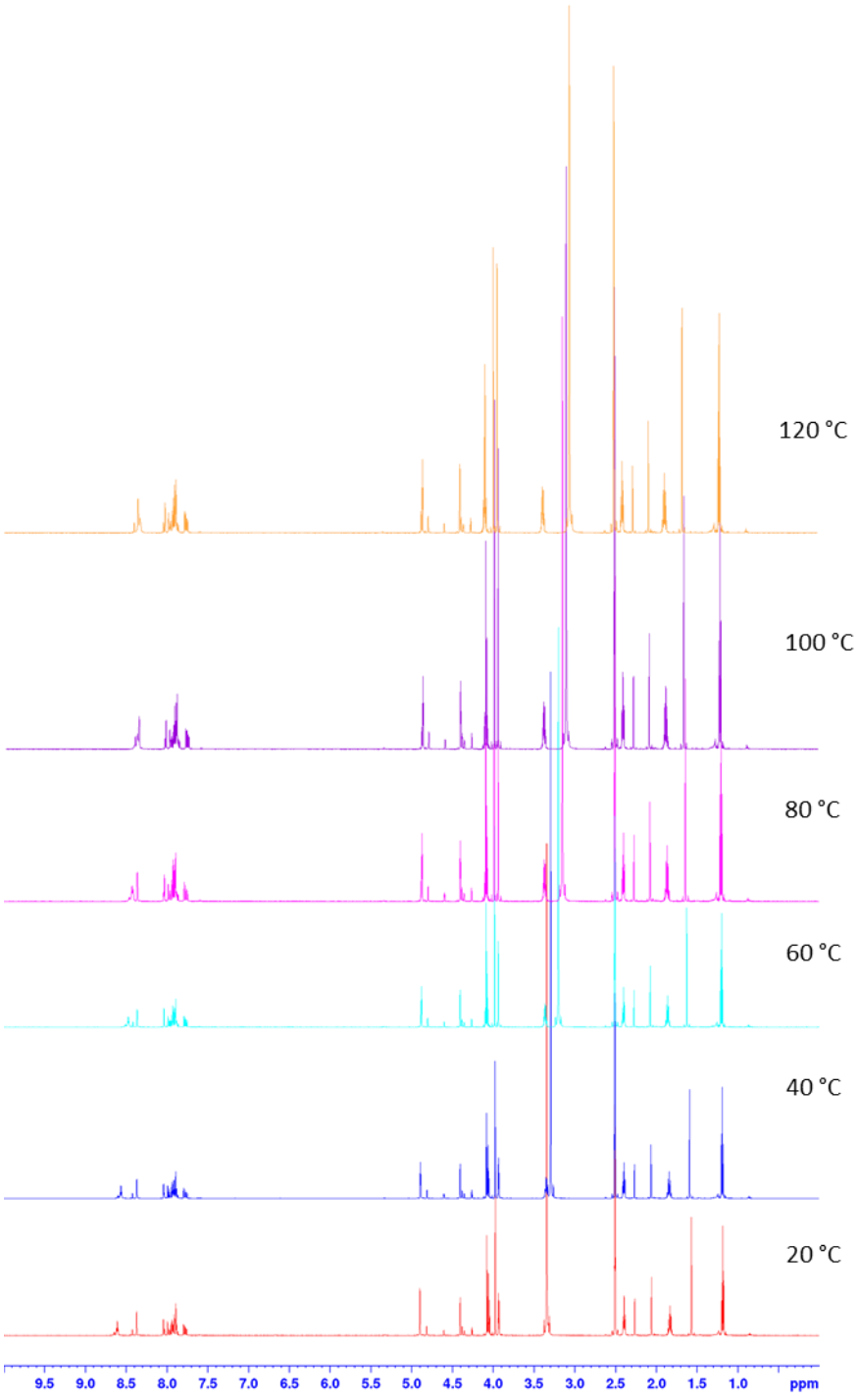

Figure 2.9: Variable temperature NMR study of *N*-(1'-methyl-6-ferrocenyl-2-naphthoyl)-γ-aminobutyric acid ethyl ester **69** at 20, 40, 60, 80, 100 and 120 °C.

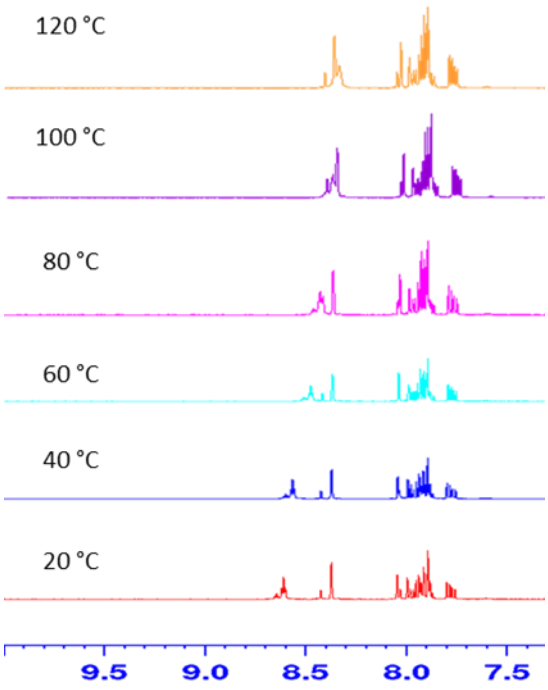

Figure 2.10: Variable temperature NMR study of *N*-(1'-methyl-6-ferrocenyl-2-naphthoyl)-γ-aminobutyric acid ethyl ester **69**: the aromatic region (7.5-10.0 ppm) of the ^{1}H NMR spectrum.

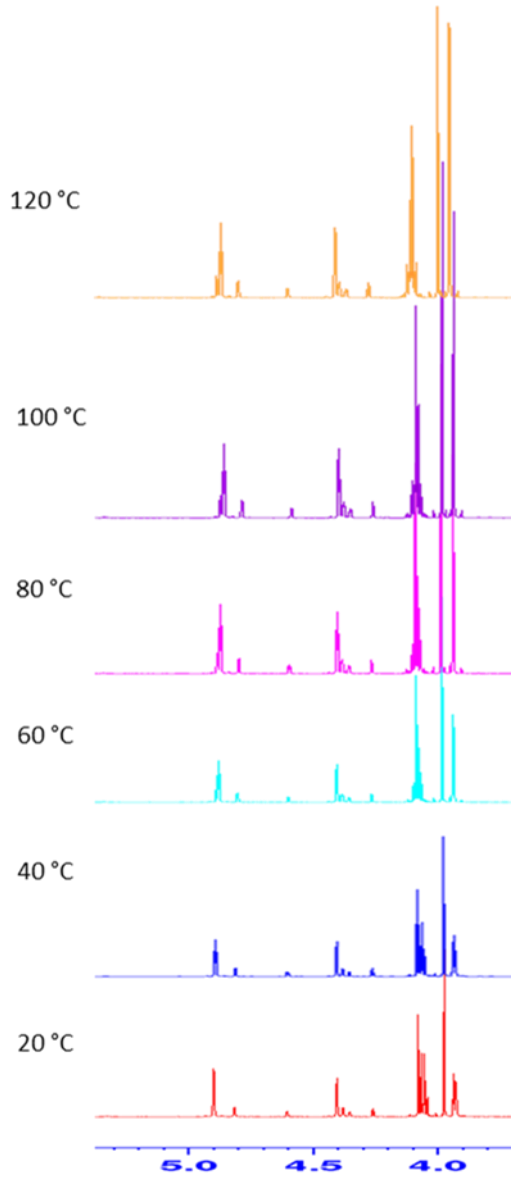

Figure 2.11: Variable temperature NMR study of *N*-(1'-methyl-6-ferrocenyl-2-naphthoyl)-γ-aminobutyric acid ethyl ester **69**: the ferrocenyl region (3.7-5.3 ppm) of the ^{1}H NMR spectrum.

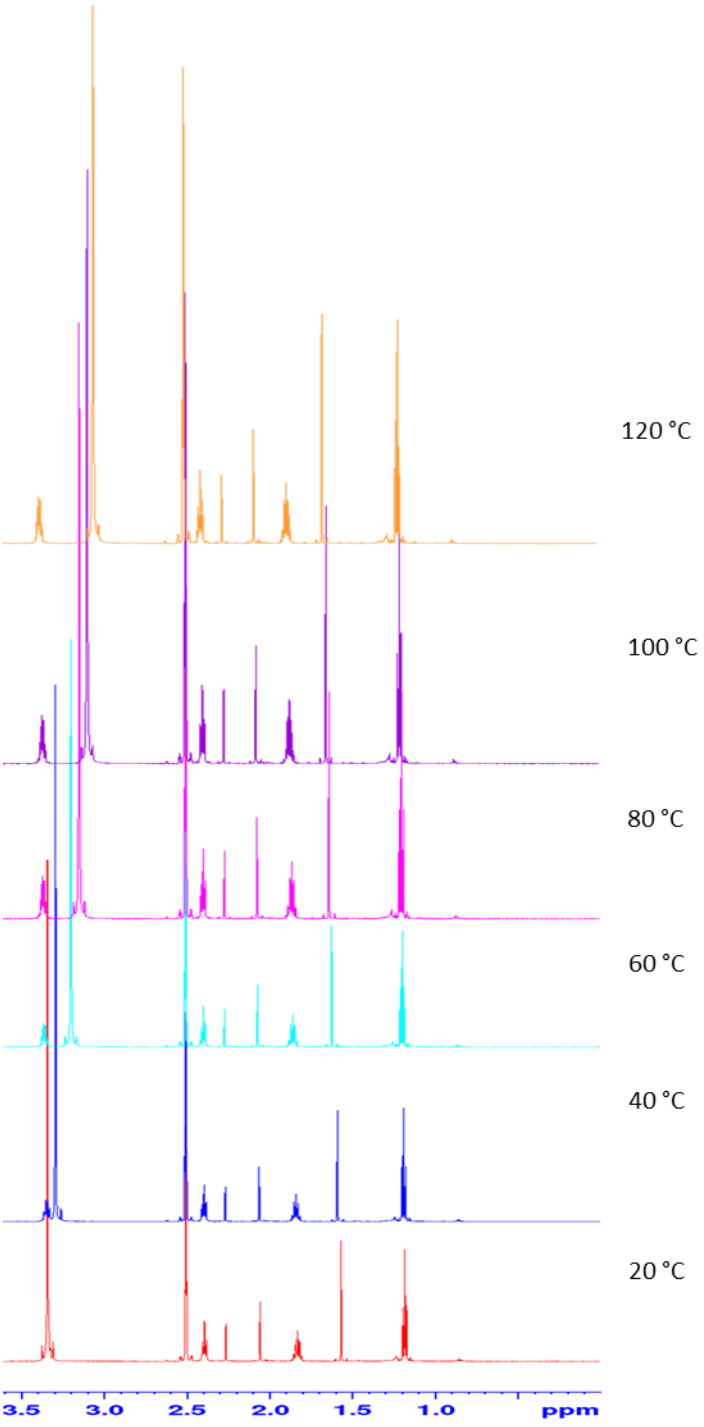

Figure 2.12: Variable temperature NMR study of *N*-(1'-methyl-6-ferrocenyl-2-naphthoyl)-γ-aminobutyric acid ethyl ester **69**: the methylene and alkyl region (0.0-3.6 ppm) of the ^{1}H NMR spectrum.

2.6.3. HPLC-UV studies of *N*-(1'-methyl-6-ferrocenyl-2-naphthoyl)-glycine-glycine ethyl ester (63)

High-performance liquid chromatography (HPLC) is a useful technique used to separate, identify and quantify each component in a mixture. [14] The chromatography detector is a device used in HPLC to detect components of the mixture being eluted off the column. There are selective detectors and universal detectors used in HPLC. Selective detectors are based on physical or chemical property of the solute, mainly have following four subtypes: absorbance detectors, fluorescence detectors, electrochemical detectors and mass spectrometric detectors. Universal detectors used to measure the difference in some physical property of the solute in mobile phase compared to the mobile phase alone. It is highly dependent of the mobile phase. Refractive index detectors and evaporating light scattering detectors are the major two types of detectors used in universal detectors. Absorbance detector is a type of the most common spectroscopic detector used to measure the ability of solutes to absorb light at wavelengths in the UV-Vis wavelength range. The UV, VIS, and PDA detectors are categorized as absorbance detectors. A standard UV detector allows the user to choose wavelengths between 195 to 370 nm. Most commonly used wavelength is 254 nm. Compared to a UV detector, a VIS detector uses longer wavelength (400 to 700 nm). There are detectors that provide wider wavelength selection, covering both UV and VIS ranges (195 to 700 nm) called UV/VIS detector. UV and VIS detectors visualize the obtained result in light intensity and time dimensions. The photo diode array detector (PDA) operates by simultaneously monitoring absorbance of solute at an entire wavelength. Light from the broad emission source such as a deuterium lamp is collimated by an achromatic lens system so that the total light passes through the detector cell onto a holographic grating. Therefore, the sample is subjected to light of all wavelengths generated by the lamp. The dispersed light from the grating is allowed to fall on to a diode array. The output from diode is recorded on to a computer. PDA adds the third dimension - wavelength. This is convenient to determine the most suitable wavelength without repeating analyses. [14 ,15]

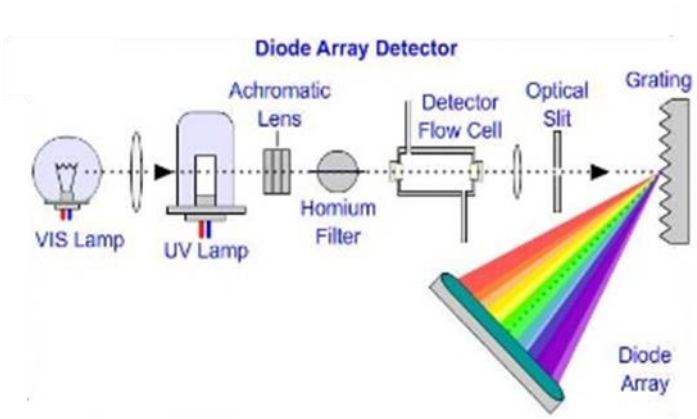

Figure 2.13: The components of a diode array detector.

In this study, UV-Vis photo diode array detector (PDA) is used with HPLC to measure the sample's absorption. Different samples may have different retention times therefore the number of atropisomers exist in the mixture can be identified.

N-(1'-methyl-6-ferrocenyl-2-naphthoyl)-glycine-glycine ethyl ester **63** was dissolved in ethanol and a C18 reversed column was used. The mixture was run at a flow rate of 4 mL min^{-1} with an injection volume of 20 μL. Two separate injections were carried out as shown in Figure 2.14. Similar signals were recorded for the sample at different concentrations.

From Figure 2.15, two main peaks were detected with retention time at 31.068 and 34.267 minutes respectively. The peak generated at 31.068 minutes have a lower left shoulder which can divided this peak area into peak area number 1 and 2. The peak area from number 1, 2 and 3 have 18%, 50% and 32% of the total peak area. Therefore, the ratio of those isomers detected from HPLC-PDA equal to 1:3:2. This result shows there are three isomers in the compound with different retention time. From ^{1}H NMR study of *N*-(1'-methyl-6-ferrocenyl-2-naphthoyl)-glycine-glycine ethyl ester **63**. The integration raised from the alkyl group were 0.5H, 1H and 1.5H respectively, which also equal to 1:2:3. Combined with the information from ^{13}C NMR and MS, compounds gave spectroscopic and analytical data in accordance with their structures.

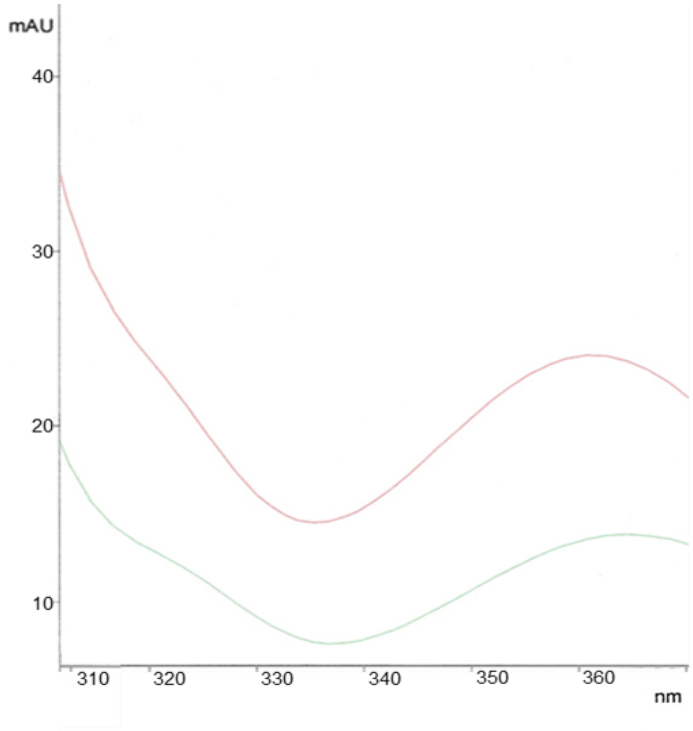

Figure 2.14: Two separate signals generated from PDA detector of *N*-(1'-methyl-6-ferrocenyl-2-naphthoyl)-glycine-glycine ethyl ester **63** at different concentrations by two injections.

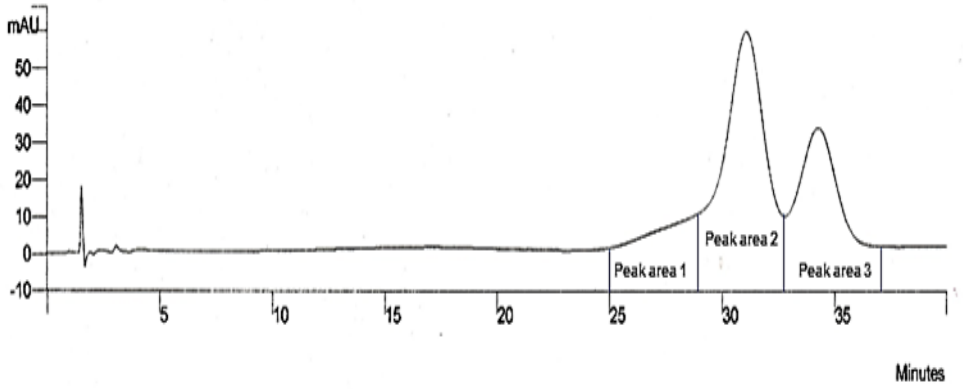

Figure 2.15: The HPLC-UV chromatogram of *N*-(1'-methyl-6-ferrocenyl-2-naphthoyl)-glycine-glycine ethyl ester **63**.

2.6.4. ^{1}H NMR studies of *N*-(1'-methyl-6-ferrocenyl-2-naphthoyl)-glycine-glycine ethyl ester (63)

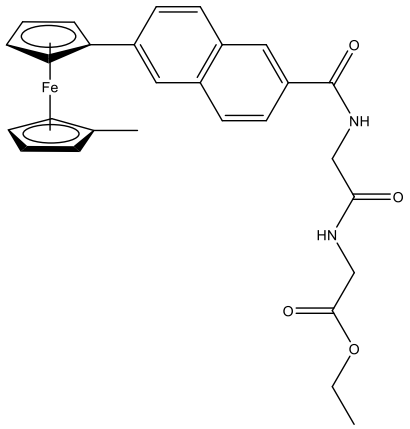

The ^{1}H NMR spectrum of *N*-(1'-methyl-6-ferrocenyl-2-naphthoyl)-glycine-glycine ethyl ester **63** was measured in $CDCl_3$ (Figure 2.16). The two amide protons (-CONH-) are positioned downfield at δ 7.53 and δ 7.18 with integration of one. The naphthoyl spacer region confirms the presence of six protons, which appears from δ 8.27 to δ 7.55. For the disubstituted ferrocene moiety, the peak due to the *ortho* of the cyclopentadiene ring attached to the naphthoyl spacer ($\eta^5C_5H_4$-naphthoyl) appears as the furthest downfield. This signal appears as a triplet at δ 4.64 and with integration of two. Similarly, the *meta* ($\eta^5C_5H_4$-naphthoyl) protons appear as a triplet at δ 4.29. The protons on the alkylated cyclopentadiene ring (η^5-C_5H_4-alkyl) appear as two triplets with an overall integration of four at δ 3.91 and δ 3.87 for protons on *meta* and *ortho*, respectively.

The methyl protons of the alkyl group (-CH_3) attached to the cyclopentadiene ring appear as three singlets at δ 2.19, δ 2.00 and δ 1.61 with a total integration as three. The methylene group of the ethyl ester (-OCH_2CH_3) is presented as a quartet at downfield δ 4.14 with a coupling constant of 7.2 Hz. The methylene proton signal (-$NHCH_2CO$-) of the glycine glycine ethyl ester moiety appears as a doublet at δ 4.21 with J = 6.1 Hz whilst another methylene proton signal (-$CONHCH_2CO$-) appear as a doublet at δ 4.02 with J = 7.3 Hz, both with corresponding integration of 2. The methyl group of the ethyl ester (-OCH_2CH_3) is present as a triplet at δ 1.17 with J = 7.2 Hz.

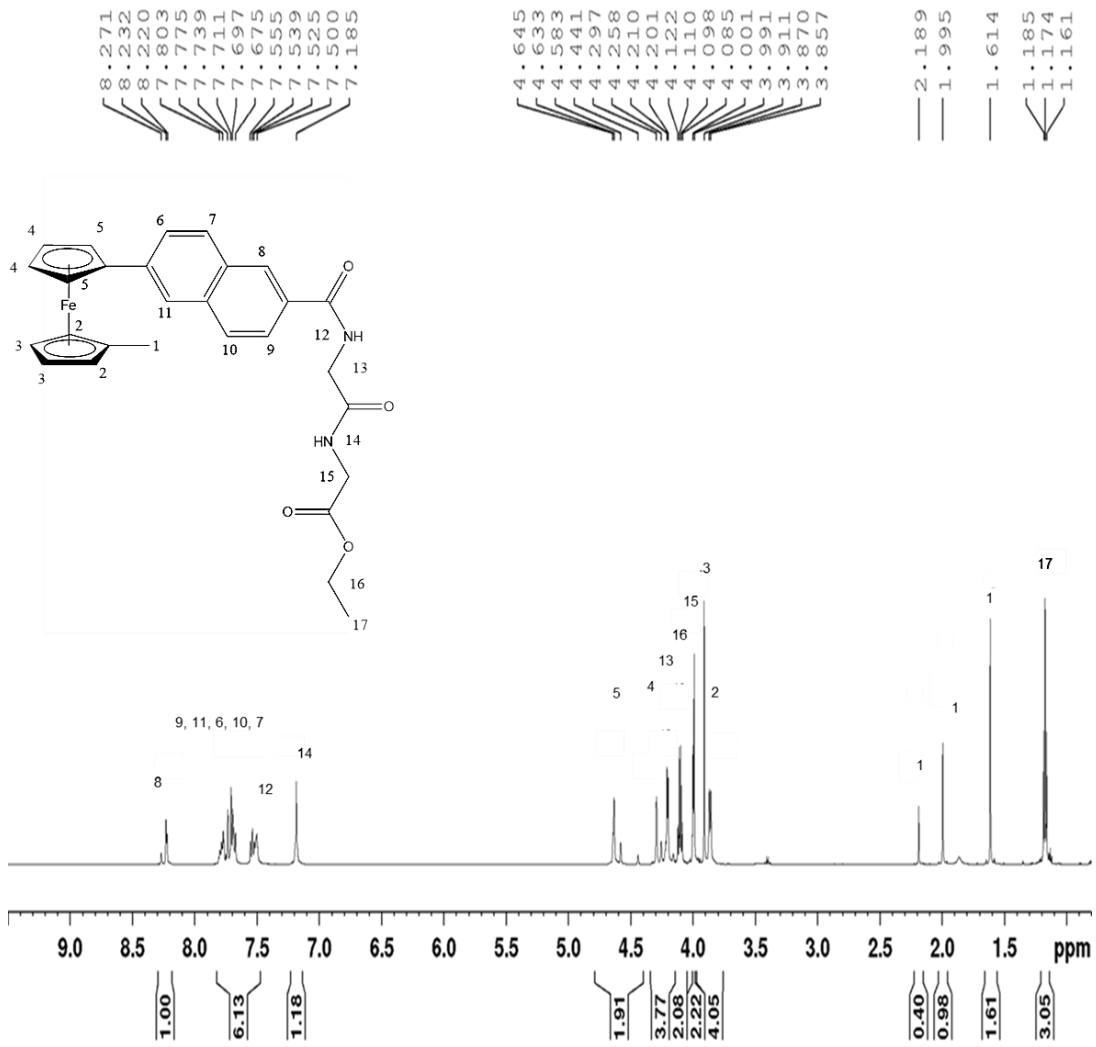

Figure 2.16: ^{1}H NMR spectrum of *N*-(1'-methyl-6-ferrocenyl-2-naphthoyl)-glycine-glycine ethyl ester **63** in $CDCl_3$.

2.7. ^{13}C NMR and DEPT-135 spectroscopic studies of *N*-(1'-methyl-6-ferrocenyl-2-naphthoyl) and *N*-(1'-ethyl-6-ferrocenyl-2-naphthoyl) amino acid and dipeptide esters

^{13}C and DEPT 135 NMR studies were carried out on all compounds. In a DEPT-135 spectrum, methine and methyl carbons appear as positive peaks, whereas methylene carbons appear as negative peaks *i.e.* below the resonance line. Carbonyl and quaternary carbons are absent in a DEPT 135 spectrum. All the ^{13}C and DEPT-135 NMR experiments were performed in $CDCl_3$. The typical ^{13}C NMR chemical shifts observed are presented in Table 2.7.

In the ^{13}C NMR spectra of *N*-(1'-methyl-6-ferrocenyl-2-naphthoyl) and *N*-(1'-ethyl-6-ferrocenyl-2-naphthoyl) amino acid and dipeptide esters, the typical peaks observed include the appearance of carbonyl signals between δ 173.9-166.6. In the amino acid derivatives only two carbonyl signals are observed whilst for the dipeptide derivatives found to have three carbonyl signals. In the aromatic region of the spectrum of these derivatives, ten unique carbon signals are observed which appear between δ 140.2- 120.8. The two quaternary carbon atoms present on the naphthoyl moiety can be easily identified by their absence in the DEPT-135 spectrum.

For the 1-alkyl-1' derivatives, six unique carbon signals are observed for the disubstituted ferrocene moiety with two ipso carbons being present. The *ipso* carbon (η^5-C_5H_4- naphthoyl) appears between δ 86.8 - 84.0, whilst the *ipso* carbon (η^5-C_5H_4-alkyl) appears between δ 92.0-88.8. The signals of *ortho* carbons on the substituted cyclopentadiene rings appear more downfield compared to the *meta* carbons due to deshielding by the naphthoyl linker and the alkyl chain attached. The carbon atom of the methyl group (-CH_3), attached to the cyclopentadiene ring appears between δ 15.3-13.7. The methylene carbon of the ethyl ester (-OCH_2CH_3) derivatives appears between δ 62.3-61.4 whilst the methyl carbon (-OCH_2CH_3) appears between δ 15.1-14.0. The carbon atom of the methyl ester (-OCH_3) derivatives appear between δ 51.3-51.8.

Table 2.7: ^{13}C and DEPT 135 NMR spectral data for *N*-(1'-methyl-6-ferrocenyl-2-naphthoyl) and *N*-(1'-ethyl-6-ferrocenyl-2-naphthoyl) amino acid and dipeptide esters.

Compound No.	C=O	*Ipso* (η^5-C_5H_4-alkyl)	*Ipso* (η^5-C_5H_4-naphthoyl)	*meta* on (η^5-C_5H_4-naphthoyl)	*meta* on (η^5-C_5H_4-alkyl)	*ortho* on (η^5-C_5H_4-alkyl)	*ortho* on (η^5-C_5H_4-naphthoyl)	-CH_3	-$\underline{C}H_2CH_3$	-$CH_2\underline{C}H_3$
62	170.3-166.6	90.2	85.1	69.5	67.1	66.3	65.7	15.0	-	-
63	172.9-167.8	90.1	86.8	71.1	69.9	69.7	67.3	15.2	-	-
64	172.5-167.5	88.8	84.0	70.5	68.1	67.9	66.2	15.0	-	-
65	173.1-167.7	89.3	85.8	71.3	68.8	67.2	65.9	14.8	-	-
66	172.6-167.5	89.1	84.2	70.6	68.1	67.4	66.3	15.3	-	-
67	173.2-167.5	89.0	84.2	71.0	69.0	67.4	66.1	14.8	-	-
68	172.9-168.0	89.1	84.9	70.2	68.8	67.3	65.8	13.8	-	-
69	173.9-167.9	89.4	84.3	70.4	68.9	67.1	64.4	13.7	-	-
70	168.9-166.6	89.9	85.7	70.2	68.4	67.4	65.8	-	21.7	14.7
71	169.7-166.9	92.0	84.2	68.9	67.1	66.4	65.6	-	21.6	14.7
72	172.5-167.4	89.3	84.2	71.7	69.3	67.1	66.2	-	20.6	14.5
73	172.-167.8	89.7	84.8	70.3	69.0	67.2	65.7	-	21.0	14.1
74	172.6-167.5	88.9	84.5	71.0	69.1	67.2	66.3	-	21.3	14.5
75	173.6-167.5	89.6	84.1	69.8	69.1	67.3	65.7	-	21.3	14.7
76	174.3-167.6	88.9	84.3	71.3	69.1	67.2	66.5	-	21.5	14.7
77	173.3-168.6	89.1	84.3	69.7	68.8	67.1	65.6	-	22.2	13.6

2.7.1. ^{13}C NMR and DEPT-135 spectroscopic studies of *N*-(1'-methyl-6-ferrocenyl-2-naphthoyl)-glycine-glycine ethyl ester (63)

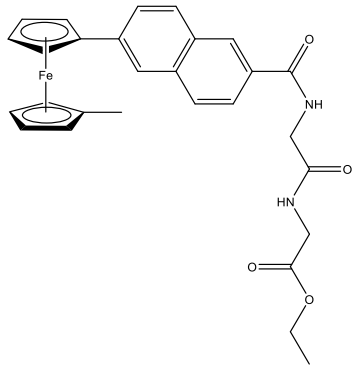

The ^{13}C NMR spectrum of *N*-(1'-methyl-6-ferrocenyl-2-naphthoyl)-glycine-glycine ethyl ester **63** displays three carbonyl carbon atoms at δ 172.9, δ 169.4 and δ 167.8. These are absent in the DEPT-135 spectrum. The aromatic region shows ten unique carbon signals, representing the ten non-equivalent carbon atoms of the 2, 6-disubstituted naphthalene group, between δ 134.8 and δ 120.8. The four quaternary carbon atoms from the naphthoyl spacer moiety at δ 134.8, δ 133.0, δ 130.7 and δ 130.2 can be easily identified by their absence in the DEPT-135 spectrum. The *ipso* carbon atom on (η^5-C_5H_4-alkyl) ring appears at δ 90.1 whilst the *ipso* on (η^5-C_5H_4- naphthoyl) ring appears at δ 86.8. These are absent in the DEPT-135 spectrum. The remaining carbon atoms on the cyclopentadiene rings are present between δ 71.7-67.3. The methylene carbon atom of the ethyl ester (-OCH_2CH_3) is observed at δ 61.5, whilst the methyl carbon atom appears at δ 14.0. The two methylene carbon atoms (-$NHCH_2$-) of the glycine glycine ethyl ester are observed at δ 43.8 and δ 41.2. The carbon atom of the methyl group (-CH_3) attached to the cyclopentadiene ring appears at δ 15.0. (Figure 2.17 and Figure 2.18)

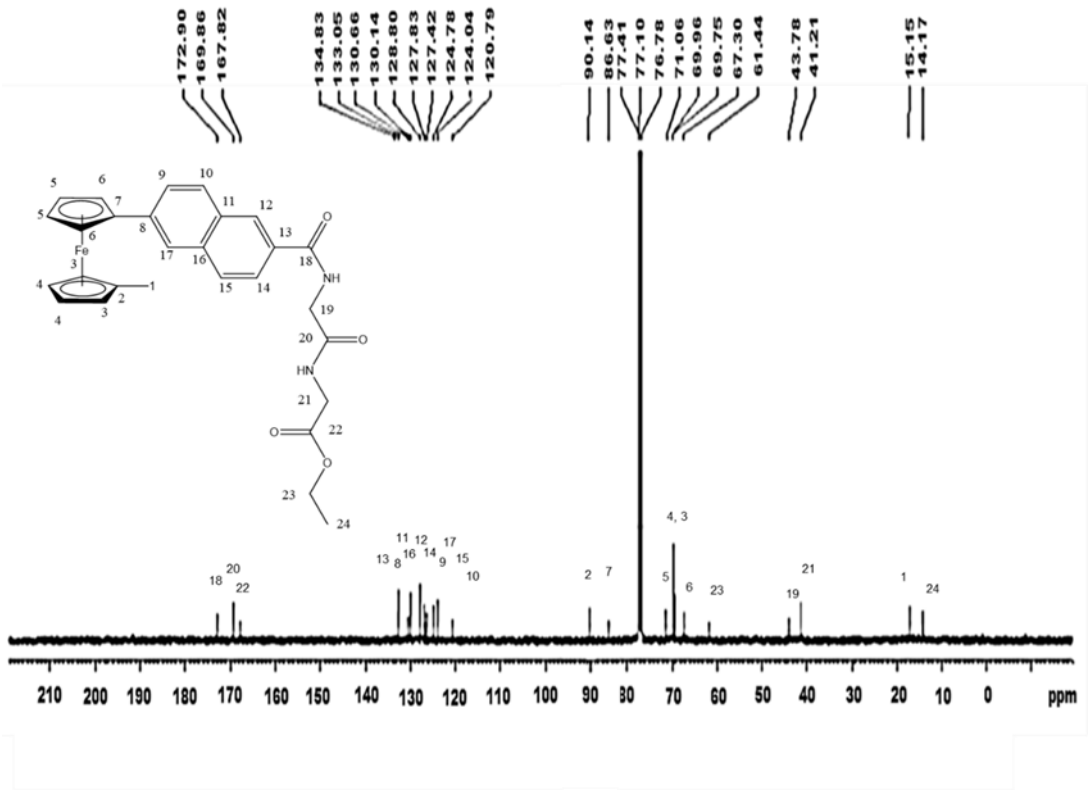

Figure 2.17: ^{13}C NMR spectrum of *N*-(1'-methyl-6-ferrocenyl-2-naphthoyl)-glycine-glycine ethyl ester **63** in $CDCl_3$.

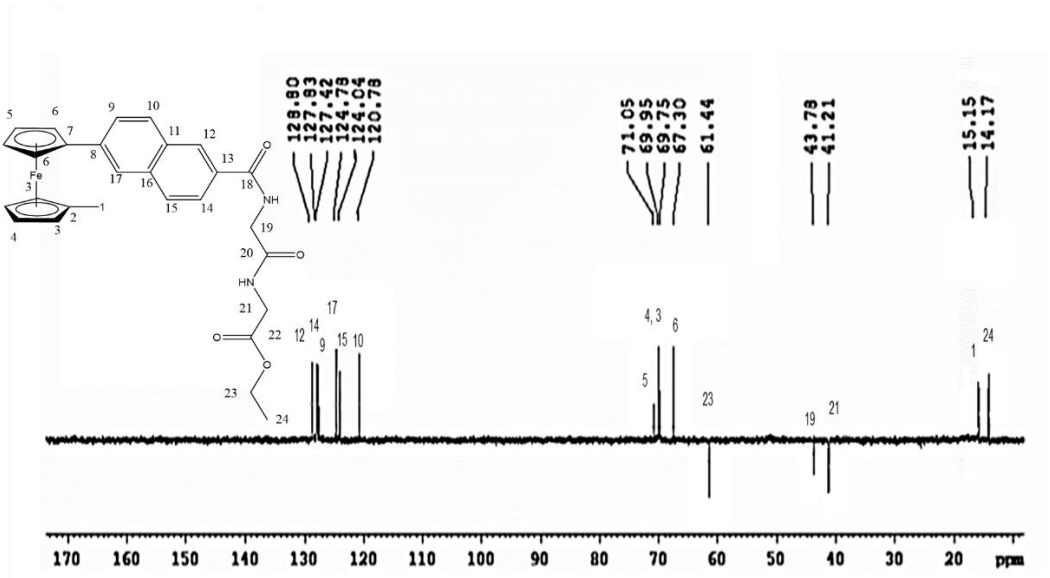

Figure 2.18: DEPT-135 NMR spectrum of *N*-(1'-methyl-6-ferrocenyl-2-naphthoyl)-glycine-glycine ethyl ester **63** in $CDCl_3$.

2.8. HMQC spectroscopic studies of *N*-(1'-methyl-6-ferrocenyl-2-naphthoyl)-γ- aminobutyric acid ethyl ester (69)

HMQC (Heteronuclear Multiplet Quantum Coherence) is a 2D NMR technique that correlates each ^{13}C atom to the proton to which it is directly attached.[12] Thus, HMQC allows assignment of proton and carbon spectra which aids in total structure elucidation. This technique correlates a carbon signal to any directly associated protons. Therefore, no signals are observed for those carbon atoms lacking protons *i.e.* carbonyl or quaternary carbon atoms. The structure and HMQC spectrum of *N*-(1'-methyl-6-ferrocenyl-2-naphthoyl)-γ-aminobutyric acid ethyl ester **69** is shown in Figure 2.19 and Figure 2.20, respectively. The positions of the C-H correlations are listed in Table 2.8.

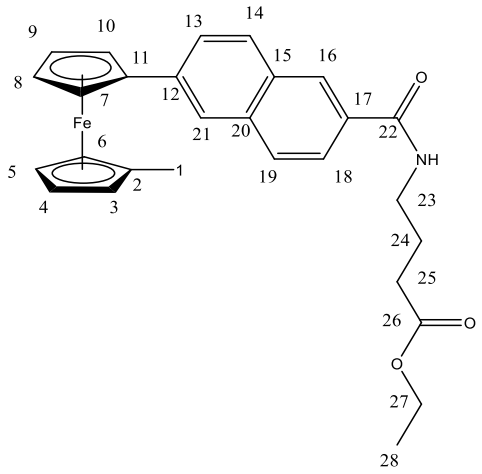

Figure 2.19: *N*-(1'-methyl-6-ferrocenyl-2-naphthoyl)-γ-aminobutyric acid ethyl ester **69**.

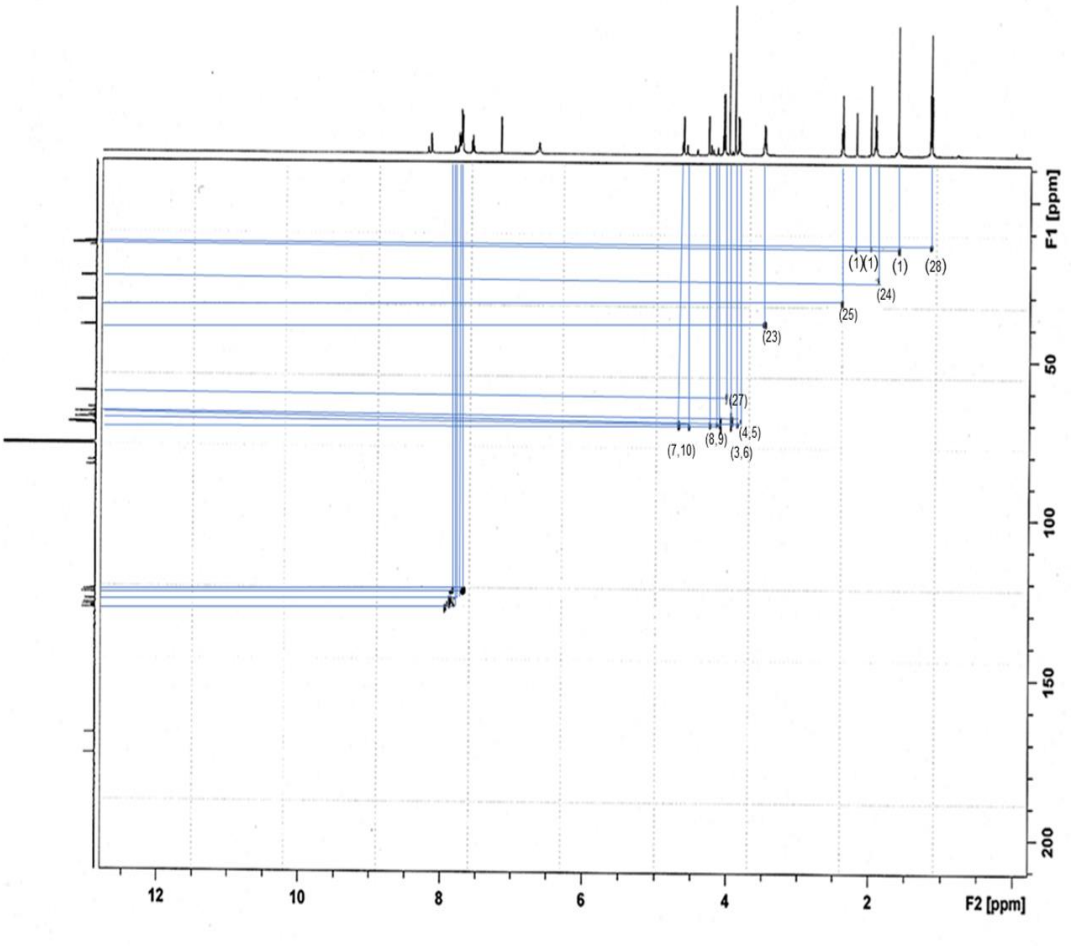

Figure 2.20: HMQC spectrum of *N*-(1'-methyl-6-ferrocenyl-2-naphthoyl)-γ-aminobutyric acid ethyl ester **69**.

Table 2.8: HMQC data for *N*-(1'-methyl-6-ferrocenyl-2-naphthoyl)-γ-aminobutyric acid ethyl ester **69**.

Site	^{1}H NMR	^{13}C NMR	HMQC
1*	2.21, 2.01, 1.63	-	13.7
2	-	89.4	-
(3, 6)*	3.86	-	67.1
(4, 5)*	4.00	-	68.9
(8, 9)*	4.29	-	70.4
(7, 10)*	4.65	-	64.4
11	-	84.3	-
12	-	135.1	-
13*	7.81	-	127.2
14*	7.61	-	123.1
15	-	131.2[a]	-
16*	8.21	-	128.8
17	-	139.5	-
18*	7.84	-	127.9
19*	7.74	-	123.9
20	-	130.7[b]	-
21*	7.78	-	126.1
22	-	173.9	-
23*	3.53	-	39.8
24*	1.94	-	24.5
25*	2.40	-	32.1
26	-	167.9	-
27*	4.10	-	60.6
28*	1.18	-	14.1

* C-H correlation site.

[a,b] Signals may be reversed.

2.9. Mass spectrometric studies of *N*-(1'-methyl-6-ferrocenyl-2-naphthoyl) and *N*-(1'-ethyl-6-ferrocenyl-2-naphthoyl) amino acid and dipeptide derivatives

Mass spectrometry enables the determination of the relative molecular mass of many different types of compounds. The mass spectrometer is composed of five distinct parts, namely the sample inlet, the ion source, the mass analyser, the detector and the data system. The sample is introduced into the ion source and this allows ionisation to occur. These ions are extracted into the analyser, where they are separated according to their mass (*m*) to charge (*z*) ratios (*m/z*). [12] The separated ions are detected and displayed as a mass spectrum. Electrospray ionization mass spectrometry (ESI-MS) was employed in the analysis of *N*-(1'-methyl-6-ferrocenyl-2-naphthoyl) and *N*-(1'-ethyl-6-ferrocenyl-2-naphthoyl) amino acid and dipeptide esters. Those compounds are non-volatile, and a soft ionization technique is employed in their analysis. The analysis confirmed the correct relative molecular mass for those compounds.

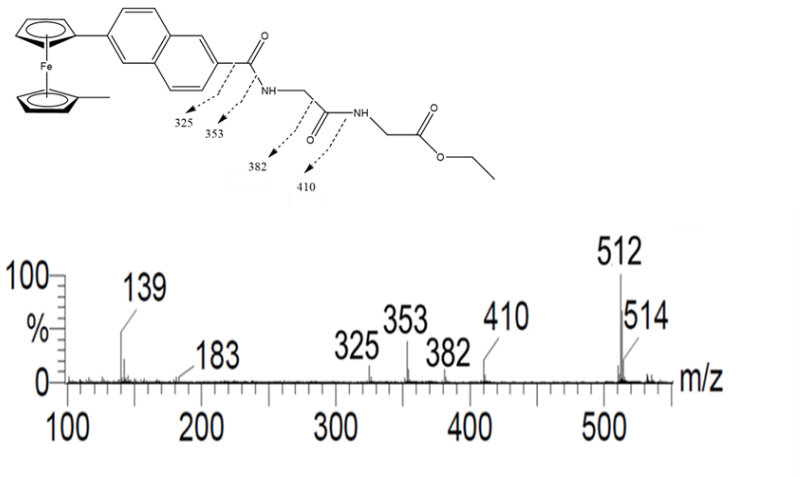

Figure 2.21: Product ions observed in the ESI-MS/MS spectrum of *N*-(1'-methyl-6-ferrocenyl-2-naphthoyl)-glycine-glycine ethyl ester **63**.

The mass spectrum for of *N*-(1'-methyl-6-ferrocenyl-2-naphthoyl)-glycine-glycine ethyl ester **63** is shown in Figure 2.21. The sequence specific fragment ions are present at *m/z* 325, *m/z* 353, *m/z* 382 and *m/z* 410. The signal at *m/z* 325 indicates the presence of a ferrocenyl naphthyl subunit while the signal at *m/z* 353 is due to cleavage at the naphthoyl carbonyl. And as expected, product ions at *m/z* 382 and *m/z* 410 were observed.

For compound **76**, similar trends were detected as shown in Figure 2.22, the sequence specific fragment ions are present at *m/z* 339 and *m/z* 367.

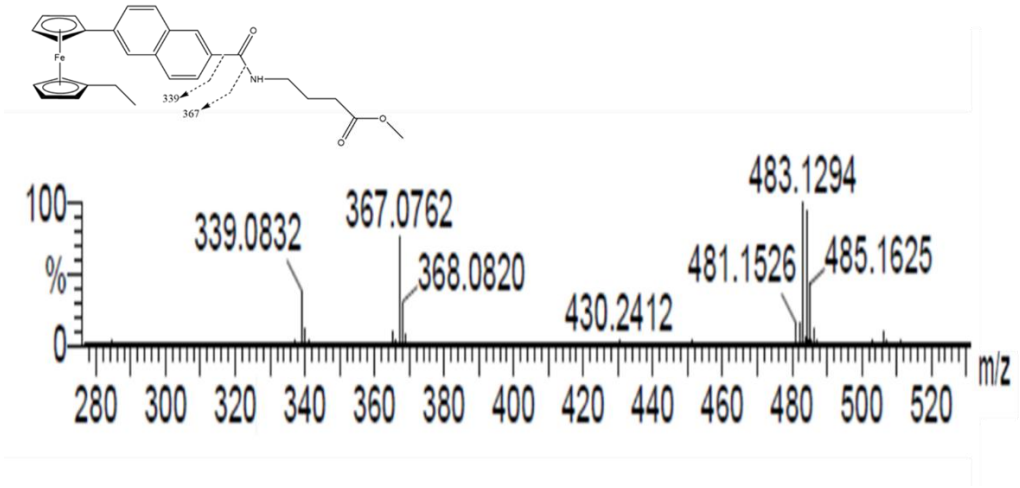

Figure 2.22: Product ions observed in the ESI-MS/MS spectrum of *N*-(1'-ethyl-6-ferrocenyl-2-naphthoyl)-γ-aminobutyric acid methyl ester **76**.

2.10. Conclusion

N-(ferrocenyl)naphthoyl amino acid and dipeptide derivatives have been identified as potential anti-cancer agents against the H1299 NSCLC and Sk-Mel-28 cell lines. [6] The project sought to further explore the structure-activity relationship (SAR) of these compounds to enhance their anti-proliferative effect. Both ferrocene and ester regions have been modified. Thus *N*-(1'-methyl-6-ferrocenyl-2-naphthoyl) and *N*-(1'-ethyl-6-ferrocenyl-2-naphthoyl) amino acid and dipeptide esters have been prepared. Each novel compound contains an electroactive alkylated ferrocene core, a conjugated aromatic linker and an amino acid or dipeptide ester chain. These novel compounds were prepared by condensation of 1'-methyl-6-ferrocenyl-2-naphthoic acid and 1'-ethyl-6-ferrocenyl-2-naphthoic acid with the amino acid or dipeptide esters under solution phase EDC/NHS coupling conditions. Purification by column chromatography furnished the required compounds as an orange solid or orange oil, in moderate yields 13% to 60%.

The *N*-(1'-methyl-6-ferrocenyl-2-naphthoyl) and *N*-(1'-ethyl-6-ferrocenyl-2-naphthoyl) amino acid and dipeptide derivatives were characterized by a range of spectroscopic techniques including ^{1}H NMR, ^{13}C NMR, DEPT-135, HMQC, IR, UV-Vis and MS. And all compounds gave spectroscopic and analytical data in accordance with their proposed structures.

Experimental Procedures

Experimental Note

All chemicals were purchased from Sigma-Aldrich or Fluorochem Limited; and used as received. Commercial grade reagents were used without further purification. When necessary, all solvents were purified and dried prior to use. Riedel-Haën silica gel was used for thin layer and column chromatography. Melting points were determined using a Griffin melting point apparatus and are uncorrected. Infrared spectra were recorded on a PerkinElmer Spectrum 100 FT-IR with ATR. UV-Vis spectra were recorded on a Hewlett Packard 8452A diode array UV-Vis spectrophotometer. ^{1}H and ^{13}C NMR spectra were recorded in deuterated solvents on either a Bruker Avance 400 or 600 NMR. The ^{1}H and ^{13}C NMR chemical shifts are reported in ppm (parts per million). Tetramethylsilane (TMS) or the residual solvent peaks have been used as an internal reference. All coupling constants (*J*) are in Hertz. The abbreviations for the peak multiplicities are as follows: s (singlet), d (doublet), dd (doublet of doublets), t (triplet), q (quartet), qt (quintet), m (multiplet) and br (broad). Electrospray ionization mass spectra were performed on a Micromass LCT mass spectrometer.

General Procedures

General procedure for the preparation of amino acid and dipeptide esters.

Glycine-glycine methyl ester hydrochloride (47)

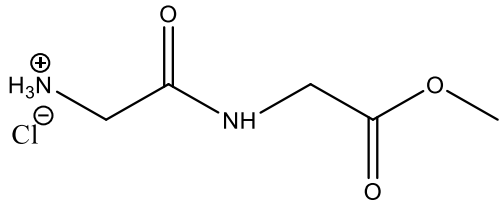

Thionyl chloride (4 ml) was added slowly to methanol (25 ml) at -5 °C and glycine-glycine (2.00 g, 15.2 mmol) was added to the solution. After 30 minutes, the reaction mixture was refluxed for 16 hours. The solvent was removed *in vacuo* to yield the title compound as a white solid (2.01g, 72%), mp: 107-109 °C;

^{1}H NMR (600 MHz) δ (DMSO-d_6): 9.07 (1H, t, J = 6.0 Hz, -CONH-), 8.38 (3H, br.s, -NH_3CH_2-), 3.94 (2H, d, J = 6.1 Hz, -NHCH_2-), 3.64 (3H, s, -OCH_3), 3.43 (2H, s, -NH_3CH_2-);

^{13}C NMR (100 MHz) δ (DMSO-d_6): 170.5 (C=O), 167.3 (C=O), 53.4 (-OCH$_3$), 41.3 (NH_3CH_2-, -ve DEPT), 40.2 (-NHCH$_2$-, -ve DEPT).

Glycine-glycine ethyl ester hydrochloride (48)

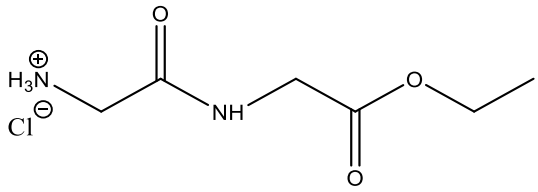

The synthesis followed that of glycine-glycine methyl ester hydrochloride using the following reagents: glycine-glycine (2.00 g, 15.2 mmol), ethanol (25 ml), thionyl chloride (4 ml). The solvent was removed *in vacuo* to yield the title compound as a white solid (1.96 g, 70%), mp: 178-179 °C;

^{1}H NMR (600 MHz) δ (DMSO-d_6): 8.89 (1H, t, J = 6.0 Hz, -CONH-), 8.19 (3H, br.s, - NH_3CH_2-), 4.14 (2H, q, J = 7.2 Hz, -OCH_2CH$_3$), 3.94 (2H, d, J = 6.1 Hz, -NHCH_2-), 3.61 (2H, s, NH_3CH_2-), 1.22 (3H, t, J = 7.2 Hz, -OCH$_2$CH_3);

^{13}C NMR (100 MHz) δ (DMSO-d_6): 169.4 (C=O), 166.5 (C=O), 60.6 (-OCH$_2$CH$_3$, -ve DEPT), 40.7 (NH_3CH_2-, -ve DEPT), 40.6 (-NHCH$_2$-, -ve DEPT), 14.0 (-OCH$_2$$CH_3$).

γ-Aminobutyric acid methyl ester hydrochloride (49)

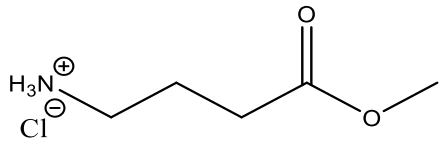

The synthesis followed that of glycine-glycine methyl ester hydrochloride using the following reagents: γ-aminobutyric acid (2.00 g, 19.4 mmol), methanol (25 ml), thionyl chloride (4 ml). The solvent was removed *in vacuo* to yield the title compound as a white solid (1.75 g, 59%), mp: 115-116 °C;

^{1}H NMR (600 MHz) δ (DMSO-d_6): 8.19 (3H, br.s, -N$\underline{H}_3$), 3.60 (3H, s, -OC$\underline{H}_3$), 2.80 (2H, t, J = 7.2 Hz, -COC$\underline{H}_2$-), 2.46 (2H, t, J = 7.2 Hz, $NH_3C\underline{H}_2$-), 1.84 (2H, qt, J = 7.2 Hz,-$CH_2C\underline{H}_2CH_2$-);

^{13}C NMR (100 MHz) δ (DMSO-d_6): 172.6 (C=O), 51.9 (-O$\underline{C}H_3$), 38.5 ($NH_3\underline{C}H_2$-, -ve DEPT), 30.9 (-CO$\underline{C}H_2$-, -ve DEPT), 22.9 (-$CH_2\underline{C}H_2CH_2$-,-ve DEPT).

γ-Aminobutyric acid ethyl ester hydrochloride (50)

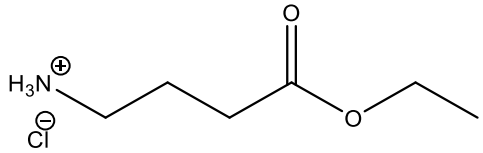

The synthesis followed that of glycine-glycine methyl ester hydrochloride using the following reagents: γ-aminobutyric acid (2.00 g, 19.4 mmol), ethanol (25 ml), thionyl chloride (4 ml). The solvent was removed *in vacuo* to yield the title compound as a white solid (2.15 g, 68%), mp: 46-48 °C;

^{1}H NMR (600 MHz) δ (DMSO-d_6): 8.04 (3H, br. s, -N$\underline{H}_3CH_2$-), 4.09 (2H, q, J =7.3 Hz, -OC$\underline{H}_2CH_3$), 3.45 (2H, t, J =7.2 Hz, -COC$\underline{H}_2$-), 2.43 (2H, t, J =7.2 Hz, $NH_3C\underline{H}_2$-), 1.84 (2H, qt, J =7.2 Hz, -$CH_2C\underline{H}_2CH_2$-), 1.19 (3H, t, J =7.3 Hz, -$OCH_2C\underline{H}_3$);

^{13}C NMR (100 MHz) δ (DMSO-d_6): 172.1 (C=O), 59.9 (-O$\underline{C}H_2CH_3$, -ve DEPT), 37.9 ($NH_3\underline{C}H_2$-, -ve DEPT), 30.4 (-CO$\underline{C}H_2$-, -ve DEPT), 22.3 (-$CH_2\underline{C}H_2CH_2$-, -ve DEPT), 14.1 (-$OCH_2\underline{C}H_3$).

General procedure for the preparation of Boc protected dipeptide esters

Boc-glycine-L-alanine-methyl ester (51)

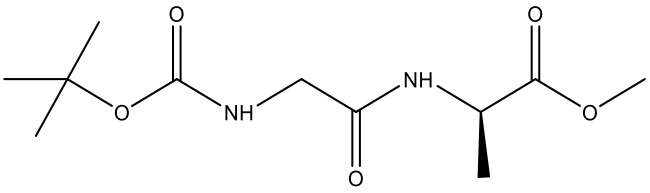

Boc-glycine (2.45 g, 14.0 mmol) was dissolved in DCM (60 ml) at 0 °C. L-alanine methyl ester hydrochloride (1.41 g, 14.0 mmol), *N*-(3-dimethylaminopropyl)-*N*'-ethylcarbodiimide hydrochloride (2.68 g, 14.0 mmol), *N*-hydroxysuccinimide (1.61 g, 14.0 mmol) and triethylamine (5 ml) were added and stirred at 0 °C for 1 hour. The reaction mixture was allowed to stir at room temperature for 48 hours. The solvent was removed *in vacuo* and the crude product was purified by column chromatography (eluent 1:1 ethyl acetate: hexane) to yield the product as a transparent oil (1.86 g, 48%);

^{1}H NMR (600 MHz) δ (DMSO-d_6): 8.20 {1H, d, J = 7.2 Hz, -CON<u>H</u>CH(CH_3)-}, 6.90 (1H, t, J = 6.2 Hz, -CON<u>H</u>-), 4.32 (1H, qt, J = 7.4 Hz, -NHC<u>H</u>-), 3.59 (3H, s, -OC<u>H</u>$_3$), 3.58 (2H, dd, J = 6.2 and 10.4 Hz, -NHC<u>H</u>$_2$-), 1.38 {9H, s, -C(C<u>H</u>$_3$)$_3$}, 1.28 (3H, d, J = 7.4 Hz, -CHC<u>H</u>$_3$);

^{13}C NMR (100 MHz) δ (DMSO-d_6): 173.5 (C=O), 170.1 (C=O), 156.5 (C=O), 78.6 (C_q), 52.2 (-O<u>C</u>H$_3$), 48.1 (-<u>C</u>HCH$_3$-), 43.4 (-NH<u>C</u>H$_2$-, -ve DEPT), 28.7 {-C(<u>C</u>H$_3$)$_3$}, 17.5 (-CH<u>C</u>H$_3$).

Boc-glycine-L-alanine-ethyl ester (52)

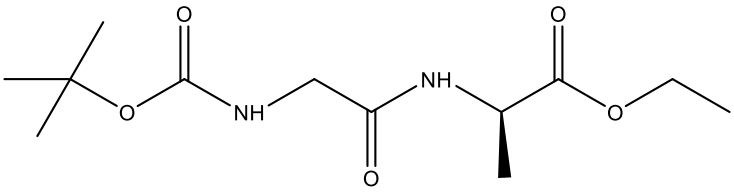

The synthesis followed that of Boc-glycine-L-alanine-methyl ester using the following reagents: Boc-glycine (2.45 g, 14.0 mmol), L-alanine ethyl ester hydrochloride (1.58 g, 14.0 mmol), *N*-(3-dimethylaminopropyl)-*N*′-ethylcarbodiimide hydrochloride (2.68 g, 14.0 mmol), *N*-hydroxysuccinimide (1.61 g, 14.0 mmol) and triethylamine (5 ml). The product was purified by column chromatography (eluent 1:1 ethyl acetate: hexane) to give the title compound as a transparent oil (1.91 g, 48%);

^{1}H NMR (600 MHz) δ (DMSO-d_6): 8.18 {1H, d, J = 7.2 Hz, -CONHCH(CH$_3$)-}, 6.91 (1H, t, J = 6.2 Hz, -CONH-), 4.28 (1H, qt, J = 7.4 Hz, -NHCH-), 4.10 (2H, q, J = 7.3 Hz, -OCH$_2$CH$_3$), 3.61 (2H, dd, J = 6.2 and 10.4 Hz, -NHCH$_2$-), 1.38 {9H, s, -(CH$_3$)$_3$}, 1.28 (3H, d, J = 7.4 Hz, -CHCH$_3$), 1.20 (3H, t, J = 7.3 Hz, -OCH$_2$CH$_3$);

^{13}C NMR (100 MHz) δ (DMSO-d_6): 173.1 (C=O), 169.9 (C=O), 156.3 (C=O), 78.8 (C$_q$), 61.3 (-OCH$_2$CH$_3$, -ve DEPT), 48.1 (-CHCH$_3$), 43.4 (-NHCH$_2$-, -ve DEPT), 28.5{-C(CH$_3$)$_3$}, 17.7 (-CHCH$_3$), 14.5 (-CH$_2$CH$_3$).

Boc-glycine-D-alanine-methyl ester (53)

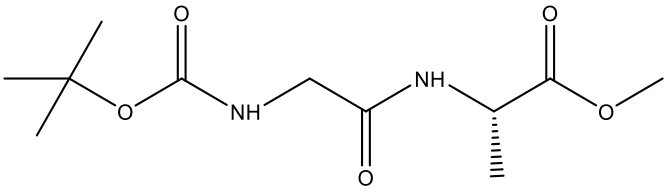

The synthesis followed that of Boc-glycine-L-alanine-methyl ester using the following reagents: Boc-glycine (2.45 g, 14.0 mmol), D-alanine methyl ester hydrochloride (1.41 g, 14.0 mmol), *N*-(3-dimethylaminopropyl)-*N′*-ethylcarbodiimide hydrochloride (2.68 g, 14.0 mmol), *N*-hydroxysuccinimide (1.61 g, 14.0 mmol) and triethylamine (5 ml). The product was purified by column chromatography (eluent 1:1 ethyl acetate:hexane) to give the title compound as a transparent oil (1.20 g, 31%);

^{1}H NMR (600 MHz) δ (DMSO-d_6): 8.21 {1H, d, J = 7.2 Hz, -CONHCH(CH$_3$)}, 6.92 (1H, t, J = 6.2 Hz, -CONH-), 4.31 (1H, qt, J = 7.4 Hz, -NHCH-), 3.62 (3H, s, -OCH$_3$), 3.58 (2H, dd, J = 6.2 and 10.4 Hz, -NHCH$_2$-), 1.38 {9H, s, -C(CH$_3$)$_3$}, 1.28 (3H, d, J = 7.4 Hz, -CHCH$_3$);

^{13}C NMR (100 MHz) δ (DMSO-d_6): 172.9 (C=O), 169. 9 (C=O), 156.5 (C=O), 78.6 (C$_q$), 52.2 (-OCH$_3$), 48.1(-CHCH$_3$-), 43.4 (-NHCH$_2$-, -ve DEPT), 28.7 {-C(CH$_3$)$_3$}, 17.5 (-CH$_2$CH$_3$).

Boc-glycine-D-alanine-ethyl ester (54)

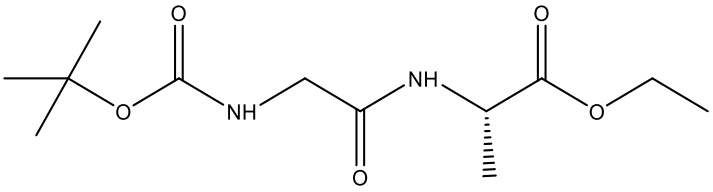

The synthesis followed that of Boc-glycine-L-alanine-methyl ester using the following reagents: Boc-glycine (2.45 g, 14.0 mmol), D-alanine ethyl ester hydrochloride (1.58 g, 14.0 mmol), *N*-(3-

dimethylaminopropyl)-*N′*-ethylcarbodiimide hydrochloride (2.68 g, 14.0 mmol), *N*-hydroxysuccinimide (1.61 g, 14.0 mmol) and triethylamine (5 ml). The product was purified by column chromatography (eluent 1:1 ethyl acetate: hexane) to give the title compound as a transparent oil (1.81 g, 44%);

^{1}H NMR (600 MHz) δ (DMSO-d_6): 8.18 {1H, d, J = 7.2 Hz, -CON<u>H</u>CH(CH_3)-}, 6.92 (1H, t, J = 6.2 Hz, -CON<u>H</u>-), 4.27 (1H, qt, J = 7.4 Hz, -NHC<u>H</u>-), 4.09 (2H, q, J = 7.3 Hz, -OC<u>H_2</u>CH_3), 3.61 (2H, dd, J = 6.2 and 10.4 Hz, -NHC<u>H_2</u>-), 1.38 {9H, s, -(C<u>H_3</u>)$_3$}, 1.28 (3H, d, J = 7.4 Hz, -CHC<u>H_3</u>), 1.20 (3H, t, J = 7.3 Hz, -OCH_2C<u>H_3</u>);

^{13}C NMR (100 MHz) δ (DMSO-d_6): 172.8 (C=O), 169. 9 (C=O), 156.4 (C=O), 78. 6 (C_q), 61.1 (-O<u>C</u>H_2CH_3, -ve DEPT), 48.1 (-<u>C</u>HCH_3), 43.6 (-NH<u>C</u>H_2-, -ve DEPT), 28.7{-C(<u>C</u>H_3)$_3$}, 17.7 (-CH<u>C</u>H_3), 14.6 (-CH_2<u>C</u>H_3).

Synthesis of starting material

Methyl ferrocene (55)

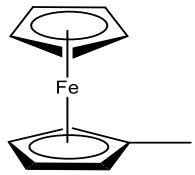

Lithium aluminium hydride (1.42 g, 37.4 mmol) was dissolved in dry diethyl ether (50 ml) under nitrogen at 0 °C. Ferrocenecarboxaldehyde (4.00 g, 18.7 mmol) was slowly added and the reaction mixture was allowed to stir for 15 minutes. Anhydrous aluminum chloride (4.99 g, 37.4 mmol) was added slowly to the reaction mixture over 30 minutes. The reaction mixture was refluxed at room temperature for 8 hours and quenched on ice after. The diethyl ether layer was washed with water and dried over $MgSO_4$. The solvent was removed *in vacuo* to yield the crude product. The crude product was purified by column chromatography {eluent 5:1 hexane: diethyl ether} yielding the title compound as dark orange solid (3.60 g, 90%), mp: 35.5-37.5 °C;

^{1}H NMR (600 MHz) δ ($CDCl_3$): 4.04 (5H, s,η^5-$C_5\underline{H}_5$), 4.01 (2H, s, *meta* on η^5-$C_5\underline{H}_4$-alkyl), 3.97 (2H, s, *ortho* on η^5-$C_5\underline{H}_4$-alkyl), 1.90 (3H, s, -$C\underline{H}_3$);

^{13}C NMR (100 MHz) δ ($CDCl_3$): 89.5 (C_{ipso} η^5-$\underline{C}_5H_4$-alkyl), 69.2 (C_{meta} η^5-$\underline{C}_5H_4$-CH_3), 68.6 (C_{ortho} η^5-$\underline{C}_5H_4$-CH_3), 67.2 (η^5-$\underline{C}_5H_5$), 14.8 (-$\underline{C}H_3$).

Ethyl ferrocene (56)

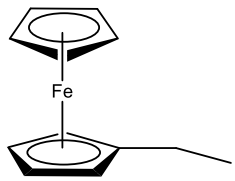

The synthesis followed that of methyl ferrocene using the following reagents: lithium aluminium hydride (1.42 g, 37.4 mmol), acetylferrocene (4.00 g, 17.5 mmol), anhydrous aluminum chloride (4.99 g, 37.4 mmol). The crude product was purified by column chromatography {eluent 5:1 hexane: diethyl ether} yielding the title compound as a dark orange oil (3.23 g, 86%);

^{1}H NMR (600 MHz) δ ($CDCl_3$): 4.08 (5H, s,η^5-$C_5\underline{H}_5$), 4.03 (2H, t, J = 1.6 Hz, *meta* on η^5-$C_5\underline{H}_4$-alkyl), 3.99 (2H, t, J = 1.6 Hz, *ortho* on η^5-$C_5\underline{H}_4$-alkyl), 2.28 (2H , q, J = 7.4 Hz, -$C\underline{H}_2CH_3$), 1.11 (3H, t, J = 7.4 Hz , -$CH_2C\underline{H}_3$);

^{13}C NMR (100 MHz) δ ($CDCl_3$): 91.1 (C_{ipso} η^5-$\underline{C}_5H_4$-alkyl), 68.4 (C_{meta} η^5-$\underline{C}_5H_4$-alkyl), 67.9 (C_{ortho} η^5-$\underline{C}_5H_4$-alkyl), 66.9 (η^5-$\underline{C}_5H_5$), 22.3 (-$\underline{C}H_2CH_3$, -ve DEPT), 14.9 (-$CH_2\underline{C}H_3$).

Methyl-6-aminonaphthalene-2-carboxylate hydrochloride (57)

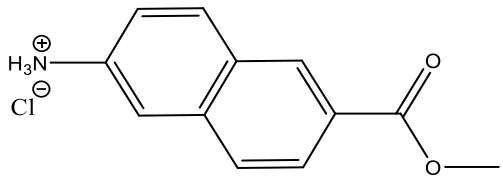

6-Amino-2-naphthoic acid (5.00 g, 26.7 mmol) was added slowly to a solution of methanol (30 ml) and thionyl chloride (8 ml) at 0 °C and refluxed for 48 hours. The solution was cooled to room temperature and the precipitate was isolated *via* vacuum filtration and washed with hexane to yield the title compound as a brown solid (4.77 g, 89%), mp: 221-223 °C (lit[13]: 250-251 °C);

^{1}H NMR (600 MHz) δ (DMSO-d_6): 8.58 (1H, s, Ar$\underline{H}$), 8.13 (1H, d, J = 8.8 Hz, Ar$\underline{H}$), 7.96-7.90 (2H, dd, J = 2.0 and 8.8 Hz, Ar$\underline{H}$), 7.62 (1H, s, Ar$\underline{H}$), 7.42 (1H, dd, J = 2.0 and 8.8 Hz, Ar$\underline{H}$), 3.90 (3H, s, -OC$\underline{H}_3$);

^{13}C NMR (100 MHz) δ (DMSO-d_6): 166.9 (C=O), 136.6 (Cq),135.4 (Cq), 131.7, 130.5, 129.2 (Cq), 127.7, 126.2 (Cq), 125.0, 121.7, 117.4, 52.5 (-O$\underline{C}H_3$).

1'-Methyl-6-ferrocenyl-methyl-2-naphthoate (58)

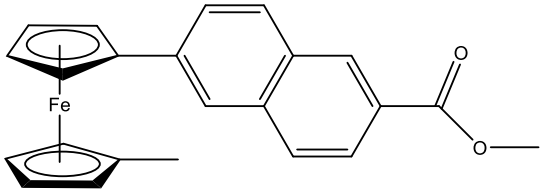

Concentrated hydrochloric acid (5 ml) was added with intermittent cooling to a solution of methyl-6-aminonaphthalene-2-carboxylate hydrochloride (2.39 g, 12.0 mmol) in 30 ml of water. A solution of sodium nitrite (0.83 g, 12.0 mmol) in 30 ml of deionised water was added slowly to this mixture with stirring, keeping the temperature below 5 ^{o}C furnishing a pale brown/yellow solution. The resulting diazo salt was added to a solution of methyl ferrocene (3.00 g, 15.0 mmol) in diethyl ether (100 ml) with polyethylene glycol (2 ml) and allowed to react for 48 hours. The reaction mixture was washed with water and brine and the ether layer was dried over $MgSO_4$. The solvent was removed *in vacuo* to yield the crude product. The crude product was purified by column chromatography {eluent 5:1 hexane: diethyl ether} yielding the title compound as an orange solid (0.92 g, 20%), mp: 170-172 °C;

^{1}H NMR (600 MHz) δ ($CDCl_3$): 8.52 (1H, t, *J* = 8.4 Hz, Ar<u>H</u>), 7.95 (1H, dd, *J* = 1.6 and 8.8 Hz, Ar<u>H</u>), 7.81-7.79 (3H, m, Ar<u>H</u>), 7.58 (1H, dd, *J* = 1.6 and 8.8 Hz, Ar<u>H</u>), 4.64 (2H, t, *J* = 2.0 Hz, *ortho* on η^5-C_5<u>H_4</u>-naphthoyl), 4.31 (2H, t, *J* = 2.0 Hz, , *meta* on η^5-C_5<u>H_4</u>-naphthoyl), 4.0 (3H, s, -OC<u>H_3</u>), 3.92 (2H, t, *J* = 2.0 Hz, *meta* on η^5-C_5<u>H_4</u>-alkyl), 3.88 (2H, t, *J* = 2.0 Hz, *ortho* on η^5-C_5<u>H_4</u>-alkyl), 2.22 (0.5H, s, -C<u>H_3</u>), 2.02 (0.9H, s, -C<u>H_3</u>), 1.64 (1.6H, s, -C<u>H_3</u>);

^{13}C NMR (100 MHz) δ ($CDCl_3$): 167.4 (C=O), 140.5 (C_q), 139.85 (C_q), 136.0 (C_q), 131.0, 129.2, 127.8, 127.5, 126.6 (C_q), 125.6, 123.1, 88.9 (C_{ipso} η^5-<u>C</u>$_5$H$_4$-alkyl), 85.4 (C_{ipso} η^5-<u>C</u>$_5$H$_4$- naphthoyl), 70.9 (C_{meta} η^5-<u>C</u>$_5$H$_4$-naphthoyl), 68.2 (C_{meta} η^5-<u>C</u>$_5$H$_4$-alkyl), 67.3 (C_{ortho} η^5-<u>C</u>$_5$H$_4$-alkyl), 65.8 (C_{ortho} η^5-<u>C</u>$_5$H$_4$-naphthoyl), 52.1 (-O<u>C</u>H$_3$), 13.9 (-<u>C</u>H$_3$).

1'-Ethyl-6-ferrocenyl-methyl-2-naphthoate (59)

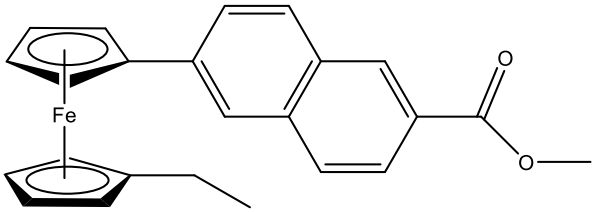

The synthesis followed that of 1'-methyl-6-ferrocenyl-methyl-2-naphthoate using the following reagents: methyl-6-aminonaphthalene-2-carboxylate hydrochloride (2.39 g, 12.0 mmol), HCl (5 ml), sodium nitrite (0.83 g, 12.0 mmol), ethyl ferrocene (3.10 g, 15.0 mmol) and polyethylene glycol (2 ml). The crude product was purified by column chromatography {eluent 5:1 hexane: diethyl ether} yielding the title compound as an orange solid (0.86 g, 17%), mp: 163-164 °C;

^{1}H NMR (400 MHz) δ ($CDCl_3$): 8.61 (1H, t, *J* = 8.4 Hz, Ar<u>H</u>), 8.06 (1H, dd, *J* = 1.6 and 8.8 Hz, Ar<u>H</u>), 7.75-7.82 (3H, m, Ar<u>H</u>), 7.71 (1H, dd, *J* = 1.6 and 8.8 Hz, Ar<u>H</u>), 4.76 (2H, t, *J* = 2.0 Hz, *ortho* on η^5-C_5<u>H_4</u>-naphthoyl), 4.40 (2H, t, *J* = 2.0 Hz, *meta* on η^5-C_5<u>H_4</u>-naphthoyl), 4.12 (2H, t, *J* = 2.0 Hz, *meta* on η^5-C_5<u>H_4</u>-alkyl), 4.03 (3H, s, -OC<u>H_3</u>), 3.98 (2H, t, *J* = 2.0 Hz, *ortho* on η^5-C_5<u>H_4</u>-alkyl), 2.72 (0.3H, q, *J* = 7.2Hz, -C<u>H_2</u>CH_3), 2.48 (0.4H, q, *J* = 7.2Hz, -C<u>H_2</u>CH_3), 2.20 (1.3H, q, *J* = 7.2Hz, -C<u>H_2</u>CH_3), 1.29 (1.5H, t, *J* = 7.2Hz, -CH_2C<u>H_3</u>), 1.08 (1.5H, t, *J* = 7.2Hz, -CH_2C<u>H_3</u>);

^{13}C NMR (100 MHz) δ ($CDCl_3$): 167.4 (C=O), 140.41 (C_q), 139.9 (C_q), 135.9 (C_q), 131.1, 130.9, 129.1, 127.6, 126.0 (C_q), 125.7, 123.1, 122.8, 89.6 (C_{ipso} η^5-<u>C_5</u>H_4-alkyl), 84.2 (C_{ipso} η^5-<u>C_5</u>H_4-naphthoyl), 70.2 (C_{meta} η^5-<u>C_5</u>H_4-naphthoyl), 69.1 (C_{meta} η^5-<u>C_5</u>H_4-alkyl), 67.2 (C_{ortho} η^5-<u>C_5</u>H_4-alkyl), 65.6 (C_{ortho} η^5-<u>C_5</u>H_4-naphthoyl), 52.2 (-O<u>C</u>H_3), 21.5 (-<u>C</u>H_2CH_3, -ve DEPT), 14.5 (-CH_2<u>C</u>H_3).

1'-Methyl-6-ferrocenyl-2-naphthoic acid (60)

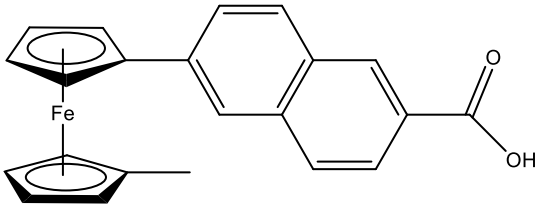

10% NaOH solution (80 ml) was added to 1'-methyl-6-ferrocenyl-methyl-2-naphthoate (5.00 g, 13.0 mmol) in 80 ml methanol and was refluxed for 12 hours. The solution was cooled on ice and acidified to pH 2 with concentrated HCl. Vacuum filtrated the precipitate and wash with deionised water yielding product as an orange solid (3.58 g, 74%), mp: 210 °C (decomp);

^{1}H NMR (600 MHz) δ (DMSO-d_6): 12.85 (1H, br. s, -COO<u>H</u>), 8.53 (1H, s, Ar<u>H</u>), 8.07-7.79 (5H, m, Ar<u>H</u>), 4.91 (2H, t, *J* = 2.0 Hz, *ortho* on η^5-C$_5$<u>H$_4$</u>-naphthoyl), 4.41 (2H, t, *J* = 2.0 Hz, , *meta* on η^5-C$_5$<u>H$_4$</u>-naphthoyl), 4.01 (2H, t, *J* = 2.0 Hz, *meta* on η^5-C$_5$<u>H$_4$</u>-alkyl), 3.92 (2H, t, *J* = 2.0 Hz, *ortho* on η^5-C$_5$<u>H$_4$</u>-alkyl), 2.27 (0.5H, s, -C<u>H$_3$</u>), 2.05 (1H, s, -C<u>H$_3$</u>), 1.57 (1.5H, s, -C<u>H$_3$</u>);

^{13}C NMR (100 MHz) δ ($CDCl_3$): 168.3 (C=O), 133.9 (C_q), 132.6 (C_q), 131.0 (C_q), 130.2, 129.6, 129.3, 128.9, 126.6 (C_q), 127.8, 125.8, 88.1 (C_{ipso} η^5-<u>C$_5$</u>H$_4$-alkyl), 84.4 (C_{ipso} η^5-<u>C$_5$</u>H$_4$- naphthoyl), 84.6 (C_{ipso} η^5-<u>C$_5$</u>H$_4$-naphthoyl), 71.0 (C_{meta} η^5-<u>C$_5$</u>H$_4$-naphthoyl), 69.6 (C_{meta} η^5-<u>C$_5$</u>H$_4$-alkyl), 68.8 (C_{ortho} η^5-<u>C$_5$</u>H$_4$-alkyl), 66.2 (C_{ortho} η^5-<u>C$_5$</u>H$_4$-naphthoyl), 14.3 (-<u>C</u>H$_3$).

1'-Ethyl-6-ferrocenyl-2-naphthoic acid (61)

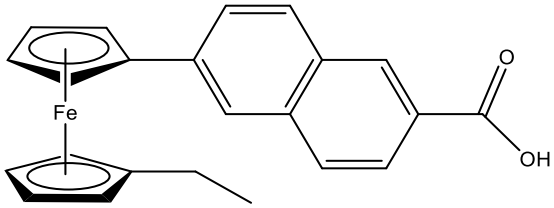

The synthesis followed that of 1'-methyl-6-ferrocenyl-methyl-2-naphthoate using the following reagents: 1'-ethyl-6-ferrocenyl-methyl-2-naphthoate (5.00 g, 12.6 mmol), methanol (80ml), 10% NaOH solution (80 ml). Vacuum filtrated the precipitate and wash with deionised water yielding product as an orange oil (3.32 g, 70%);

^{1}H NMR (400 MHz) δ (DMSO): 12.73 (1H, br. s, -COOH), 8.58 (1H, t, *J* = 8.4 Hz, ArH), 8.03 (1H, dd, *J* = 1.6 and 8.8 Hz, ArH), 7.85-7.76 (3H, m, ArH), 7.64 (1H, dd, *J* = 1.6 and 8.8 Hz, ArH), 4.65 (2H, t, *J* = 2.0 Hz, *ortho* on η^5-C_5H_4-naphthoyl), 4.23 (2H, t, *J* = 2.0 Hz, , *meta* on η^5-C_5H_4-naphthoyl), 3.94 (2H, t, *J* = 2.0 Hz, *meta* on η^5-C_5H_4-alkyl), 3.98 (2H, t, *J* = 2.0 Hz, *ortho* on η^5-C_5H_4-alkyl), 2.41 (1H, q, *J* = 7.2Hz, -$CH_2$$CH_3$), 2.12 (1H, q, *J* = 7.2Hz, -$CH_2$$CH_3$), 1.25 (1H, t, *J* = 7.2Hz, -CH_2CH_3), 1.00 (2H, t, *J* = 7.2Hz, -CH_2CH_3);

^{13}C NMR (100 MHz) δ ($CDCl_3$): 168.5 (C=O), 134.8 (C_q), 132.9 (C_q), 131.8 (C_q), 131.4, 128.3, 128.6, 127.7, 126.7 (C_q), 124.1, 123.0, 89.4 (C_{ipso} η^5-C_5H_4-alkyl), 84.0 (C_{ipso} η^5-C_5H_4- naphthoyl), 71.4 (C_{meta} η^5-C_5H_4-naphthoyl), 69.4 (C_{meta} η^5-C_5H_4-alkyl), 68.5 (C_{ortho} η^5-C_5H_4-alkyl), 65.9 (C_{ortho} η^5-C_5H_4-naphthoyl), 21.5 (-CH_2CH_3, -ve DEPT), 14.7 (-CH_2CH_3).

General procedure for the synthesis of N-(1'-methyl-6-ferrocenyl-2-naphthoyl) amino acid and dipeptide esters

_N_-(1'-methyl-6-ferrocenyl-2-naphthoyl)-glycine-glycine methyl ester (62)

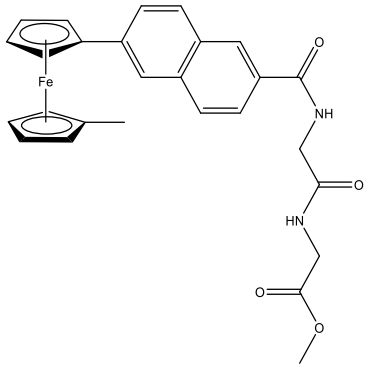

1'-Methyl-6-ferrocenyl-2-naphthoic acid (1.00 g, 0.27 mmol) was dissolved in dichloromethane (100 ml) at 0 °C. *N*-(3-dimethylaminopropyl)-*N*'-ethylcarbodiimide hydrochloride (0.05 g, 0.27 mmol), *N*-hydroxysuccinimide (0.03 g, 0.27 mmol), glycine-glycine methyl ester (0.39 g, 0.27 mmol) and triethylamine (3 ml) were added and the reaction mixture was stirred at 0 °C. After 45 minutes, the solution was raised to room temperature and stirred for 48 hours. The reaction mixture was washed with water. The organic layer was dried over $MgSO_4$ and the solvent was removed *in vacuo.* The crude product was purified by column chromatography {eluent 1:1 hexane: ethyl acetate} yielding the title compound as an orange solid (0.24 g, 18%), mp: 162 - 164 °C;

I.R. υ_{max} (neat): 3307 (NH), 3264 (NH), 1748 ($C=O_{ester}$), 1629 ($C=O_{amide\ I}$),1623 ($C=O_{amide\ I}$), 1600 ($C=O_{amide\ II}$) cm^{-1};

UV-Vis λ_{max} (CH_3CN): 369, 450 nm;

^{1}H NMR (400 MHz) δ ($CDCl_3$): 8.28-8.24 (1H, m, Ar<u>H</u>), 7.82-7.75 (4H, m, Ar<u>H</u>), 7.57 (1H, dd, *J* = 1.6 and 8.8 Hz, Ar<u>H</u>), 7.13 (1H, t, *J* = 5.6 Hz, -CON<u>H</u>-), 6.73 (1H, t, *J* = 5.6 Hz, -CON<u>H</u>-), 4.59 (2H, t, *J* = 2.0 Hz, *ortho* on η^5-C_5<u>H_4</u>-naphthoyl), 4.26 (2H, t, *J* = 2.0 Hz, *meta* on η^5-C_5<u>H_4</u>-naphthoyl), 4.21 (2H, d, *J* = 6.1 Hz, -NHC<u>H_2</u>CO-), 4.12 (3H, s, -OC<u>H_3</u>), 4.02 (2H, d, *J* = 6.1 Hz, -NHC<u>H_2</u>CO-), 3.91 (2H, t, *J* = 2.0 Hz, *meta* on η^5-C_5<u>H_4</u>-alkyl), 3.87 (2H, t, *J* = 2.0 Hz, *ortho* on η^5-C_5<u>H_4</u>-alkyl), 2.22 (0.5H, s, -C<u>H_3</u>), 2.03 (1H, s, -C<u>H_3</u>), 1.64 (1.5H, s, -C<u>H_3</u>);

^{13}C NMR (100 MHz) δ ($CDCl_3$): 170.3 (C=O), 169.9 (C=O), 166.6 (C=O), 139.4 (C_q), 135.0 (C_q), 131.0 (C_q), 130.4 (C_q), 129.3, 128.0, 127.5, 125.9, 124.1, 122.8, 90.2 (C_{ipso} η^5-<u>C</u>$_5$H$_4$-alkyl), 85.1 (C_{ipso} η^5-<u>C</u>$_5$H$_4$-naphthoyl), 69.5 (C_{meta} η^5-<u>C</u>$_5$H$_4$-naphthoyl), 67.1 (C_{meta} η^5-<u>C</u>$_5$H$_4$-alkyl), 66.3 (C_{ortho} η^5-<u>C</u>$_5$H$_4$-alkyl), 65.7 (C_{ortho} η^5-<u>C</u>$_5$H$_4$-naphthoyl), 51.7 (-O<u>C</u>H$_3$), 44.7 (-NH<u>C</u>H$_2$-, -ve DEPT), 40.5 (-NH<u>C</u>H$_2$-, -ve DEPT), 15.0 (-<u>C</u>H$_3$).

***N*-(1'-methyl-6-ferrocenyl-2-naphthoyl)-glycine-glycine ethyl ester (63)**

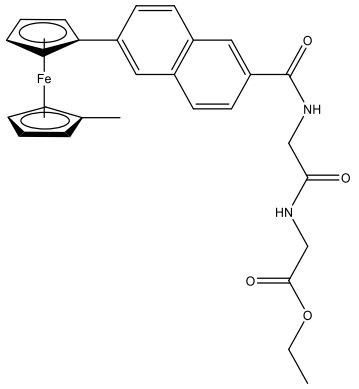

The synthesis followed that of *N*-(1'-methyl-6-ferrocenyl-2-naphthoyl)-glycine-glycine methyl ester using the following reagent: glycine-glycine ethyl ester (0.42 g, 0.27 mmol). The crude product was purified by column chromatography {eluent 1:1 hexane: ethyl acetate} yielding the title compound as an orange solid (0.50 g, 37%), mp: 125 - 127 ^{o}C;

HRMS (ESI^{+}) *m/z*: 512.1171 $[M]^{+\bullet}$, $C_{28}H_{28}N_2O_4Fe$ requires 512.1398;

I.R. υ_{max} (neat): 3300 (NH), 3276 (NH), 1740 ($C=O_{ester}$), 1630 ($C=O_{amide\ I}$), 1626 ($C=O_{amide\ I}$), 1608 ($C=O_{amide\ II}$) cm^{-1};

UV-Vis λ_{max} (CH_3CN): 367, 450 nm;

^{1}H NMR (600 MHz) δ ($CDCl_3$): 8.27-8.20 (1H, m, ArH), 7.80-7.73 (4H, m, ArH), 7.55 (1H, dd, *J* = 1.6 and 8.8 Hz, ArH), 7.53 (1H, t, *J* = 5.6 Hz, -CONH-), 7.18 (1H, t, *J* = 5.6 Hz, -CONH-), 4.64 (2H, t, *J* = 2.0 Hz, *ortho* on η^5-C_5H_4-naphthoyl), 4.29 (2H, t, *J* = 2.0 Hz, *meta* on η^5-C_5H_4-naphthoyl), 4.21 (2H, d, *J* = 6.1 Hz, -NHCH_2CO-), 4.14 (2H, q, *J* = 7.2 Hz, -OCH_2CH$_3$), 4.02 (2H, d, *J* = 7.3 Hz, -CONHCH_2CO-), 3.91 (2H, t, *J* = 2.0 Hz , *meta* on η^5-C_5H_4-alkyl), 3.87（2H, t, *J* = 2.0 Hz , *ortho* on η^5-C_5H_4-alkyl), 2.19 (0.5H, s, -CH$_3$), 2.00 (1H, s, -CH$_3$), 1.61 (1.5H, s, -CH$_3$), 1.17 (3H, t, *J* = 7.2 Hz, -OCH$_2$CH$_3$);

^{13}C NMR (100 MHz) δ ($CDCl_3$): 172.9 (C=O), 169.4 (C=O), 167.8 (C=O), 134.8 (C_q), 133.0 (C_q), 130.7 (C_q), 130.2 (C_q), 128.8, 127.8, 127.4, 124.8, 124.0, 120.8, 90.1 (C_{ipso} η^5-C_5H_4-alkyl), 86.5 (C_{ipso} η^5-C_5H_4-naphthoyl), 71.7 (C_{meta} η^5-C_5H_4-naphthoyl), 69.9 (C_{meta} η^5-C_5H_4-alkyl), 69.7 (C_{ortho} η^5-C_5H_4-alkyl), 67.3 (C_{ortho} η^5-C_5H_4-naphthoyl), 61.5 (-OCH$_2$CH$_3$, -ve DEPT), 43.8 (-NHCH$_2$-, -ve DEPT), 41.2 (-NHCH$_2$-, -ve DEPT), 15.2 (-CH$_3$), 14.1 (-OCH$_2$$CH_3$).

***N*-(1'-methyl-6-ferrocenyl-2-naphthoyl)-glycine-L-alanine methyl ester (64)**

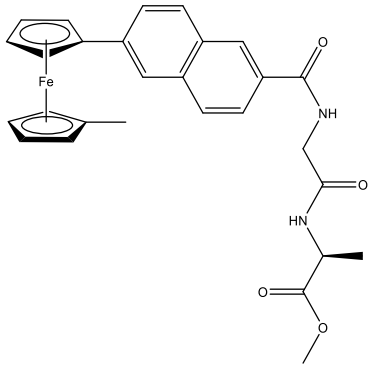

The synthesis followed that of *N*-(1'-methyl-6-ferrocenyl-2-naphthoyl)-glycine-glycine methyl ester using the following reagent: glycine-L-alanine methyl ester (0.43 g, 0.27 mmol). The crude product was purified by column chromatography {eluent 1:1 hexane: ethyl acetate} yielding the title compound as a light orange solid (0.24 g, 17%), mp: 142 - 144 ^{o}C;

I.R. υ_{max} (neat): 3290 (NH), 3090 (NH), 1747 (C=O$_{ester}$), 1640 (C=O$_{amide\ I}$), 1620 (C=O$_{amide\ I}$), 1521 (C=O$_{amide\ II}$) cm^{-1};

UV-Vis λ_{max} (CH_3CN): 376, 452 nm;

^{1}H NMR (400 MHz) δ ($CDCl_3$): 8.13-8.04 (1H, m, ArH), 7.79-7.73 (4H, m, ArH), 7.48 (1H, dd, *J* = 1.6 and 8.8 Hz, ArH), 7.21 (1H, t, *J* = 5.6 Hz, -CONH-), 6.84 (1H, t, *J* = 5.6 Hz, -CONH-), 4.62 (2H, t, *J* = 2.0 Hz, *ortho* on η^5-C_5H_4-naphthoyl), 4.54 (1H, q, *J* = 7.3 Hz, -CHCH$_3$), 4.29 (2H, t, *J* = 2.0 Hz, *meta* on η^5-C_5H_4-naphthoyl), 4.26 (2H, d, *J* = 7.3 Hz, -NHCH$_2$-), 4.00 (2H, t, *J* = 2.0 Hz , *meta* on η^5-C_5H_4-alkyl), 3.87 (2H, t, *J* = 2.0 Hz , *ortho* on η^5-C_5H_4-alkyl), 3.63 (3H, s, -OCH$_3$), 2.21 (0.5H, s, -CH$_3$), 2.04 (1H, s, -CH$_3$), 1.62 (1.5H, s, -CH$_3$), 1.32 (3H, d, *J* = 7.3 Hz, -CHCH$_3$);

^{13}C NMR (100 MHz) δ ($CDCl_3$): 172.5 (C=O), 169.0 (C=O), 167.5 (C=O), 139.4 (C$_q$), 136.0 (C$_q$), 131.3 (C$_q$), 130.4 (C$_q$), 128.7, 128.0, 126.9, 126.0, 124.4, 122.8, 88.8 (C$_{ipso}$ η^5-C$_5$H$_4$-alkyl), 84.0 (C$_{ipso}$ η^5-C$_5$H$_4$-naphthoyl), 70.5 (C$_{meta}$ η^5-C$_5$H$_4$-naphthoyl), 68.1 (C$_{meta}$ η^5-C$_5$H$_4$-alkyl), 67.9 (C$_{ortho}$ η^5-C$_5$H$_4$-alkyl), 66.2 (C$_{ortho}$ η^5-C$_5$H$_4$-naphthoyl), 51.7 (-OCH$_3$), 49.6 (-CHCH$_3$), 43.0 (-NHCH$_2$-, -ve DEPT), 18.1 (-CHCH$_3$), 15.0 (-CH$_3$).

***N*-(1'-methyl-6-ferrocenyl-2-naphthoyl)-glycine-L-alanine ethyl ester (65)**

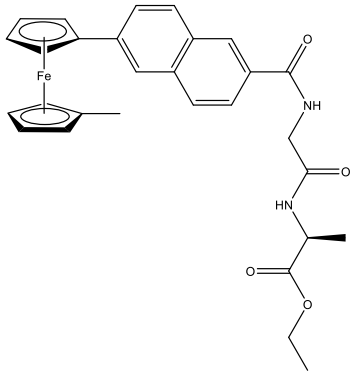

The synthesis followed that of *N*-(1'-methyl-6-ferrocenyl-2-naphthoyl)-glycine-glycine methyl ester using the following reagent: glycine-L-alanine ethyl ester (0.47g, 0.27 mmol). The crude product was purified by column chromatography {eluent 1:1 hexane: ethyl acetate} yielding the title compound as a dark orange solid (0.34 g, 23%), mp: 154 - 156 ^{o}C;

I.R. υ_{max} (neat): 3289 (NH), 3079 (NH), 1734 (C=O_{ester}), 1640 (C=$O_{amide\ I}$), 1624 (C=$O_{amide\ I}$), 1522 (C=$O_{amide\ II}$) cm^{-1};

UV-Vis λ_{max} (CH_3CN): 373, 453 nm;

^{1}H NMR (600 MHz) δ ($CDCl_3$): 8.30-8.24 (1H, m, ArH), 7.84-7.73 (4H, m, ArH), 7.61 (1H, dd, *J* = 1.6 and 8.8 Hz, ArH), 7.22 (1H, t, *J* = 5.6 Hz, -CONH-), 6.83 (1H, t, *J* = 5.6 Hz, -CONH-), 4.63 (2H, t, *J* = 2.0 Hz, *ortho* on η^5-C_5H_4-naphthoyl), 4.54 (1H, q, *J* = 7.3 Hz, -CHCH$_3$), 4.29 (2H, t, *J* = 2.0 Hz, *meta* on η^5-C_5H_4-naphthoyl), 4.26 (2H, d, *J* = 7.3 Hz, -NHCH_2-), 4.21 (2H, q, *J* = 7.2 Hz, -OCH_2CH$_3$), 4.00 (2H, t, *J* = 2.0 Hz, *meta* on η^5-C_5H_4-alkyl), 3.85 (2H, t, *J* = 2.0 Hz , *ortho* on η^5-C_5H_4-alkyl), 2.21 (0.5H, s, -CH$_3$), 2.02 (1H, s, -CH$_3$), 1.63 (1.5H, s, -CH$_3$), 1.40 (3H, d, *J* =7.3 Hz, -CHCH$_3$), 1.22 (3H, t, *J* = 7.2 Hz, -OCH$_2$CH$_3$);

^{13}C NMR (100 MHz) δ ($CDCl_3$): 173.1 (C=O), 169.0 (C=O), 167.7 (C=O), 139.2 (C_q), 135.6 (C_q), 131.6 (C_q), 130.3 (C_q), 128.9, 128.4, 127.9, 126.1, 124.0, 122.9, 89.3 (C_{ipso} η^5-C_5H_4-alkyl), 85.8 (C_{ipso} η^5-C_5H_4-naphthoyl), 71.3 (C_{meta} η^5-C_5H_4-naphthoyl), 68.8 (C_{meta} η^5-C_5H_4-alkyl), 67.2 (C_{ortho} η^5-C_5H_4-alkyl), 65.9 (C_{ortho} η^5-C_5H_4-naphthoyl), 61.7 (-OCH$_2$CH$_3$, -ve DEPT), 48.4 (-CHCH$_3$), 43.6 (-NHCH$_2$-, -ve DEPT), 18.3 (-CHCH$_3$), 14.9 (-OCH$_2$CH$_3$), 14.8 (-CH$_3$).

***N*-(1'-methyl-6-ferrocenyl-2-naphthoyl)-glycine-D-alanine methyl ester (66)**

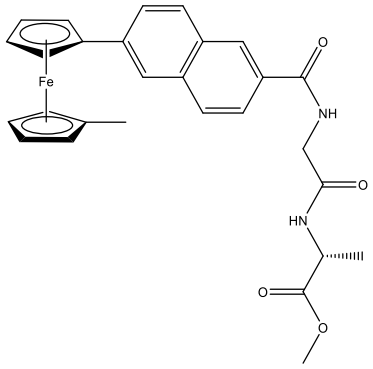

The synthesis followed that of *N*-(1'-methyl-6-ferrocenyl-2-naphthoyl)-glycine-glycine methyl ester using the following reagent: glycine-D-alanine methyl ester (0.43 g, 0.27 mmol). The crude product was purified by column chromatography {eluent 1:1 hexane: ethyl acetate} yielding the title compound as a light orange solid (0.28 g, 20%), mp: 139 - 140 ^{o}C;

I.R. υ_{max} (neat): 3286 (NH), 3078 (NH), 1739 (C=O_{ester}), 1643 (C=$O_{amide\ I}$), 1625 (C=$O_{amide\ I}$), 1521 (C=$O_{amide\ II}$) cm^{-1};

UV-Vis λ_{max} (CH_3CN): 376, 455 nm;

^{1}H NMR (400 MHz) δ ($CDCl_3$): 8.25 (1H, t, *J* = 8.4 Hz, Ar<u>H</u>), 7.79-7.73 (4H, m, Ar<u>H</u>), 7.60 (1H, dd, *J* = 1.6 and 8.8 Hz, Ar<u>H</u>), 7.35 (1H, t, *J* = 5.6 Hz, -CON<u>H</u>-), 7.09 (1H, t, *J* = 5.6 Hz, -CON<u>H</u>-), 4.67 (2H, t, *J* = 2.0 Hz, *ortho* on η^5-C_5<u>H_4</u>-naphthoyl), 4.59 (1H, q, *J* = 7.3 Hz, -C<u>H</u>CH_3), 4.32 (2H, t, *J* = 2.0 Hz, *meta* on η^5-C_5<u>H_4</u>-naphthoyl), 4.22 (2H, d, *J* = 7.3 Hz, -NHC<u>H_2</u>-), 3.94 (2H, t, *J* = 2.0 Hz , *meta* on η^5-C_5<u>H_4</u>-alkyl), 3.90 (2H, t, *J* = 2.0 Hz , *ortho* on η^5-C_5<u>H_4</u>-alkyl), 3.69 (3H, s, -OC<u>H_3</u>), 2.21 (0.5H, s, -C<u>H_3</u>), 2.02 (1H, s, -C<u>H_3</u>), 1.63 (1.5H, s, -C<u>H_3</u>), 1.41 (3H, d, *J* = 7.3 Hz, -CHC<u>H_3</u>);

^{13}C NMR (100 MHz) δ ($CDCl_3$): 172.6 (C=O), 169.3 (C=O), 167.5 (C=O), 139.2 (C_q), 135.2 (C_q), 131.1 (C_q), 130.6 (C_q), 129.0, 128.4, 127.9, 126.0, 124.2, 122.8, 89.1 (C_{ipso} η^5-<u>C</u>$_5H_4$-alkyl), 84.2 (C_{ipso} η^5-<u>C</u>$_5H_4$-naphthoyl), 70.6 (C_{meta} η^5-<u>C</u>$_5H_4$-naphthoyl), 68.1 (C_{meta} η^5-<u>C</u>$_5H_4$-alkyl), 67.4 (C_{ortho} η^5-<u>C</u>$_5H_4$-alkyl), 66.3 (C_{ortho} η^5-<u>C</u>$_5H_4$-naphthoyl), 51.6 (-O<u>C</u>H_3), 49.6 (-<u>C</u>HCH_3), 43.1 (-NH<u>C</u>H_2-, -ve DEPT), 18.2 (-CH<u>C</u>H_3), 15.3 (-<u>C</u>H_3).

***N*-(1'-methyl-6-ferrocenyl-2-naphthoyl)-glycine-D-alanine ethyl ester (67)**

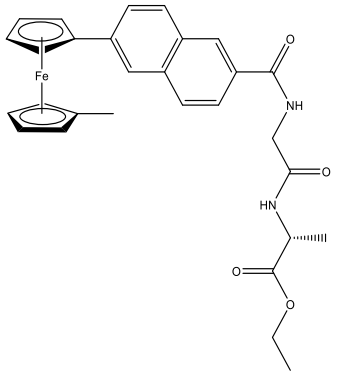

The synthesis followed that of *N*-(1'-methyl-6-ferrocenyl-2-naphthoyl)-glycine-glycine methyl ester using the following reagent: glycine-D-alanine ethyl ester (0.47g, 0.27 mmol) The crude product was purified by column chromatography {eluent 1:1 hexane: ethyl acetate} yielding the title compound as a dark orange solid (0.22 g, 15%), mp: 142 - 143 ^{o}C;

I.R. υ_{max} (neat): 3286 (NH), 3093 (NH), 1736 (C=O_{ester}), 1626 (C=$O_{amide\ I}$), 1608 (C=$O_{amide\ I}$), 1518 (C=$O_{amide\ II}$) cm^{-1};

UV-Vis λ_{max} (CH_3CN): 379, 455 nm;

^{1}H NMR (600 MHz) δ ($CDCl_3$): 8.23(1H, t, *J* = 8.4 Hz, Ar<u>H</u>), 7.80-7.73 (4H, m, Ar<u>H</u>), 7.74 (1H, dd, *J* = 1.6 and 8.8 Hz, Ar<u>H</u>), 6.98 (1H, t, *J* = 5.6 Hz, -CON<u>H</u>-), 6.51 (1H, t, *J* = 5.6 Hz, -CON<u>H</u>-), 4.74 (2H, t, *J* = 2.0 Hz, *ortho* on η^5-C_5<u>H</u>$_4$-naphthoyl), 4.58 (1H, t, *J* = 7.3 Hz, -C<u>H</u>CH_3), 4.39 (2H, t, *J* = 2.0 Hz, *meta* on η^5-C_5<u>H</u>$_4$-naphthoyl), 4.18 (2H, d, *J* = 7.3 Hz, -NHC<u>H</u>$_2$-), 4.13 (2H, q, *J* = 7.2 Hz, -OC<u>H</u>$_2$$CH_3$), 4.07 (2H, t, *J* = 2.0 Hz , *meta* on η^5-C_5<u>H</u>$_4$-alkyl), 3.97 (2H, t, *J* = 2.0 Hz , *ortho* on η^5-C_5<u>H</u>$_4$-alkyl), 2.17 (0.5H, s, -C<u>H</u>$_3$), 2.02 (1H, s, -C<u>H</u>$_3$), 1.61 (1.5H, s, -C<u>H</u>$_3$), 1.39 (3H, d, *J* =7.3 Hz, -CHC<u>H</u>$_3$), 1.24 (3H, t, *J* = 7.2 Hz, -OCH$_2$C<u>H</u>$_3$);

^{13}C NMR (100 MHz) δ ($CDCl_3$): 173.2 (C=O), 169.3 (C=O), 167.5 (C=O), 139.1 (C_q), 135.8 (C_q), 131.3 (C_q), 130.7 (C_q), 128.6, 128.4, 127.0, 126.8, 124.8, 122.2, 89.0 (C_{ipso} η^5-<u>C</u>$_5$H$_4$-alkyl), 84.2 (C_{ipso} η^5-<u>C</u>$_5$H$_4$- naphthoyl), 71.0 (C_{meta} η^5-<u>C</u>$_5$H$_4$-naphthoyl), 69.0 (C_{meta} η^5-<u>C</u>$_5$H$_4$-alkyl), 67.4 (C_{ortho} η^5-<u>C</u>$_5$H$_4$-alkyl), 66.1 (C_{ortho} η^5-<u>C</u>$_5$H$_4$-naphthoyl), 61.6 (-O<u>C</u>H$_2$$CH_3$, -ve DEPT), 47.9 (-<u>C</u>HCH_3), 43.6 (-NH<u>C</u>H$_2$-, -ve DEPT), 17.9 (-CH<u>C</u>H$_3$), 15.0 (-OCH$_2$<u>C</u>H$_3$), 14.8 (-<u>C</u>H$_3$).

***N*-(1'-methyl-6-ferrocenyl-2-naphthoyl)-γ-aminobutyric acid methyl ester (68)**

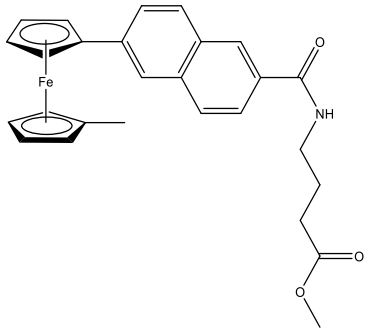

The synthesis followed that of *N*-(1'-methyl-6-ferrocenyl-2-naphthoyl)-glycine-glycine methyl ester using the following reagent: gamma-aminobutyric acid methyl ester (0.31 g, 0.27 mmol). The crude product was purified by column chromatography {eluent 1:1 hexane: ethyl acetate} yielding the title compound as a dark orange solid (0.72 g, 57%), mp: 175 - 178 ^{o}C;

HRMS (ESI^{+}) *m/z*: 469.1082 $[M]^{+\bullet}$, $C_{27}H_{27}NO_3Fe$ requires 469.1340;

I.R. υ_{max} (neat): 3280 (NH), 1721 ($C{=}O_{ester}$), 1600 ($C{=}O_{amide}$) cm^{-1};

UV-Vis λ_{max} (CH_3CN): 379, 454 nm;

^{1}H NMR (600 MHz) δ ($CDCl_3$): 8.23-8.17 (1H, m, Ar<u>H</u>), 7.86-7.58 (4H, m, Ar<u>H</u>), 7.50-7.45 (1H, m, Ar<u>H</u>), 6.65 (1H, t, *J* = 5.6 Hz, -CON<u>H</u>-), 4.66 (2H, t, *J* = 2.0 Hz, *ortho* on η^5-C_5<u>H</u>$_4$-naphthoyl), 4.29 (2H, t, *J* = 2.0 Hz, *meta* on η^5-C_5<u>H</u>$_4$-naphthoyl), 4.00 (2H, t, *J* = 2.0 Hz , *meta* on η^5-C_5<u>H</u>$_4$-alkyl), 3.87 (2H, t, *J* = 2.0 Hz, *ortho* on η^5-C_5<u>H</u>$_4$-alkyl), 3.61 (3H, s, -OC<u>H</u>$_3$), 3.52 (2H, q, *J* = 6.5 Hz, -NHC<u>H</u>$_2$CH$_2$CH$_2$-), 2.44 (2H, t, *J* = 6.5 Hz, -NHCH$_2$CH$_2$C<u>H</u>$_2$CO-), 1.92 (2H, qt, *J* = 6.5 Hz, -NHCH$_2$C<u>H</u>$_2$CH$_2$-), 2.21 (0.5H, s, -C<u>H</u>$_3$), 2.01 (1H, s, -C<u>H</u>$_3$), 1.63 (1.5H, s, -C<u>H</u>$_3$),;

^{13}C NMR (100 MHz) δ ($CDCl_3$): 172.9 (C=O), 168.0 (C=O), 139.5 (C_q), 138.9 (C_q), 134.6 (C_q), 131.7 (C_q), 129.0, 128.4, 127.7, 126.6, 123.9, 123.0, 89.1 (C_{ipso} η^5-<u>C</u>$_5$H$_4$-alkyl), 84.9 (C_{ipso} η^5-<u>C</u>$_5$H$_4$-naphthoyl), 70.2 (C_{meta} η^5-<u>C</u>$_5$H$_4$-naphthoyl), 68.8 (C_{meta} η^5-<u>C</u>$_5$H$_4$-alkyl), 67.3 (C_{ortho} η^5-<u>C</u>$_5$H$_4$-alkyl), 65.8 (C_{ortho} η^5-<u>C</u>$_5$H$_4$-naphthoyl), 51.7 (-O<u>C</u>H$_3$), 39.8 (-NH<u>C</u>H$_2$CH$_2$CH$_2$-, -ve DEPT), 31.8 (-NHCH$_2$CH$_2$<u>C</u>H$_2$-, -ve DEPT), 24.6 (-NHCH$_2$<u>C</u>H$_2$CH$_2$-, -ve DEPT), 13.8 (-<u>C</u>H$_3$).

***N*-(1'-methyl-6-ferrocenyl-2-naphthoyl) -γ-aminobutyric acid ethyl ester (69)**

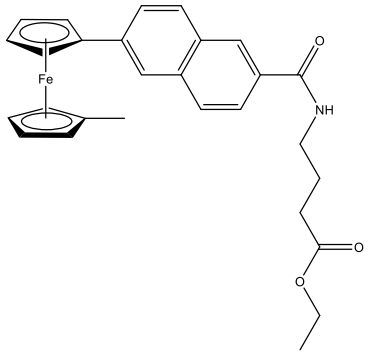

The synthesis followed that of *N*-(1'-methyl-6-ferrocenyl-2-naphthoyl)-glycine-glycine methyl ester using the following reagent: gamma-aminobutyric acid ethyl ester (0.34 g, 0.27 mmol). The crude product was purified by column chromatography {eluent 1:1 hexane: ethyl acetate} yielding the title compound as a dark orange solid (0.34 g, 32%), mp: 196 - 198 ^{o}C;

HRMS (ESI^{+}) *m/z*: 483.1474 $[M]^{+\bullet}$, $C_{28}H_{29}NO_3Fe$ requires 483.1497;

I.R. υ_{max} (neat): 3283 (NH), 1726 ($C{=}O_{ester}$), 1605 ($C{=}O_{amide}$) cm^{-1};

UV-Vis λ_{max} (CH_3CN): 371, 447 nm;

^{1}H NMR (600 MHz) δ ($CDCl_3$): 8.21-8.17 (1H, m, Ar<u>H</u>), 7.84-7.74 (4H, m, Ar<u>H</u>), 7.61 (1H, dd, *J* = 1.6 and 8.8 Hz, Ar<u>H</u>), 6.68 (1H, t, *J* = 5.6 Hz, -CON<u>H</u>-), 4.65 (2H, t, *J* = 2.0 Hz, *ortho* on η^5-C_5<u>H_4</u>-naphthoyl), 4.29 (2H, t, *J* = 2.0 Hz, *meta* on η^5-C_5<u>H_4</u>-naphthoyl), 4.10 (2H, q, *J* = 7.3 Hz, -OC<u>H_2</u>CH_3), 4.00 (2H, t, *J* = 2.0 Hz , *meta* on η^5-C_5<u>H_4</u>-alkyl), 3.86 (2H, t, *J*= 2.0 Hz ,*ortho* on η^5-C_5<u>H_4</u>-alkyl), 3.53 (2H, q, *J* = 6.5 Hz, -NHC<u>H_2</u>CH_2CH_2-), 2.40 (2H, t, *J* = 6.5 Hz, -$NHCH_2CH_2$C<u>H_2</u>-), 2.21 (0.5H, s, -C<u>H_3</u>), 2.01 (1H, s, -C<u>H_3</u>), 1.94 (2H, qt, *J* = 6.5 Hz, -$NHCH_2$C<u>H_2</u>CH_2-), 1.63 (1.5H, s, -C<u>H_3</u>), 1.18 (3H, t, *J* = 7.3 Hz ,- OCH_2C<u>H_3</u>);

^{13}C NMR (100 MHz) δ ($CDCl_3$): 173.9 (C=O), 167.9 (C=O), 139.5 (C_q), 135.1 (C_q), 131.2 (C_q), 130.7 (C_q), 128.8, 127.9, 127.2, 126.1, 123.9, 123.1, 89.4 (C_{ipso} η^5-<u>C</u>$_5H_4$-alkyl), 84.3 (C_{ipso} η^5-<u>C</u>$_5H_4$-naphthoyl), 70.4 (C_{meta} η^5-<u>C</u>$_5H_4$-naphthoyl), 68.9 (C_{meta} η^5-<u>C</u>$_5H_4$-alkyl), 67.1 (C_{ortho} η^5-<u>C</u>$_5H_4$-alkyl), 64.4 (C_{ortho} η^5-<u>C</u>$_5H_4$-naphthoyl), 60.6 (-O<u>C</u>H_2CH_3, -ve DEPT), 39.8 (-NH<u>C</u>$H_2CH_2CH_2$-, -ve DEPT), 32.1 (-$NHCH_2CH_2$<u>C</u>H_2-, -ve DEPT), 24.5 (-$NHCH_2$<u>C</u>H_2CH_2-, -ve DEPT), 14.1 (-OCH_2<u>C</u>H_3), 13.7 (-<u>C</u>H_3).

General procedure for the synthesis of N-(1'-ethyl-6-ferrocenyl-2-naphthoyl) amino acid and dipeptide esters

_N_-(1'-ethyl-6-ferrocenyl-2-naphthoyl)-glycine-glycine methyl ester (70)

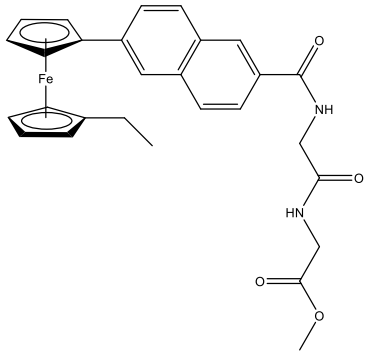

1'-Ethyl-6-ferrocenyl-2-naphthoic acid (1.12 g, 0.27 mmol) was dissolved in dichloromethane (100 ml) at 0 ^{o}C. *N*-(3-dimethylaminopropyl)-*N*'-ethylcarbodiimide hydrochloride (0.05 g, 0.27 mmol), *N*-hydroxysuccinimide (0.03 g, 0.27 mmol), glycine-glycine methyl ester (0.42 g, 0.27 mmol) and triethylamine (3 ml) were added and the reaction mixture was stirred at 0 ^{o}C. After 45 minutes, the solution was raised to room temperature and stir for 48 hours. The reaction mixture was washed with water. The organic layer was dried over $MgSO_4$ and the solvent was removed *in vacuo.* The crude product was purified by column chromatography {eluent 1:1 hexane: ethyl acetate} yielding the title compound as an orange oil (0.17 g, 13%);

HRMS (ESI^+) *m/z*: 512.1429 $[M]^{+\bullet}$, $C_{28}H_{28}N_2O_4Fe$ requires 512.1398;

I.R. υ_{max} (neat): 3303 (NH), 3081 (NH), 1744 ($C=O_{ester}$), 1643 ($C=O_{amide\ I}$), 1626 ($C=O_{amide\ I}$), 1522 ($C=O_{amide\ II}$) cm^{-1};

UV-Vis λ_{max} (CH_3CN): 368, 454 nm;

^{1}H NMR (400 MHz) δ ($CDCl_3$): 8.28-8.24 (1H, m, Ar<u>H</u>), 7.90-7.76 (4H, m, Ar<u>H</u>), 7.63 (1H, dd, *J* = 1.6 and 8.8 Hz, Ar<u>H</u>), 7.14 (1H, t, *J* = 5.4 Hz, -CON<u>H</u>-), 6.79 (1H, t, *J* = 5.4 Hz, -CON<u>H</u>-), 4.67 (2H, t, *J* = 2.0 Hz, *ortho* on η^5-C_5<u>H_4</u>-naphthoyl), 4.31 (2H, t, *J* = 2.0 Hz, *meta* on η^5-C_5<u>H_4</u>-naphthoyl), 4.23 (2H, d, *J* = 6.0 Hz, -NHC<u>H_2</u>$COOCH_3$), 4.06 (2H, d, *J* = 6.0 Hz, -CONHC<u>H_2</u>CO-), 4.04 (3H, s, -OC<u>H_3</u>), 3.94-3.71 (4H, m, η^5-C_5<u>H_4</u>-alkyl), 2.62 (0.5H, q, *J* = 8.0 Hz, -C<u>H_2</u>CH_3), 2.39 (0.5H, q, *J* = 8.0 Hz, -C<u>H_2</u>CH_3), 2.14 (1H, q, *J* = 8.0 Hz, -C<u>H_2</u>CH_3), 1.21 (1.5H, t, *J* = 8.0 Hz, -CH_2C<u>H_3</u>), 0.99 (1.5H, t, *J* = 8.0 Hz, -CH_2C<u>H_3</u>);

^{13}C NMR (100 MHz) δ ($CDCl_3$): 169.8 (C=O), 169.6 (C=O), 166.6 (C=O), 139.3 (C_q), 134.4 (C_q), 132.3 (C_q), 131.2 (C_q), 128.7, 127.9, 126.7, 123.3, 123.0, 122.5, 89.9 (C_{ipso} η^5-<u>C</u>$_5H_4$-alkyl), 85.7 (C_{ipso} η^5-<u>C</u>$_5H_4$-naphthoyl), 70.2 (C_{meta} η^5-<u>C</u>$_5H_4$-naphthoyl), 68.4 (C_{meta} η^5-<u>C</u>$_5H_4$-alkyl), 67.4 (C_{ortho} η^5-<u>C</u>$_5H_4$-

alkyl), 65.8 (C_{ortho} η^5-$\underline{C}_5H_4$-naphthoyl), 51.8 (-O$\underline{C}H_3$), 43.4 (-NH$\underline{C}H_2$-, -ve DEPT), 40.7 (-NH$\underline{C}H_2$-, -ve DEPT), 21.7 (-$\underline{C}H_2CH_3$, -ve DEPT), 14.7 (-$CH_2\underline{C}H_3$).

***N*-(1'-ethyl-6-ferrocenyl-2-naphthoyl)-glycine-glycine ethyl ester (71)**

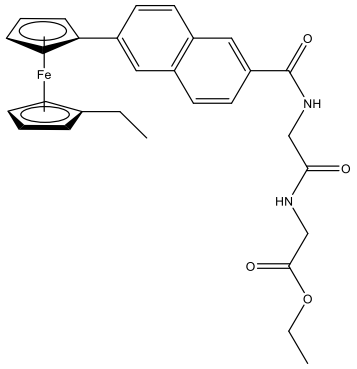

The synthesis followed that of *N*-(1'-ethyl-6-ferrocenyl-2-naphthoyl)-glycine-glycine methyl ester using the following reagent: glycine-glycine ethyl ester (0.39 g, 0.27 mmol). The crude product was purified by column chromatography {eluent 1:1 hexane: ethyl acetate} yielding the title compound as an orange oil (0.21 g, 16%);

I.R. υ_{max} (neat): 3371 (NH), 3350 (NH), 1733 ($C=O_{ester}$), 1645 ($C=O_{amide\ I}$), 1626 ($C=O_{amide\ I}$), 1523 ($C=O_{amide\ II}$) cm^{-1};

UV-Vis λ_{max} (CH_3CN): 367, 454 nm;

^{1}H NMR (600 MHz) δ ($CDCl_3$): 7.93-7.90 (1H, m, Ar<u>H</u>), 7.76-7.74 (4H, m, Ar<u>H</u>), 7.06 (1H, dd, *J* = 1.6 and 8.8 Hz, Ar<u>H</u>), 6.99 (1H, t, *J* = 5.6 Hz, -CON<u>H</u>-), 6.51 (1H, t, *J* = 5.6 Hz, -CON<u>H</u>-), 4.68 (2H, t, *J* = 2.0 Hz, *ortho* on η^5-C_5<u>H_4</u>-naphthoyl), 4.33 (2H, t, *J* = 2.0 Hz, *meta* on η^5-C_5<u>H_4</u>-naphthoyl), 4.21 (2H, d, *J* = 6.0 Hz, -NHC<u>H_2</u>CO-), 4.18 (2H, q, *J* = 7.2 Hz, -OC<u>H_2</u>CH_3), 4.05 (2H, d, *J* = 6.0 Hz, -CONHC<u>H_2</u>CO-), 3. 95-3.91 (4H, m , η^5-C_5<u>H_4</u>-alkyl), 2.54 (1H, q, *J* = 8.0 Hz, -C<u>H_2</u>CH_3), 2.08 (1H, q, *J* = 8.0 Hz, -C<u>H_2</u>CH_3), 1.08 (3H, t, *J* = 8.0 Hz, -CH_2C<u>H_3</u>), 0.97 (3H, t, *J* = 7.2 Hz, -OCH_2C<u>H_3</u>);

^{13}C NMR (100 MHz) δ ($CDCl_3$): 169.7 (C=O), 168.2 (C=O), 166.9 (C=O), 139.4 (C_q), 135.4 (C_q), 131.2 (C_q), 130.0 (C_q), 128.9, 128.1, 127.8, 126.1, 124.2, 122.9, 92.0 (C_{ipso} η^5-<u>C</u>$_5H_4$-alkyl), 84.2 (C_{ipso} η^5-<u>C</u>$_5H_4$-naphthoyl), 68.9 (C_{meta} η^5-<u>C</u>$_5H_4$-naphthoyl), 67.1 (C_{meta} η^5-<u>C</u>$_5H_4$-alkyl), 66.4 (C_{ortho} η^5-<u>C</u>$_5H_4$-alkyl), 65.6 (C_{ortho} η^5-<u>C</u>$_5H_4$-naphthoyl), 62.3 (-O<u>C</u>H_2CH_3, -ve DEPT), 44.4 (-NH<u>C</u>H_2-, -ve DEPT), 40.8 (-NH<u>C</u>H_2-, -ve DEPT), 21.6 (-<u>C</u>H_2CH_3, -ve DEPT), 14.9 (-OCH_2<u>C</u>H_3), 14.7 (-CH_2<u>C</u>H_3).

***N*-(1'-ethyl-6-ferrocenyl-2-naphthoyl)-glycine-L-alanine methyl ester (72)**

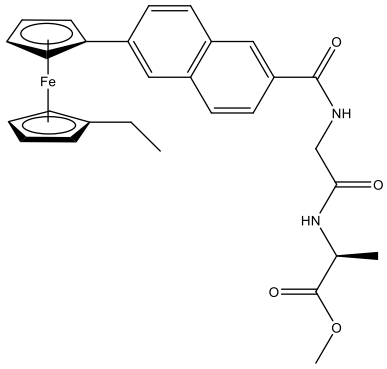

The synthesis followed that of *N*-(1'-ethyl-6-ferrocenyl-2-naphthoyl)-glycine-glycine methyl ester using the following reagent: glycine-L-alanine methyl ester (0.43 g, 0.27 mmol). The crude product was purified by column chromatography {eluent 1:1 hexane: ethyl acetate} yielding the title compound as a light orange oil (0.25 g, 18%);

I.R. υ_{max} (neat): 3387 (NH), 3090 (NH), 1737 ($C=O_{ester}$), 1642 ($C=O_{amide\ I}$), 1627($C=O_{amide\ I}$), 1529 ($C=O_{amide\ II}$) cm^{-1};

UV-Vis λ_{max} (CH_3CN): 373, 452 nm;

^{1}H NMR (400 MHz) δ ($CDCl_3$): 8.29 (1H, t, *J* = 8.4 Hz, Ar<u>H</u>), 7.90-7.73 (4H, m, Ar<u>H</u>), 7.54 (1H, dd, *J* = 1.6 and 8.8 Hz, Ar<u>H</u>), 7.25 (1H, t, *J* = 5.6 Hz, -CON<u>H</u>-), 6.91 (1H, t, *J* = 5.6 Hz, -CON<u>H</u>-), 4.56 (2H, t, *J* = 2.0 Hz, *meta* on η^5-C_5<u>H_4</u>-naphthoyl), 4.44 (1H, q, *J* = 7.3 Hz, -C<u>H</u>CH_3), 4.29 (2H, t, *J* = 2.0 Hz, *ortho* on η^5-C_5<u>H_4</u>-naphthoyl), 4.27 (2H, d, *J* = 7.3 Hz, -NHC<u>H_2</u>-), 3.92-3.86 (4H, m, η^5-C_5<u>H_4</u>-alkyl), 3.68 (3H, s, -OC<u>H_3</u>), 2.60 (0.8H, q, *J* = 7.2 Hz, - C<u>H_2</u>CH_3), 2.16 (1.2H, q, *J* = 7.2 Hz, -C<u>H_2</u>CH_3), 1.40 (3H, d, *J* =7.3 Hz, -CHC<u>H_3</u>), 1.18 (3H, t, *J* = 7.2 Hz, -CH_2C<u>H_3</u>);

^{13}C NMR (100 MHz) δ ($CDCl_3$): 172.5 (C=O), 169.1 (C=O), 167.4 (C=O), 139.4 (C_q), 135.1 (C_q), 131.3 (C_q), 130.4 (C_q), 129.6, 128.3, 127.9, 125.4, 123.3, 123.0, 89.3 (C_{ipso} η^5-<u>C</u>$_5H_4$-alkyl), 84.2 (C_{ipso} η^5-<u>C</u>$_5H_4$-naphthoyl), 71.7 (C_{meta} η^5-<u>C</u>$_5H_4$-naphthoyl), 69.3 (C_{meta} η^5-<u>C</u>$_5H_4$-alkyl), 67.1(C_{ortho} η^5-<u>C</u>$_5H_4$-alkyl), 66.2 (C_{ortho} η^5-<u>C</u>$_5H_4$-naphthoyl), 51.7 (-O<u>C</u>H_3), 49.6 (-<u>C</u>HCH_3), 43.0 (-NH<u>C</u>H_2-, -ve DEPT), 20.6 (-<u>C</u>H_2CH_3, -ve DEPT), 17.5 (-CH<u>C</u>H_3), 14.5 (-CH_2<u>C</u>H_3).

***N*-(1'-ethyl-6-ferrocenyl-2-naphthoyl)-glycine-L-alanine ethyl ester (73)**

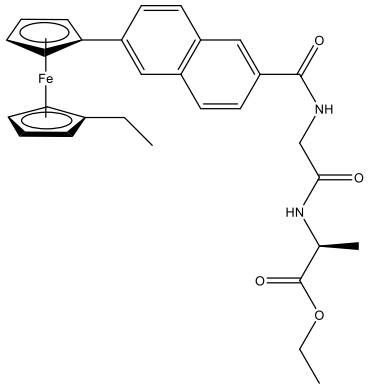

The synthesis followed that of *N*-(1'-ethyl-6-ferrocenyl-2-naphthoyl)-glycine-glycine methyl ester using the following reagent: glycine-L-alanine ethyl ester (0.47g, 0.27 mmol). The crude product was purified by column chromatography {eluent 1:1 hexane: ethyl acetate} yielding the title compound as a dark orange oil (0.35 g, 23%);

I.R. υ_{max} (neat): 3315 (NH), 3061 (NH), 1750 (C=O_{ester}), 1643 (C=$O_{amide\ I}$), 1629 (C=$O_{amide\ I}$), 1535 (C=$O_{amide\ II}$) cm^{-1};

UV-Vis λ_{max} (CH_3CN): 372, 452 nm;

^{1}H NMR (400 MHz) δ ($CDCl_3$): 8.28-8.24 (1H, m, Ar<u>H</u>), 7.82-7.69 (5H, m, Ar<u>H</u>), 7.29 (1H, t, *J* = 5.6 Hz, -CON<u>H</u>-), 6.96 (1H, t, *J* = 5.6 Hz, -CON<u>H</u>-), 4.71 (2H, t, *J* = 2.0 Hz, *ortho* on η^5-C_5<u>H_4</u>-naphthoyl), 4.53 (1H, q, *J* = 7.3 Hz, -C<u>H</u>CH_3), 4.35 (2H, t, *J* = 2.0 Hz, *meta* on η^5-C_5<u>H_4</u>-naphthoyl), 4.21 (2H, d, *J* = 7.3 Hz, -NHC<u>H_2</u>-), 4.16 (2H, q, *J* = 7.2 Hz, -OC<u>H_2</u>CH_3), 4.05 (2H, t, *J*= 2.0 Hz , *meta* on η^5-C_5<u>H_4</u>-alkyl), 3.93 (2H, t, *J* = 2.0 Hz , *ortho* on η^5-C_5<u>H_4</u>-alkyl), 2.45 (1.3H, q, *J* = 7.2 Hz, -C<u>H_2</u>CH_3), 2.34 (0.5H, q, *J* = 7.2 Hz, -C<u>H_2</u>CH_3), 2.04 (0.2H, q, *J* = 7.2 Hz, -C<u>H_2</u>CH_3), 1.41 (3H, d, *J* =7.3 Hz, -CHC<u>H_3</u>), 1.19 (3H, t, *J* = 7.2 Hz, -OCH_2C<u>H_3</u>), 1.17 (3H, t, *J* = 7.2 Hz, -CH_2C<u>H_3</u>);

^{13}C NMR (100 MHz) δ ($CDCl_3$): 172.1 (C=O), 169.6 (C=O), 167.8 (C=O), 140.2 (C_q), 136.2 (C_q), 131.3 (C_q), 130.9 (C_q), 129.7, 128.3, 127.7, 125.4, 123.3, 123.2, 89.7 (C_{ipso} η^5-<u>C</u>$_5H_4$-alkyl), 84.8 (C_{ipso} η^5-<u>C</u>$_5H_4$-naphthoyl), 70.3 (C_{meta} η^5-<u>C</u>$_5H_4$-naphthoyl), 69.0 (C_{meta} η^5-<u>C</u>$_5H_4$-alkyl), 67.2 (C_{ortho} η^5-<u>C</u>$_5H_4$-alkyl), 65.7 (C_{ortho} η^5-<u>C</u>$_5H_4$-naphthoyl), 61.6 (-O<u>C</u>H_2CH_3, -ve DEPT), 49.4 (-<u>C</u>HCH_3), 42.6 (-NH<u>C</u>H_2-, -ve DEPT), 21.0 (-<u>C</u>H_2CH_3, -ve DEPT), 18.8 (-CH<u>C</u>H_3), 14.9 (-OCH_2<u>C</u>H_3), 14.1 (-CH_2<u>C</u>H_3).

***N*-(1'-ethyl-6-ferrocenyl-2-naphthoyl)-glycine-D-alanine methyl ester (74)**

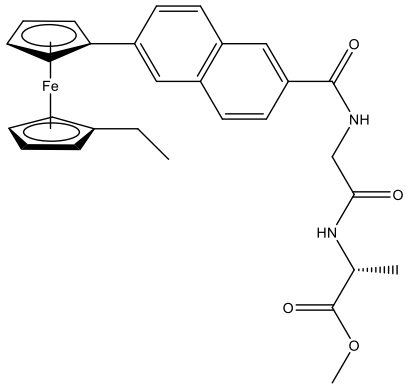

The synthesis followed that of *N*-(1'-ethyl-6-ferrocenyl-2-naphthoyl)-glycine-glycine methyl ester using the following reagent: glycine-D-alanine methyl ester (0.43 g, 0.27 mmol). The crude product was purified by column chromatography {eluent 1:1 hexane: ethyl acetate} yielding the title compound as a light orange oil (0.26 g, 17%);

I.R. υ_{max} (neat): 3379 (NH), 3090 (NH), 1734 (C=O_{ester}), 1642 (C=$O_{amide\ I}$), 1627 (C=$O_{amide\ I}$), 1531 (C=$O_{amide\ II}$) cm^{-1};

UV-Vis λ_{max} (CH_3CN): 376, 450 nm;

^{1}H NMR (400 MHz) δ ($CDCl_3$): 8.23(1H, t, *J* = 8.4 Hz, Ar<u>H</u>), 7.79-7.61 (5H, m, Ar<u>H</u>), 7.00 (1H, t, *J* = 5.6 Hz, -CON<u>H</u>-), 6.56 (1H, t, *J* = 5.6 Hz, -CON<u>H</u>-), 4.68 (2H, t, *J* = 2.0 Hz, *ortho* on η^5-C_5<u>H_4</u>-naphthoyl), 4.58 (1H, qt, *J* = 7.3 Hz, -C<u>H</u>CH_3), 4.26 (2H, t, *J* = 2.0 Hz, *meta* on η^5-C_5<u>H_4</u>-naphthoyl), 4.17 (2H, d, *J* = 7.2 Hz, -NHC<u>H_2</u>-), 3.93-3.88 (4H, m, η^5-C_5<u>H_4</u>-alkyl), 3.71 (3H, s, -OC<u>H_3</u>), 2.40 (1H, q, *J* = 7.2 Hz, -C<u>H_2</u>CH_3), 2.05 (1H, q, *J* = 7.2 Hz, -C<u>H_2</u>CH_3), 1.40 (3H, d, *J* =7.3Hz, -CHC<u>H_3</u>), 1.12 (3H, t, *J* = 7.2 Hz, -CH_2C<u>H_3</u>);

^{13}C NMR (100 MHz) δ ($CDCl_3$): 172.6 (C=O), 169.0 (C=O), 167.5 (C=O), 139.2 (C_q), 135.1 (C_q), 133.1 (C_q), 130.4(C_q), 129.3, 128.0, 127.2, 125.3, 123.2, 122.8, 88.9 (C_{ipso} η^5-<u>C_5</u>H_4-alkyl), 84.5 (C_{ipso} η^5-<u>C_5</u>H_4- naphthoyl), 71.0 (C_{meta} η^5-<u>C_5</u>H_4-naphthoyl), 69.1 (C_{meta} η^5-<u>C_5</u>H_4-alkyl), 67.2 (C_{ortho} η^5-<u>C_5</u>H_4-alkyl), 66.3 (C_{ortho} η^5-<u>C_5</u>H_4-naphthoyl), 51.3 (-O<u>C</u>H_3), 49.6 (-<u>C</u>HCH_3), 43.1 (-NH<u>C</u>H_2-, -ve DEPT), 21.3 (-<u>C</u>H_2CH_3, -ve DEPT), 17.8 (-CH<u>C</u>H_3), 14.5 (-CH_2<u>C</u>H_3).

***N*-(1'-ethyl-6-ferrocenyl-2-naphthoyl)-glycine-D-alanine ethyl ester (75)**

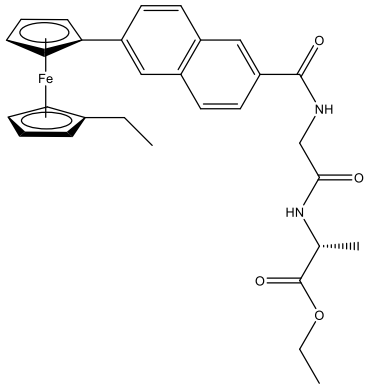

The synthesis followed that of *N*-(1'-ethyl-6-ferrocenyl-2-naphthoyl)-glycine-glycine methyl ester using the following reagent: glycine-D-alanine ethyl ester (0.47g, 0.27 mmol). The crude product was purified by column chromatography {eluent 1:1 hexane: ethyl acetate} yielding the title compound as a dark orange oil (0.22 g, 15%);

I.R. υ_{max} (neat): 3305 (NH), 3061 (NH), 1734 ($C=O_{ester}$), 1642 ($C=O_{amide\ I}$), 1628 ($C=O_{amide\ I}$), 1523 ($C=O_{amide\ II}$) cm^{-1};

UV-Vis λ_{max} (CH_3CN): 380, 452 nm;

^{1}H NMR (400 MHz) δ ($CDCl_3$): 8.28 (1H, t, *J* = 8.4 Hz, Ar<u>H</u>), 7.82-7.60 (5H, m, Ar<u>H</u>), 7.33 (1H, t, *J* = 5.6 Hz, -CON<u>H</u>-), 6.99 (1H, t, *J* = 5.6 Hz, -CON<u>H</u>-), 4.66 (2H, t, *J* = 2.0 Hz, *ortho* on η^5-C_5<u>H_4</u>-naphthoyl), 4.56 (1H, qt, *J* = 7.3 Hz, -C<u>H</u>CH_3), 4.29 (2H, t, *J* = 2.0 Hz, *meta* on η^5-C_5<u>H_4</u>-naphthoyl), 4.21(2H, d, *J* = 7.3 Hz, -NHC<u>H_2</u>-), 4.16 (2H, q, *J* = 7.2 Hz, -OC<u>H_2</u>CH_3), 4.11-3.93 (4H, m, η^5-C_5<u>H_4</u>-alkyl), 2.63 (1.2H, q, *J* = 7.2 Hz, -C<u>H_2</u>CH_3), 2.10 (0.8H, q, *J* = 7.2 Hz, -C<u>H_2</u>CH_3), 1.41 (3H, d, *J* =7.3 Hz, -CHC<u>H_3</u>), 1.22 (3H, t, *J* = 7.2 Hz, -OCH$_2$C<u>H_3</u>), 1.18 (3H, t, *J* = 7.2 Hz, -CH$_2$C<u>H_3</u>);

^{13}C NMR (100 MHz) δ ($CDCl_3$): 173.6 (C=O), 169.8 (C=O), 167.5 (C=O), 139.2 (C_q), 136.2 (C_q), 131.3 (C_q), 130.7 (C_q), 129.0, 128.4, 127.7, 125.8, 123.8, 123.2, 89.6 (C_{ipso} η^5-<u>C_5</u>H_4-alkyl), 84.1 (C_{ipso} η^5-<u>C_5</u>H_4-naphthoyl), 69.8 (C_{meta} η^5-<u>C_5</u>H_4-naphthoyl), 69.1 (C_{meta} η^5-<u>C_5</u>H_4-alkyl), 67.3 (C_{ortho} η^5-<u>C_5</u>H_4-alkyl), 65.7 (C_{ortho} η^5-<u>C_5</u>H_4-naphthoyl), 61.8 (-O<u>C</u>H_2CH_3, -ve DEPT), 49.7 (-<u>C</u>HCH_3), 42.6 (-NH<u>C</u>H_2-, -ve DEPT), 21.3 (-<u>C</u>H_2CH_3, -ve DEPT), 17.9 (-CH<u>C</u>H_3), 14.8 (-OCH$_2$<u>C</u>H_3), 14.7 (-CH$_2$<u>C</u>H_3).

***N*-(1'-ethyl-6-ferrocenyl-2-naphthoyl)-γ-aminobutyric acid methyl ester (76)**

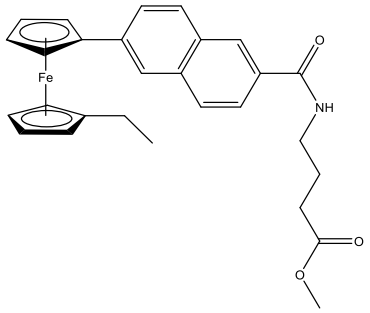

The synthesis followed that of *N*-(1'-ethyl-6-ferrocenyl-2-naphthoyl)-glycine-glycine methyl ester using the following reagent: gamma-aminobutyric acid methyl ester (0.31 g, 0.27 mmol). The crude product was purified by column chromatography {eluent 1:1 hexane: ethyl acetate} yielding the title compound as a dark orange oil (0.47 g, 36%);

HRMS (ESI^+) *m/z*: 483.1294 $[M]^{+\bullet}$, $C_{28}H_{29}NO_3Fe$ requires 483.1497;

I. R. υ_{max} (neat): 3274 (NH), 1730 ($C{=}O_{ester}$), 1622 ($C{=}O_{amide}$) cm^{-1};

UV-Vis λ_{max} (CH_3CN): 372, 449 nm;

^1H NMR (400 MHz) δ ($CDCl_3$): 8.21-8.15 (1H, m, ArH), 7.84-7.73 (4H, m, ArH), 7.61 (1H, dd, *J* = 1.6 and 8.8 Hz, ArH), 6.62 (1H, t, *J* = 5.4Hz, -CONH-), 4.62 (2H, t, *J* = 2.0 Hz, *ortho* on η^5-C_5H_4-naphthoyl), 4.27 (2H, t, *J* = 2.0 Hz, *meta* on η^5-C_5H_4-naphthoyl), 4.00-3.85 (4H, m, η^5-C_5H_4-alkyl), 3.58 (3H, s, -OCH_3), 3.49 (2H, q, *J* = 6.5 Hz, -$NHCH_2CH_2CH_2$-), 2.40 (2H, t, *J* = 6.5 Hz, -$NHCH_2CH_2CH_2CO$-), 2.62 (0.3H, q, *J* = 7.2, -CH_2CH_3), 2.39 (0.4H, q, *J* = 7.2, -CH_2CH_3), 2.14 (1.3H, q, *J* = 7.2 Hz, -CH_2CH_3), 1.93 (2H, qt, *J* = 6.5 Hz, -$NHCH_2CH_2CH_2$-), 1.21 (1.5H, t, *J* = 7.2, -CH_2CH_3), 0.99 (1.5H, t, *J* = 7.2 Hz, -CH_2CH_3);

^{13}C NMR (100 MHz) δ ($CDCl_3$): 174.3 (C=O), 167.6 (C=O), 134.7 (C_q), 132.6 (C_q), 131.6 (C_q), 131.1 (C_q), 128.9, 128.4, 127.8, 126.7, 123.7, 123.5, 88.9 (C_{ipso} η^5-C_5H_4-alkyl), 84.3 (C_{ipso} η^5-C_5H_4-naphthoyl), 71.3 (C_{meta} η^5-C_5H_4-naphthoyl), 69.1 (C_{meta} η^5-C_5H_4-alkyl), 67.2 (C_{ortho} η^5-C_5H_4-alkyl), 66.5 (C_{ortho} η^5-C_5H_4-naphthoyl), 51.8 (-OCH_3), 39.8 (-$NHCH_2CH_2CH_2$-, -ve DEPT), 31.8 (-$NHCH_2CH_2CH_2$-, -ve DEPT), 24.4 (-$NHCH_2CH_2CH_2$-, -ve DEPT), 21.5 (-CH_2CH_3, -ve DEPT),14.7 (-CH_2CH_3).

***N*-(1'-ethyl-6-ferrocenyl-2-naphthoyl)-γ-aminobutyric acid ethyl ester (77)**

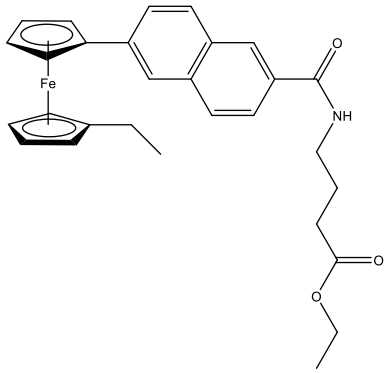

The synthesis followed that of *N*-(1'-ethyl-6-ferrocenyl-2-naphthoyl)-glycine-glycine methyl ester using the following reagent: gamma-aminobutyric acid ethyl ester (0.34 g, 0.27 mmol). The crude product was purified by column chromatography {eluent 1:1 hexane: ethyl acetate} yielding the title compound as a dark orange oil (0.54 g, 60%);

HRMS (ESI^+) *m/z*: 497.1524 $[M]^{+\bullet}$, $C_{29}H_{31}NO_3Fe$ requires 497.1653;

I.R. υ_{max} (neat): 3318 (NH), 1729 ($C{=}O_{ester}$), 1636 ($C{=}O_{amide}$) cm^{-1};

UV-Vis λ_{max} (CH_3CN): 370, 447 nm;

^1H NMR (400 MHz) δ ($CDCl_3$): 8.23-8.19 (1H, m, Ar<u>H</u>), 7.85-7.75 (4H, m, Ar<u>H</u>), 7.62 (1H, dd, *J* = 1.6 and 8.8 Hz, Ar<u>H</u>), 6.67 (1H, t, *J* = 5.4 Hz, -CON<u>H</u>-), 4.76 (2H, t, *J* = 2.0 Hz, *ortho* on η^5-$C_5\underline{H}_4$-naphthoyl), 4.38 (2H, t, *J* = 2.0 Hz, *meta* on η^5-$C_5\underline{H}_4$-naphthoyl), 4.13 (2H, q, *J* = 8.0 Hz, -OC<u>H_2</u>CH_3), 4.02-3.96 (4H, m, η^5-$C_5\underline{H}_4$-alkyl), 3.62 (2H, q, *J* = 6.5 Hz, -NHC<u>H_2</u>CH_2CH_2-), 2.64 (0.6H, q, *J* = 7.2 Hz, -C<u>H_2</u>CH_3), 2.56 (2H, t, *J* = 6.5 Hz, -$NHCH_2CH_2$C<u>H_2</u>-), 2.45 (0.4H, q, *J* = 7.2 Hz, -C<u>H_2</u>CH_3), 2.18 (1H, q, *J* = 7.2 Hz, -C<u>H_2</u>CH_3), 2.15 (2H, qt, *J* = 6.5 Hz, -$NHCH_2$C<u>H_2</u>CH_2-), 1.29 (3H, t, *J* = 8.0 Hz, -OCH_2C<u>H_3</u>), 0.99 (1.5H, t, *J* = 7.2 Hz, -CH_2C<u>H_3</u>), 0.89 (1.5H, t, *J* = 7.2 Hz, -CH_2C<u>H_3</u>);

^{13}C NMR (100 MHz) δ ($CDCl_3$): 173.3 (C=O), 168.6 (C=O), 134.7 (C_q), 133.3 (C_q), 131.6 (C_q), 132.5 (C_q), 128.7, 128.3, 127.6, 126.4, 123.9, 123.2, 89.1 (C_{ipso} η^5-<u>C</u>$_5H_4$-alkyl), 84.3 (C_{ipso} η^5-<u>C</u>$_5H_4$-naphthoyl), 69.7 (C_{meta} η^5-<u>C</u>$_5H_4$-naphthoyl), 68.8 (C_{meta} η^5-<u>C</u>$_5H_4$-alkyl), 67.1 (C_{ortho} η^5-<u>C</u>$_5H_4$-alkyl), 65.6 (C_{ortho} η^5-<u>C</u>$_5H_4$-naphthoyl), 61.4 (-O<u>C</u>H_2CH_3, -ve DEPT), 40.1 (-NH<u>C</u>$H_2CH_2CH_2$-, -ve DEPT), 31.7 (-$NHCH_2CH_2$<u>C</u>H_2-, -ve DEPT), 23.9 (-$NHCH_2$<u>C</u>H_2CH_2-, -ve DEPT), 22.2 (-<u>C</u>H_2CH_3, -ve DEPT), 15.1 (-OCH_2<u>C</u>H_3), 13.6 (-<u>C</u>H_3).

References

1. B. W. Harper, A. M. Krause-Heuer, M. P. Grant, M. Manohar, K. B. Garbutcheon-Singh and J. R. Aldrich-Wright, *Chemistry*, 2010, **16**, 7064-7077.
2. G. Jaouen, A. Vessieres and S. Top, *Chem Soc Rev*, 2015, **44**, 8802-8817.
3. N. B. Souza, A. C. Aguiar, A. C. Oliveira, S. Top, P. Pigeon, G. Jaouen, M. O. Goulart and A. U. Krettli, *Memórias do Instituto Oswaldo Cruz*, 2015, **110**, 981-988.
4. C. Biot, F. Nosten, L. Fraisse, D. Ter-Minassian, J. Khalife and D. Dive, *Parasite*, 2011, **18**, 207-214.
5. Z. H. Chohan, *Applied Organometallic Chemistry*, 2006, **20**, 112-116.
6. Á. Mooney, R. Tiedt, T. Maghoub, N. O'Donovan, J. Crown, B. White and P. T. M. Kenny, *Journal of Medicinal Chemistry*, 2012, **55**, 5455-5466.
7. P. P. Yong Wang, Siden Top, Michael J. Mcglinchey, Gérard Jaouen, *Angewandte Chemie International Edition*, 2015, **54**, 10230-10233.
8. Á. Mooney, A. J. Corry, C. Ni Ruairc, T. Mahgoub, D. O'Sullivan, N. O'Donovan, J. Crown, S. Varughese, S. M. Draper, D. K. Rai and P. T. M. Kenny, *Dalton Transactions*, 2010, **39**, 8228-8239.
9. A. J. Corry, N. O'Donovan, Á. Mooney, D. O'Sullivan, D. K. Rai and P. T. M. Kenny, *Journal of Organometallic Chemistry*, 2009, **694**, 880-885.
10. A. J. Corry, Á. Mooney, D. O'Sullivan and P. T. M. Kenny, *Inorganica Chimica Acta*, 2009, **362**, 2957-2961.
11. A. G. Harry, W. E. Butler, J. C. Manton, M. T. Pryce, N. O'Donovan, J. Crown, D. K. Rai and P. T. M. Kenny, *Journal of Organometallic Chemistry*, 2014, **757**, 28-35.
12. D. L. Pavia, G. M. Lampman, G. S. Kriz and J. R. Vyvyan, *Introduction to spectroscopy*, 2014.
13. R. Tiedt, Ph.D Thesis, Dublin City University, 2014.
14. David and Victor, *Essentials in modern HPLC separations*, Elsevier, 2012.
15. U. D. Neue, *HPLC columns: theory, technology, and practice*, Wiley-VCH, 1997.

Chapter 3

Biological Evaluation of *N*-(1'-methyl-6-ferrocenyl-2-naphthoyl) and *N*-(1'-ethyl-6-ferrocenyl-2-naphthoyl) amino acid and dipeptide esters

3.1. Introduction

Recent studies have shown *N*-(6-ferrocenyl-2-naphthoyl)-glycine-glycine ethyl ester **30** is the most active compound of the *N*-ferrocenyl amino acid and dipeptide esters to date in Kenny's research group, with an IC_{50} value of 0.13 ± 0.02 μM in H1299 NSCLC cells. [1] Harry *et al.* synthesized disubstituted derivatives of *N*-(ferrocenyl)benzoyl amino acid and dipeptide esters, and have shown a greater cytotoxicity than the monosubstituted ones. 1-methyl-1'-*N*-{*para*-(ferrocenyl)-benzoyl}-glycine-glycine ethyl ester **31** have IC_{50} value of 2.8 ± 1.23 μM in H1299 cell line. [2]

In a further structure-activity relationship (SAR) study of the ferrocenyl peptide conjugates, a series of *N*-(1'-methyl-6-ferrocenyl-2-naphthoyl) and *N*-(1'-ethyl-6-ferrocenyl-2-naphthoyl) amino acid and dipeptide esters have been prepared maintaining the most active amino acid and dipeptide esters whilst altering the ferrocenyl moiety and the ester functionality. In total, 14 compounds were tested for their anti-proliferative effect on human cervical carcinoma cells (ATCC HTB-35, SiHa) and human liver cells (ATCC CCL-13, Chang liver, HeLa markers).

3.2. Miniaturised *in vitro* methods

Miniaturised *in vitro* colorimetric assay is a simple and sensitive technique which has been widely used in the determination of a substance's ability to enhance cell growth or promote cell death. [3] The most commonly used measure of toxicity is impairment of cell growth by reduced cell numbers when comparing between treated samples and untreated controls.

Colorimetric end-point assays are not possible to distinguish the cell death due to cytotoxic or cytostatic effect. Cytotoxic effect leads to cell death by either apoptosis, necrosis or autophagy, while cytostatic effect is only a temporary manner. Apoptosis is programmed cell death that occurs in multicellular organisms, necrosis is an unprogrammed cell death caused by disease, cellular injury, or failure of the blood supply, and autophagy is a self-degrative process that delivers cytoplasmic constituents to the lysosome. [5] A substance will lose its anti-proliferative activity once the cytostatic agent is removed. [3 4 5]

Several miniaturised *in vitro* colorimetric assays have been developed for the quantification of cell growth. The most common assays used are MTT assay [6] , acid phosphatase assay [7] and WST-1 assay [8].

3.2.1. MTT dye assay

The MTT test is a colorimetric assay based on the formation of a coloured insoluble formazan salt. The amount of formazan produced, and the viable cell numbers have a direct proportional relationship thus this method can be used to measure cell viability and proliferation. The yellow water-soluble tetrazolium salt MTT (3-(4,5-dimethylthiazolyl-2)-2,5-diphenyltetrazolium bromide) can be reduced into a purple insoluble formazan product by the mitochondrial succinate dehydrogenase. The resulting intracellular purple insoluble crystals can be solubilized in DMSO and quantified by spectrophotometric means at 570 nm. Nonetheless, the MTT assay have a number of problems: the intensity of the reduction varies in different cell lines; the reaction rate varies with a few factors (*e.g.* cellular and medium glucose levels, and pH). [6]

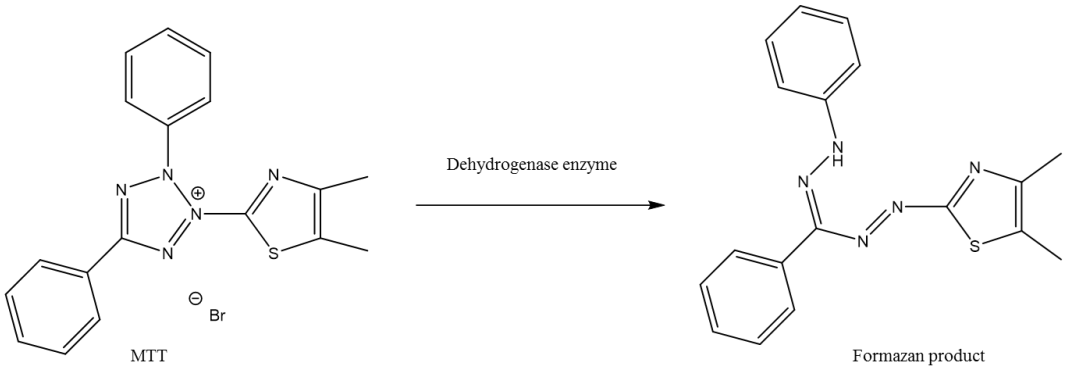

Figure 3.1: The dehydrogenase enzyme conversion of the MTT dye to the formazan product.

3.2.2. Acid phosphatase assay

Acid Phosphatases are a group of enzymes that non-specifically catalyse the production of inorganic phosphate from *p*-nitrophenolate phosphate (pNPP) at an acidic pH. The ability of phosphatases to catalyse the hydrolysis of pNPP to *p*-nitrophenol is measured by spectrometric means. The addition of strong base not only ceases the reaction but also yields alkaline conditions in which p-nitrophenolate is yellow. Colorimetric analysis of the *p*-nitrophenolate anion indirectly measures of the inhibition of cell growth. A direct correlation of the yellow intensity and viable cell number can be measured by spectrophotometric means at 405nm. The acid phosphatase assay is a simple and sensitive method with excellent reproducibility. It involves fewer steps hence uses fewer reagents. [7]

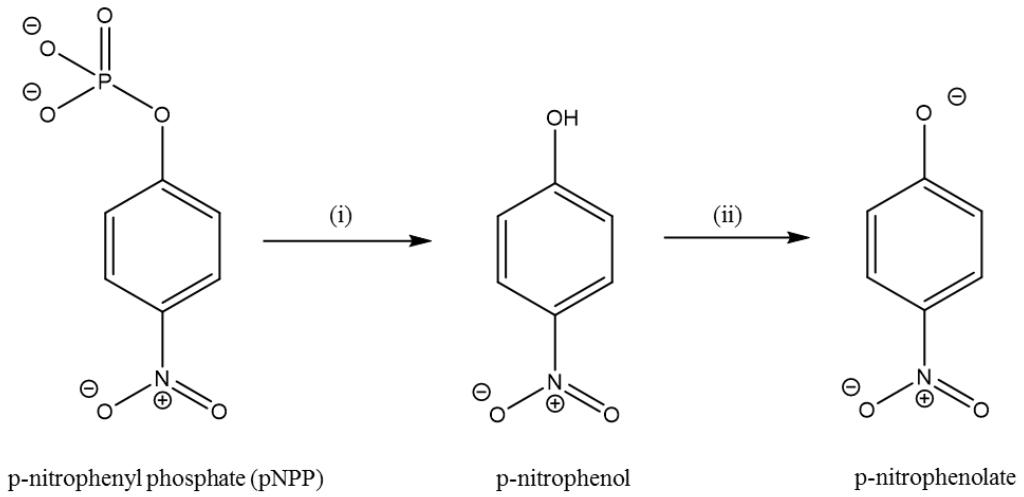

Figure 3.2: Acid phosphatase end-point assay: (i) phosphatase catalysed reaction (H_2O); (ii) colorimetric reaction in strong alkaline conditions (NaOH).

3.2.3. WST-1 assay

More recently, modified tetrazolium salts like WST-1 have become available. The assay principle is based on the conversion of the tetrazolium salt WST-1 (4-[3-(4-iodophenyl)-2-(4-nitrophenyl)- -2H-5-tetrazolio]-1,3-benzene disulfonate) into a coloured dye by mitochondrial dehydrogenase enzymes. The soluble salt is released into the media. Within a given period, the reaction produces a colour change which directly correlates to the amount of mitochondrial dehydrogenase in a given culture.

The major advantage of this substance is that it can only be converted by viable cells to a water-soluble formazan, which leads to a wider linear range and a higher stability. [8] No solubilization of the products is necessary as required in the MTT dye assay. In addition, the WST-1 is a ready-to-use solution. This convenient colorimetric assay is performed in the same microtiter plate where the cells were cultivated. Therefore, the entire step can be done in only one 96-well plate and the absorbance of the coloured solution is measured at 450 nm. For these reasons, the WST-1 assay was the chosen colorimetric end-point assay for the *in vitro* biological evaluation of *N*-(1'-methyl-6-ferrocenyl-2-naphthoyl) and *N*-(1'-ethyl-6-ferrocenyl-2-naphthoyl) amino acid and dipeptide derivatives.

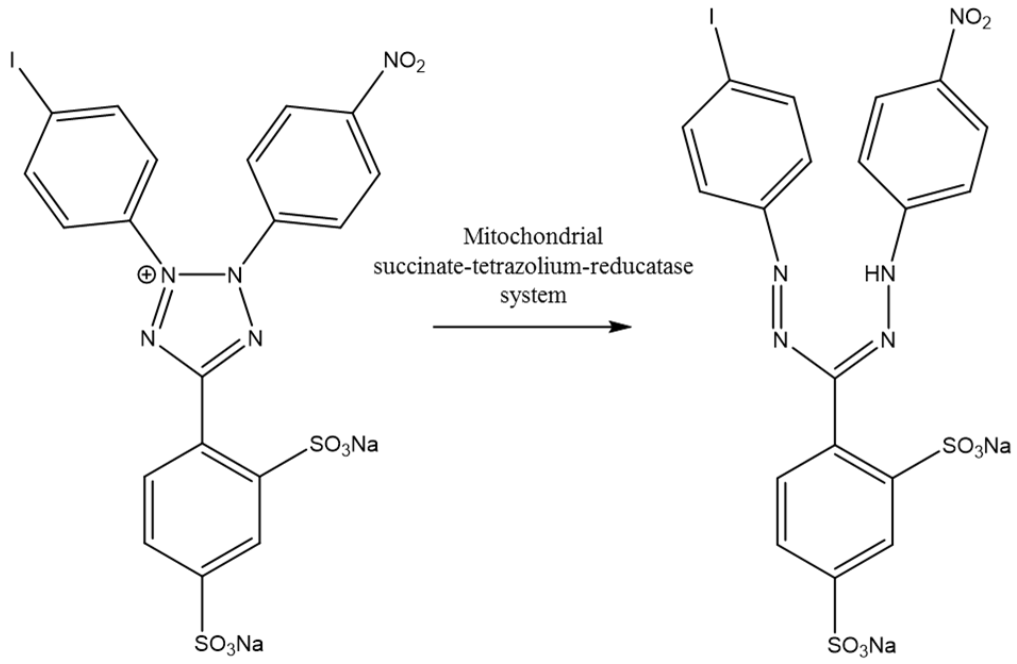

Figure 3.3: Cleavage of the tetrazolium salt WST-1 to formazan.

3.3. Biological evaluation of *N*-(1'-alkyl-6-ferrocenyl-2-naphthoyl) amino acid and dipeptide derivatives

The *in vitro* cytotoxicity of the *N*-(1'-methyl-6-ferrocenyl-2-naphthoyl) and *N*-(1'-ethyl-6-ferrocenyl-2-naphthoyl) amino acid and dipeptide derivatives were evaluated at a single dose (200 μM) in the human cervical carcinoma cell line (SiHa) and liver cell line (Chang). The endpoint of the growth inhibition was evaluated by the WST-1 assay. The screening of the compounds was performed in collaboration with Dr. Patricia González-Barranco and Dr. Mónica A. Ramírez-Cabrera of the School of Chemical Sciences, Universidad Autónoma de Nuevo León, México, and Karen G. Ontiveros-Castillo of the School of Chemical Sciences, Dublin City University.

The preliminary screenings were performed in triplicate by treating individual wells of a 96-well plate containing SiHa and Chang cells with a 200 μM solution of each test compound prepared in DMSO/H_2O/EtOH. A positive reference vincristine, a negative control (untreated cells with media) and blank control (empty wells) were included in the assays. The cells were incubated for 24 hours, until cell confluency was reached. At this point, cell survival was established through WST-1 assay. The results of the comprehensive screens are expressed as the percentage cell viability ± standard deviation (relative to the negative control). Standard deviations have been calculated using data obtained from three independent experiments. The student's t-test was performed to determine significant difference between results obtained from ferrocenyl bioconjugates and vincristine, all results showed a p-value < 0.05. Therefore, there is significant difference in toxicity between these novel compounds and vincristine. The results of the preliminary screen are presented in Figure 3.4 to 3.7.

3.3.1. *In vitro* study of *N*-(1'-alkyl-6-ferrocenyl-2-naphthoyl) amino acid and dipeptide derivatives in the human cervical carcinoma cell line (SiHa)

N-(1'-methyl-6-ferrocenyl-2-naphthoyl) amino acid and dipeptide derivatives **62**, **63**, **65-69** and reference compound vincristine were both tested against SiHa cervical carcinoma cell lines at 200 μM. As can be seen in Figure 3.4 and Table 3.1, all compounds show excellent growth inhibition, with a general anti-proliferative effect above 60%. The results shown these novel compounds are more toxic than chemotherapeutic medication vincristine. Strong growth inhibition also found for *N*-(1'-ethyl-6-ferrocenyl-2-naphthoyl) amino acid and dipeptide derivatives **70**, **71**, **73-77** (Figure 3.5 and Table 3.2). Except compound **77**, rest compounds are more active than vincristine. A general trend was observed in these compounds: the gamma-aminobutyric esters are less active than the Gly-Gly, Gly-L-Ala and Gly-D-Ala derivatives.

Table 3.1: Percentage cell viability at 200 µM on SiHa cervical carcinoma cells for *N*-(1'-methyl-6-ferrocenyl-2-naphthoyl) amino acid and dipeptide derivatives **62**, **63**, **65-69** and reference compound vincristine.

Alkyl	Linker	Amino acid and dipeptide esters	Compound No.	% cell viability at 200 µM
$-CH_3$	naphthoyl	Gly-Gly-OMe	**62**	4.45 ± 1.01
		Gly-Gly-OEt	**63**	30.47 ± 2.04
		Gly-L-Ala-OEt	**65**	1.77 ± 1.24
		Gly-D-Ala-OMe	**66**	10.13 ± 3.98
		Gly-D-Ala-OEt	**67**	18.50 ± 2.19
		GABA-OMe	**68**	22.49 ± 2.40
		GABA-OEt	**69**	40.31 ± 1.28
			Vincristine	42.47 ± 2.79

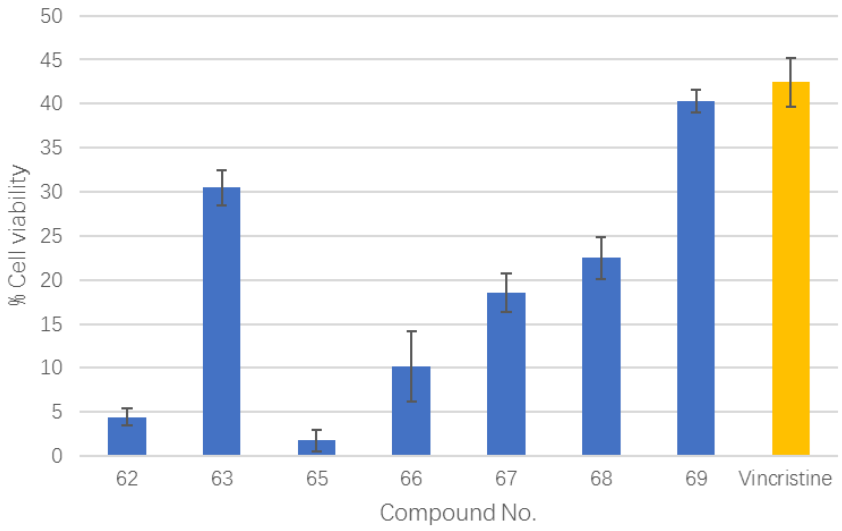

Figure 3.4: Percentage cell viability at 200 µM on SiHa cervical carcinoma cells for *N*-(1'-methyl-6-ferrocenyl-2-naphthoyl) amino acid and dipeptide derivatives **62**, **63**, **65-69** and reference compound vincristine. Error bars represent the standard deviation of triplicate experiments.

Table 3.2: Percentage cell viability at 200 µM on SiHa cervical carcinoma cells for *N*-(1'-ethyl-6-ferrocenyl-2-naphthoyl) amino acid and dipeptide derivatives **70**, **71**, **73-77** and reference compound vincristine.

Alkyl	Linker	Amino acid and dipeptide esters	Compound No.	% cell viability at 200 µM
$-CH_2CH_3$	naphthoyl	Gly-Gly-OMe	**70**	11.59 ± 1.83
		Gly-Gly-OEt	**71**	2.54 ± 0.60
		Gly-L-Ala-OEt	**73**	20.75 ± 1.83
		Gly-D-Ala-OMe	**74**	20.47 ± 0.14
		Gly-D-Ala-OEt	**75**	5.33 ± 0.72
		GABA-OMe	**76**	21.34 ± 2.90
		GABA-OEt	**77**	55.60 ± 1.19
			Vincristine	42.47 ± 2.79

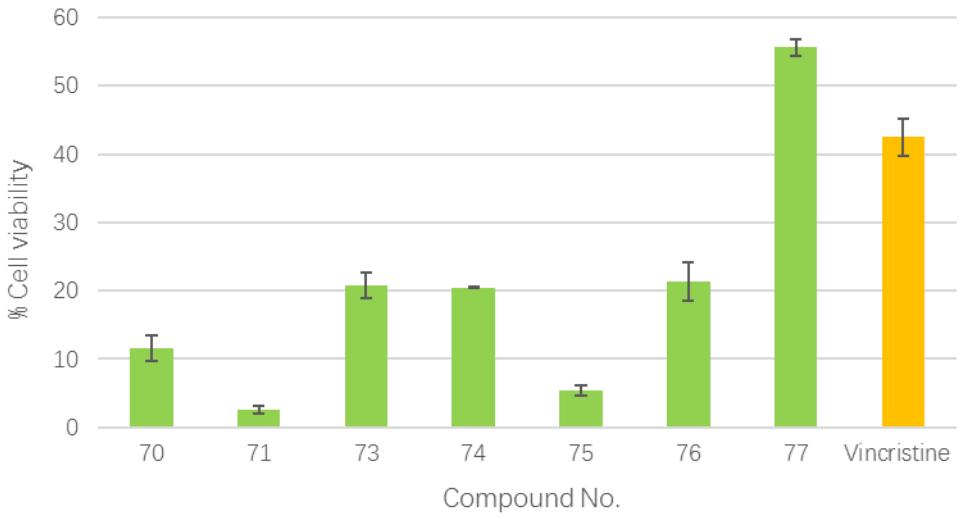

Figure 3.5: Percentage cell viability at 200 µM on SiHa cervical carcinoma cells for *N*-(1'-ethyl-6-ferrocenyl-2-naphthoyl) amino acid and dipeptide derivatives **70**, **71**, **73-77** and reference compound vincristine. Error bars represent the standard deviation of triplicate experiments.

3.3.2. *In vitro* study of *N*-(1'-alkyl-6-ferrocenyl-2-naphthoyl) amino acid and dipeptide derivatives in the human liver cell line (Chang)

N-(1'-alkyl-6-ferrocenyl-2-naphthoyl) amino acid and dipeptide derivatives **62**, **63**, **65-71** and **73-77** were tested against Chang normal liver cells at 200 μM (Figure 3.6 and Figure 3.7). Compound **62**, **65**, **66**, **70**, **71**, **73** and **74** were shown to have strong growth inhibition above 80%. However, *N*-(1'-methyl-6-ferrocenyl-2-naphthoyl)-glycine-D-alanine ethyl ester **67**, *N*-(1'-methyl-6-ferrocenyl-2-naphthoyl)-γ-aminobutyric acid methyl ester **68** and *N*-(1'-methyl-6-ferrocenyl-2-naphthoyl) -γ-aminobutyric acid ethyl ester **69** were have inhibition around 76%, 53% and 64%. Similar trend was obtained for *N*-(1'-ethyl-6-ferrocenyl-2-naphthoyl) amino acid and dipeptide derivatives; compound **75**, **76** and **77** with glycine-D-alanine ethyl ester, γ-aminobutyric acid methyl ester and γ-aminobutyric acid ethyl ester have lower toxicity against Chang liver cells.

Table 3.3: Percentage cell viability at 200 µM on Chang liver cells for *N*-(1'-methyl-6-ferrocenyl-2-naphthoyl) amino acid and dipeptide derivatives **62**, **63**, **65-69**.

Alkyl	Linker	Amino acid and dipeptide esters	Compound No.	% cell viability at 200 µM
-CH_3	naphthoyl	Gly-Gly-OMe	**62**	3.57 ± 1.72
		Gly-Gly-OEt	**63**	26.92 ± 2.66
		Gly-L-Ala-OEt	**65**	0.80 ± 0.24
		Gly-D-Ala-OMe	**66**	9.61 ± 3.06
		Gly-D-Ala-OEt	**67**	23.95 ± 0.45
		GABA-OMe	**68**	46.78 ± 0.03
		GABA-OEt	**69**	45.12 ± 1.79

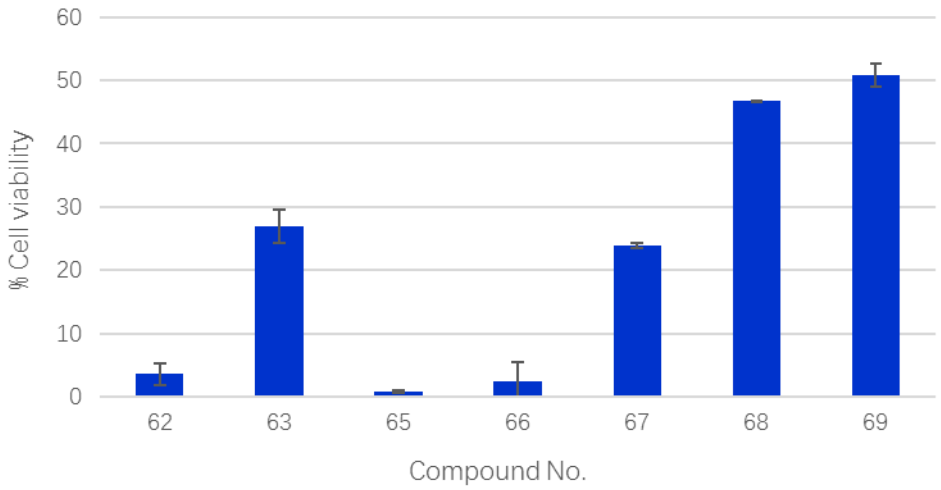

Figure 3.6: Percentage cell viability at 200 µM on Chang liver cells for *N*-(1'-methyl-6-ferrocenyl-2-naphthoyl) amino acid and dipeptide derivatives **62**, **63**, **65-69**. Error bars represent the standard deviation of triplicate experiments.

Table 3.4: Percentage cell viability at 200 μM on Chang liver cells for *N*-(1'-ethyl-6-ferrocenyl-2-naphthoyl) amino acid and dipeptide derivatives **70**, **71**, **73-77**.

Alkyl	Linker	Amino acid and dipeptide esters	Compound No.	% cell viability at 200 μM
$-CH_2CH_3$	naphthoyl	Gly-Gly-OMe	**70**	9.58 ± 0.61
		Gly-Gly-OEt	**71**	0.92 ± 0.25
		Gly-L-Ala-OEt	**73**	3.78 ± 2.30
		Gly-D-Ala-OMe	**74**	12.05 ± 1.76
		Gly-D-Ala-OEt	**75**	41.01 ± 3.37
		GABA-OMe	**76**	50.90 ± 0.88
		GABA-OEt	**77**	56.30 ± 0.50

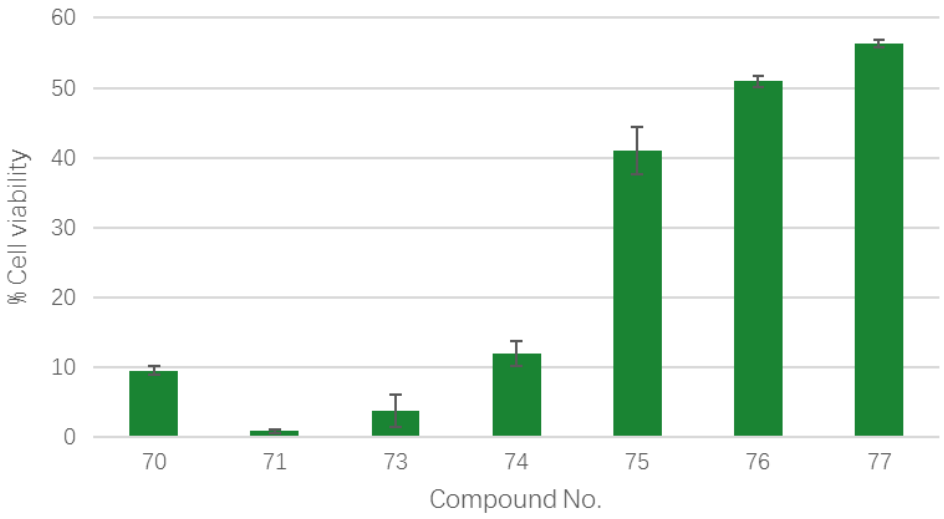

Figure 3.7: Percentage cell viability at 200 μM on Chang liver cells for *N*-(1'-ethyl-6-ferrocenyl-2-naphthoyl) amino acid and dipeptide derivatives **70**, **71**, **73-77**. Error bars represent the standard deviation of triplicate experiments.

3.3.3. *In vitro* comparison study of *N*-(1'-alkyl-6-ferrocenyl-2-naphthoyl) amino acid and dipeptide derivatives against the human cervical carcinoma cell line (SiHa) and the human liver cell line (Chang)

Toxicity is a common side effect of chemotherapeutic agents. [5] In recent years, the Chang cell line was widely used as a human hepatocyte model. [9] [10] *N*-(1'-methyl-6-ferrocenyl-2-naphthoyl) amino acid and dipeptide derivatives **62**, **63**, **65-69** and *N*-(1'-ethyl-6-ferrocenyl-2-naphthoyl) amino acid and dipeptide derivatives **70**, **71**, **73-77** were both tested against cervical carcinoma cell SiHa and human liver cells Chang at 200 μM. To compare the inhibitory effects between SiHa and Chang cell lines, the observations can suggest there might be differences in susceptibilities to ferrocenyl amino acid and dipeptide bioconjugates toxicity by different cells. Therefore, the compounds show stronger anti-proliferative effect on SiHa and with less toxicity against Chang cells will be selected for further IC_{50} determination.

For *N*-(1'-methyl-6-ferrocenyl-2-naphthoyl) amino acid and dipeptide derivatives, compound **68** and **69** are less toxic than others in Chang cell lines, with more than 45% cell growth. And compound **75**, **76** and **77** are less toxic than the rest from *N*-(1'-ethyl-6-ferrocenyl-2-naphthoyl) amino acid and dipeptide esters against Chang cells, have more than 40% cell viability. Despite compound **77**, other compounds **68**, **69**, **75**, **76** have more than 50% cell inhibition against SiHa cells. Therefore, compound **68**, **69**, **75, 76** were selected for IC_{50} determination.

Table 3.5: Comparison of percentage cell viability at 200 μM in SiHa and Chang cell lines for compound **62**, **63**, **65-71** and **73-77**.

Compound name	Compound No.	% cell viability in SiHa cells	% cell viability in Chang cells
N-(1'-methyl-6-ferrocenyl-2-naphthoyl)-Gly-Gly-OMe	**62**	4.45 ± 1.01	3.57 ± 1.72
N-(1'-methyl-6-ferrocenyl-2-naphthoyl)-Gly-Gly-OEt	**63**	30.47 ± 2.04	26.92 ± 2.66
N-(1'-methyl-6-ferrocenyl-2-naphthoyl)-Gly-L-Ala-OEt	**65**	1.77 ± 1.24	0.80 ± 0.24
N-(1'-methyl-6-ferrocenyl-2-naphthoyl)-Gly-D-Ala-OMe	**66**	10.13 ± 3.98	9.61 ± 3.06
N-(1'-methyl-6-ferrocenyl-2-naphthoyl)-Gly-D-Ala-OEt	**67**	18.50 ± 2.19	23.95 ± 0.45
N-(1'-methyl-6-ferrocenyl-2-naphthoyl)-GABA-OMe	**68**	22.49 ± 2.40	46.78 ± 0.03
N-(1'-methyl-6-ferrocenyl-2-naphthoyl)-GABA-OEt	**69**	40.31 ± 1.28	45.12 ± 1.79
N-(1'-ethyl-6-ferrocenyl-2-naphthoyl)-Gly-Gly-OMe	**70**	11.59 ± 1.83	9.58 ± 0.61
N-(1'-ethyl-6-ferrocenyl-2-naphthoyl)-Gly-L-Ala-OMe	**71**	2.54 ± 0.60	0.92 ± 0.25
N-(1'-ethyl-6-ferrocenyl-2-naphthoyl)-Gly-L-Ala-OEt	**73**	20.75 ± 1.83	3.78 ± 2.30
N-(1'-ethyl-6-ferrocenyl-2-naphthoyl)-Gly-D-Ala-OMe	**74**	20.47 ± 0.14	12.05 ± 1.76
N-(1'-ethyl-6-ferrocenyl-2-naphthoyl)-Gly-D-Ala-OEt	**75**	5.33 ± 0.72	41.01 ± 3.37
N-(1'-ethyl-6-ferrocenyl-2-naphthoyl)-GABA-OMe	**76**	21.34 ± 2.90	50.90 ± 0.88
N-(1'-ethyl-6-ferrocenyl-2-naphthoyl)-GABA-OEt	**77**	55.60 ± 1.19	56.30 ± 0.50

3.3.4. IC_{50} value determination for *N*-(1'-alkyl-6-ferrocenyl-2-naphthoyl) amino acid and dipeptide derivatives

The effect of selected compounds **68**, **69**, **75, 76** on SiHa cell growth was expressed as an IC_{50} value, which corresponds to the concentration of the drug required for 50% inhibition of cell growth. To determine the IC_{50} values of the four target compounds, individual 96-well plates containing SiHa cells were treated with the test compounds at concentrations ranging from 3.125 μg/mL to 100 μg/mL. The cells were incubated for 5-6 days, until cell confluency was reached. Cell survival was determined by performing the WST-1 assay. The IC_{50} value for each compound was calculated using Calcusyn software, and standard deviations have been calculated using data obtained from three independent experiments. The values obtained are listed in Table 3.6.

Table 3.6: IC_{50} values in SiHa cell line.

Compound Name	**Compound No.**	**IC_{50} values (μM)**
N-(1'-methyl-6-ferrocenyl-2-naphthoyl)-GABA-OMe	**68**	50.83 ± 1.29
N-(1'-methyl-6-ferrocenyl-2-naphthoyl)-GABA-OEt	**69**	61.81 ± 2.52
N-(1'-ethyl-6-ferrocenyl-2-naphthoyl)-Gly-D-Ala-OEt	**75**	8.76 ± 0.98
N-(1'-ethyl-6-ferrocenyl-2-naphthoyl)-GABA-OMe	**76**	44.27 ± 2.89

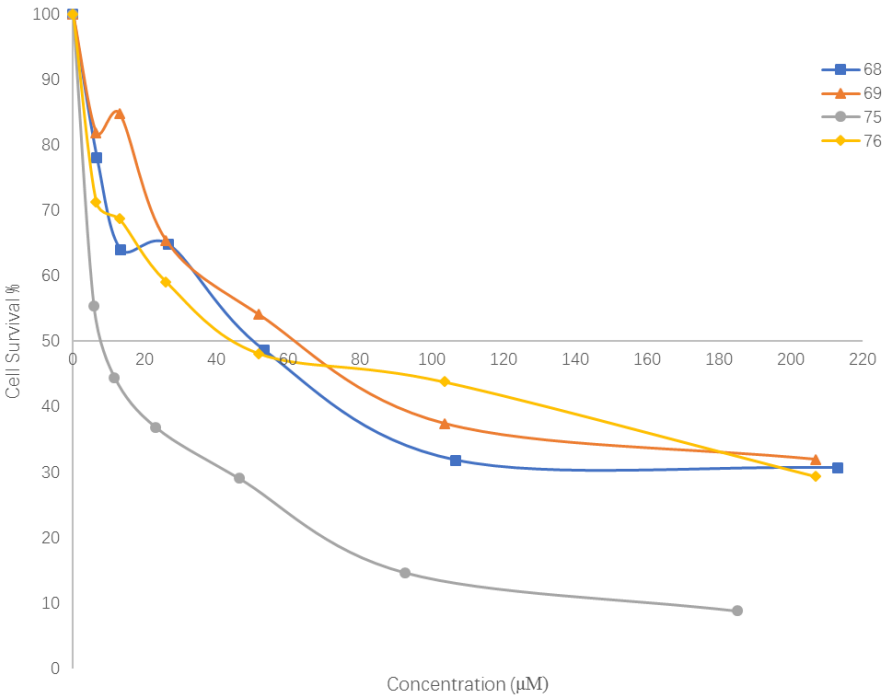

Figure 3.8: IC_{50} plot for selected compounds in SiHa cell line.

The four *N*-(1'-alkyl-6-ferrocenyl-2-naphthoyl) amino acid and dipeptide derivatives were shown to exert an anti-proliferative effect in the SiHa cell lines. The *N*-(1'-methyl-6-ferrocenyl-2-naphthoyl)-γ-aminobutyric acid methyl ester **68**, *N*-(1'-methyl-6-ferrocenyl-2-naphthoyl)-γ-aminobutyric acid ethyl ester **69** and *N*-(1'-ethyl-6-ferrocenyl-2-naphthoyl)-γ-aminobutyric acid methyl ester **76** display an IC_{50} value of 50.83 ± 1.29, 61.81 ± 2.52 and 44.27 ± 2.89 respectively. Compound *N*-(1'-ethyl-6-ferrocenyl-2-naphthoyl)-glycine-D-alanine ethyl ester **75** is the most active one with the IC_{50} value below 10 µM. Since those compounds show stronger anti-proliferative effect on human cervical carcinoma cells (SiHa) and with less toxicity against human liver cells (Chang), they have some selectivity for cancer treatment.

3.4. Conclusion

A series of *N*-(1'-methyl-6-ferrocenyl-2-naphthoyl) and *N*-(1'-ethyl-6-ferrocenyl-2-naphthoyl) amino acid and dipeptide esters have been prepared and evaluated for their biological activities. These novel-ferrocenyl bioconjugates exhibited a moderate to strong anti-proliferative effect in the human cervical carcinoma cells (ATCC HTB-35, SiHa). Except *N*-(1'-ethyl-6-ferrocenyl-2-naphthoyl)-γ-aminobutyric acid ethyl ester, all compounds have over 60% growth inhibition and found to be more active than anti-cancer drug vincristine. A general trend was observed: the gamma-aminobutyric esters are less toxic than the Gly-Gly, Gly-L-Ala and Gly-D-Ala derivatives. Those compounds were also tested against human liver cells (ATCC CCL-13, Chang liver, HeLa markers). *N*-(1'-methyl-6-ferrocenyl-2-naphthoyl)-γ-aminobutyric acid methyl ester **68**, *N*-(1'-methyl-6-ferrocenyl-2-naphthoyl)-γ-aminobutyric acid ethyl ester **69**, *N*-(1'-ethyl-6-ferrocenyl-2-naphthoyl)-glycine-D-alanine ethyl ester **75**, *N*-(1'-ethyl-6-ferrocenyl-2-naphthoyl)-γ-aminobutyric acid methyl ester **76** and *N*-(1'-ethyl-6-ferrocenyl-2-naphthoyl)-γ-aminobutyric acid ethyl ester **77** did not exhibit strong inhibition effect. Due to the less toxicity against Chang cells than SiHa, compound **68**, **69**, **75, 76** were selected for further investigation. Compound **68**, **69**, **75, 76** have IC_{50} value (μM**)** of 50.83 ± 1.29, 61.81 ± 2.52, 8.76 ± 0.98 and 44.27 ± 2.89 respectively in SiHa cell line. The observations can suggest that there are differences in susceptibilities to novel ferrocenyl amino acid and dipeptide bioconjugates toxicity between cancer and normal cells. Therefore compound **75** is a potential anti-cancer agent with selectivity.

Materials and Methods

Cells and cell culture

The SiHa HTB-35 and Chang CCL-13 cell lines were obtained from the American Type Culture Collection (ATCC). All cell culture work was carried out in laminar airflow cabinet (Thermo Fischer Scientific). Before and after use the laminar airflow, cabinet was cleaned with 70% industrial methylated spirits (IMS). Any items brought to the airflow cabinet were swabbed using IMS. At any one time, only one cell line was used in the laminar airflow cabinet and after completion of work, the laminar airflow cabinet was allowed stand for 10 minutes before use. This was to eliminate any possibility of cross contamination between cell lines.

The cells were thawed and placed in culture flasks by adding 4 mL of minimal essential medium EMEM (Caisson) supplemented with 10% fetal bovine serum (Corning) and 1% antibiotic penicillin-streptomycin (Sigma-Aldrich). EMEM was changed every 3 days. Cells were fed with fresh media when confluency reached 80%, washed twice with 4 mL of a PBS solution, dead cells were removed along with other residues. 1 mL of 0.25% trypsin-EDTA was added to the cell and incubated at 37 ° C for less than 3 minutes. Trypsin (Corning) was neutralized with 2 mL of EMEM. Cells were centrifuged to remove the medium with trypsin. 3 mL of EMEM were added after. Cell pellet formed was re-suspended, 20 μL of the suspension was taken to determine the cell concentration by counting cells in a Neubauer chamber with an inverted microscope. Once the cell concentration is obtained, a dilution was performed to obtain a 10,000 cell/100 μL concentration, which were deposited in a 96-well plate. After 24 hours, both lines were grown as a monolayer culture at 37 °C, under a humidified atmosphere of 95 % O_2 and 5 % CO_2.

In vitro proliferation assays

Assessment of cell survival in the presence of test sample was determined by the WST-1 assay. After a monolayer formed in the 96-well plate, plates were exposed with test samples with different concentrations. Plates were incubated at 37 ˚C for 24 hours. For the full comprehensive screen, cell growth percentage in the presence of each sample was calculated relative to the vincristine (positive control), cells with medium (negative control), and wells (blank control). After incubation time, medium was removed, and two washes were performed with 100μL of PBS. 100μL of 5% EMEM(Caisson) with 5% WST-1(Roche) was added, and the initial optical density reading was recorded at 450 nm on the ELx800 microplate reader (BIOTEK). The plates were incubated further for 2 hours under the same conditions as above, and the absorbance of each well was read.

Statistical analysis

IC_{50} values were calculated using CalcuSyn Software (BioSoft). Student t-test (two tailed with unequal variances) was used to compare the activity of test compounds to their corresponding control group, and p-value < 0.05 was considered.

References

1. Á. Mooney, R. Tiedt, T. Maghoub, N. O'Donovan, J. Crown, B. White and P. T. M. Kenny, *Journal of Medicinal Chemistry*, 2012, **55**, 5455-5466.
2. A. G. Harry, W. E. Butler, J. C. Manton, M. T. Pryce, N. O'Donovan, J. Crown, D. K. Rai and P. T. M. Kenny, *Journal of Organometallic Chemistry*, 2014, **757**, 28-35.
3. J. Davey and J. M. Lord, *Essential cell biology: a practical approach*, Oxford University Press, 2003.
4. R. I. Freshney, *Culture of Animal Cells : A Manual of Basic Technique and Specialized Applications*, Wiley, Hoboken, U.S., 2010.
5. R. J. B. King and M. W. Robins, *Cancer Biology*, Pearson Education M.U.A., 2006.
6. P. R. Twentyman and M. Luscombe, *British Journal of Cancer*, 1987, **56**, 279-285.
7. L. Corte-Real, A. P. Matos, I. Alho, T. S. Morais, A. I. Tomaz, M. H. Garcia, I. Santos, M. P. Bicho and F. Marques, *Microscopy and Microanalysis*, 2013, **19**, 1122-1130.
8. E. Hodgson and R. C. Smart, *Molecular and Biochemical Toxicology*, John Wiley & Sons Inc, 2008.
9. K.-C. NGAI, C.-Y. YEUNG and C.-S. LEUNG, *Journal of Paediatrics and Child Health*, 2000, **36**, 51-55.
10. S. M. Jazayeri and S. M. Alavian, *Hepatology*, 2011, **54**, 1889-1890.

Chapter 4

Synthesis and structural characterisation of *N*-(ferrocenylmethylamino acid)-fluorinated benzene carboxamides.

4.1. Introduction

The incorporation of amino acids in bioconjugations is a common strategy in medicinal chemistry research. [1,2] Antihypertensive agent Valsartan **78** and the DNA alkylating agent Mephalan **79** are drugs containing amino acid on the market. Valsartan **78** is an angiotensin II receptor agonist while Mephalan **79** is a nitrogen mustard alkylating agent with phenylalanine moiety. Similarly, Levodopa **80** contains an amino acid group that can be recognized by the phenylalanine transporter.

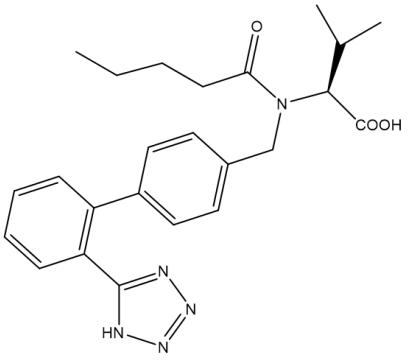

Valsartan

78

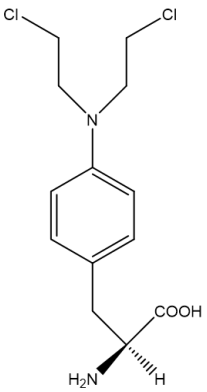

Mephalan

79

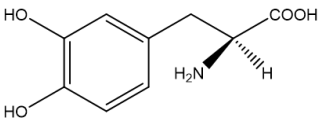

Levodopa

80

Fluorine substitution has been frequently used to increase the biological activity of a drug. [3] There were many fluorinated derivatives approved by the FDA for use as an anti-cancer, antidepressant and antibacterial agents. [4] There are over 150 fluorinated drugs on the market, including the anti-cancer Tegafur **81**, [5] the anti-depressant Lexapro **82** and anti-bacterial Levaquine **83** and ciprofloxacin **84**. [4,6] Tegafur **81** is a prodrug of 5-fluorouracil that interferes with DNA synthesis by blocking the thymidylate synthetase conversion. Lexapro **82** acts in the brain by blocking the

reuptake of the neurotransmitter serotonin into presynaptic cells. Levaquine **83** and Ciprofloxacin **84** are from the fluoroquinolone antibiotic family. They can bind to DNA gyrase (topoisomerase II) of bacterial hence prevents bacteria's cell replication. [3, 4] It has emerged that to have fluorine atom on 9-position of the quinolone ring is essential.

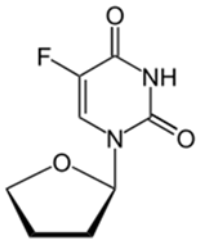

Tegafur

81

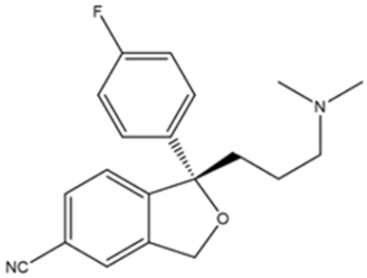

Lexapro

82

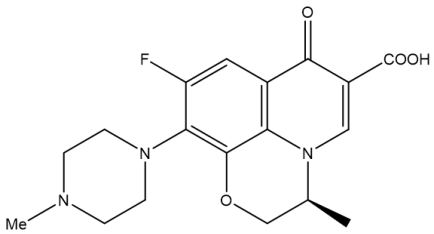

Levaquin

83

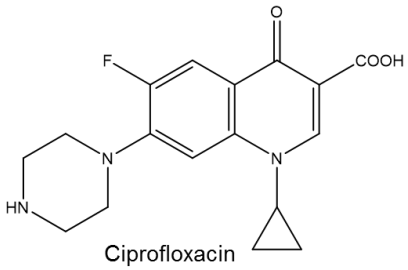

Ciprofloxacin

84

Fluorine is highly electronegative, lipophilic with small atomic size, those properties aids its addition to other active molecules to improve biological activity. Replace the hydroxyl groups with fluorine atoms to the parent compound resveratrol, an increasing anti-proliferative effect was reported by Moran *et al*. The general structure of **85** is shown below. [7]

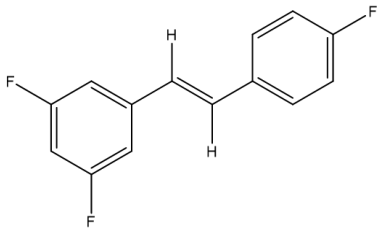

85

A preliminary structure-activity relationship (SAR) study of *N*-(ferrocenylmethyl) fluorinated benzene carboxamide derivatives was conducted by Kelly *et al*. and Butler *et al*. [8, 9] The results demonstrated that the derivatives are effective at inhibiting the *in vitro* proliferation of breast cancer cell lines MDA-MB-435-SF and MCF-7. Their research gave IC_{50} data in the range of 11μM to 50μM on the MDA-MB-435-SF cell line and 2.84 μM to 46.5 μM on the MCF-7 cell line (Table 4.1). [8, 9] The position and the number of fluorine atoms on the aromatic ring were investigated, 3,4,5-trifluoro and 2,3,4,5,6-pentafluoro analogues were identified as having an excellent inhibitory effect on MCF-7 cell line. [9]

Table 4.1: IC_{50} values for the most active compounds in the *N*-(ferrocenylmethyl) fluorinated benzene carboxamide derivatives against MCF-7 cell line.

Compound	**No.**	**IC_{50} (μM)**
N-(ferrocenylmethyl-L-alanine)-3,4,5-trifluorobenzene carboxamide	**28**	2.84 ± 0.10
N-(ferrocenylmethyl-L-alanine)-2,3,4,5,6-pentafluorobenzene carboxamide	**86**	10.3 ± 0.12
N-(ferrocenylmethylglycine)-2,3,4,5,6-pentafluorobenzene carboxamide	**87**	11.1 ± 0.12

The primary objective of this research is to explore the SAR of these novel *N*-(ferrocenylmethylamino acid) fluorobenzene carboxamide derivatives in order to enhance their cytotoxic effect. Since the position and the number of fluorine atoms on the aromatic ring have been investigated, it is now focused on varying the amino acid or peptide chains to determine the contributions toward the biological effect. This was carried out by substituting various amino acids and dipeptides between the ferrocene and the aromatic ring containing 3,4,5-trifluoro or 2,3,4,5,6-pentafluoro moiety. A series of compounds synthesized and discussed in this chapter have three key moieties (Figure 4.1): a redox active ferrocenyl centre; an amino acid or dipeptide moiety and a fluorinated aromatic ring.

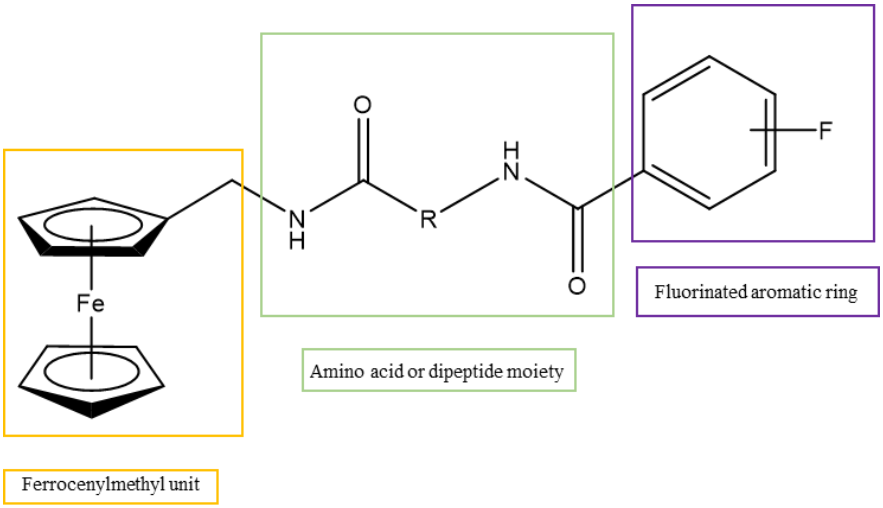

Figure 4.1: General structure of the *N*-(ferrocenylmethyl) fluorinated benzene carboxamides **28, 86, 87, 101-108**.

4.2. The synthesis of *N*-(ferrocenylmethylamino acid) fluorinated benzene carboxamides

The *N*-(ferrocenylmethylamino acid) fluorinated benzene carboxamides were prepared *via* standard peptide coupling methods using conventional *N*-(3-dimethylaminopropyl)-*N*'-ethylcarbodiimide hydrochloride (EDC) and *N*-hydroxysuccinimide (NHS) coupling protocol. A solution of *N*-(fluorobenzoyl) amino acids or dipeptides in dichloromethane at 0 °C, was treated with EDC, NHS and triethylamine (Et_3N) and allowed to stir for 45 minutes. Ferrocenylmethylamine was added to the solution with stirring. Subsequent to coupling, the crude compounds were purified *via* column chromatography. The eluent used in all the column chromatography was hexane : ethyl acetate mixture (2:1). Scheme 4.1 and Scheme 4.2 outline the synthetic route employed.

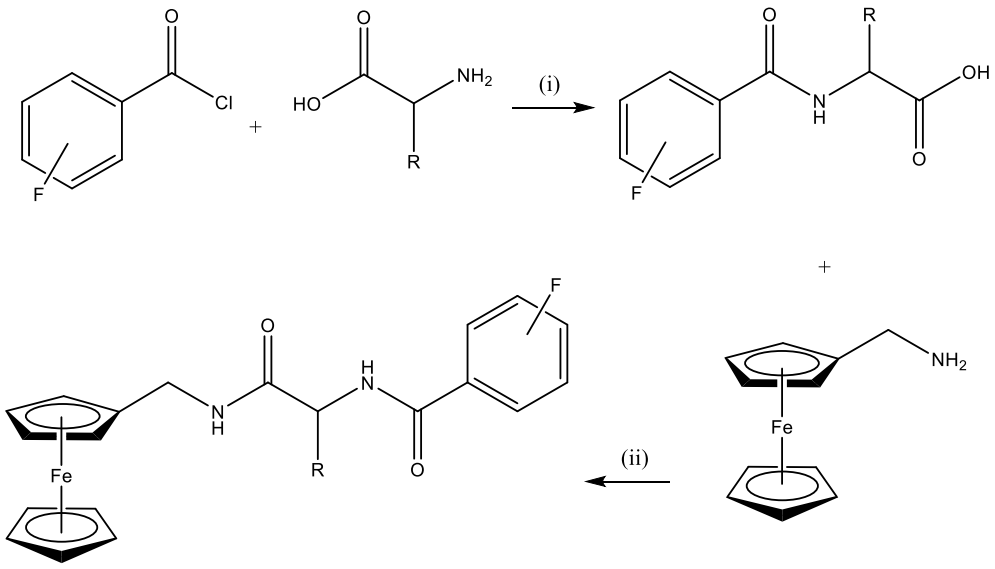

R = -H, -CH_3, -CH_2CH_3, -$CH_2CH_2CH_3$, -$CH_2(CH_2)_2CH_3$, -$CH_2CH(CH_3)_2$, -$CH_2CH_2SCH_3$, -Ph.

(i) 2M NaOH (ii) EDC, NHS, Et_3N.

Scheme 4.1: The general reaction scheme for the synthesis of *N*-(ferrocenylmethylamino acid) fluorinated benzene carboxamide using *N*-(fluorobenzoyl) amino acids.

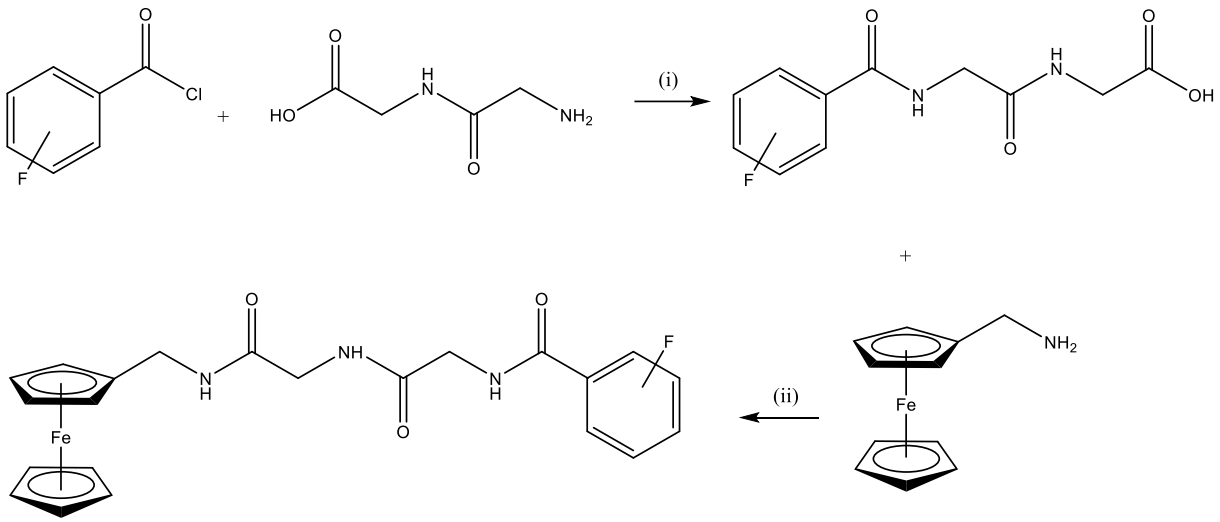

(i) 2M NaOH (ii) EDC, NHS, Et_3N.

Scheme 4.2: The reaction scheme for the synthesis of *N*-(ferrocenylmethyl-glycine-glycine) fluorinated benzene carboxamide **108** using *N*-(fluorobenzoyl)-glycine-glycine.

4.2.1. Synthesis of ferrocenecarbaldoxime

The synthesis of ferrocenecarbaldoxime is outlined in Scheme 4.3. The amine of the hydroxylamine hydrochloride attacks the carbonyl group of the ferrocenecarboxaldehyde hence a dipolar tetrahedral intermediate formed. An amino alcohol formed due to intermolecular proton transfer form nitrogen to oxygen. Protonation of the oxygen produces a good leaving group, and loss of water yields an oxime ion. Transfer of a proton to water produces the oxime. [10]

Reaction yields of the ferrocenecarboaldoxime ranged between 80% and 89%. After complete drying, ferrocenecarboaldoxime was reduced to ferrocenylmethylamine by using lithium aluminum hydride (Scheme 4.4), with around 97% yield.

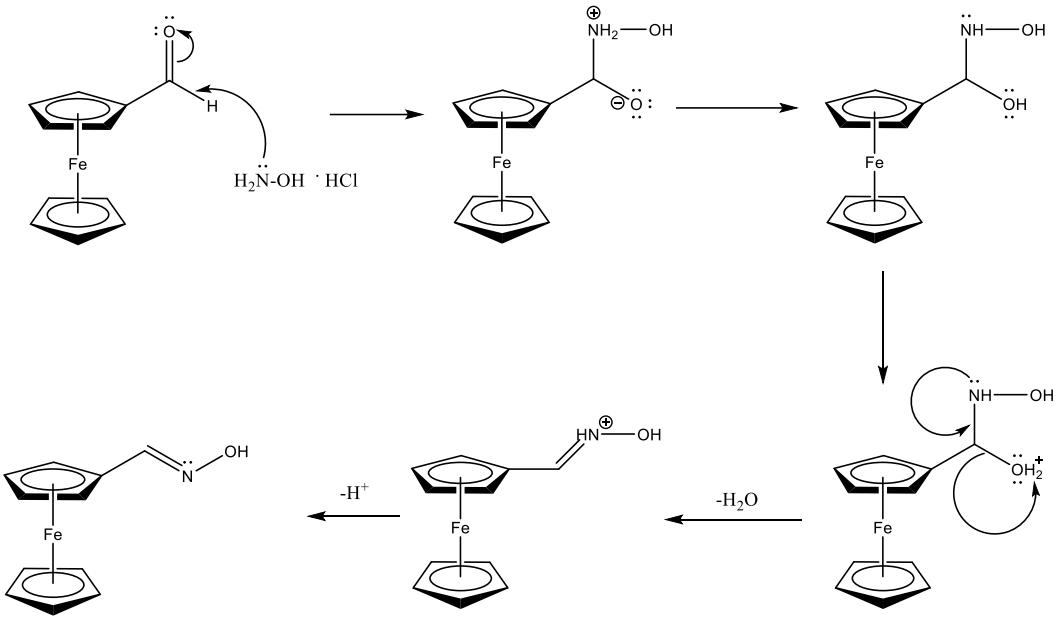

Scheme 4.3: Reaction mechanism for the synthesis of ferrocenecarbaldoxime.

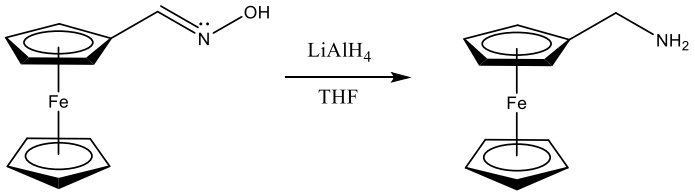

Scheme 4.4: Synthesis of ferrocenylmethylamine *via* reduction of ferrocenecarbaldoxime.

4.2.2. Synthesis of *N*-(fluorobenzoyl) amino acids and dipeptides

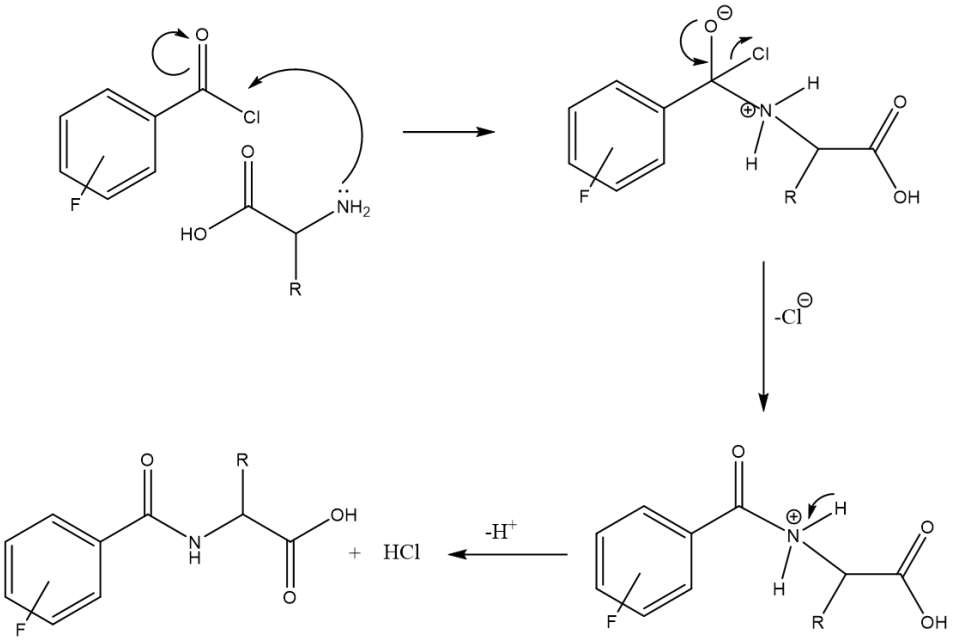

Scheme 4.5: Schotten Baumann reaction mechanism of fluorobenzoyl chlorides with the amino acids and dipeptides.

N-(fluorobenzoyl) amino acids and dipeptides were synthesized *via* Schotten Baumann reaction (Scheme 4.5). This two-phase system of immiscible water and dichloromethane allowing the formation of the amino acid intermediates and the neutralisation of the excess acid formed during the reaction. [11] The desired products were with percentage yields varying between 19.6-49 %.

4.2.3. Preparation of *N*-(ferrocenylmethylamino acid)-fluorinated benzene carboxamides

EDC/NHS coupling reactions were used to facilitate the attachment of the ferrocenylmethylamine to the various *N*-(fluorobenzoyl) amino acids and dipeptides. *N*-(fluorobenzoyl) amino acids or dipeptides was treated with EDC, NHS and triethylamine (Et_3N) in dichloromethane at 0 °C, ferrocenylmethylamine was added to mixture to stir for 48 hours. The crude product was purified by column chromatography {eluent 2:1 hexane: ethyl acetate} yielding the title compound as an orange solid.

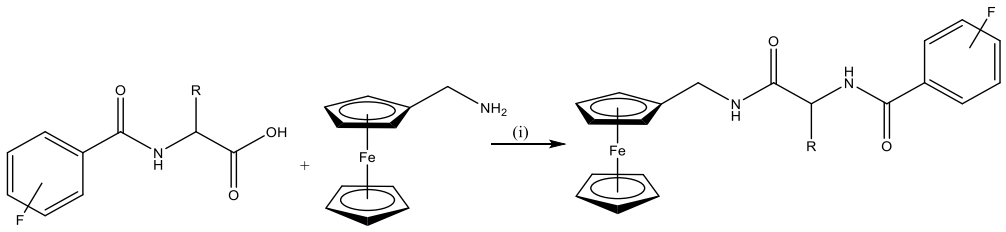

R = -H, -CH_3, -CH_2CH_3, -$CH_2CH_2CH_3$, -$CH_2(CH_2)_2CH_3$, -$CH_2CH(CH_3)_2$, -$CH_2CH_2SCH_3$, -Ph.

(i) EDC, NHS, Et_3N

Scheme 4.6: Synthesis of *N*-(ferrocenylmethylamino acid)-fluorinated benzene carboxamides **28**, **86**, **87**, **101-107**.

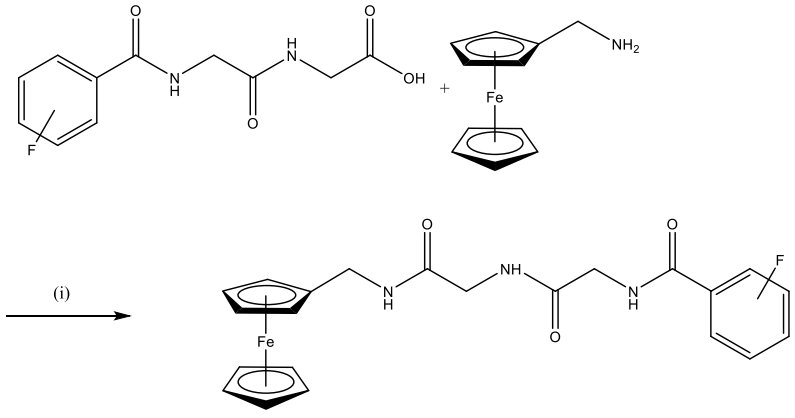

(i) EDC, NHS, Et_3N

Scheme 4.7: Synthesis of *N*-(ferrocenylmethyl-glycine-glycine)-2,3,4,5,6-pentafluorobenzene carboxamide **108**.

4.3. Purification and yields of *N*-(ferrocenylmethylamino acid)-fluorinated benzene carboxamides

The *N*-(ferrocenylmethylamino acid)-fluorinated benzene carboxamides were synthesized by the condensation of various *N*-(fluorobenzoyl) amino acids and dipeptides with ferrocenylmethylamine, under the standard EDC/NHS coupling conditions. Crude products were purified in the usual manner by column chromatography, using a mixture of hexane and ethyl acetate as the eluent. The purified compounds were furnished as orange solids, with yields in the range of 11 % to 52 %, shown in Table 4.2. All compounds gave spectroscopic and analytical data in accordance with their proposed structures. Yields were found to vary according to the amino acids and dipeptides. General trend showed the larger the side chain of the amino acid the lower the yield. For example, compound **103** have the lowest yield as 11% whereas compound **28** have highest yield 52%. Such low yield may be due to the side chain to exert greater steric hindrance.

Table 4.2: Percentage yields for *N*-(ferrocenylmethylamino acid)-fluorinated benzene carboxamides

Compound Name	**Compound No.**	**%Yields**
N-(ferrocenylmethyl-L-alanine)-3,4,5-trifluorobenzene carboxamide	**28**	52
N-(ferrocenylmethyl-L-2-aminobutyric acid)-3,4,5-trifluorobenzene carboxamide	**101**	34
N-(ferrocenylmethyl-L-norvaline)-3,4,5-trifluorobenzene carboxamide	**102**	17
N-(ferrocenylmethyl-L-leucine)-3,4,5-trifluorobenzene carboxamide	**103**	11
N-(ferrocenylmethyl-L-norleucine)-3,4,5-trifluorobenzene carboxamide	**104**	13
N-(ferrocenylmethyl-L-methionine)-3,4,5-trifluorobenzene carboxamide	**105**	13
N-(ferrocenylmethyl-L-(+)-α-phenylglycine)-3,4,5-trifluorobenzene carboxamide	**106**	15
N-(ferrocenylmethylglycine)-2,3,4,5,6-pentafluorobenzene carboxamide	**87**	28
N-(ferrocenylmethyl-L-alanine)-2,3,4,5,6-pentafluorobenzene carboxamide	**86**	29
N-(ferrocenylmethyl-L-(+)-α-phenylglycine)-2,3,4,5,6-pentafluorobenzene carboxamide	**107**	12
N-(ferrocenylmethyl-glycine-glycine)-2,3,4,5,6-pentafluorobenzene carboxamide	**108**	16

4.4. Infra-red studies of *N*-(ferrocenylmethylamino acid)-fluorinated benzene carboxamides

The IR spectra of the *N*-(ferrocenylmethylamino acid)-fluorinated benzene carboxamides were obtained as pure solids and shown in Table 4.3. The spectra of these compounds generally showed strong bands around 3200 cm^{-1} that correspond to the N-H stretching from amide groups. Bands observed in the region of 2960 to 2850 cm^{-1} correspond for the saturated C-H stretches in methylene and methyl groups. The two or three bands between 1600 and 1475 cm^{-1} are due to the C=C ring stretch of the aromatic ring system.

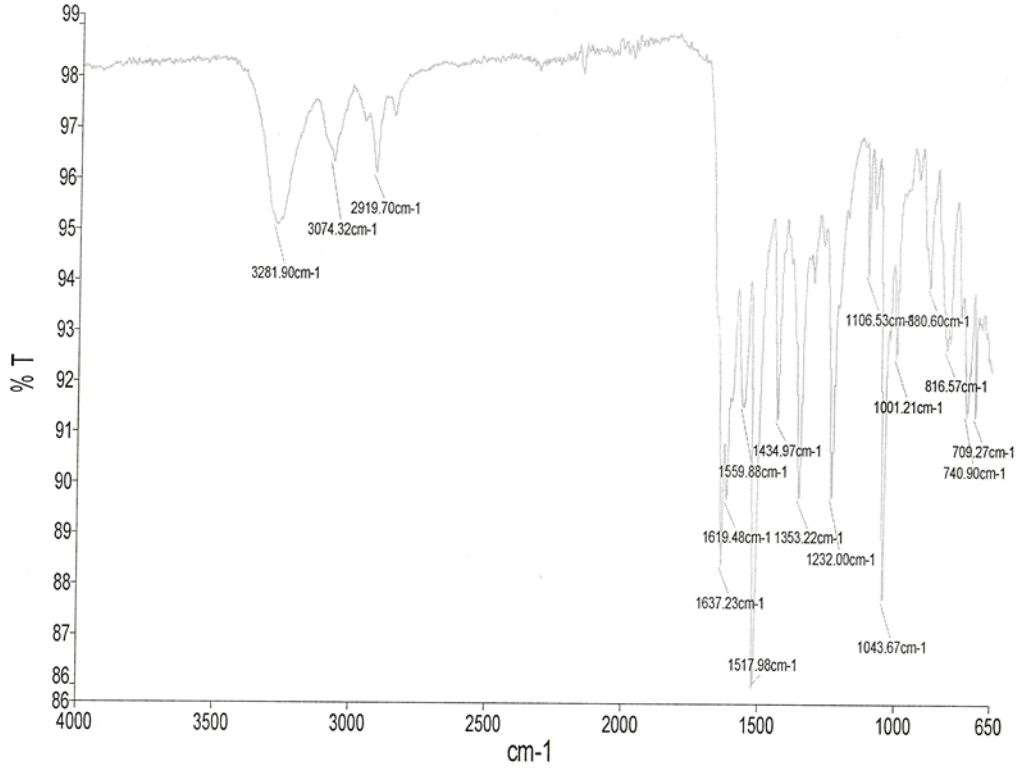

Figure 4.2: IR spectrum of *N*-(ferrocenylmethyl-L-methionine)-3,4,5-trifluorobenzene carboxamide **105**.

Table 4.3: IR data for *N*-(ferrocenylmethylamino acid)-fluorinated benzene carboxamides. Values are given in cm^{-1}.

Compound No.	N-H	C-H	C=O	Aromatic
28	3290	3075	1641	1621-1559
101	3282	2926	1639	1518
102	3307	3094	1638	1621-1519
103	3289	3067	1637	1604-1516
104	3242	3073	1634	1619-1520
105	3281	3074	1637	1619-1517
106	3282	2957	1664	1623-1518
87	3309	3067	1653	1506
86	3286	3051	1653	1621-1506
107	3257	2926	1669	1631-1519
108	3239	3057	1649	1523

4.5. UV-Vis studies of *N*-(ferrocenylmethylamino acid)-fluorinated benzene carboxamides

In this UV-Vis study, the spectra of all compounds were obtained at a concentration of 5 x 10^{-4} M in acetonitrile. The molar extinction coefficient ε is calculated from the Beer-Lambert Law A=εcl, where A is the absorbance, c is the concentration and l is the path length of the sample cell.

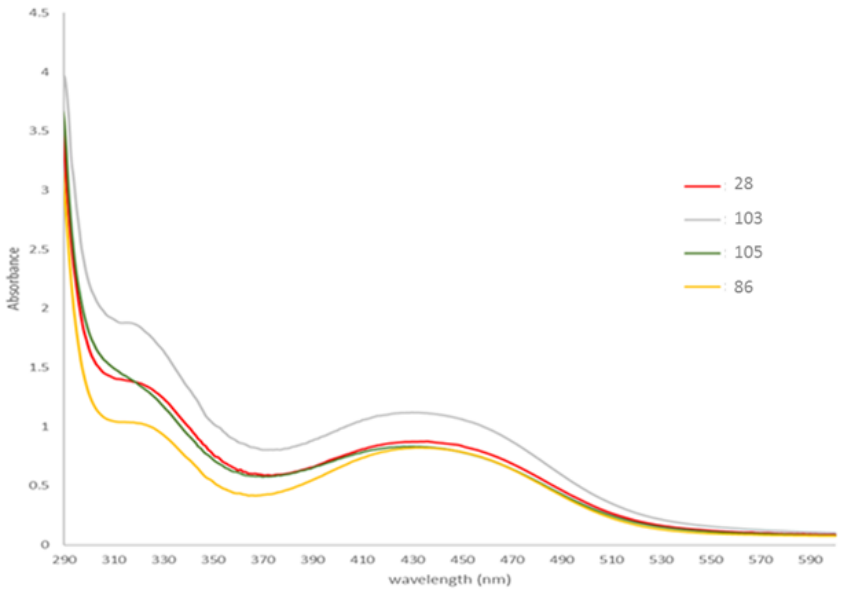

Figure 4.3: UV-Vis data for selected *N*-{ferrocenylmethyl(L-alanine), (L-leucine), (L-methionine)}-3, 4, 5-trifluorobenzene carboxamides **28**, **103**, and **105**. *N*-{ferrocenylmethyl (L-alanine)}-2, 3, 4, 5, 6-pentafluorobenzene carboxamide **86**.

Table 4.4: UV-Vis data for selected *N*-(ferrocenylmethylamino acid)-fluorinated benzene carboxamides.

Compound No.	$\lambda_{max1\ (nm)}$	ε_1	$\lambda_{max2\ (nm)}$	ε_2
28	432	2483	317	2940
103	429	2312	313	2894
105	430	2019	315	2687
86	427	2895	314	3320

From the UV-Vis data for *N*-(1'-methyl-6-ferrocenyl-2-naphthoyl) and *N*-(1'-ethyl-6-ferrocenyl-2-naphthoyl) amino acid and dipeptide esters shown in Figure 4.3 and Table 4.4, the strongest absorptions in the UV spectrum with local maxima at 375 nm and 450 nm respectively. The absorptions are similar with those of the *N*-(6-ferrocenyl-2-naphthoyl) derivatives. [12] Low energy bands observed approximately at 450 nm with a distinct $\lambda_{max\ 2}$ value can be assigned as metal to ligand charge transfer (MLCT) band transitions arising from the ferrocene moiety. The high energy band around 375 nm, with distinct λ_{max1} values are due to the π - π^* transitions of the aromatic spacer group.

4.6. ^{1}H NMR studies of *N*-(ferrocenylmethylamino acid)-fluorinated benzene carboxamides

All the ^{1}H NMR experiments were performed in DMSO-*d6* as the *N*-(ferrocenylmethylamino acid) fluorinated benzene carboxamide derivatives showed limited solubility in other deuterated solvents. Table 4.5 summarises the main features of the ^{1}H NMR spectra.

In the ^{1}H NMR spectra of the *N*-(ferrocenylmethylamino acid) fluorinated benzene carboxamides, the amide protons peaks appear downfield from δ 9.82-8.16. The equivalent protons in the *ortho*-position of the aromatic ring are split by fluorine coupling, appear as a doublet of doublets with integration of two for trifluorinated derivatives. This signal absences for pentafluorinated compounds.

The ^{1}H NMR spectra of the *N*-(ferrocenylmethylamino acid) fluorinated benzene carboxamides derivatives showed peaks in the range of δ 4.19-4.02 that are representative of a monosubstituted ferrocene derivative. The signal for the unsubstituted (η^5-C_5H_5) cyclopentadienyl ring and the protons in the *ortho* position on the substituted ring (η^5-C_5H_5) occur as a multiplet between δ 4.20 and δ 4.02. This multiplet with an integration of seven protons is observed due to the overlap of signals. The *meta* protons of the substituted (η^5-C_5H_5) cyclopentadienyl ring appears as a triplet between δ 4.14 and δ 4.02 for most derivatives, except for compound **101** and **107** that the signal overlaps with either ferrocenyl protons or methylene protons attached to ferrocene. The peaks belong to methylene group from Fc-CH_2 appears between δ 4.15 - δ 3.92, integrating for two.

Table 4.5: ^{1}H NMR spectral data for *N*-(ferrocenylmethylamino acid)-fluorinated benzene carboxamides.

Compound No.	CONH	$FcCH_2NH$	ArH	αH	(η^5-C_5H_5) & *ortho* on (η^5-C_5H_4)	*meta* on (η^5-C_5H_4)	$FcCH_2$
28	8.75	8.18	7.93	4.50	4.19-4.17	4.08	4.05-3.90
101	8.62	8.16	7.91	4.40	4.17-4.16	4.08-4.04	4.08-4.04
102	8.64	8.16	7.90	4.48	4.16-4.15	4.09	4.06-3.97
103	8.72	8.28	7.92	4.58	4.18-4.15	4.08	4.06-3.92
104	8.69	8.24	7.91	4.46	4.07-4.04	4.03	3.99-3.94
105	8.75	8.25	7.90	4.55	4.16-4.13	4.04	3.99-3.94
106	9.16	8.55	7.94	5.74	4.15-4.07	4.02	3.97-3.92
87	9.20	8.20	-	-	4.20-4.17	4.10	4.05
86	9.24	8.32	-	4.57	4.19-4.16	4.12	4.15-4.05
107	9.82	8.70	-	5.80	4.14-4.02	4.14-4.02	3.97-3.95
108	9.16, 8.01	8.28	-	-	4.19-4.17	4.09	4.03-4.00

4.6.1. ^{1}H NMR spectroscopic studies of *N*-(ferrocenylmethyl-L-2-aminobutyric acid)-3,4,5-trifluorobenzene carboxamide (101)

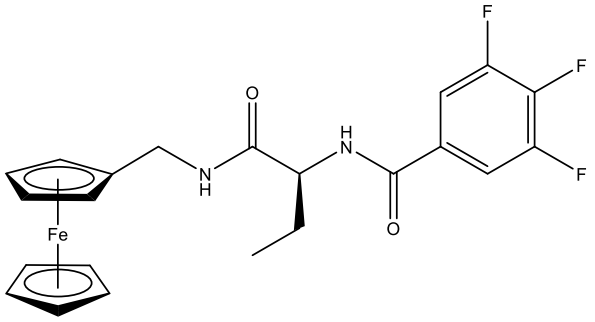

In the ^{1}H NMR spectrum of *N*-(ferrocenylmethyl-L-2-aminobutyric acid)-3,4,5-trifluorobenzene carboxamide **101**, two amide protons occur at the relatively downfield positions of δ 8.62 and δ 8.16 respectively. They appear as a doublet and a triplet due to the coupling of the nearby methine group of aminobutyric acid group and methylene group of the ferrocenylmethylamine moiety. The coupling constants observed for the amide protons at δ 8.62 and δ 8.16 were both 8.0 Hz.

The aromatic protons appear as a doublet of doublets at δ 7.91 due to the fluorine-proton coupling. This was observed in all trifluorinated derivatives synthesized. The aromatic peak integrates as two hydrogens.

The signal for the unsubstituted (η^5-C_5H_5) cyclopentadienyl ring and the protons in the *ortho* position on the substituted ring (η^5-C_5H_4) occur as a multiplet between δ 4.17 and δ 4.16. A multiplet with an integration of seven protons is observed due to the overlap of signals. The *meta* protons of the substituted (η^5-C_5H_4) cyclopentadienyl ring and the protons attached to ferrocenyl group appear as a multiplet between δ 4.08-4.04 with integration of four.

The methylene and methyl protons belong to aminobutyric acid were appear as a multiplet and a triplet at δ 1.83-1.72 and δ 0.94, with corresponding integration of two and three.

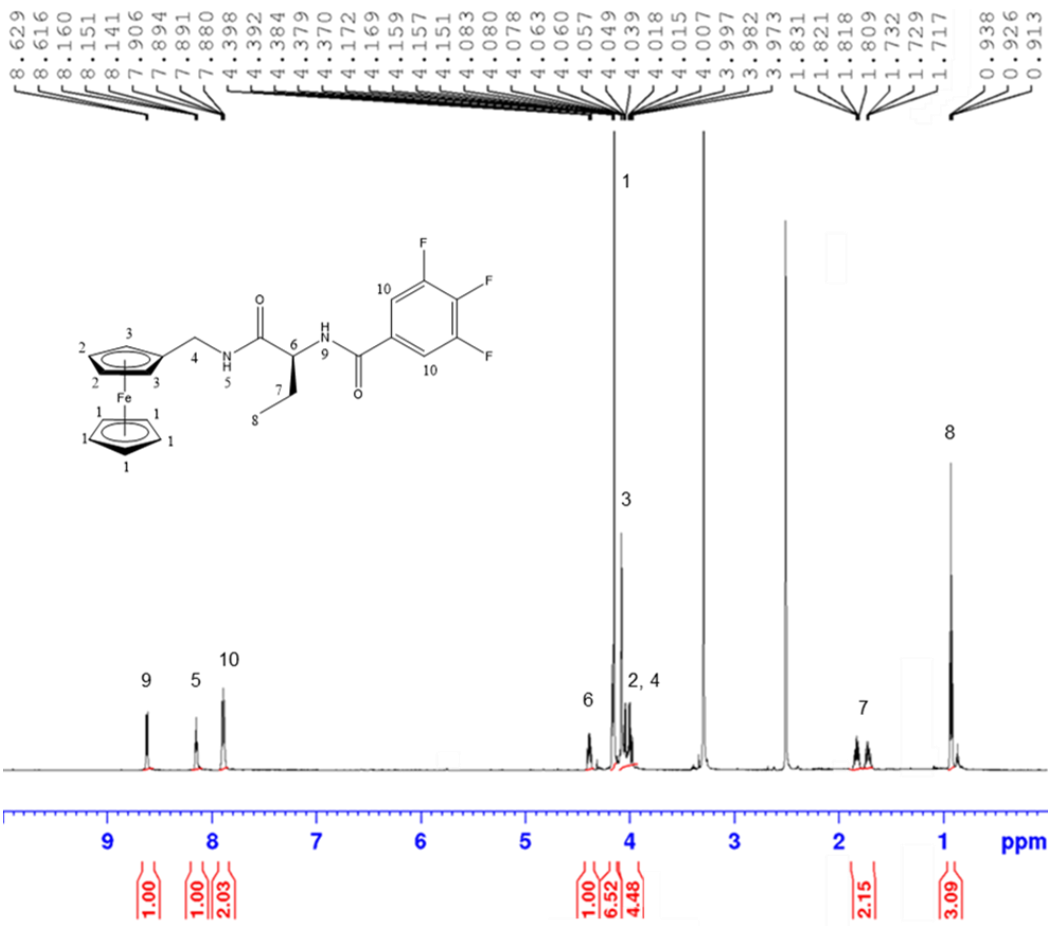

Figure 4.4: ^{1}H NMR spectrum of *N*-(ferrocenylmethyl-L-2-aminobutyric acid)-3,4,5-trifluorobenzene carboxamide **101**.

4.6.2. ^{1}H NMR spectroscopic studies of *N*-(ferrocenylmethyl-glycine-glycine)-2,3,4,5,6-pentafluorobenzene carboxamide (108)

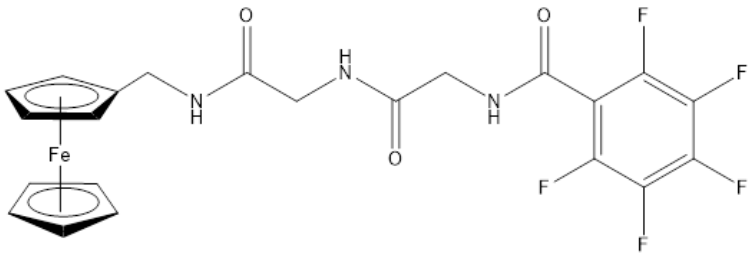

In the ^{1}H NMR spectrum of *N*-(ferrocenylmethyl-glycine-glycine)-2,3,4,5,6-pentafluorobenzene carboxamide **108**, three amide protons occur at δ 9.16, δ 8.28 and δ 8.01 respectively. All amide groups appear as triplets due to the coupling of the nearby methylene groups of glycine and of the ferroceneylmethylamine moiety. The coupling constants observed for the amide protons at δ 9.16 and δ 8.01 were 7.2 Hz while at δ 8.28 was 8.0 Hz.

The signal for the unsubstituted (η^5-C_5H_5) cyclopentadienyl ring and the protons in the *ortho* position on the substituted ring (η^5-C_5H_4) occur as a multiplet between δ 4.19 and δ 4.17. This signal has an integration of seven protons because of the overlap of signals. The *meta* protons of the substituted (η^5-C_5H_4) cyclopentadienyl ring occurs as a triplet at δ 4.09.

The methylene protons belong to the ferrocenylmethylamine group and glycine group appear as a multiplet between δ 4.03-4.00. And another methylene group of the amino acid occur most upfield is split into a doublet at δ 3.78 with a coupling constant of 5.6 Hz.

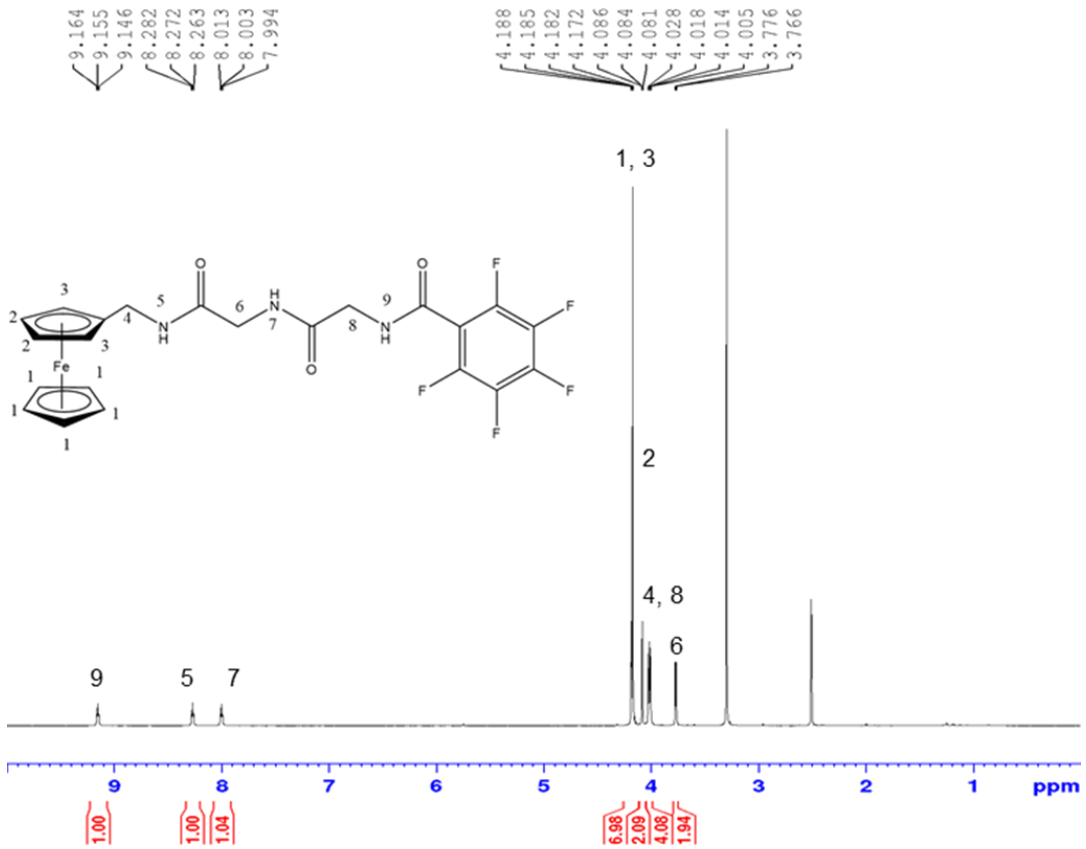

Figure 4.5: ^{1}H NMR spectrum of *N*-(ferrocenylmethyl-glycine-glycine)-2,3,4,5,6-pentafluorobenzene carboxamide **108**.

4.7. ^{13}C NMR and DEPT-135 spectroscopic studies of *N*-(ferrocenylmethylamino acid)-fluorinated benzene carboxamides

^{13}C and DEPT 135 NMR studies were carried out on all compounds. In a DEPT-135 spectrum, methine and methyl carbons appear as positive peaks, whereas methylene carbons appear as negative peaks. Carbonyl and quaternary carbons are absent in a DEPT-135 spectrum. All the ^{13}C and DEPT-135 NMR experiments were performed in $CDCl_3$. The typical ^{13}C NMR chemical shifts observed were recorded in Table 4.6.

In the ^{13}C NMR spectra of *N*-(ferrocenylmethylamino acid)-fluorinated benzene carboxamides, the amide carbonyl peak appears between δ 168.5 and δ 171.5 as a triplet due to the effect of ^{19}F-^{13}C coupling, and the carbonyl carbon atoms of the benzene carbonyl carbon atoms appear in the region of δ 167.9 to δ 156.8 for all the derivatives synthesized. In the amino acid derivatives only two carbonyl signals are observed whilst for the dipeptide derivatives three carbonyl signals are observed. Carbon signals belong to trisubstituted derivatives appears four peaks, due to four unique carbons. Pentafluoro derivatives have six distinct peaks. This effect is due to ^{19}F-^{13}C coupling in the ^{13}C NMR spectra.

The ferrocenyl carbon atoms appear in the region between δ 86.7 and δ 67.2. The unsubstituted cyclopentadienyl ring (η^5-C_5H_5) appears as an intense peak in the range of δ 69.0 to δ 68.3, while the other ferrocenyl peaks, the *ortho* and *meta* carbons of the substituted cyclopentadienyl ring (η^5-C_5H_4) produce chemical shifts between δ 68.8 and δ 67.2. The *ipso* carbon on the substituted cyclopentadienyl ring appears in the range of δ 86.7 to δ 85.9. This peak does not appear in any of the DEPT 135 NMR spectra.

The methylene carbon atom of ferrocenylmethylamine appears in the region of δ 38.1 to δ 37.4. And the α carbon belongs to amino acid groups has peak between δ 57.2 and δ 49.7. The methylene carbon belongs to amino acid or dipeptide have signal between δ 42.9 and δ 19.4 while the methyl groups from amino acid or dipeptide shows signal around δ 23.1 to δ 11.2.

Table 4.6: ^{13}C and DEPT 135 NMR spectral data for *N*-(ferrocenylmethylamino acid)-fluorinated benzene carboxamides

Compound No.	C=O	*Ipso* (η^5-C_5H_4)	(η^5-C_5H_5)	*ortho* on (η^5-C_5H_4)	*meta on* (η^5-C_5H_4)	α-C	Fc-CH_2
28	170.5, 167.9	86.2	68.4	67.5	67.1	49.7	37.4
101	171.3, 163.7	86.7	68.8	68.0	67.7	55.7	38.0
102	171.5, 163.6	86.7	68.8	68.0	67.7	54.0	38.0
103	171.3, 162.9	86.2	68.8	68.0	67.7	52.0	37.4
104	171.1, 163.1	86.1	68.3	67.5	67.2	53.8	37.6
105	171.0, 163.8	86.6	68.8	68.0	67.7	53.6	38.1
106	168.9, 156.8	86.6	69.0	68.8	67.7	57.2	38.1
87	168.3, 165.1	85.9	68.3	67.8	67.3	-	37.5
86	170.6, 164.9	86.2	68.3	67.5	67.2	49.8	37.4
107	168.9, 156.8	86.4	69.0	68.8	67.7	57.2	37.4
108	168.5, 168.4, 147.5	86.4	68.8	68.4	67.7	-	38.1

4.7.1. ^{13}C NMR and DEPT-135 spectroscopic studies of *N*-(ferrocenylmethyl-L-(+)-α-phenylglycine)-2,3,4,5,6-pentafluorobenzene carboxamide (107)

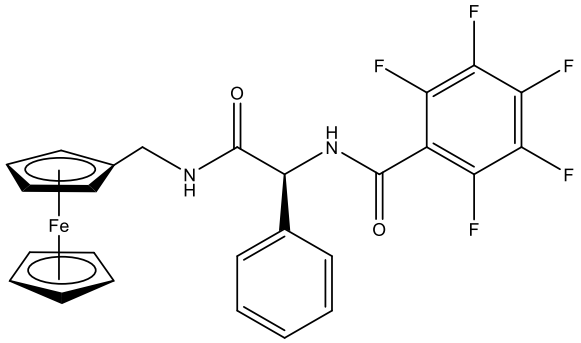

The ^{13}C NMR spectrum of *N*-(ferrocenylmethyl-L-(+)-α-phenylglycine)-2,3,4,5,6-pentafluorobenzene carboxamide **107** displays two carbonyl carbon atoms at δ 168.9 and δ 156.8. These are not present in the DEPT-135 spectrum. The fluorinated aromatic region shows six unique carbon signals, representing the six non-equivalent quaternary carbon atoms, between δ 143.0 and δ 112.9. Each of the carbon atoms on the fluorinated aromatic ring appear as multiplets and triplet (*J* = 14.0 Hz) due to the effect of ^{19}F-^{13}C coupling. These six quaternary carbon atoms can be identified by their absence in the DEPT-135 spectrum. Four peaks from the aromatic protons belong to phenylglycine appear between δ 144.6 to δ 127.5.

The carbon located at δ 86.4, is the *ipso* carbon. This peak is not present in the DEPT-135 spectrum. The 5 equivalent carbons of the unsubstituted (η^5-C_5H_5) cyclopentadienyl ring occurs at δ 69.0. The carbons of the substituted cyclopentadienyl ring, in the positions of *ortho* and *meta*, occur at δ 68.8 and δ 67.7 respectively.

The α-C from phenylglycine appear at δ 57.2. The methylene group belongs to ferrocenylamine is easily assigned, as it shows negative resonance in the DEPT-135 at δ 38.1.

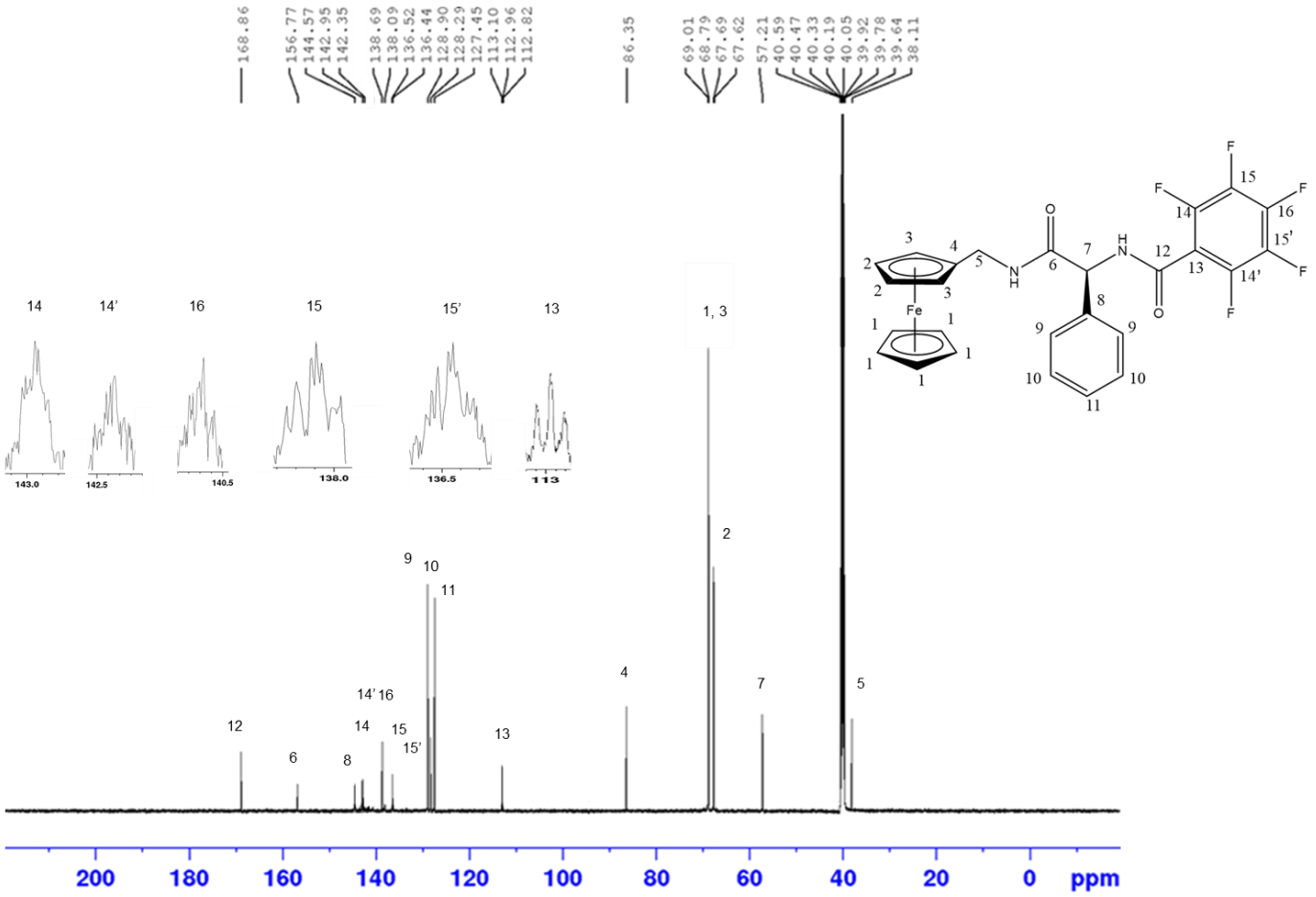

Figure 4.6: ^{13}C NMR spectrum of *N*-(ferrocenylmethyl-L-(+)-α-phenylglycine)-2,3,4,5,6-pentafluorobenzene carboxamide **107**.

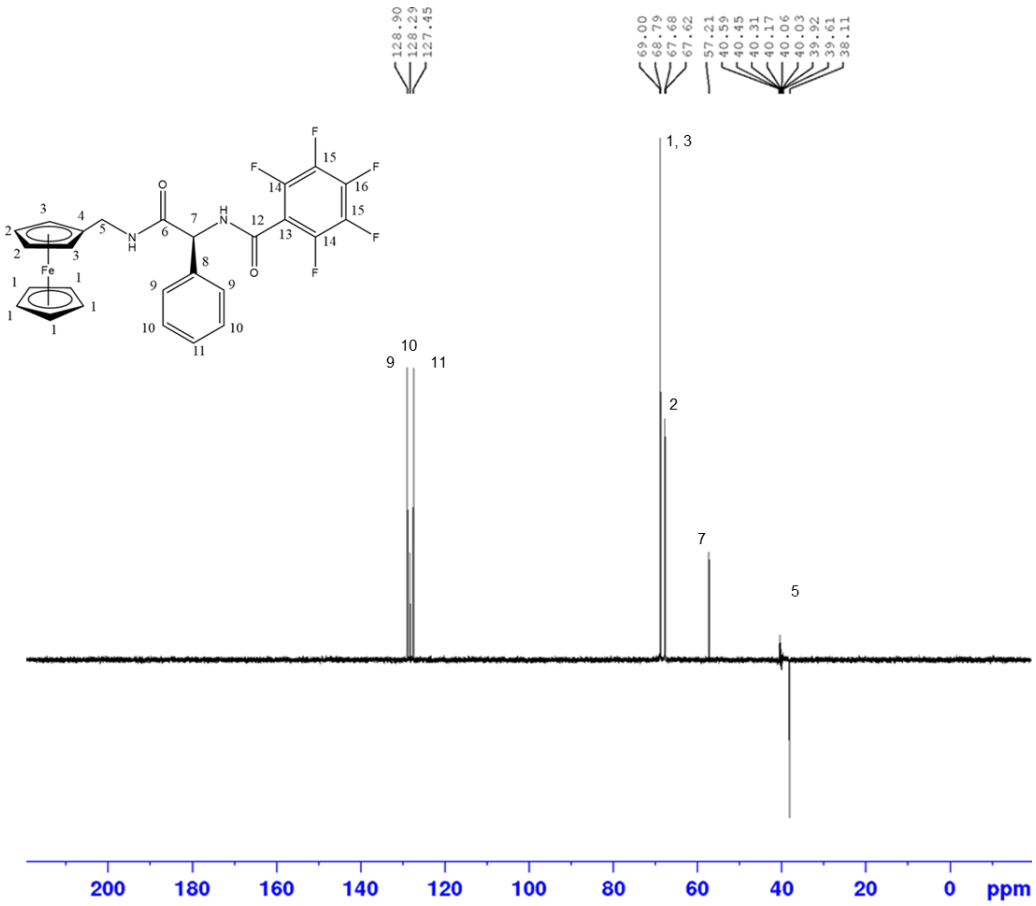

Figure 4.7: DEPT-135 NMR spectrum of *N*-(ferrocenylmethyl-L-(+)-α-phenylglycine)-2,3,4,5,6-pentafluorobenzene carboxamide **107.**

4.8. ^{19}F NMR spectroscopic studies of *N*-(ferrocenylmethylamino acid) fluorinated benzene carboxamide derivatives

For the characterization of *N*-(ferrocenylmethylamino acid) fluorinated benzene carboxamide derivatives, fluorine was identified *via* ^{19}F NMR spectroscopy. The position and the number of fluorine atoms on the aromatic moiety of the *N*-(ferrocenylmethylamino acid) fluorobenzene carboxamides played a vital role in the characterization of the compounds.

For trisubstituted derivatives, the *meta* fluorines appear as a doublet of doublets with integration of two, this splitting is caused by the one adjacent *para* fluorine ($^3J_{FmFp}$ = 22.6 Hz) and two *ortho* hydrogens ($^3J_{FmHo}$ = 7.5 Hz) coupling. The *para* fluorine occurs as a triplet of triplets with integration of one. It is a triplet of triplets because of the two adjacent *meta* fluorine atoms ($^3J_{FpFm}$ = 22.6 Hz) and two *ortho* hydrogens ($^4J_{FpHo}$ = 7.5 Hz).

The pentafluoro derivatives show a distinctive pattern in the ^{19}F NMR. The fluorine atoms in the *ortho* positions appear as a doublet of doublets. The fluorine atoms couple with the *meta* fluorine atoms to give a coupling constant of 22.6 Hz and with each other giving a decreased coupling constant of 7.5 Hz. The *para*-fluoro substituent appears as a triplet with coupling constant equal to 22.6 Hz. This signal is caused by coupling with two *meta* fluorine atoms. The integration of this peak gives a value of one. The *meta* fluorine atoms on the aromatic moiety is observed as a triplet of doublets with integration as two. The fluorine atoms in these positions couple with each other, the *ortho* fluorine atoms and the *para* fluorine atom.

The chemical shifts appear in the negative region within the range of δ -134.3 to δ -161.7. Figure 4.8 and Figure 4.9 present the ^{19}F NMR spectrum for compound **104** and **107**.

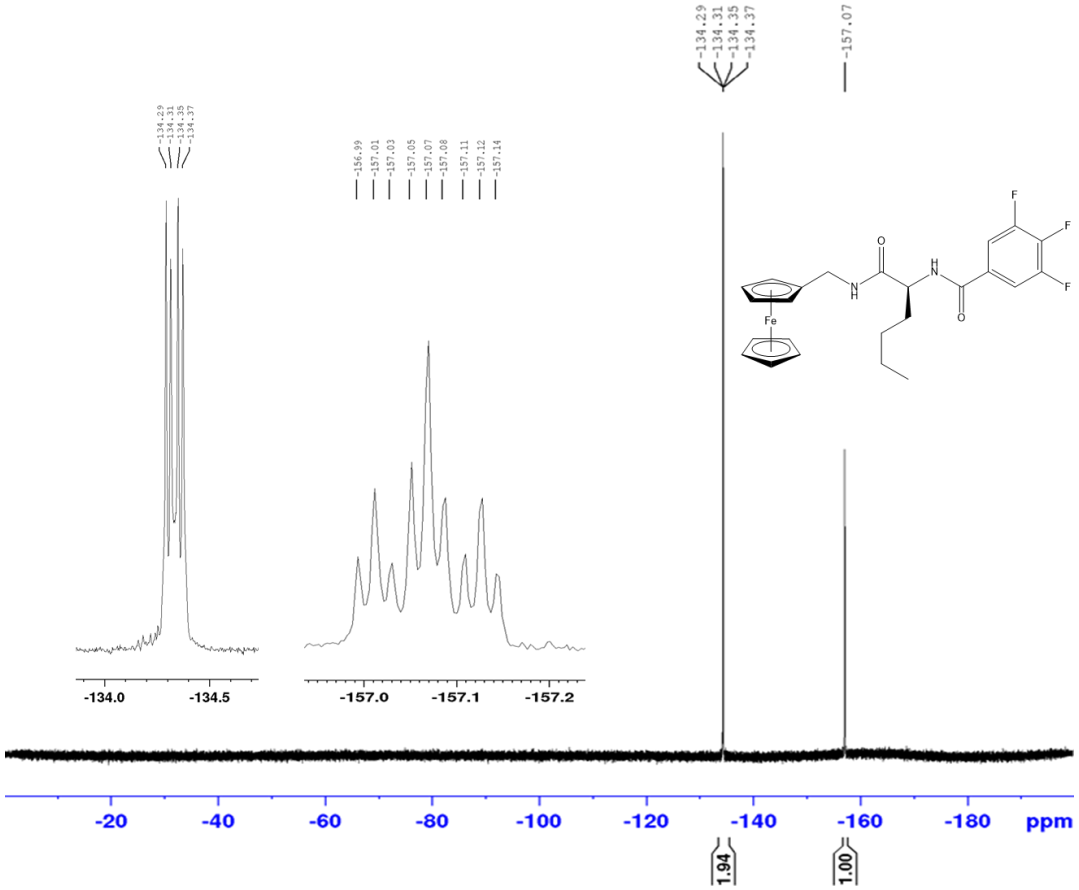

Figure 4.8: ^{19}F NMR spectrum of *N*-(ferrocenylmethyl-L-norleucine)-3,4,5-trifluorobenzene carboxamide **104**.

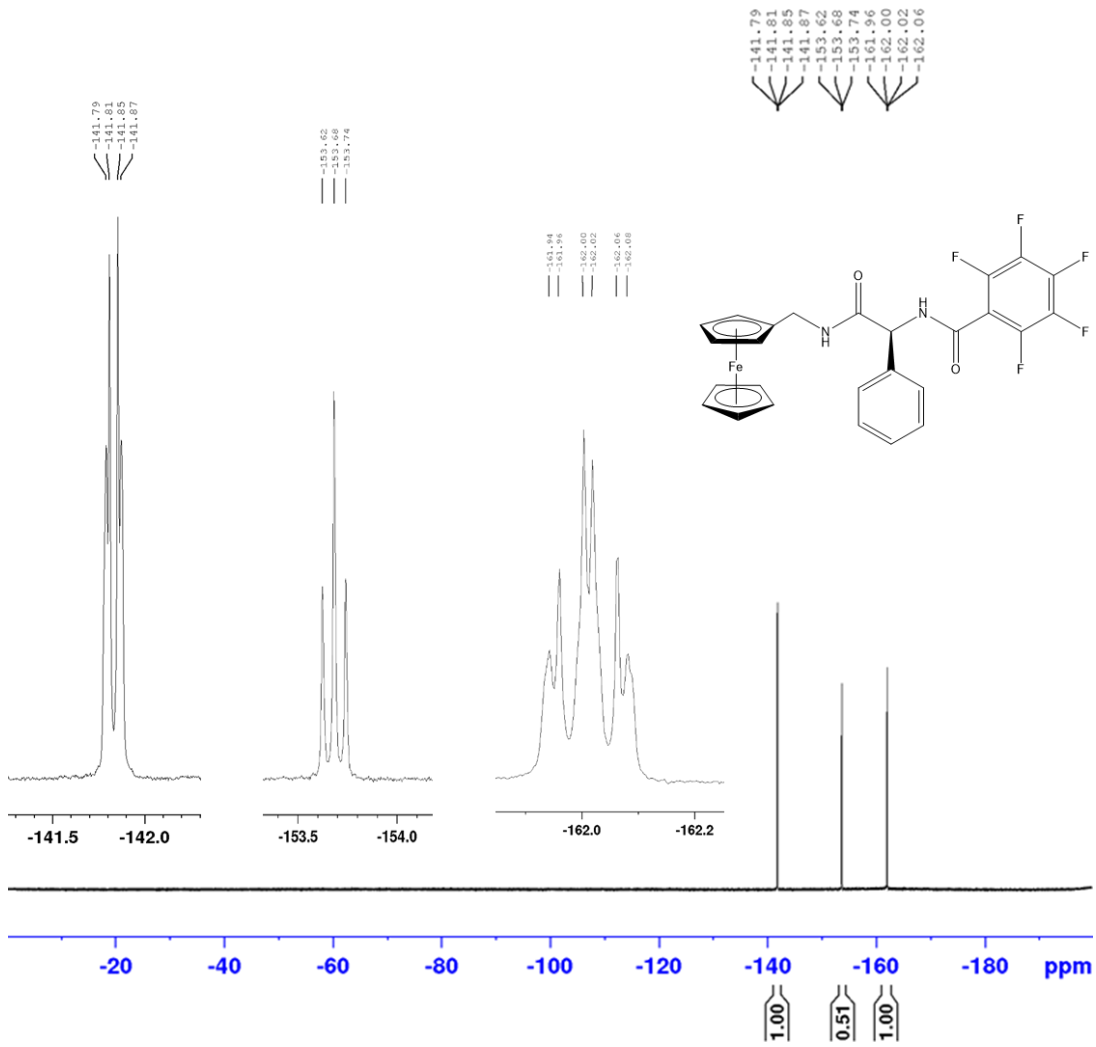

Figure 4.9: ^{19}F NMR spectrum of *N*-(ferrocenylmethyl-L-(+)-α-phenylglycine)-2,3,4,5,6-pentafluorobenzene carboxamide **107**.

4.9. COSY study of *N*-(ferrocenylmethyl-L-norvaline)-3,4,5-trifluorobenzene carboxamide (102)

COSY (Correlation Spectroscopy) is a two-dimensional experiment that indicates all the spin-spin coupled protons in one spectrum. In the COSY spectrum, two essentially identical chemical shift axes are plotted orthogonally. All peaks that are mutually spin-spin coupled are shown by cross-peaks in the third dimension, which are placed symmetrically about the diagonal. [13]

The structure and COSY spectrum of *N*-(ferrocenylmethyl-L-norvaline)-3,4,5-trifluorobenzene carboxamide **102** is shown in Figure 4.10 and Figure 4.11, respectively. The amide proton of the L-norvaline amino acid **a** (δ 8.64) correlates with the methine group of the amino acid **b** (δ 4.48), while the amide proton of the ferrocenylmethylamine **f** (δ 8.16) correlates with the methylene group of adjacent to it **g** (δ 4.06-3.97). Correlation is also present between the *meta* and *ortho* protons of the substituted ring (η^5-C_5H_4), *i.e.* **i** (δ 4.16) and **j** (δ 4.09). The central methylene group of the L-norvaline chain **c** (δ 1.75-1.70) is easily identified due to its coupling with the methine proton **b** (δ 4.48) and **d** (δ 1.33-1.22) positioned on either side. The proton **d** (δ 1.33-1.22) have correlation with proton **e** (δ 0.19).

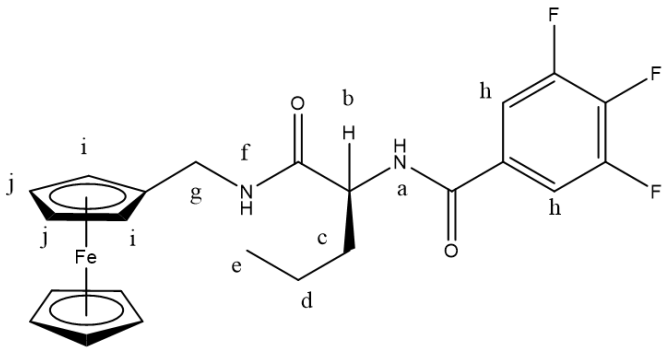

Figure 4.10: *N*-(ferrocenylmethyl-L-norvaline)-3,4,5-trifluorobenzene carboxamide **102.**

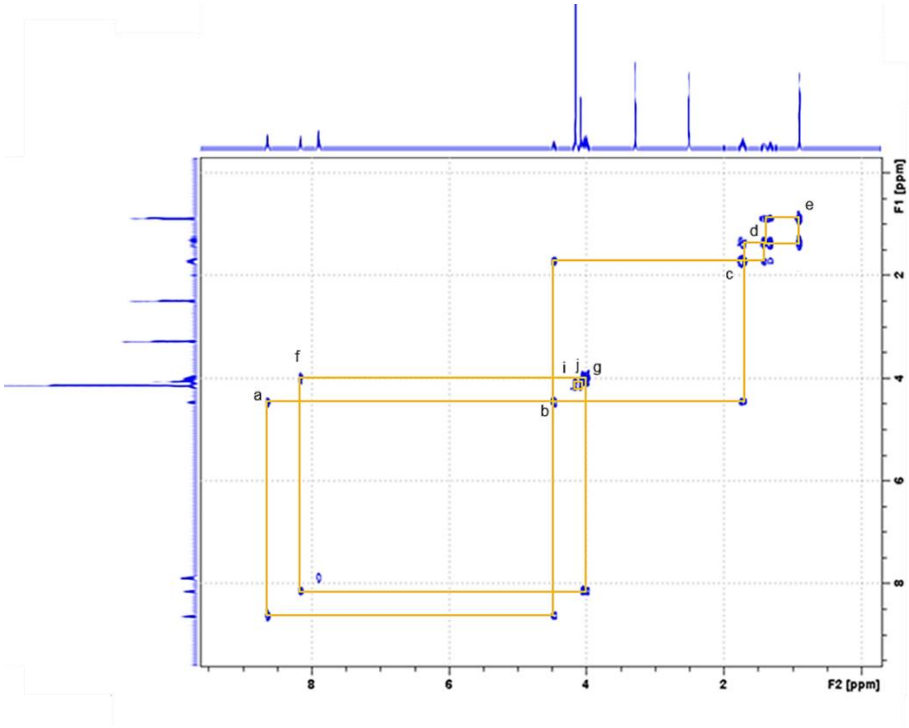

Figure 4.11: COSY spectrum of *N*-(ferrocenylmethyl-L-norvaline)-3,4,5-trifluorobenzene carboxamide **102**.

4.10. Conclusion

N-(ferrocenylmethyl)-fluorobenzene carboxamide derivatives have been identified as potential anti-cancer agents on the MDA-MB-435-SF and MCF-7 cancer cell lines. [8,9] This project sought to further explore the structure-activity relationship (SAR) of these compounds to enhance the anti-proliferative effect. Thus, various amino acids and dipeptides were modified between the ferrocene moiety and fluorinated aromatic group. Those novel compounds were prepared by EDC/NHS condensation and purified by column chromatography furnished the required compounds as orange solids, in moderate yields (11 % to 52 %).

The *N*-(ferrocenylmethyl)-fluorobenzene carboxamides were characterized by a range of spectroscopic techniques including ^{1}H NMR, ^{13}C NMR, DEPT-135, ^{19}F, COSY, IR and UV-Vis. All compounds gave spectroscopic and analytical data in accordance with their proposed structures.

Experimental Procedures

Experimental Note

All chemicals were purchased from Sigma-Aldrich or Fluorochem Limited, and used as received. Commercial grade reagents were used without purification. When necessary, all solvents were purified and dried prior to use. Riedel-Haën silica gel was used for thin layer and column chromatography. Melting points were determined using a Griffin melting point apparatus and are uncorrected. Infrared spectra were recorded on a PerkinElmer Spectrum 100 FT-IR with ATR. UV-Vis spectra were recorded on a Hewlett Packard 8452A diode array UV-Vis spectrophotometer. NMR spectra were obtained on a Bruker AC 400 NMR spectrometer operating at 400 MHz for ^{1}H NMR, 376 MHz for ^{19}F NMR and 100 MHz for ^{13}C NMR. The ^{1}H and ^{13}C NMR chemical shifts (δ) are relative to tetramethylsilane and the ^{19}F NMR chemical shifts (δ) are relative to trifluoroacetic acid. All coupling constants (*J*) are in Hertz. The abbreviations for the peak multiplicities are as follows: s (singlet), d (doublet), dd (doublet of doublets), t (triplet), q (quartet), and m (multiplet).

General Procedures

General procedure for the preparation of starting materials for N-(ferrocenylmethylamino acid)-fluorinated benzene carboxamides.

Ferrocenecarbaldoxime (88)

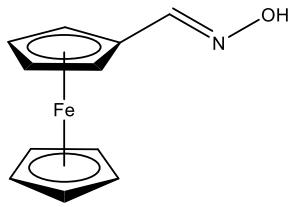

Ferrocenecarboxaldehyde (2.02 g, 9.4 mmol) was dissolved in warm ethanol (10 ml). Sodium acetate (2.28 g, 27.8 mmol) and hydroxylamine hydrochloride (1.75 g, 25.2 mmol) were dissolved thoroughly in distilled water (15 ml). The solutions were combined and refluxed for 40 minutes. After cooling to room temperature, diethyl ether (50 ml) was added to mixture. The ether layer was washed with water and dried over $MgSO_4$. The solvent was removed in *vacuo* to yield an orange solid. (1.90 g, 89 %), mp: 135-136 °C (Lit [9]: 135-136 °C);

^{1}H NMR (400 MHz) δ (DMSO-d_6): 10.97 (1H, s, -O<u>H</u>), 7.17 (1H, s, C<u>H</u>NOH), 4.78 (2H, t, J = 1.6 Hz, *ortho* on η^5-C_5<u>H_4</u>), 4.35, (2H, t, J = 1.6 Hz, *meta* on η^5-C_5<u>H_4</u>), 4.19 (5H, s, η^5-C_5<u>H_5</u>);

^{13}C NMR (100 MHz) δ (DMSO-d_6): 144.9 (<u>C</u>HNOH), 73.5 (C_{ipso} η^5-<u>C_5</u>H_4), 70.9 (C_{ortho} η^5-<u>C_5</u>H_4), 69.34 (C_{meta} η^5-<u>C_5</u>H_4), 68.6 (η^5-<u>C_5</u>H_5).

Ferrocenylmethylamine (89)

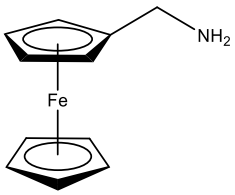

Lithium aluminium hydride (2.63 g, 69.4 mmol) was dissolved in anhydrous tetrahydrofuran (20 ml) under nitrogen. Ferrocenecarbaldoxime (3.00 g, 13.1 mmol) was dissolved in anhydrous tetrahydrofuran (20 ml) and added slowly to the $LiAlH_4$ solution *via* syringe. The reaction was stirred for 48 hours. The reaction flask was cooled to 0 °C. Ethyl acetate (30 ml) and 3 M sodium hydroxide (10 ml) were added. The reaction mixture was filtered and diethyl ether (100 ml) was added. The ether layer was washed with water and dried over $MgSO_4$. The solvent was removed in *vacuo* to yield the crude product as an orange oil (2.75 g, 97 %);

^{1}H NMR (400 MHz) δ (DMSO-d_6): 8.14-8.06 (2H, m, -N$\underline{H}_2$), 4.18-4.15 (7H, m, η^5-$C_5\underline{H}_5$ and *ortho* on η^5-$C_5\underline{H}_4$), 4.08 (2H, t, J = 5.6 Hz, *meta* on η^5-$C_5\underline{H}_4$), 3.95-3.91 (2H, m, -C$\underline{H}_2$NH$_2$);

^{13}C NMR (100 MHz) δ (DMSO-d_6): 86.1 (C$_{ipso}$ η^5-$\underline{C}_5H_4$), 68.4 (C$_{ortho}$ η^5-$\underline{C}_5H_4$), 67.7 (C$_{meta}$ η^5-$\underline{C}_5H_4$), 67.1 (η^5-$\underline{C}_5H_5$), 37.3 (-$\underline{C}$H$_2$NH$_2$).

General procedure for the synthesis of N-(fluorobenzoyl) amino acids:

_N_-(3,4,5-trifluorobenzoyl)-L-alanine (90)

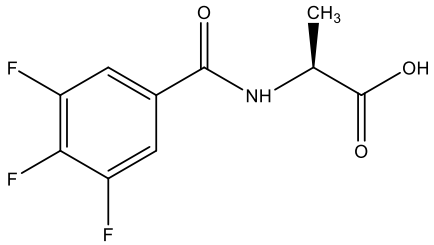

L-alanine (1.00 g, 11.3 mmol) was dissolved in dichloromethane (20 ml). 3,4,5-Trifluorobenzoyl chloride (1.50 ml, 11.4 mmol) was added slowly *via* a syringe. 2 M sodium hydroxide (10 ml) was added, and the reaction mixture was stirred for 48 hours. Concentrated hydrochloric acid was added to the aqueous layer until a precipitate formed. Vacuum filtration yielded a white powder (0.75 g, 23.3 %), mp: 199-200 °C (Lit [9]: 199-201 °C);

^{1}H NMR (400 MHz) δ (DMSO-d_6): 12.27 (1H, bs, -COO<u>H</u>), 8.94 (1H, d, *J* = 7.2 Hz, CON<u>H</u>), 7.89-7.79 (2H, m, Ar<u>H</u>), 4.40 (1H, q, *J* = 7.2 Hz, -NHC<u>H</u>), 1.39 {3H, d, *J* = 7.2 Hz, -CH(C<u>H</u>$_3$)};

^{13}C NMR (100 MHz) δ (DMSO-d_6): 173.9 (C=O), 162.8 (C=O), 151.2 (d, *J* = 166 Hz, -ArC_3 & -ArC_5), 148.6 (t, *J* = 166 Hz , -ArC_4), 130.2 (t, *J* = 4 Hz, -ArC_1), 112.4 (d, *J* = 12 Hz, -ArC_2 & -ArC_6), 48.6 {-<u>C</u>H(CH$_3$)}, 16.5 (-<u>C</u>H$_3$).

_N_-(3,4,5-trifluorobenzoyl)-L-2-aminobutyric acid (91)

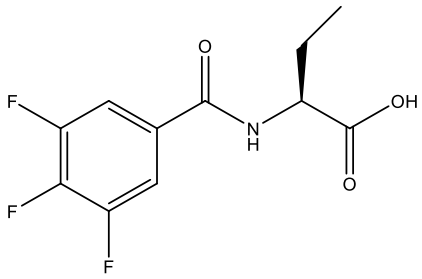

The synthesis followed that of *N*-(3,4,5-trifluorobenzoyl)-L-alanine using the following reagents: L-2-aminobutyric acid (1.17 g, 11.3 mmol), 3,4,5-trifluorobenzoyl chloride (1.50 ml, 11.4 mmol), 2 M sodium hydroxide (10 ml). Vacuum filtrated the precipitate yielded product as a white powder (0.98 g, 33.3 %), mp: 206-207 °C;

^{1}H NMR (400 MHz) δ (DMSO-d_6): 12.10 (1H, bs, -COOH), 8.71 (1H, d, *J* = 7.2 Hz, CONH), 7.94-7.85 (2H, m, ArH), 4.51-4.42 (1H, m, -NHCH), 1.84-1.70 (2H, m, -$CH_2$$CH_3$), 0.95 (3H, t, *J* = 7.3 Hz, -CH_2CH_3);

^{13}C NMR (100 MHz) δ (DMSO-d_6): 171.0 (C=O), 164.0 (C=O), 154.4 (d, *J* = 166 Hz, -ArC_3 & -ArC_5), 146.4 (t, *J* = 166 Hz , -ArC_4), 130.1 (t, *J* = 4 Hz, -ArC_1), 113.2 (d, *J* = 12 Hz, -ArC_2 & -ArC_6), 54.0 (-NHCH), 25.5 (-CH_2CH_3, -ve DEPT), 11.0 (-CH_2CH_3).

_N_-(3,4,5-trifluorobenzoyl)-L-norvaline (92)

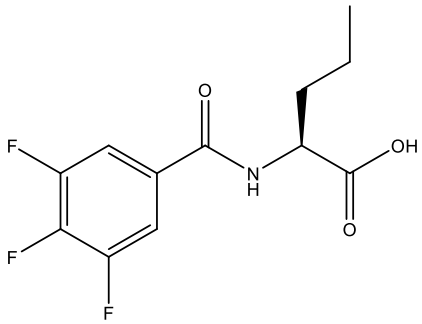

The synthesis followed that of *N*-(3,4,5-trifluorobenzoyl)-L-alanine using the following reagents: L-norvaline (1.34 g, 11.4 mmol), 3,4,5-trifluorobenzoyl chloride (1.50 ml, 11.4 mmol), 2 M sodium hydroxide (10 ml). Vacuum filtrated the precipitate yielded product as a white powder (0.68 g, 21.7 %), mp: 213-215 °C;

^{1}H NMR (400 MHz) δ (DMSO-d_6): 12.24 (1H, bs, -COOH), 8.71 (1H, d, *J* = 7.2 Hz, CONH), 7.96-7.88 (2H, m, ArH), 4.54-4.48 (1H, m, -NHCH), 1.75-1.70 (2H, m, -$CH_2CH_2CH_3$), 1.35-1.32 (2H, m, -$CH_2CH_2CH_3$), 0.93 (3H, t, *J* = 7.3 Hz, -$CH_2CH_2CH_3$);

^{13}C NMR (100 MHz) δ (DMSO-d_6): 171.4 (C=O), 163.5 (C=O), 155.2 (d, *J* = 166 Hz, -ArC_3 & -ArC_5), 146.3 (t, *J* = 166 Hz, -ArC_4), 131.2 (t, *J* = 4 Hz, -ArC_1), 113.2 (d, *J* = 12 Hz, -ArC_2 & -ArC_6), 54.0 (-NHCH), 34.0 (-$CH_2CH_2CH_3$, -ve DEPT), 19.2 (-$CH_2CH_2CH_3$, -ve DEPT), 14.9 (-$CH_2CH_2CH_3$).

_N_-(3,4,5-trifluorobenzoyl)-L-norleucine (93)

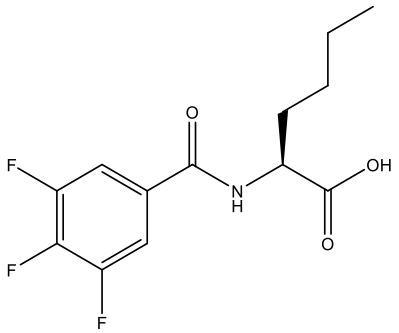

The synthesis followed that of *N*-(3,4,5-trifluorobenzoyl)-L-alanine using the following reagents: L-norleucine (1.49 g, 11.3 mmol), 3,4,5-trifluorobenzoyl chloride (1.50 ml, 11.4 mmol), 2 M sodium hydroxide (10 ml). Vacuum filtrated the precipitate yielded product as a white powder (0.64 g, 19.6 %), mp: 219-220 °C;

^{1}H NMR (400 MHz) δ (DMSO-d_6): 12.31 (1H, bs, -COOH), 8.68 (1H, d, J = 7.2 Hz, CONH), 7.93-7.85 (2H, m, ArH), 4.49-4.42 (1H, m, -NHCH), 1.83-1.64 (2H, m, -$CH_2CH_2CH_2CH_3$), 1.45-1.31 (4H, m, -$CH_2CH_2CH_2CH_3$), 0.93 (3H, t, J = 7.3 Hz, -$CH_2CH_2CH_2CH_3$);

^{13}C NMR (100 MHz) δ (DMSO-d_6): 171.0 (C=O), 163.3 (C=O), 151.4 (d, J = 166 Hz, -ArC_3 & -ArC_5), 142.3 (t, J = 166 Hz , -ArC_4), 130.1 (t, J = 4 Hz, -ArC_1), 112.5 (d, J = 12 Hz, -ArC_2 & -ArC_6), 54.0 (-NHCH), 31.3 (-$CH_2CH_2CH_2CH_3$, -ve DEPT), 27.9 (-$CH_2CH_2CH_2CH_3$, -ve DEPT), 22.0 (-$CH_2CH_2CH_2CH_3$, -ve DEPT), 13.6 (-$CH_2CH_2CH_2CH_3$).

_N_-(3,4,5-trifluorobenzoyl)-L-leucine (94)

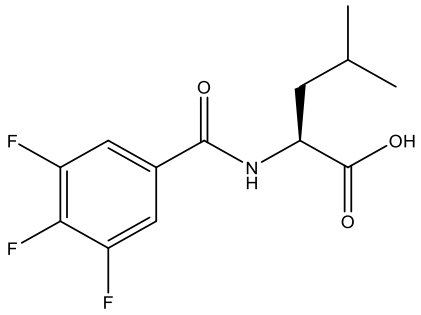

The synthesis followed that of *N*-(3,4,5-trifluorobenzoyl)-L-alanine using the following reagents: L-leucine (1.51 g, 11.5 mmol), 3,4,5-trifluorobenzoyl chloride (1.50 ml, 11.4 mmol), 2 M sodium hydroxide (10 ml). Vacuum filtrated the precipitate yielded product as a white powder (1.50 g, 45 %), mp: 203-205 °C;

^{1}H NMR (400 MHz) δ (DMSO-d_6): 12.36 (1H, bs, -COOH), 8.99 (1H, d, J = 8.0 Hz, CONH), 7.97-7.86 (2H, m, ArH), 4.49-4.45 (1H, m, -NHCH), 1.86-1.75 {2H, m, -CHCH_2CH$(CH_3)_2$}, 1.68-1.61 {1H, m, -CHCH_2CH$(CH_3)_2$}, 0.98 {6H, dd, J = 4.0 and 8.0 Hz, -CHCH_2CH$(CH_3)_2$};

^{13}C NMR (100 MHz) δ (DMSO-d_6): 171.4 (C=O), 164.6 (C=O), 151.0 (d, J = 166 Hz, -ArC_3 & -ArC_5), 142.2 (t, J = 166 Hz , -ArC_4), 130.1 (t, J = 4 Hz, -ArC_1), 113.0 (d, J = 12 Hz, -ArC_2 & -ArC_6), 52.1 (-NHCH), 30.6 {-CHCH$_2$CH$(CH_3)_2$, -ve DEPT}, 24.8 {-CHCH$_2$CH$(CH_3)_2$}, 22.9 {-CHCH$_2$CH$(CH_3)_2$}, 21.0 {-CHCH$_2$CH$(CH_3)_2$}.

_N_-(3,4,5-trifluorobenzoyl)-L-methionine (95)

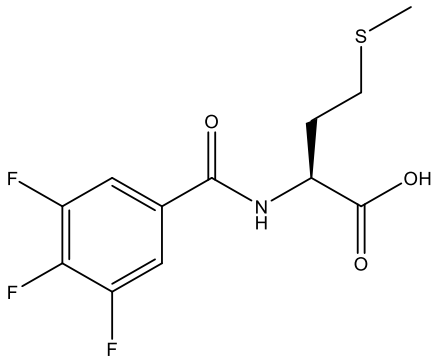

The synthesis followed that of *N*-(3,4,5-trifluorobenzoyl)-L-alanine using the following reagents: L-methionine (1.72 g, 11.5 mmol), 3,4,5-trifluorobenzoyl chloride (1.50 ml, 11.4 mmol), 2 M sodium hydroxide (10 ml). Vacuum filtrated the precipitate yielded product as a white powder (1.08 g, 31%), mp: 234-236 °C;

^{1}H NMR (400 MHz) δ (DMSO-d_6): 12.13 (1H, bs, -COOH), 9.01 (1H, d, J = 7.2 Hz, CONH), 7.92-7.85 (2H, m, ArH), 4.52-4.47 (1H, m, -NHCH), 2.51 (2H, t, J = 2.0 Hz, -CH$_2$CH$_2$SCH$_3$), 2.10-2.06 (2H, m, -CH$_2$CH$_2$SCH$_3$), 2.05 (3H, s, -CH$_2$CH$_2$SCH$_3$);

^{13}C NMR (100 MHz) δ (DMSO-d_6): 171.7 (C=O), 163.5 (C=O), 151.4 (d, J = 166 Hz, -ArC$_3$ & -ArC$_5$), 148.1 (t, J = 166 Hz , -ArC$_4$), 130.0 (t, J = 4 Hz, -ArC$_1$), 113.2 (d, J = 12 Hz, -ArC$_2$ & -ArC$_6$), 54.2 (-NHCH), 31.7 (-CH$_2$CH$_2$SCH$_3$, -ve DEPT), 29.7 (-CH$_2$CH$_2$SCH$_3$, -ve DEPT), 15.6 (-CH$_2$CH$_2$SCH$_3$).

***N*-(3,4,5-trifluorobenzoyl)-L-(+)-α-phenylglycine (96)**

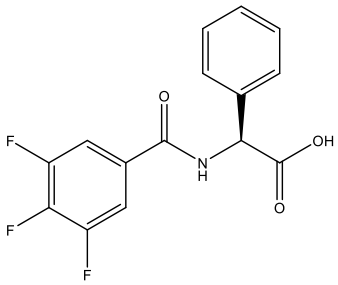

The synthesis followed that of *N*-(3,4,5-trifluorobenzoyl)-L-alanine using the following reagents: L-(+)-α-phenylglycine (1.74 g, 11.5 mmol), 3,4,5-trifluorobenzoyl chloride (1.50 ml, 11.4 mmol), 2 M sodium hydroxide (10 ml). Vacuum filtrated the precipitate yielded product as a white powder (1.34 g, 38 %), mp: 251-252 °C;

^{1}H NMR (400 MHz) δ (DMSO-d_6): 12.27 (1H, bs, -COO<u>H</u>), 9.28 (1H, d, *J* = 7.2 Hz, CON<u>H</u>), 7.54-7.32 { (5H, m, -CH(C$_6$<u>H</u>$_5$) }, 5.56 { (1H, d, *J* = 8.0 Hz, -C<u>H</u>(C$_6$H$_5$) };

^{13}C NMR (100 MHz) δ (DMSO-d_6): 168.9 (C=O), 156.8 (C=O), 144.6 (d, *J* = 166 Hz, -ArC$_3$ & -ArC$_5$), 138.7 (t, *J* = 166 Hz , -ArC$_4$), 136.5 (t, *J* = 4 Hz, -ArC$_1$), 128.9, 128.3, 127.5, 113.1 (d, *J* = 12 Hz, -ArC$_2$ & -ArC$_6$)**,** 109.5, 57.2 (-NH<u>C</u>H).

_N_-(2,3,4,5,6-pentafluorobenzoyl)-glycine (97)

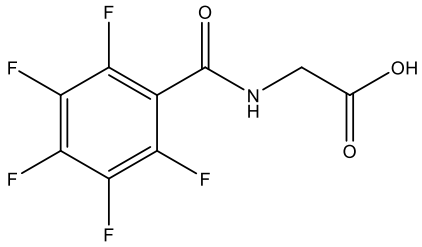

The synthesis followed that of *N*-(3,4,5-trifluorobenzoyl)-L-alanine using the following reagents: glycine (0.86 g, 11.5 mmol), 2,3,4,5,6-pentafluorobenzoyl chloride (1.74 ml, 11.4 mmol), 2 M sodium hydroxide (10 ml). Vacuum filtrated the precipitate yielded product as a white powder (0.77 g, 25.2 %), mp: 189-190 °C (Lit [9]: 188-190 °C);

^{1}H NMR (400 MHz) δ (DMSO-d_6): 11.82 (1H, bs, -COOH), 9.46 (1H, t, J = 5.6 Hz, -CONH), 3.98 (2H, d, J = 5.6 Hz, -NHCH_2);

^{13}C NMR (100 MHz) δ (DMSO-d_6): 168.4 (C=O), 165.0 (C=O), 155.3-155.2 (m, -ArC_2), 154.6-154.4 (m, -ArC_6), 133.8-133.6 (m, -ArC_4), 130.2-130.0 (m, -ArC_3), 130.0-129.9 (m, -ArC_5), 115.1 (t, J = 12 Hz, -ArC_1), 42.0 (-NHCH_2, -ve DEPT).

_N_-(2,3,4,5,6-pentafluorobenzoyl)-L-alanine (98)

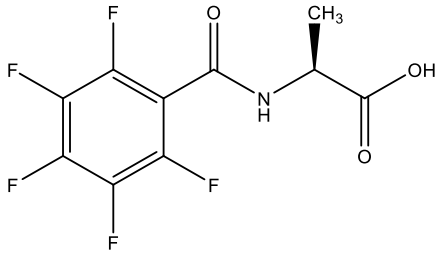

The synthesis followed that of *N*-(3,4,5-trifluorobenzoyl)-L-alanine using the following reagents: L-alanine (1.02 g, 11.5 mmol), 2,3,4,5,6-pentafluorobenzoyl chloride (1.74 ml, 11.4 mmol), 2 M sodium hydroxide (10 ml). Vacuum filtrated the precipitate yielded product as a white powder (0.91 g, 28.3 %), mp: 201-202 °C (Lit [9]: 200-203 °C);

^{1}H NMR (400 MHz) δ (DMSO-d_6): 12.15 (1H, bs, -COOH), 9.30 (1H, t, *J* = 7.2 Hz, -CONH), 4.43 (1H, q, *J* = 7.2 Hz, -NHCH),1.40 {3H, d, *J* = 5.6 Hz, -NHCH(CH$_3$)};

^{13}C NMR (100 MHz) δ (DMSO-d_6): 171.8 (C=O), 164.9 (C=O), 144.6-144.4 (m, -ArC$_2$), 142.9-142.8 (m, -ArC$_6$), 136.6-136.5 (m, -ArC$_4$), 130.2-130.0 (m, -ArC$_3$), 129.8-129.6 (m, -ArC$_5$), 115.3 (t, *J* = 12 Hz, -ArC$_1$), 48.6 (-NHCH), 16.7 (-CHCH$_3$).

_N_-(2,3,4,5,6-pentafluorobenzoyl)-L-(+)-α-phenylglycine (99)

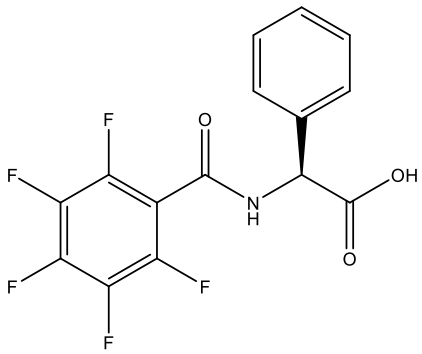

The synthesis followed that of *N*-(3,4,5-trifluorobenzoyl)-L-alanine using the following reagents: L-(+)-α-phenylglycine (1.74 g, 11.5 mmol), 2,3,4,5,6-pentafluorobenzoyl chloride (1.74 ml, 11.4 mmol), 2 M sodium hydroxide (10 ml). Vacuum filtrated the precipitate yielded product as a white powder (1.54 g, 39 %), mp: 263-265 °C;

^{1}H NMR (400 MHz) δ (DMSO-d_6): 12.37 (1H, bs, -COO<u>H</u>), 9.80 (1H, d, *J* = 8.0 Hz, CON<u>H</u>), 7.48-7.34 { 5H, m, -CH(C$_6$<u>H</u>$_5$) }, 5.56 {1H, d, *J* = 8.0 Hz, -C<u>H</u>(C$_6$H$_5$)};

^{13}C NMR (100 MHz) δ (DMSO-d_6): 168.9 (C=O), 156.8 (C=O), 144.4 (C$_q$), 144.0-143.9 (m, -ArC$_2$), 143.5-143.2 (m, -ArC$_6$), 140.9-140.5 (m, -ArC$_4$), 138.6-138.3 (m, -ArC$_3$), 136.5-136.2 (m, -ArC$_5$), 128.9, 128.3, 127.5, 113.1 (t, *J* = 12 Hz, -ArC$_1$), 57.2 (-NH<u>C</u>H).

***N*-(2,3,4,5,6-pentafluorobenzoyl)-glycine-glycine (100)**

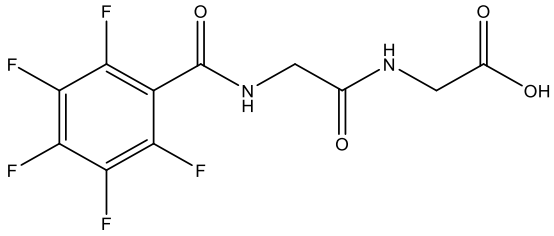

The synthesis followed that of *N*-(3,4,5-trifluorobenzoyl)-L-alanine using the following reagents: glycine-glycine (1.52 g, 11.5 mmol), 2,3,4,5,6-pentafluorobenzoyl chloride (1.74 ml, 11.4 mmol), 2 M sodium hydroxide (10 ml). Vacuum filtrated the precipitate yielded product as a white powder (1.82 g, 49 %), mp: 288-290 °C;

^{1}H NMR (400 MHz) δ (DMSO-d_6): 12.46 (1H, bs, -COOH), 9.10 (1H, t, J = 8.0 Hz, CONH), 8.01 (1H, t, J = 8.0 Hz, CONH), 4.02-4.00 (4H, m, -NHCH_2- and -NHCH_2COOH);

^{13}C NMR (100 MHz) δ (DMSO-d_6): 168.5 (C=O), 168.2 (C=O), 147.5 (C=O), 145.3-145.0 (m, -ArC_2), 144.4-144.2 (m, -ArC_6), 141.5-141.3 (m, -ArC_4), 136.4-136.3 (m, -ArC_3), 136.0-135.7 (m, -ArC_5), 112.8 (t, J = 12 Hz, -ArC_1), 43.0 (-NHCH_2-, -ve DEPT)), 42.5 (-NHCH_2COOH, -ve DEPT).

General procedure for the synthesis of N-(ferrocenylmethylamino acid)-fluorinated benzene carboxamides.

_N_-(ferrocenylmethyl-L-alanine)-3,4,5-trifluorobenzene carboxamide (28)

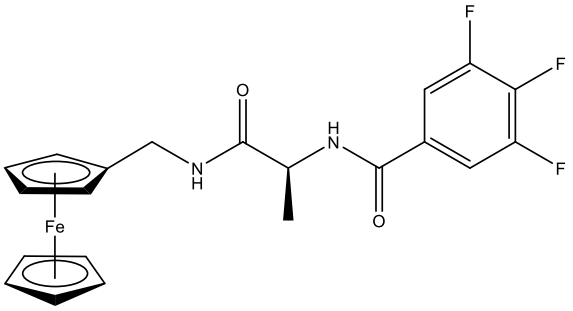

N-(3,4,5-trifluorobenzoyl)-L-alanine (0.92 g, 3.7 mmol) was dissolved in DCM (20 ml) at 0 °C. Ferrocenylmethylamine (0.80 g, 3.7 mmol), *N*-(3-dimethylaminopropyl)-*N*'-ethylcarbodiimide hydrochloride (0.58 g, 3.7 mmol), *N*-hydroxysuccinimide (0.43 g, 3.7 mmol) and triethylamine (3 ml) were added and stirred at 0 °C for 1 hour. The reaction mixture was allowed to stir at room temperature for 48 hours. The solvent was removed *in vacuo* and the crude product was purified by column chromatography (eluent 2:1 ethyl acetate: hexane) to yield the product as a orange powder (0.85 g, 52 %), mp: 134 –135 °C (Lit [9]: 134-136 °C);

I.R. υ_{max} (neat): 3290, 3075, 1647, 1620, 1557, 1231, 1043 cm^{-1};

UV-Vis λ_{max} (CH_3CN): 317, 432 nm;

^{1}H NMR (400 MHz) δ (DMSO-d_6): 8.75 (1H, d, *J* = 8.0 Hz, -CONH), 8.18 (1H, t, *J* = 8.0 Hz, $FcCH_2NH$), 7.93 (2H, dd, *J* = 4.0 and 8.0 Hz, ArH), 4.50 (1H, q, *J* = 7.2 Hz, -NHCH), 4.19-4.17 (7H, m, η^5-C_5H_5 and *ortho* on η^5-C_5H_4), 4.08 (2H, t, *J* = 2 Hz, *meta* on η^5-C_5H_4), 4.05-3.90 (2H, m, $FcCH_2$), 1.39 {3H, d, *J* = 7.2 Hz, -CH(CH_3)};

^{13}C NMR (100 MHz) δ (DMSO-d_6): 170.5 (C=O), 167.9 (C=O), 155.9 (d, *J* = 166 Hz, -ArC_3 & -ArC_5), 147.5 (t, *J* = 166 Hz , -ArC_4), 130.2 (t, *J* = 4 Hz, -ArC_1), 112.7 (d, *J* = 12 Hz, -ArC_2 & -ArC_6), 86.2 (C_{ipso} η^5-C_5H_4), 68.4 (η^5-C_5H_5), 67.5 (C_{ortho} η^5-C_5H_4), 67.1 (C_{meta} η^5-C_5H_4), 49.7 {-CH(CH_3)}, 37.4 ($FcCH_2$, -ve DEPT), 17.9 (-CH_3);

^{19}F NMR (376 MHz) δ (DMSO-d_6): -134.3 (2F, dd, *J* = 22.6 and 7.5 Hz), -157.0 (1F, tt, *J* = 22.6 and 7.5 Hz).

***N*-(ferrocenylmethyl-L-2-aminobutyric acid)-3,4,5-trifluorobenzene carboxamide (101)**

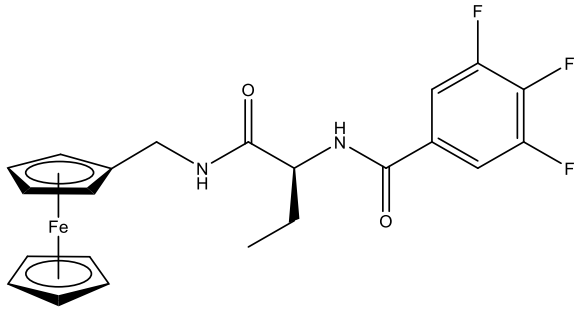

The synthesis followed that of *N*-(ferrocenylmethyl-L-alanine)-3,4,5-trifluorobenzene carboxamide using the following reagents: *N*-(3,4,5-trifluorobenzoyl)-L-2-aminobutyric acid (0.80 g, 3.7 mmol), ferrocenylmethylamine (0.80 g, 3.7 mmol), *N*-(3-dimethylaminopropyl)-*N*'-ethylcarbodiimide hydrochloride (0.58 g, 3.7 mmol), *N*-hydroxysuccinimide (0.43 g, 3.7 mmol) and triethylamine (3 ml). The product was purified by column chromatography (eluent 2:1 ethyl acetate: hexane) to give the title compound as a yellow solid (0.58 g, 34 %), mp: 138 –140 °C;

I.R. υ_{max} (neat): 3282, 3214, 2926, 1639, 1621, 1518, 1356, 1231, 1045 cm^{-1};

UV-Vis λ_{max} (CH_3CN): 322, 416 nm;

^{1}H NMR (400 MHz) δ (DMSO-d_6): 8.62 (1H, d, *J* = 8.0 Hz, -CONH), 8.16 (1H, t, *J* = 8.0 Hz, $FcCH_2NH$), 7.91 (2H, dd, *J* = 4.0 and 8.0 Hz, ArH), 4.40 (1H, qt, *J* = 7.2 Hz, -NHCH), 4.17-4.16 (7H, m, η^5-C_5H_5 and *ortho* on η^5-C_5H_4), 4.08-4.04 (4H, m, *meta* on η^5-C_5H_4 and $FcCH_2$), 1.83-1.72 (2H, m, $-CH_2CH_3$), 0.94 (3H, t, *J* = 7.3 Hz, $-CH_2CH_3$);

^{13}C NMR (100 MHz) δ (DMSO-d_6): 171.3 (C=O), 163.7 (C=O), 155.9 (d, *J* = 166 Hz, $-ArC_3$ & $-ArC_5$), 146.8 (t, *J* = 166 Hz , $-ArC_4$), 131.0 (t, *J* = 4 Hz, $-ArC_1$), 113.2 (d, *J* = 12 Hz, $-ArC_2$ & $-ArC_6$), 86.7 (C_{ipso} η^5-C_5H_4), 68.8 (η^5-C_5H_5), 68.0 (C_{ortho} η^5-C_5H_4), 67.7 (C_{meta} η^5-C_5H_4), 55.7 (-NHCH), 38.0 ($FcCH_2$, -ve DEPT), 25.5 ($-CH_2CH_3$, -ve DEPT), 11.2 ($-CH_2CH_3$);

^{19}F NMR (376 MHz) δ (DMSO-d_6): -134.3 (2F, dd, *J* = 22.6 and 7.5 Hz), -157.1 (1F, tt, *J* = 22.6 and 7.5 Hz).

***N*-(ferrocenylmethyl-L-norvaline)-3,4,5-trifluorobenzene carboxamide (102)**

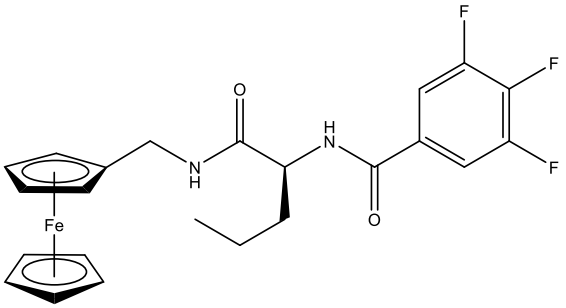

The synthesis followed that of *N*-(ferrocenylmethyl-L-alanine)-3,4,5-trifluorobenzene carboxamide using the following reagents: *N*-(3,4,5-trifluorobenzoyl)-L-norvaline (1.02 g, 3.7 mmol), ferrocenylmethylamine (0.80 g, 3.7 mmol), *N*-(3-dimethylaminopropyl)-*N*'-ethylcarbodiimide hydrochloride (0.58 g, 3.7 mmol), *N*-hydroxysuccinimide (0.43 g, 3.7 mmol) and triethylamine (3 ml). The product was purified by column chromatography (eluent 2:1 ethyl acetate: hexane) to give the title compound as a yellow solid (0.63 g, 36 %), mp: 163-165 °C;

I.R. υ_{max} (neat): 3307, 3248, 3094, 2960, 2926, 1666, 1621, 1519, 1232, 1046 cm^{-1};

UV-Vis λ_{max} (CH_3CN): 320, 428 nm;

^{1}H NMR (400 MHz) δ (DMSO-d_6): 8.64 (1H, d, *J* = 8.0 Hz, -CONH), 8.16 (1H, t, *J* = 8.0 Hz, $FcCH_2NH$), 7.90 (2H, dd, *J* = 4.0 and 8.0 Hz, ArH), 4.48 (1H, qt, *J* = 7.2 Hz, -NHCH), 4.16-4.15 (7H, m, η^5-C_5H_5 and *ortho* on η^5-C_5H_4), 4.09 (2H, t, *J* = 2 Hz, *meta* on η^5-C_5H_4), 4.06-3.97 (2H, m, $FcCH_2$), 1.75-1.70 (2H, m, -$CH_2CH_2CH_3$), 1.33-1.32 (2H, m, -$CH_2CH_2CH_3$), 0.91 (3H, d, *J* = 7.3 Hz, -$CH_2CH_2CH_3$);

^{13}C NMR (100 MHz) δ (DMSO-d_6): 171.5 (C=O), 163.6 (C=O), 155.8 (d, *J* = 166 Hz, -ArC_3 & -ArC_5), 146.8 (t, *J* = 166 Hz, -ArC_4), 131.1 (t, *J* = 4 Hz, -ArC_1), 113.2 (d, *J* = 12 Hz, -ArC_2 & -ArC_6), 86.7 (C_{ipso} η^5-C_5H_4), 68.8 (η^5-C_5H_5), 68.0 (C_{ortho} η^5-C_5H_4), 67.7 (C_{meta} η^5-C_5H_4), 54.0 (-NHCH), 38.0 ($FcCH_2$, -ve DEPT), 34.2 (-$CH_2CH_2CH_3$, -ve DEPT), 19.4 (-$CH_2CH_2CH_3$, -ve DEPT), 14.1 (-$CH_2CH_2CH_3$);

^{19}F NMR (376 MHz) δ (DMSO-d_6): -134.3 (2F, dd, *J* = 22.6 and 7.5 Hz), -157.1 (1F, tt, *J* = 22.6 and 7.5 Hz).

***N*-(ferrocenylmethyl-L-leucine)-3,4,5-trifluorobenzene carboxamide (103)**

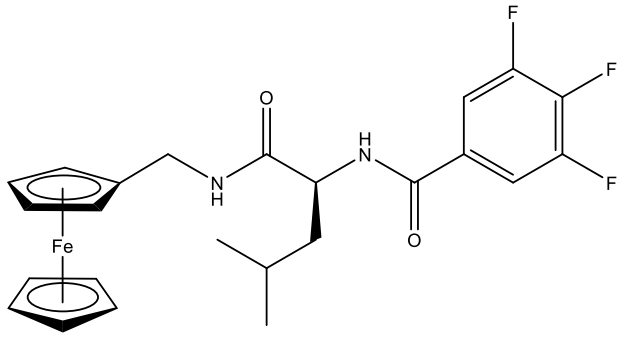

The synthesis followed that of *N*-(ferrocenylmethyl-L-alanine)-3,4,5-trifluorobenzene carboxamide using the following reagents: *N*-(3,4,5-trifluorobenzoyl)-L-leucine (1.07 g, 3.7 mmol), ferrocenylmethylamine (0.80 g, 3.7 mmol), *N*-(3-dimethylaminopropyl)-*N*'-ethylcarbodiimide hydrochloride (0.58 g, 3.7 mmol), *N*-hydroxysuccinimide (0.43 g, 3.7 mmol) and triethylamine (3 ml). The product was purified by column chromatography (eluent 2:1 ethyl acetate: hexane) to give the title compound as a yellow solid (0.19 g, 11 %), mp: 144 –145 °C;

I.R. υ_{max} (neat): 3289, 3067, 2957, 1663, 1637, 1604, 1556, 1516, 1233, 1107, 1043 cm^{-1};

UV-Vis λ_{max} (CH_3CN): 313, 429 nm;

^{1}H NMR (400 MHz) δ (DMSO-d_6): 8.72 (1H, d, *J* = 8.0 Hz, -CONH), 8.28 (1H, t, *J* = 8.0 Hz, $FcCH_2NH$), 7.92 (2H, dd, *J* = 4.0 and 8.0 Hz, ArH), 4.58 (1H, qt, *J* = 7.2 Hz, -NHCH), 4.18-4.15 (7H, m, η^5-C_5H_5 and *ortho* on η^5-C_5H_4), 4.08 (2H, t, *J* = 2 Hz, *meta* on η^5-C_5H_4), 4.06-3.92 (2H, m, $FcCH_2$), 1.76-1.62 {2H, m, $-CHCH_2CH(CH_3)_2$}, 1.57-1.51 {1H, m, $-CHCH_2CH(CH_3)_2$}, 0.96 {6H, dd, *J* = 4.0 and 8.0 Hz, $-CHCH_2CH(CH_3)_2$};

^{13}C NMR (100 MHz) δ (DMSO-d_6): 171.3(C=O), 162.9 (C=O), 151.2 (d, *J* = 166 Hz, $-ArC_3$ & $-ArC_5$), 142.0 (t, *J* = 166 Hz, $-ArC_4$), 130.3 (t, *J* = 4 Hz, $-ArC_1$), 112.7(d, *J* = 12 Hz, $-ArC_2$ & $-ArC_6$), 86.2 (C_{ipso} η^5-C_5H_4), 68.8 (η^5-C_5H_5), 68.0 (C_{ortho} η^5-C_5H_4), 67.7 (C_{meta} η^5-C_5H_4), 52.0 (-NHCH), 37.4 ($FcCH_2$, -ve DEPT), 30.7 {$-CHCH_2CH(CH_3)_2$, -ve DEPT}, 24.4 {$-CHCH_2CH(CH_3)_2$ }, 23.1 {$-CHCH_2CH(CH_3)_2$};

^{19}F NMR (376 MHz) δ (DMSO-d_6): -134.3 (2F, dd, *J* = 22.6 and 7.5 Hz), -157.0 (1F, tt, *J* = 22.6 and 7.5 Hz).

***N*-(ferrocenylmethyl-L-norleucine)-3,4,5-trifluorobenzene carboxamide (104)**

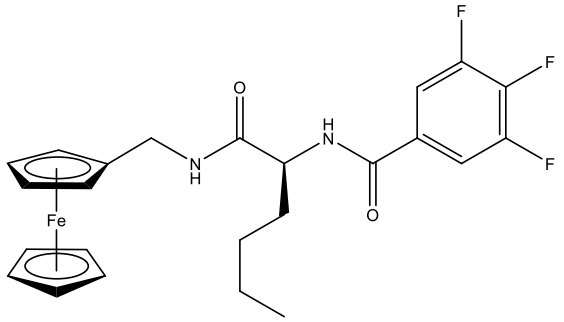

The synthesis followed that of *N*-(ferrocenylmethyl-L-alanine)-3,4,5-trifluorobenzene carboxamide using the following reagents: *N*-(3,4,5-trifluorobenzoyl)-L-norleucine (1.07 g, 3.7 mmol), ferrocenylmethylamine (0.80 g, 3.7 mmol), *N*-(3-dimethylaminopropyl)-*N*'-ethylcarbodiimide hydrochloride (0.58 g, 3.7 mmol), *N*-hydroxysuccinimide (0.43 g, 3.7 mmol) and triethylamine (3 ml). The product was purified by column chromatography (eluent 2:1 ethyl acetate: hexane) to give the title compound as a yellow solid (0.24 g, 13 %), mp: 170-172 °C;

I.R. υ_{max} (neat): 3242, 3073, 2966, 1662, 1634, 1619, 1549, 1520, 1233, 1106, 1045 cm^{-1};

UV-Vis λ_{max} (CH_3CN): 317, 430 nm;

^{1}H NMR (400 MHz) δ (DMSO-d_6): 8.69 (1H, d, *J* = 8.0 Hz, -CONH), 8.24 (1H, t, *J* = 8.0 Hz, $FcCH_2NH$), 7.91 (2H, dd, *J* = 4.0 and 8.0 Hz, ArH), 4.46 (1H, q, *J* = 7.2 Hz, -NHCH), 4.07-4.04 (7H, m, η^5-C_5H_5 and *ortho* on η^5-C_5H_4), 4.03 (2H, t, *J* = 2 Hz, *meta* on η^5-C_5H_4), 3.99-3.94 (2H, m, $FcCH_2$), 1.79-1.69 (2H, m, -$CH_2CH_2CH_2CH_3$), 1.36-1.24 (4H, m, -$CH_2CH_2CH_2CH_3$), 0.88 (3H, t, *J* = 7.3 Hz, -$CH_2CH_2CH_2CH_3$);

^{13}C NMR (100 MHz) δ (DMSO-d_6): 171.1(C=O), 163.1 (C=O), 151.4 (d, *J* = 166 Hz, -ArC_3 & -ArC_5), 142.0 (t, *J* = 166 Hz , -ArC_4), 130.3 (t, *J* = 4 Hz, -ArC_1), 112.7 (d, *J* = 12 Hz, -ArC_2 & -ArC_6), 86.1 (C_{ipso} η^5-C_5H_4), 68.3 (η^5-C_5H_5), 67.5 (C_{ortho} η^5-C_5H_4), 67.2 (C_{meta} η^5-C_5H_4), 53.8 (-NHCH), 37.6 ($FcCH_2$, -ve DEPT), 31.3 (-$CH_2CH_2CH_2CH_3$, -ve DEPT), 27.9 (-$CH_2CH_2CH_2CH_3$, -ve DEPT), 21.8 (-$CH_2CH_2CH_2CH_3$, -ve DEPT), 13.8 (-$CH_2CH_2CH_2CH_3$);

^{19}F NMR (376 MHz) δ (DMSO-d_6): -134.3 (2F, dd, *J* = 22.6 and 7.5 Hz), -157.0 (1F, tt, *J* = 22.6 and 7.5 Hz).

***N*-(ferrocenylmethyl-L-methionine)-3,4,5-trifluorobenzene carboxamide (105)**

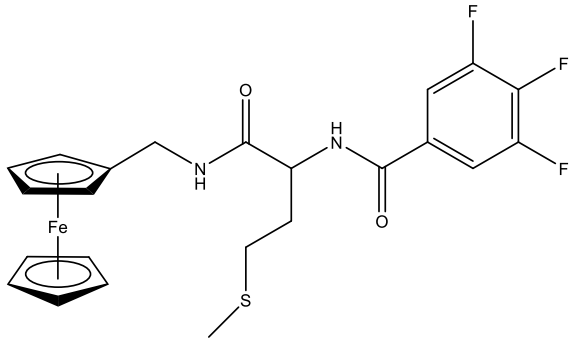

The synthesis followed that of *N*-(ferrocenylmethyl-L-alanine)-3,4,5-trifluorobenzene carboxamide using the following reagents: *N*-(3,4,5-trifluorobenzoyl)-L-methionine (0.28 g, 0.9 mmol), ferrocenylmethylamine (0.19 g, 0.9 mmol), *N*-(3-dimethylaminopropyl)-*N*'-ethylcarbodiimide hydrochloride (0.14 g, 0.9 mmol), *N*-hydroxysuccinimide (0.10 g, 0.9 mmol) and triethylamine (1.5 ml). The product was purified by column chromatography (eluent 2:1 ethyl acetate: hexane) to give the title compound as a yellow solid (0.06 g, 13 %), mp: 193 –194 °C;

I.R. υ_{max} (neat): 3281, 3074, 2919, 1669, 1637, 1619, 1559, 1517, 1232, 1106, 1043 cm^{-1};

UV-Vis λ_{max} (CH_3CN): 318, 430 nm;

^{1}H NMR (400 MHz) δ (DMSO-d_6): 8.75 (1H, d, *J* = 8.0 Hz, -CONH), 8.25 (1H, t, *J* = 8.0 Hz, $FcCH_2NH$), 7.90 (2H, dd, *J* = 4.0 and 8.0 Hz, ArH), 4.55 (1H, qt, *J* = 7.2 Hz, -NHCH), 4.16-4.13 (7H, m, η^5-C_5H_5 and *ortho* on η^5-C_5H_4), 4.04 (2H, t, *J* = 2 Hz, *meta* on η^5-C_5H_4), 3.99-3.94 (2H, m, $FcCH_2$), 2.51 (2H, t, *J* = 2.0 Hz, -$CH_2CH_2SCH_3$), 2.12-1.93 (5H, m, -$CH_2CH_2SCH_3$ and -$CH_2CH_2SCH_3$);

^{13}C NMR (100 MHz) δ (DMSO-d_6): 171.0 (C=O), 163.8 (C=O), 151.3 (d, *J* = 166 Hz, -ArC_3 & -ArC_5), 149.6 (t, *J* = 166 Hz , -ArC_4), 130.9 (t, *J* = 4 Hz, -ArC_1), 113.2 (d, *J* = 12 Hz, -ArC_2 & -ArC_6), 86.6 (C_{ipso} η^5-C_5H_4), 68.8 (η^5-C_5H_5), 68.0 (C_{ortho} η^5-C_5H_4), 67.7 (C_{meta} η^5-C_5H_4), 53.6 (-NHCH), 38.1 ($FcCH_2$, -ve DEPT), 31.9 (-$CH_2CH_2SCH_3$, -ve DEPT), 30.5 (-$CH_2CH_2SCH_3$, -ve DEPT), 15.1 (-$CH_2CH_2SCH_3$);

^{19}F NMR (376 MHz) δ (DMSO-d_6): -134.3 (2F, dd, *J* = 22.6 and 7.5 Hz), -157.0 (1F, tt, *J* = 22.6 and 7.5 Hz).

***N*-(ferrocenylmethyl-L-(+)-α-phenylglycine)-3,4,5-trifluorobenzene carboxamide (106)**

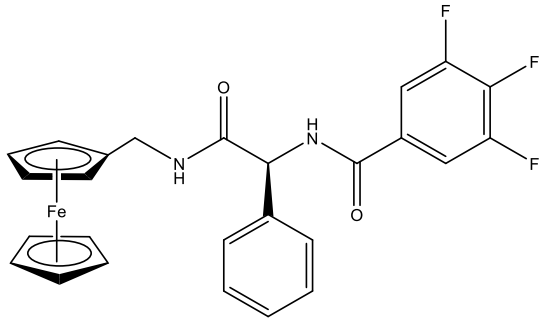

The synthesis followed that of *N*-(ferrocenylmethyl-L-alanine)-3,4,5-trifluorobenzene carboxamide using the following reagents: *N*-(3,4,5-trifluorobenzoyl)-L-(+)-α-phenylglycine (0.43 g, 1.4 mmol), ferrocenylmethylamine (0.30 g, 1.4 mmol), *N*-(3-dimethylaminopropyl)-*N*'-ethylcarbodiimide hydrochloride (0.22 g, 1.4 mmol), *N*-hydroxysuccinimide (0.16 g, 1.4 mmol) and triethylamine (1.5 ml). The product was purified by column chromatography (eluent 2:1 ethyl acetate: hexane) to give the title compound as a yellow solid (0.11 g, 15 %), mp: 201 –202 °C;

I.R. υ_{max} (neat): 3282, 2957, 1664, 1623, 1552, 1518, 1256, 1106 cm^{-1};

UV-Vis λ_{max} (CH_3CN): 315, 416 nm;

^{1}H NMR (400 MHz) δ (DMSO-d_6): 9.16 (1H, d, *J* = 8.0 Hz, -CONH), 8.55 (1H, t, *J* = 8.0 Hz, $FcCH_2NH$), 7.94 (2H, dd, *J* = 4.0 and 8.0 Hz, ArH), 7.57 (2H, dt, *J* = 4.0 and 8.0 Hz, *meta* on -CHC_6H_5), 7.40 (1H, tt, *J* = 4.0 and 8.0 Hz, *ortho* on -CHC_6H_5), 7.35 (1H, tt, *J* = 4.0 and 8.0 Hz, *para* on -CHC_6H_5), 5.74 (1H, d, *J* = 7.2 Hz, -NHCH), 4.15-4.07 (7H, m, η^5-C_5H_5 and *ortho* on η^5-C_5H_4), 4.02 (2H, t, *J* = 2 Hz, *meta* on η^5-C_5H_4), 3.97-3.92 (2H, m, $FcCH_2$);

^{13}C NMR (100 MHz) δ (DMSO-d_6): 168.9 (C=O), 156.8 (C=O), 144.6 (d, *J* = 166 Hz, -ArC_3 & -ArC_5), 138.7 (t, *J* = 166 Hz , -ArC_4), 136.5 (t, *J* = 4 Hz, -ArC_1), 128.9, 128.3, 127.5, 113.1 (d, *J* = 12 Hz, -ArC_2 & -ArC_6), 109.5, 86.6 (C_{ipso} η^5-C_5H_4), 69.0 (η^5-C_5H_5), 68.8 (C_{ortho} η^5-C_5H_4), 67.7 (C_{meta} η^5-C_5H_4), 57.2 (-NHCH), 38.1 ($FcCH_2$, -ve DEPT);

^{19}F NMR (376 MHz) δ (DMSO-d_6): -134.3 (2F, dd, *J* = 22.6 and 7.5 Hz), -157.1 (1F, tt, *J* = 22.6 and 7.5 Hz).

***N*-(ferrocenylmethylglycine)-2,3,4,5,6-pentafluorobenzene carboxamide (87)**

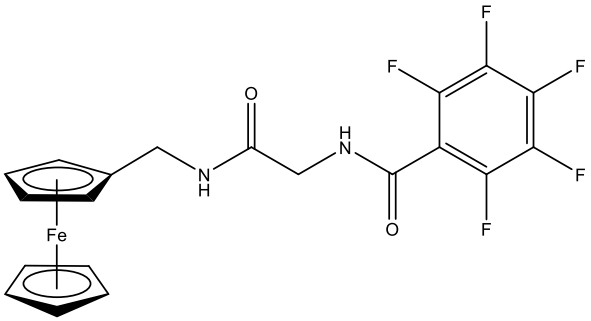

The synthesis followed that of *N*-(ferrocenylmethyl-L-alanine)-3,4,5-trifluorobenzene carboxamide using the following reagents: *N*-(2,3,4,5,6-pentafluorobenzoyl)-glycine (0.37 g, 1.4 mmol), ferrocenylmethylamine (0.30 g, 1.4 mmol), *N*-(3-dimethylaminopropyl)-*N*'-ethylcarbodiimide hydrochloride (0.22 g, 1.4 mmol), *N*-hydroxysuccinimide (0.16 g, 1.4 mmol) and triethylamine (1.5 ml). The product was purified by column chromatography (eluent 2:1 ethyl acetate: hexane) to give the title compound as a yellow solid (0.19 g, 28.6 %), mp: 138 –139 °C (Lit [9]: 138-140 °C);

I.R. υ_{max} (neat): 3309, 3067, 1693, 1653, 1559, 1506, 1223, 1107 cm^{-1};

UV-Vis λ_{max} (CH_3CN): 327, 420 nm;

^{1}H NMR (400 MHz) δ (DMSO-*d*$_6$): 9.20 (1H, t, *J* = 7.6 Hz, -CONH), 8.20 (1H, t, *J* = 8.0 Hz, FcCH$_2$NH), 4.20-4.17 (7H, m, η^5-C$_5$H$_5$ and *ortho* on η^5-C$_5$H$_4$), 4.10 (2H, t, *J* = 2.0 Hz, *meta* on η^5-C$_5$H$_4$), 4.05 (2H, d, *J* = 5.6 Hz, FcCH$_2$), 3.96 (2H, d, *J* = 5.6 Hz, -NHCH$_2$);

^{13}C NMR (100 MHz) δ (DMSO-*d6*): 168.3 (C=O), 165.1 (C=O), 156.9-156.8 (m, -ArC$_2$), 156.6-156.4 (m, -ArC$_6$), 133.7-133.6 (m, -ArC$_4$), 130.2-130.1 (m, -ArC$_3$), 130.0-129.9 (m, -ArC$_5$), 115.1 (t, *J* = 12 Hz, -ArC$_1$), 85.9 (C$_{ipso}$ η^5-C$_5$H$_4$), 68.3 (η^5-C$_5$H$_5$), 67.8 (C$_{ortho}$ η^5-C$_5$H$_4$), 67.3 (C$_{meta}$ η^5-C$_5$H$_4$), 42.6 (-NHCH$_2$-, -ve DEPT), 37.5 (FcCH$_2$, -ve DEPT);

^{19}F NMR (376 MHz) δ (DMSO-*d*$_6$): -141.5 (2F, dd, *J* = 22.6 and 7.5 Hz), -153.6 (1F, t, *J* = 22.6 Hz), -161.6 (2F, td, *J* = 22.6 and 7.5 Hz).

***N*-(ferrocenylmethyl-L-alanine)-2,3,4,5,6-pentafluorobenzene carboxamide (86)**

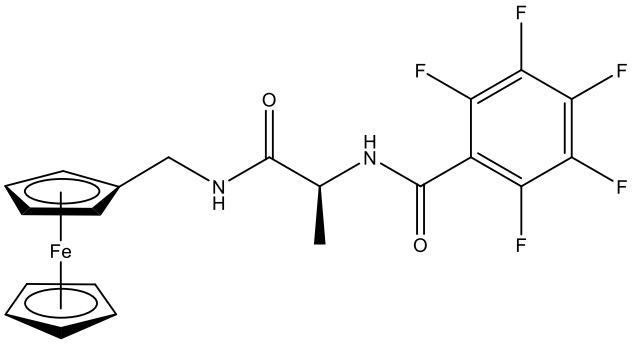

The synthesis followed that of *N*-(ferrocenylmethyl-L-alanine)-3,4,5-trifluorobenzene carboxamide using the following reagents: *N*-(2,3,4,5,6-pentafluorobenzoyl)-L-alanine (0.40 g, 1.4 mmol), ferrocenylmethylamine (0.30 g, 1.4 mmol), *N*-(3-dimethylaminopropyl)-*N*'-ethylcarbodiimide hydrochloride (0.22 g, 1.4 mmol), *N*-hydroxysuccinimide (0.16 g, 1.4 mmol) and triethylamine (1.5 ml). The product was purified by column chromatography (eluent 2:1 ethyl acetate: hexane) to give the title compound as a yellow solid (0.20 g, 29.0 %), mp: 123 –125 °C (Lit [9]: 123-125 °C);

I.R. υ_{max} (neat): 3286, 1653, 1621, 1559, 1506, 1373, 1260, 1105 cm^{-1};

UV-Vis λ_{max} (CH_3CN): 314, 427 nm;

^{1}H NMR (400 MHz) δ (DMSO-d_6): 9.24 (1H, t, *J* = 7.2 Hz, -CONH), 8.32 (1H, t, *J* = 8.0 Hz, $FcCH_2NH$), 4.57 (1H, q, *J* = 7.2 Hz, -NHCH), 4.19-4.16 (7H, m, η^5-C_5H_5 and *ortho* on η^5-C_5H_4), 4.12 (2H, t, *J* = 2.0 Hz, *meta* on η^5-C_5H_4), 4.15-4.05 (2H, m, $FcCH_2$), 1.32 {3H, d, *J* =7.2 Hz, -$CH(CH_3)$};

^{13}C NMR (100 MHz) δ (DMSO-*d6*)**:** 170.6 (C=O), 164.9 (C=O), 163.6-163.5 (m, -ArC_2), 162.9-162.6 (m, -ArC_6), 136.6-136.5 (m, -ArC_4), 130.2-130.1 (m, -ArC_3), 129.8-129.7 (m, -ArC_5), 115.3 (t, *J* = 12 Hz, -ArC_1), 86.2 (C_{ipso} η^5-C_5H_4), 68.3 (η^5-C_5H_5), 67.5 (C_{ortho} η^5-C_5H_4), 67.2 (C_{meta} η^5-C_5H_4), 49.8 (-NHCH), 37.4 ($FcCH_2$, -ve DEPT), 18.4 (-CH_3);

^{19}F NMR (376 MHz) δ (DMSO-d_6): -141.4 (2F, dd, *J* = 22.6 and 7.5 Hz), -153.1 (1F, t, *J* = 22.6 Hz), -161.5 (2F, td, *J* = 22.6 and 7.5 Hz).

***N*-(ferrocenylmethyl-L-(+)-α-phenylglycine)-2,3,4,5,6-pentafluorobenzene carboxamide (107)**

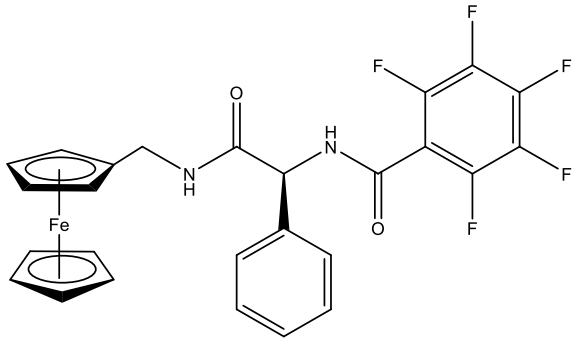

The synthesis followed that of *N*-(ferrocenylmethyl-L-alanine)-3,4,5-trifluorobenzene carboxamide using the following reagents: *N*-(2,3,4,5,6-pentafluorobenzoyl)-L-(+)-α-phenylglycine (1.45 g, 4.2 mmol), ferrocenylmethylamine (0.90 g, 4.2 mmol), *N*-(3-dimethylaminopropyl)-*N*'-ethylcarbodiimide hydrochloride (0.65 g, 4.2 mmol), *N*-hydroxysuccinimide (0.48 g, 4.2 mmol) and triethylamine (3 ml). The product was purified by column chromatography (eluent 2:1 ethyl acetate: hexane) to give the title compound as a yellow solid (0.27 g, 12 %), mp: 207 –209 °C;

I.R. υ_{max} (neat): 3257, 2926, 1669, 1631, 1549, 1519, 1045 cm^{-1};

UV-Vis λ_{max} (CH_3CN): 316, 416 nm;

^{1}H NMR (400 MHz) δ (DMSO-d_6): 9.82 (1H, d, *J* = 8.0 Hz, -CONH), 8.70 (1H, t, *J* = 8.0 Hz, $FcCH_2NH$), 7.55 (2H, dd, *J* = 4.0 and 8.0 Hz, ArH), 7.43 (2H, dd, *J* = 4.0 and 8.0 Hz, *meta* on -CHC_6H_5), 7.35 (1H, dt, *J* = 4.0 and 8.0 Hz, *ortho* on -CHC_6H_5), 7.35 (1H, tt, *J* = 4.0 and 8.0 Hz, *para* on -CHC_6H_5), 5.80 (1H, d, *J* = 7.2 Hz, -NHCH), 4.14-4.02 (9H, m, η^5-C_5H_5, *ortho* on η^5-C_5H_4 and *meta* on η^5-C_5H_4), 3.97-3.95 (2H, m, $FcCH_2$);

^{13}C NMR (100 MHz) δ (DMSO-d_6): 168.9 (C=O), 156.8 (C=O), 144.6 (C_q), 143.0-142.9 (m, -ArC_2), 142.5-142.2 (m, -ArC_6), 140.9-140.5 (m, -ArC_4), 138.3-137.9 (m, -ArC_3), 136.6-136.2 (m, -ArC_5), 128.9, 128.3, 127.5, 113.1 (t, *J* = 12 Hz, -ArC_1), 86.4 (C_{ipso} η^5-C_5H_4), 69.0 (η^5-C_5H_5), 68.8 (C_{ortho} η^5-C_5H_4), 67.7 (C_{meta} η^5-C_5H_4), 57.2 (-NHCH), 38.1 ($FcCH_2$, -ve DEPT);

^{19}F NMR (376 MHz) δ (DMSO-d_6): -141.8 (2F, dd, *J* = 22.6 and 7.5 Hz), -153.6 (1F, t, *J* = 22.6 Hz), -162.0 (2F, td, *J* = 22.6 and 7.5 Hz).

***N*-(ferrocenylmethyl-glycine-glycine)-2,3,4,5,6-pentafluorobenzene carboxamide (108)**

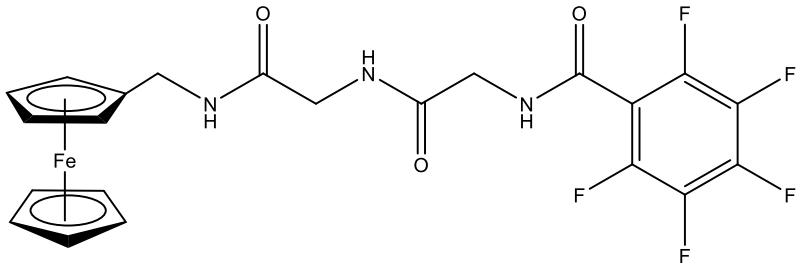

The synthesis followed that of *N*-(ferrocenylmethyl-L-alanine)-3,4,5-trifluorobenzene carboxamide using the following reagents: *N*-(2,3,4,5,6-pentafluorobenzoyl)-glycine-glycine (1.37 g, 4.2 mmol), ferrocenylmethylamine (0.90 g, 4.2 mmol), *N*-(3-dimethylaminopropyl)-*N*'-ethylcarbodiimide hydrochloride (0.65 g, 4.2 mmol), *N*-hydroxysuccinimide (0.48 g, 4.2 mmol) and triethylamine (3 ml). The product was purified by column chromatography (eluent 2:1 ethyl acetate: hexane) to give the title compound as a yellow solid (0.35 g, 16 %), mp: 221 –223 °C;

I.R. υ_{max} (neat): 3352, 3239, 3057, 2924, 1693, 1649, 1537, 1500, 1223, 1106 cm^{-1};

UV-Vis λ_{max} (CH_3CN): 329, 426 nm;

^{1}H NMR (400 MHz) δ (DMSO-d_6): 9.16 (1H, t, *J* = 7.2 Hz, -CONH), 8.28 (1H, t, *J* = 8.0 Hz, $FcCH_2NH$), 8.01 (1H, t, *J* = 7.2 Hz, -CONH), 4.19-4.17 (7H, m, η^5-C_5H_5 and *ortho* on η^5-C_5H_4), 4.09 (2H, t, *J* = 2.0 Hz, *meta* on η^5-C_5H_4), 4.03-4.00 (4H, m, $FcCH_2$ and -$NHCH_2$), 3.78 (2H, d, *J* = 5.6 Hz, -$NHCH_2$);

13C NMR (100 MHz) δ (DMSO-*d6*)**:** 168.5 (C=O), 168.4 (C=O), 147.5 (C=O), 145.3-145.0 (m, -ArC_2), 144.3-144.2 (m, -ArC_6), 141.6-141.3 (m, -ArC_4), 136.6-136.3 (m, -ArC_3), 136.2-136.0 (m, -ArC_5), 112.7 (t, *J* = 12 Hz, -ArC_1), 86.4 (C_{ipso} η^5-C_5H_4), 68.8 (η^5-C_5H_5), 68.4 (C_{ortho} η^5-C_5H_4), 67.7 (C_{meta} η^5-C_5H_4), 42.9 (-$NHCH_2$, -ve DEPT), 42.5 (-$NHCH_2$, -ve DEPT), 38.1 ($FcCH_2$, -ve DEPT);

^{19}F NMR (376 MHz) δ (DMSO-d_6): -141.4 (2F, dd, *J* = 22.6 and 7.5 Hz), -153.1 (1F, t, *J* = 22.6 Hz), -161.6 (2F, td, *J* = 22.6 and 7.5 Hz).

References

1. D. Gaspar, A. S. Veiga and M. A. Castanho, *Front Microbiol*, 2013, **4**, 294.
2. A. K. Jain and S. Jain, *Expert Opinion on Drug Delivery*, 2016, **13**, 1759-1775.
3. F. M. D. Ismail, *Journal of Fluorine Chemistry*, 2002, **118**, 27–33.
4. D. O'Hagan, *Journal of Fluorine Chemistry*, 2010, **131**, 1071-1081.
5. S. Jaferian, B. Negahdari and A. Eatemadi, *Biomedicine & Pharmacotherapy*, 2016, **84**, 780-788.
6. B. E. Smart, *Journal of Fluorine Chemistry*, 2001, **109**, 3-11.
7. B. W. Moran, F. P. Anderson, A. Devery, S. Cloonan, W. E. Butler, S. Varughese, S. M. Draper and P. T. Kenny, *Bioorganic & Medicinal Chemistry*, 2009, **17**, 4510-4522.
8. P. N. Kelly, A. Prêtre, S. Devoy, I. O'Rielly, R. Devery, A. Goel, J. F. Gallagher, A. J. Lough and P. T. M. Kenny, *Journal of Organometallic Chemistry*, 2007, **692**, 1327-1331.
9. W. E. Butler, P. N. Kelly, A. G. Harry, R. Tiedt, B. White, R. Devery and P. T. M. Kenny, *Applied Organometallic Chemistry*, 2013, **27**, 361-365.
10. G. Solomons and C. Fryhle, *Organic Chemistry*, Wiley, 7th edn., 2002.
11. J. Clayden, N. Greeves and S. Warren, *Organic Chemistry*, Oxford University Press, 2012.
12. R. Tiedt, Ph.D thesis, Dublin City University, 2014.
13. D. L. Pavia, G. M. Lampman, G. S. Kriz and J. R. Vyvyan, *Introduction To Spectroscopy*, CENGAGE Learning, 2014.

Chapter 5

Biological evaluation of *N*-(ferrocenylmethylamino acid)-fluorinated benzene carboxamides

5.1. Introduction

A preliminary structure-activity relationship (SAR) study of *N*-(ferrocenylmethyl) fluorinated benzene carboxamide derivatives was conducted by Kenny's research group, *N*-(ferrocenylmethyl-L-alanine)-3,4,5-trifluorobenzene carboxamide **28**, *N*-(ferrocenylmethyl-L-alanine)-2,3,4,5,6-pentafluorobenzene carboxamide **86** and *N*-(ferrocenylmethylglycine)-2,3,4,5,6-pentafluorobenzene carboxamide **87** were reported as the most active ones, with an IC_{50} value as 2.84 ± 0.10, 10.3 ± 0.12 and 11.1 ± 0.12 μM in MCF-7 cells after 6 days treatment .[1 2] As a further SAR and biological evaluation study, a series of 3,4,5-trifluoro and 2,3,4,5,6-pentafluoro analogues were synthesized with various amino acids and dipeptides.

As discussed in chapter 3, several miniaturised *in vitro* colorimetric assays have been developed for the quantification of cell growth. There are a number of factors should be considered when carrying out *in vitro* toxicity tests, including the cell line being used in the particular assay has a suitable level of sensitivity, cell number analysed is within a sufficient range, and choose the best system for the analysis of cell number under the certain experimental conditions.

The aims of this research project were to optimize the conditions used in the acid phosphatase assay for *N*-(ferrocenylmethyl) fluorinated benzene carboxamide derivatives and extend the SAR study of this class of compounds. Compound **28**, **86** and **87** were used for acid phosphatase assay's development. Parameters (*i.e.* cell number, concentration of DMSO and incubation time against test compounds) were analyzed. It was thought that higher accuracy will be achieved by improving sensitivity. This screening was performed in collaboration with Dr. Rosaleen Devery, of the School of Biotechnology, Dublin City University. Now the preliminary screening and *in vitro* toxicity tests for the newly synthesised ferrocenyl carboxamide derivatives are carried out in collaboration with Dr. Patricia González-Barranco and Dr. Mónica A. Ramírez-Cabrera of the School of Chemical Sciences, Universidad Autónoma de Nuevo León, México, and Karen G. Ontiveros-Castillo of the School of Chemical Sciences, Dublin City University.

5.2. Acid phosphatase assay development and optimization

The acid phosphatase assay was the chosen colorimetric end-point assay for the *in vitro* biological evaluation of this study. A distinct advantage the acid phosphatase assay has over other cytotoxicity assays is in its simplistic protocol. Once alkaline conditions are introduced, the plates are set to be read directly. Fewer steps in this semi-automated assay reduces the possibility of human error. The assay also requires less reagents, is less expensive and has better reproducibility. The sensitivity is high, but as a consequence, it has a low range of linearity between optical density and cell number. Therefore, a few parameters were considered in assay's optimization. [3]

5.2.1. The relationship between cell number and optical density in acid phosphatase assay against MCF-7 cell line in different time range

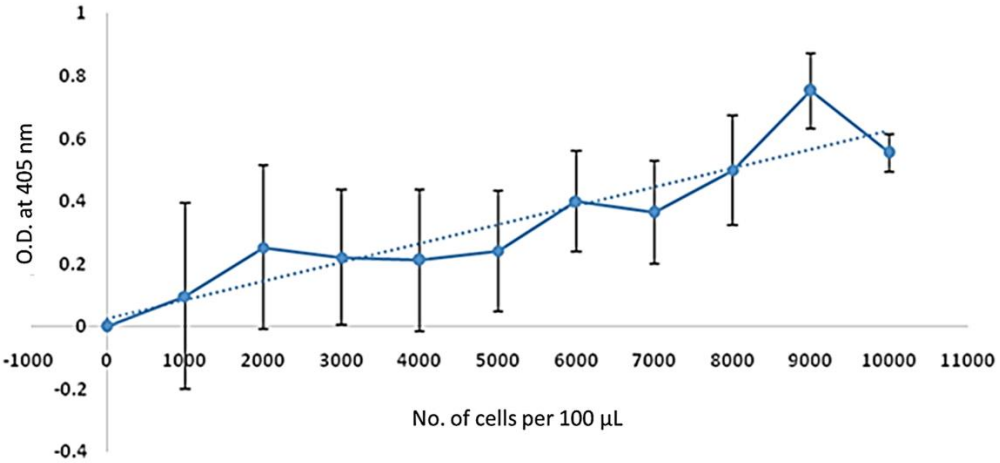

Figure 5.1: The acid phosphatase activity against MCF-7 cells after 24 hours. Error bars represent the standard deviation of triplicate experiments.

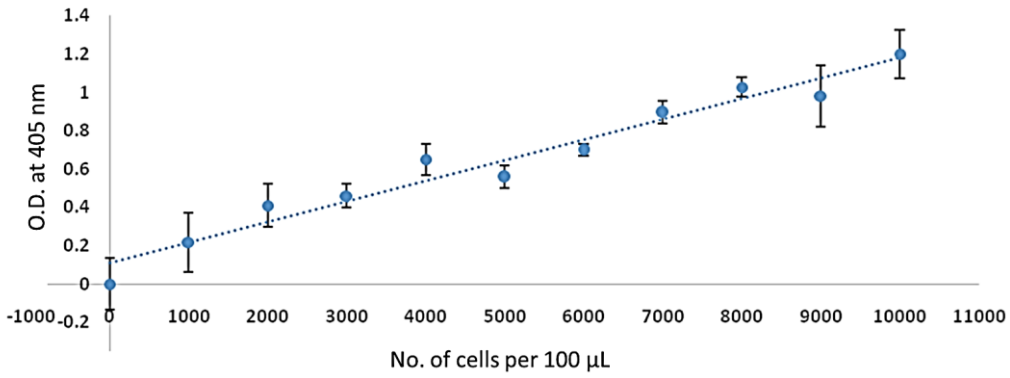

Figure 5.2: The acid phosphatase activity against MCF-7 cells after 72 hours. Error bars represent the standard deviation of triplicate experiments.

Figure 5.1 and 5.2 show the linear relationship between assay duration and O.D. after 24 to 72 hours in MCF-7 cell line, over a complete range of cell densities (0-10,000 cells per 100 µL). To investigate the effect time had on the linear relationship between acid phosphatase activity and cell number. A 10,000 cells per 100 µL stock solution was serially diluted to represent a 0-10,000 cell population in each respective well. Results show that the acid phosphatase activity, after 24 and 72 hours, is a function of MCF-7 cell number. Overall it appeared that while increased incubation time improved assay sensitivity, the linearity did not generally suffer, as the assay was still linear to high cell densities. Therefore, the sensitivity of the assay was upheld across differing time points. From these results, 1000 cells per well are used for further *in vitro* proliferation assays.

5.2.2. DMSO tolerance study in acid phosphatase assay against MCF-7 cell line

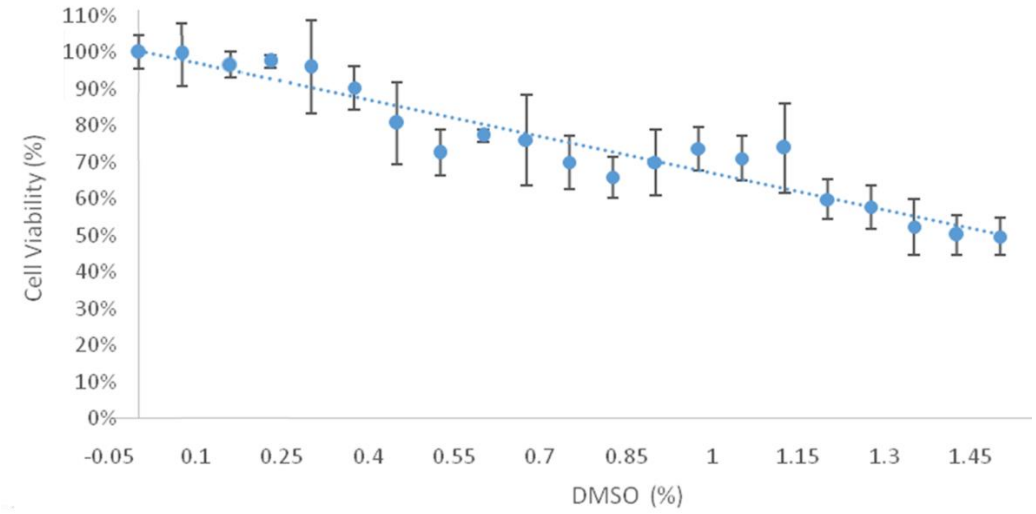

Figure 5.3: Percentage cell viability between 0 and 1.5 μM DMSO on MCF-7 cell line after 48 hours. Error bars represent the standard deviation of triplicate experiments.

DMSO tolerance is a common factor considered into toxicity assays. [4] [5] Ferrocenyl derivatives have limited solubility other than DMSO. Therefore, it is important to ascertain whether or not DMSO, in concentrations likely to be encountered, causes any significant interference in the acid phosphatase assay (e.g., by affecting enzyme activity or product fluorescence). An increasing increment of 0.075% DMSO was applied in the range of 0-1.5%. The dose response curve was plotted after 72 hours incubation time in a 37ºC, 5% CO_2 incubator. Plates were seeded for treatment at a cell density of 1000 cells per well. Control cells were untreated in media with a cell density of 1000 cells per well.

As can be seen in Figure 5.3, concentrations of DMSO is a function of percentage cell viability against MCF-7 cells. Clearly, the effect of DMSO on MCF-7 is too strong with 0.4% or higher, thus the DMSO level are maintained as 0.25% for further *in vitro* cytotoxicity investigation.

5.3. IC_{50} value determination of *N*-(ferrocenylmethylamino acid)-fluorinated benzene carboxamides in MCF-7 cell line after 24, 48 and 72 hours

N-(ferrocenylmethyl-L-alanine)-3,4,5-trifluorobenzene carboxamide **28**, *N*-(ferrocenylmethyl-L-alanine)-2,3,4,5,6-pentafluorobenzene carboxamide **86** and *N*-(ferrocenylmethylglycine)-2,3,4,5,6-pentafluorobenzene carboxamide **87** were tested against MCF-7 breast cancer cells to find the relationship between incubation time and IC_{50} results. To determine the IC_{50} values of the target compounds, individual 96-well plates containing MCF-7 cells were treated with the *N*-(ferrocenylmethylamino acid)-fluorinated benzene carboxamides at concentrations ranging from 0.25 to 50 μM. The endpoint of the growth inhibition was evaluated by the acid phosphatase assay after 24, 48 and 72 hours. The IC_{50} value for each compound was calculated using Calcusyn software, and standard deviations have been calculated using data obtained from three independent experiments.

Table 3.7: IC_{50} values for selected compounds in the MCF-7 cell line after 24, 48 and 72 hours.

Assay time (hours)	Compound No.	IC_{50} values (μM)
24	**28**	0.86 ± 0.02
	86	2.41 ± 0.05
	87	3.71 ± 0.05
48	**28**	0.53 ± 0.01
	86	1.43 ± 0.03
	87	2.06 ± 0.34
72	**28**	0.57 ± 0.03
	86	0.76 ± 0.02
	87	2.19 ± 0.04

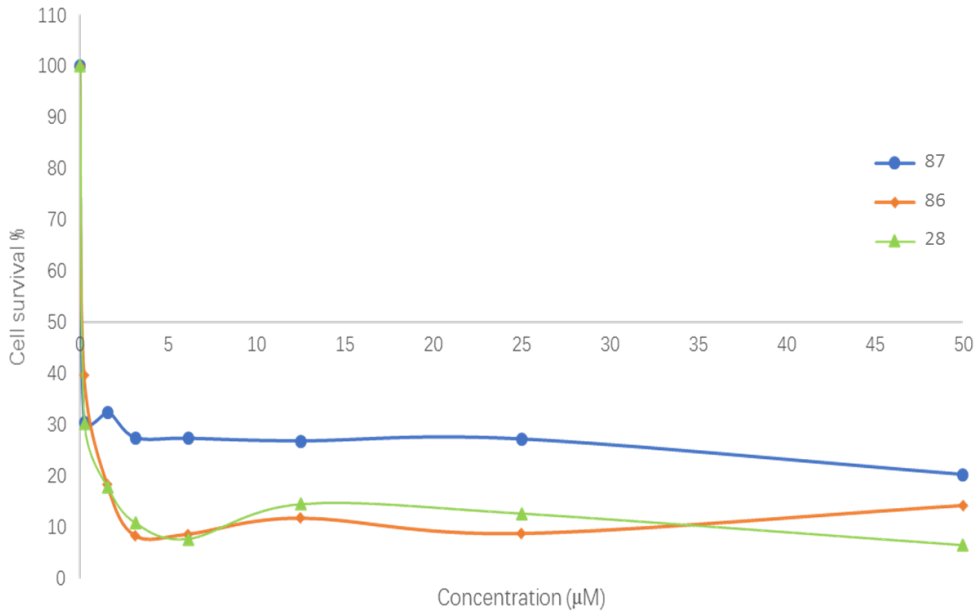

Figure 5.4: IC_{50} plot for compound **28**, **86** and **87** in MCF-7 cell line after 24 hours growth.

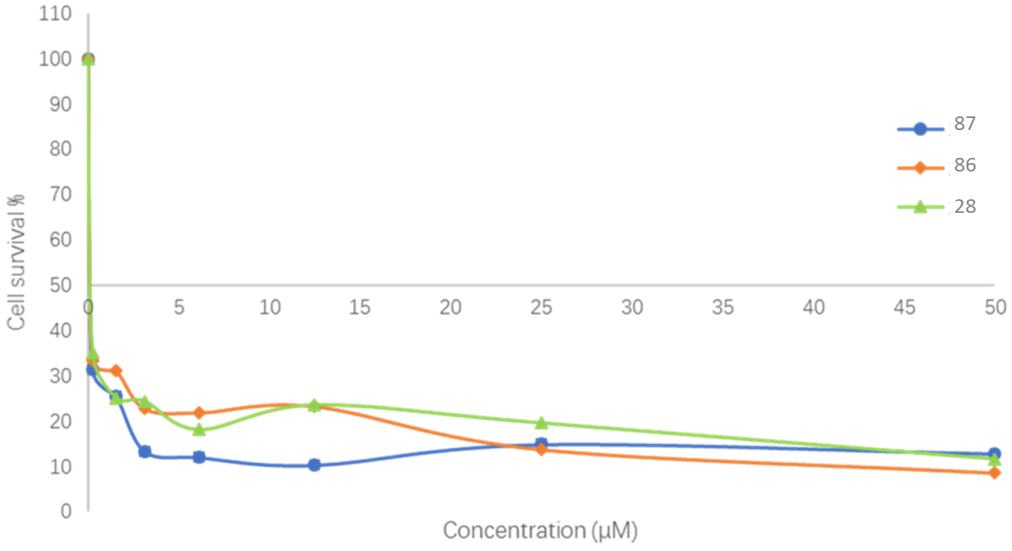

Figure 5.5: IC_{50} plot for compound **28**, **86** and **87** in MCF-7 cell line after 48 hours growth.

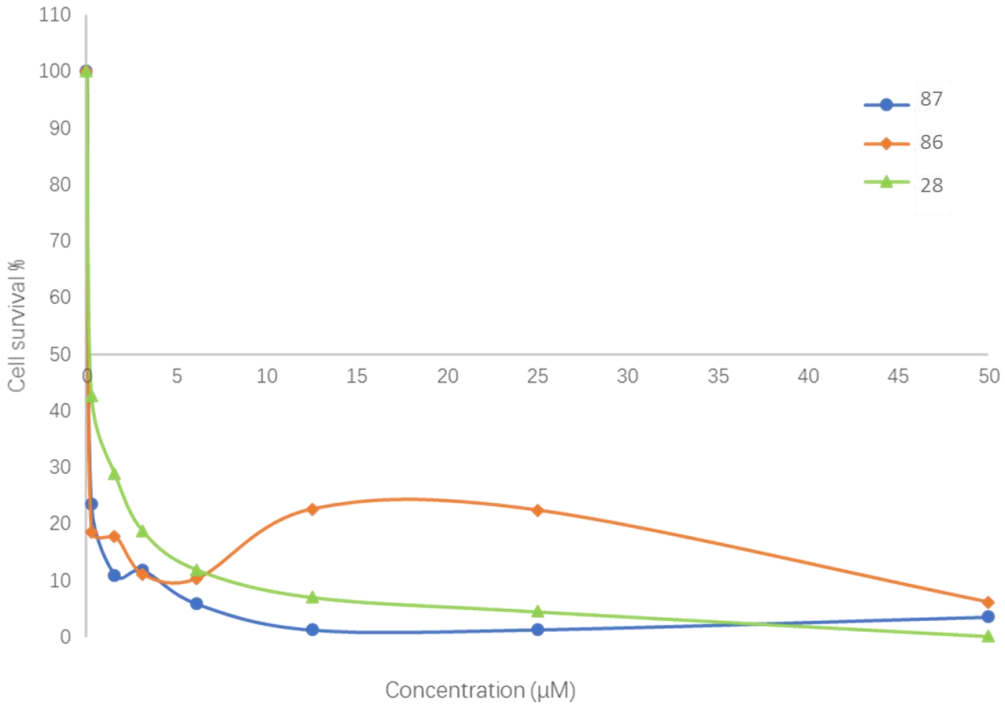

Figure 5.6: IC_{50} plot for compound **28**, **86** and **87** in MCF-7 cell line after 72 hours growth.

All *N*-(ferrocenylmethylamino acid)-fluorinated benzene carboxamides were shown to exert an anti-proliferative effect in the MCF-7 cell line. In general, the longer the breast cancer cells exposed to the test compounds, the lower the IC_{50} values are. For example, the IC_{50} dramatically decreased from 2.41 to 1.43 and 0.76 μM after 24, 48 and 72 hours test point for *N*-(ferrocenylmethyl-L-alanine)-2,3,4,5,6-pentafluorobenzene carboxamide **86**. The IC_{50} results are 3.71 (24 hours), 2.06 (48 hours) and 2.19 (72 hours) μM for compound **87**. The strongest cell growth inhibitions were found for compound *N*-(ferrocenylmethyl-L-alanine)-3,4,5-trifluorobenzene carboxamide **28** at all test points. Initially, the IC_{50} value dropped from 0.86 to 0.53 μM, and increased slightly to 0.57 μM. Butler *et al* reported the IC_{50} values belong to compound **28**, **86** and **87**, as 2.84 ± 0.10, 10.3 ± 0.12 and 11.1 ± 0.12 μM in MCF-7 cells after 6 days treatment. After optimization, lower IC_{50} values were obtained with smaller standard deviation between 24 to 72 hours' time frame. Therefore, optimization of the acid phosphatase assay has positive effect on IC_{50} determination.

5.4. Conclusion

A series of *N*-(ferrocenylmethylamino acid)-fluorinated benzene carboxamides have been prepared and evaluated for their biological activities. Compound **28**, **86** and **87** were selected for optimization of the acid phosphatase assay. A few parameters were optimized and found: the effect time have a linear relationship between acid phosphatase activity and cell number; 0.25% DMSO had negligible effects on the cell viability. Therefore, 1000 cell per well and 0.25% DMSO were used for further *in vitro* proliferation investigation. All selected carboxamides were shown to exert an anti-proliferative effect against the MCF-7 cell line. Found that longer the breast cancer cells exposed to the test compounds, the lower the IC_{50} values obtained. After optimization, lower IC_{50} values with smaller standard deviation were obtained after 24, 48 and 72 hours. Therefore, optimization of the acid phosphatase assay has positive effect on IC_{50} determination.

Materials and Methods

Cells and cell culture

Cell culture media, supplements and related solutions were purchased from Sigma-Aldrich (Dublin, Ireland) unless otherwise stated. The MCF-7 breast cancer cell line was obtained from the Health Protection Agency. The cells were grown in modified eagles' medium with 5 % foetal bovine serum (FBS). Cell lines were grown as a monolayer culture at 37 °C, under a humidified atmosphere of 95 % O_2, and 5 % CO_2 in 75 cm^2 flasks. All cell culture work was carried out in a class II laminar airflow cabinet (Holten LaminAir). All experiments involving cytotoxic compounds were conducted in a cytoguard laminar airflow cabinet (Holten LaminAir Maxisafe). Before and after use the laminar airflow cabinet was cleaned with 70 % industrial methylated spirits (IMS). Any items brought to the airflow cabinet were swabbed using IMS. At any one time, only one cell line was used in the laminar airflow cabinet and after completion of work with the cell line, the laminar airflow cabinet was allowed stand for 15 minutes before use. This was to eliminate any possibility of cross contamination between cell lines. The Laminar Airflow was cleaned daily with industrial disinfectants (Virkon or Tego) and also with IMS. These disinfectants were alternated fortnightly. Cells were fed with fresh media or subcultured when confluency reached 70 % in order to maintain active cell growth.

Subculture techniques of cell lines

Media and Trypsin/EDTA solution (0.25 % trypsin (Gibco), 0.01 % EDTA (Sigma Aldrich) solution in PBS) were incubated at 37 °C for 20 min in a water bath. The cell culture medium was removed from the tissue culture flask and discarded into a sterile bottle. The flask was rinsed with PBS (7 ml) to ensure the removal of any residual media. Once removed to a sterile waste bottle, fresh trypsin/EDTA solution (4 ml) was added and incubated at 37 °C until all the cells were detached from the inside surface of the tissue culture flask. The trypsin was deactivated by adding PBS (6 ml). The cell suspension was removed from the flask and placed in a sterile universal container and centrifuged at 2000 rpm for 5 minutes. The supernatant was removed and discarded from the universal container and the pellet was suspended in complete medium. A cell count was performed. Depending on number of tests, an aliquot of cells was used to reseed a flask at the required density, topping up the flask with fresh medium.

Assessment of cell number

Cells were trypsinised, pelleted and resuspended in media. An aliquot (10 μL) of the cell suspension was applied to a universal vial and dye was added. This was applied to the chamber of a glass cover slip enclosed haemocytometer. Cells in the 16 squares of the four grids of the chamber were counted. The average cell number, per 16 squares, was multiplied by a factor of 10^4 and the relevant dilution factor to determine the number of cells per ml in the original cell suspension.

***In vitro* proliferation assays**

Confluent cells in the exponential growth phase were harvested by trypsination and a cell suspension of 5 x 10^4 cells/ml was prepared in fresh culture medium. The cell suspension (40 μL) was added to a flat bottom 96 well plate (Costar 3599), followed by culture medium (60 μL). The plate was slightly agitated in order to ensure complete dispersion of the cells. The cells were incubated for an initial 24 hours in a 37 °C, 5 % CO_2 incubator to allow the adhesion of cells to flat bottom wells. The compounds for testing were prepared in 1 μM stocks. The different concentrations used for IC_{50} data studies were made up accordingly by adding the desired amount of compound stock solution to fresh culture media. Once the compounds and media were added to the 96 well flat bottom plates, the plate was gently agitated and incubated at 37 °C, 5 % CO_2. Following an incubation period of 24, 48 and 72 hours, drug media was removed from the 96-well plate and each well was washed with 100 μL of PBS. This was removed and 100 μL of freshly prepared phosphatase substrate (10 mM p-nitrophenol phosphate in 0.1M sodium acetate, 0.1% triton X-100, pH 5.5) was added to each well. The plate was incubated at 37 °C for 2 hours. The enzymatic reaction was stopped upon addition of 1M NaOH (50 μL) to each well. The absorbance of each well was read in a dual beam reader (Synergy HT, Bio-Tek, USA) at 405 nm with a reference wavelength of 620 nm.

Assessment of cell survival in the presence of test sample was determined by the acid phosphatase assay. For the IC_{50} data studies, the concentration of drug that causes 50 % growth inhibition was determined by plotting the percentage (%) survival of cells (relative to control cells) against the concentration of the test sample. In relation to IC_{50} data studies, IC_{50} values were calculated using Calcusyn software (Biosoft, UK).

Statistical Analysis

IC_{50} values were calculated using CalcuSyn Software (BioSoft). Student t-test (two tailed with unequal variances) was used to compare the activity of test compounds to their corresponding control group, and p-value < 0.05 was considered.

References

1. P. N. Kelly, A. Prêtre, S. Devoy, I. O'Rielly, R. Devery, A. Goel, J. F. Gallagher, A. J. Lough and P. T. M. Kenny, *Journal of Organometallic Chemistry*, 2007, **692**, 1327-1331.
2. W. E. Butler, P. N. Kelly, A. G. Harry, R. Tiedt, B. White, R. Devery and P. T. M. Kenny, *Applied Organometallic Chemistry*, 2013, **27**, 361-365.
3. J. Friedrich, W. Eder, J. Castaneda, M. Doss, E. Huber, R. Ebner and L. A. Kunz-Schughart, *Journal of Biomolecular Screening*, 2007, **12**, 925-937.
4. M. A and C. M., *Cytotechnology*, 1993, **11**, 49-58.
5. F. Kalalinia, F. Mosaffa and J. Behravan, in *Breast Cancer - Focusing Tumor Microenvironment, Stem cells and Metastasis*, 2011.